UNIVERSITÄTSKLINIKUM HAMBURG-EPPENDORF

Institut für Immunologie

Prof. Dr. Marcus Altfeld

Expression, modulation and function of the P2X7 receptor on human immune cells

Dissertation

zur Erlangung des Doktorgrades Dr. rer. biol. hum. / PhD
an der Medizinischen Fakultät der Universität Hamburg.

vorgelegt von:

Arnau Serracant Prat
aus Barcelona, Spanien

Hamburg 2018

(wird von der Medizinischen Fakultät ausgefüllt)

Angenommen von der
Medizinischen Fakultät der Universität Hamburg am: _14.12.2018_

Veröffentlicht mit Genehmigung der
Medizinischen Fakultät der Universität Hamburg.

Prüfungsausschuss, der/die Vorsitzende: _Prof. Dr. Eva Tolosa_

Prüfungsausschuss, zweite/r Gutachter/in: _Prof. Dr. Tim Magnus_

Prüfungsausschuss, dritte/r Gutachter/in: _Prof. Dr. Stefan Linder_

TABLE OF CONTENTS

1. <u>INTRODUCTION</u>

1.1 THE IMMUNE SYSTEM

The interaction of organisms with the environment and the subsequent exposure to multiple insults has driven the evolution of a multi-layered defence system, the immune system. A pivotal feature of the immune system is to distinguish between foreign (non-self) antigens and self-components (Delves and Roitt, 2000). While most of the inferior organisms only react to threats by recognizing conserved structures displayed by pathogens (Smith, 2016), the immune system of vertebrates is able to mount a specific response to pathogens and to generate long-lived memory cells. Immunological memory results in highly efficient responses following re-encounter with the same pathogen (Flajnik and Kasahara, 2010; Boehm, 2012).

1.1.1 <u>The immune response</u>

The entrance of a pathogen alerts the immune system, activating several effector molecules and tissue-resident and/or circulating immune cells that generate an immune response. The immune response relies on the close cooperation between two distinct parts of the immune system, the innate and the adaptive arm. Each branch has crucial and special properties, but the coordination between both ensures protection against pathogens throughout life (Janeway, 1989; Dempsey, Vaidya and Cheng, 2003).

1.1.1.1 The innate immune response

The first line of defence is provided by physical barriers (skin, mucous membranes and body secretions), which prevent pathogens from entering the body. Next, cells of the innate immune system (phagocytes, natural killer cells and other innate lymphoid cells) and effector plasma proteins react immediately after pathogen recognition. The potential to mount a rapid response relies upon recognition of highly conserved molecules shared by several families of pathogens. The recognition of pathogen-associated molecular patterns (PAMPs) is mediated by germline-encoded pattern recognition receptors (PRRs). PRRs can be found attached to cell membranes, such as the toll-like receptors (TLRs) and C-type lectin receptors (CLRs) or free in the cytoplasm, such as the NOD-like receptors (NLRs) and RIG-I-like receptors (RLRs). In addition, plasma proteins such as the complement system or serum amyloid A, contribute to the inflammatory process and clearance of pathogens by recruiting effector immune cells to the site of infection. Activation of the complement system cascade potentiates the recruitment of macrophages and neutrophils and enhances their

phagocytic ability. Additionally, the binding of different complement factors to the surface of bacteria induces the formation of a transmembrane channel (membrane attack complex), leading to cell lysis and bacterial death (Dunkelberger and Song, 2010).

Neutrophils are one of the first populations to be recruited to the site of inflammation and are essential in avoiding the dissemination of infection. Upon arrival, neutrophils sense and phagocytose microbes, and release large amounts of antimicrobial particles and enzymes (Mayadas, Cullere and Lowell, 2014). Basophils, eosinophils and mast cells are also an important source of antimicrobial peptides, enzymes and other cytotoxic substances, which are pivotal in the fight against extracellular bacteria and parasites. These cells, however, are involved in the generation of allergic reactions (Stone, Prussin and Metcalfe, 2010). Phagocytes, namely monocytes, macrophages, conventional dendritic cells (cDCs) and neutrophils, are key players in innate immunity for their ability to ingest and eliminate pathogens in a process known as phagocytosis. Among these immune cell populations, monocytes, macrophages and dendritic cells (DCs) can in addition process and present antigens to T cells via the major histocompatibility complex (MHC). Antigen presentation to T cells promotes a specific immune response against a particular antigen epitope. Thus, antigen presentation by professional antigen presenting cells (APCs) to T cells serves as a bridge between innate and adaptive immunity (Charles A Janeway *et al.*, 2001a).

Plasmacytoid Dendritic Cells (pDCs) are a distinct subset of DCs that react to viral infections by producing massive amounts of type one Interferons (IFN), mainly IFN-α and IFN-β. The release of these mediators promotes cytotoxic responses against virus-infected cells by activating natural killer (NK) and CD8 T cells (Colonna, Trinchieri and Liu, 2004). NK cells account for up to 15% of circulating lymphocytes, but are also present in higher numbers in peripheral organs (Yu, Freud and Caligiuri, 2013). They are extremely important in tumor surveillance and their presence is crucial for the rapid and effective elimination of viral-infected cells. Human NK cells respond through a variety of activating receptors (killer cell immunoglobulin-like receptors (KIR-S), CD16, natural cytotoxicity receptors (NCRs), NTBA, 2B4 or NKG2D) or inhibitory receptors (KIR-L, CD94/NKG2A, LILRB1) encoded in the germline. NK cells attack cells with absent or aberrantly low expression of MHC class I, but are also activated by antibodies, viral peptides, recognition of MHC class I via activating KIRs (Vély, Golub and Vivier, 2016), and cytokines like IL-2, IL-12, IL-15 and IL-18 (Freeman et al., 2015). Their activity depends on a fine balance between activating and inhibitory signals. NK cell cytotoxicity is mediated by release of perforin and granzymes, antibody-dependent cell-mediated cytotoxicity (ADCC) and Fas/FasL-induced apoptosis of infected cells. They also release tumor necrosis factor α (TNF-α) and IFN-γ, which can enhance macrophage activity and T cell responses (Vivier, Tomasello et al. 2008).

Innate lymphoid cells (ILCs) are lymphoid cells lacking rearranged antigen receptors and myeloid markers (Spits and Cupedo, 2012). They initially develop in the fetal liver or bone marrow, and then migrate to mucosal tissues. ILC subpopulations are identified based on their function and the transcription factors they express. Group 1 ILCs are inflammatory cells that rely on the T-box transcription factor T-bet and secrete mainly IFN-γ in response to intracellular pathogens. Of note, cytotoxic NK cells have been recently included within this group owing to the large amounts of IFN-γ they produce (Zhang and Huang, 2017). Group 2 ILCs are under the control of the GATA-binding protein 3 (GATA3) and retinoic acid receptor related orphan receptor-α (ROR-α) transcription factors, and produce cytokines such as IL-4, IL-5, IL-9 and IL-13 in response to parasite infections. Group 3 ILCs are defined by the secretion of IL-17 and/or IL-22 and depend on the transcription factor ROR-γt (Spits et al., 2013). They are important for the maintenance of intestinal homeostasis. This group include lymphoid tissue inducers (LTi), an immune cell subset involved in the development and maintenance of lymphoid organs (Meier *et al.*, 2007; Vermijlen and Prinz, 2014).

1.1.1.2 The adaptive immune response

The adaptive immune response provides a specific response against a particular antigen. Upon antigen recognition, adaptive T cells clonally expand and differentiate into effector cells. Consequently, the onset of an adaptive response does require several days. In contrast to the innate PRRs, the specificity of the antigen receptors is not encoded and inherited in the germline, but acquired during life. The genetic rearrangement of a limited number of genes encoding for the T cell receptor (TCR) and B cell receptor (BCR) results in an extensive diversity of receptors.

Lymphocytes are the major players in adaptive immunity. They are found constantly recirculating in blood and the lymphatic system, or as resident cells in almost all tissues in the body. Every single B and T cell presents a unique specificity against a singular antigen. Upon antigen encounter, naïve or immature T and B cells become effector cells, leave the secondary lymphoid organs (SLO) and migrate to target tissues. Some effector cells develop into long-lived memory cells and remain in blood or in tissues as tissue-resident memory (TRM) cells (Schenkel and Masopust, 2014). Immunological memory is a crucial feature of the adaptive immunity, and it provides long-term protection by inducing faster and more efficient responses after a possible re-encounter with the same antigen.

1.1.1.2.1 T cells

T cells are pivotal in cell-mediated immunity. The majority of human T cells undergo rearrangement of the alpha and beta chains to constitute the TCR, and are therefore termed αβ T cells (Tαβ). Receptor diversity originates from random rearrangements of different variable (V), diversity (D) and

join (J) segments encoded in the *TRA* and *TRB* genes; and the insertion, deletion and substitution of additional nucleotides between these segments. These events enable the generation of about 10^{16} different TCRs out of a limited number of genes (Charles A Janeway *et al.*, 2001b; Nikolich-Zugich, Slifka and Messaoudi, 2004). At the final stages of maturation in the thymus, T cells commonly express CD3 and CD4 or CD8 on their surface, which act as co-receptors that stabilize the interaction of the TCR complex with MHC molecules. Surviving mature thymocytes leave the thymus and egress to periphery as naïve T cells. The complete activation of these conventional T cells requires two further signals: first, a direct cell-cell interaction between the costimulatory molecules CD28 and CD80/CD86, and second, signalling induced by the cytokines present during antigen presentation.

<u>CD4^{+} T cells</u>

CD4^{+} T cells, also named T helper (Th) cells, provide assistance to other immune cell populations and they are referred to as the orchestrators of the immune response. Th cell functions are mediated by release of a wide range of cytokines, which are involved in many immunological processes, such as the activation of cytotoxic CD8^{+} T cells, B cell isotype switching and potentiation of the antimicrobial activity of phagocytic cells. CD4^{+} T cells differentiate into different subtypes depending on the cytokine signals received, and produce specific sets of cytokines. Th1 cells are proinflammatory cells that secrete mainly IFN-y and are critical for the clearance of intracellular pathogens upon activation of macrophages. Th2 cells secrete IL-4, IL-5 and IL-13, important in the response against parasites. Th17 cells secrete IL-17 and are essential during infections with extracellular pathogens and fungi (Zhu, Yamane and Paul, 2010). Th1 and Th17 cells play a major role in the development of autoimmunity (Tabarkiewicz *et al.*, 2015), while Th2 cells are involved in allergic reactions. Several other subtypes of Th cells have been described, e.g.: Th9 cells, Th22 cells and follicular helper T cells (Tfh). Th9 cells are involved in fighting helminth infections (Licona-Limón *et al.*, 2013) as well as in allergic and autoimmune responses (Deng *et al.*, 2017). Th22 cells play a role in host defence and inflammatory diseases in the skin (Eyerich *et al.*, 2009), while Tfh cells are crucial for the formation of germinal centres and optimal B cell differentiation and function (Ma *et al.*, 2012).

<u>CD8^{+} T cells</u>

CD8^{+} T cells or cytotoxic T cells are responsible for the elimination of cells infected with viruses or intracellular bacteria, tumour cells and injured cells. Unlike CD4^{+} T cells, which are restricted by MHC class II molecules; CD8^{+} T cells are restricted by MHC class I molecules. MHC class I is expressed in all nucleated cells and displays endogenous antigens to the extracellular surface. Peripheral CD8^{+} T cells commonly express CD8 molecules as a αβ heterodimer, but can also exist as CD8αα homodimers at mucosal surfaces. Cytotoxic T cells induce cell death by releasing granzymes and perforins, but also

through the Fas/Fas-ligand pathway. Furthermore, they secrete proinflammatory cytokines, such as IFN-γ and TNF.

<u>Regulatory T cells</u>

Regulatory T cells (Tregs) are essential in maintaining peripheral tolerance and controlling immune responses after antigen clearance. A major type of Tregs express the transcription factor Forkhead Box P3 (FoxP3) and express the IL2α chain (CD25) constitutively (Sakaguchi, 2004). FoxpP3^{+} Treg may develop in the thymus already as Treg cells (natural Tregs) or can be peripherally-induced (inducible Tregs) (Hori, Nomura and Sakaguchi, 2003). The latter arise from CD4^{+} T cells undergoing reprogramming after TCR stimulation in the presence of transforming growth factor β (TGF-β) and IL-2 (Schmitt and Williams, 2013). They dampen immune responses using different suppressive mechanisms, namely release of the immunosuppressive cytokines IL-10 and TGF-β, inhibition of T cell proliferation by deprivation of IL-2, induction of cell death, inhibition of T cell activation by inhibitory costimulatory molecules and conversion of adenosine triphosphate (ATP) into adenosine (Ado) (Curotto de Lafaille and Lafaille, 2009; A. Rissiek *et al.*, 2015).

1.1.1.2.2 B cells

B cells mediate the humoral response by secreting antibodies (Abs). In contrast to T cells, B cells are able to recognize whole pathogens and soluble antigens in their native form through the BCR; and therefore, they are not restricted to presentation by MHC molecules. Activation of B cells commonly occurs with the cooperation of Tfh cells, which results in the generation of high-affinity antibodies. B cell activation may also occur independently of T cell interaction, by TLR receptor signalling or by crosslinking of several BCRs. T-cell independent activation of B cells leads to a quicker response, but antibodies with lower affinity (Vos *et al.*, 2000). The majority of B cells differentiate eventually into plasma cells and produce large amounts of immunoglobulins (Igs), and then relocate to the bone marrow. Additionally, B cells may also present antigen to T cells upon BCR-mediated antigen endocytosis (Malhotra *et al.*, 2009).

1.1.1.3 Innate-like lymphocytes

Beyond the fully adaptive conventional T cells, a small subset of T cells termed innate-like lymphocytes (ILLs) share properties of both adaptive and innate immunity (**Figure 1**). On the one hand, ILLs undergo rearrangement of their TCR, recognize antigens presented by APCs, and differentiate into memory cells, as seen in adaptive immunity. On the other hand, they recognize conserved antigens (Vermijlen and Prinz, 2014), and also respond shortly after antigen encounter.

The best described ILLs are γδ$^+$ T cells, mucosal associated invariant T cells (MAIT) and natural Killer T (NKT) cells.

Specificity	Limited: Recognition of conserved patterns present in different pathogens	High: recognition of antigenic epitopes (few aminoacids)
Receptor diversity	Limited: germline-encoded receptors (i.e. TLRs, NLRs, KIRs)	High: TCR and BCR, arising from somatic recombination (T and B cells) hypermutation (only B cells)
Memory	Absent: equal response upon repeated exposure	Present: faster and amplified responses upon repeated exposure
Response kinetics	Immediate (minutes to hours)	Slow (several days)
Relevance	• First line of defence for control of pathogens (antimicrobial activity, phagocytosis, cytotoxicity, cytokine production) • Efficient recruitment of other immune cells to site of infection (chemoattractants) • Activation of adaptive immunity (antigen presentation by APCs)	• Highly specific and effective clearance of pathogens and infected-cells (cytotoxicity, antibody production) • Enhancement of the function of other immune cells activity by cytokine production (i.e. macrophages)

APCs (antigen presenting cells); BCR (B cell receptor); DC (dendritic cell); Mo (monocyte); ILC (innate lymphoid cell); iNKT (invariant natural killer T cell); KIRs (Killer-cell immunoglobulin-like receptors); MAIT (mucosal associated invariant T cell); NLRs (NOD-like receptors); Tc (cytotoxic T cell); TCR (T cell receptor); Th (T helper cell); TLRs (toll-like receptors); Treg (regulatory T cell).

Figure 1. Classification of immune cell subsets according to their role in the immune response. The immune system is split in two distinct arms: the innate and the adaptive; each of them characterised by different immune cell types and effector molecules that protect the body against external invaders. Innate-like lymphocytes (ILLs), such as γδ$^+$ T cells (Tγδ), mucosal associated invariant T cells (MAIT) and invariant natural

killer T cells (iNKT) share properties from both arms and are therefore positioned at the interface between both systems. ILLs display an invariant or highly restricted TCR repertoire and recognise conserved microbial elements. These cells become activated at early stages of infections and can be activated both in a TCR-dependent or independent fashion.

1.1.1.3.1 γδ$^+$ T cells

γδ$^+$ T cells rearrange the gamma (γ) and a delta (δ) chain instead of the conventional α and β chains. The TCR gamma (*TRG*) and TCR delta (*TRD*) genes contain lower number of variable segments than the *TRA* and *TRB* genes, therefore generating lower diversity than the αβ TCR. Three main Vδ gene elements (Vδ1, Vδ2 and Vδ3) are commonly used by human Tγδ cells, being Vδ2 and Vδ1 the most represented in peripheral blood. Receptor diversity is also reduced by the preferential pairing of these three Vδ elements with a limited or exclusive number Vγ elements (Prinz, Silva-Santos and Pennington, 2013).

γδ$^+$ T cells emerge from the thymus and represent 1-10% of circulating T cells, but they can also be found in tissues, especially in epithelial layers. Early γδ T cell development in mice occurs in different waves of functionally distinct γδ$^+$ T cell subsets carrying specific Vγ segments (Prinz, Silva-Santos and Pennington, 2013). In humans, it is not yet known whether a similar pattern exists. γδ$^+$ T cells recognize both microbial and self-derived compounds presented by MHC-like molecules, but also intact antigens such as lipids and stress-induced proteins (Born, Kemal Aydintug and O'Brien, 2013).

Vδ2$^+$ cells are often paired to the Vγ9 chain and constitute up to 95% of the γδ$^+$ T cell population in adult blood. Vδ2$^+$Vγ9$^+$ cells recognize the pathogen-associated phosphoantigen (E)-4-Hydroxy-3-methyl-but-2-enyl pyrophosphate (HMBPP), but also the self-derived phosphoantigens Isopentenyl pyrophosphate (IPP) and Dimethylallyl pyrophosphate (DMAPP) (Tanaka *et al.*, 1995), presented by butyrophilins and other non-classical MHC molecules (Harly *et al.*, 2012). Vδ2$^+$ cells are crucial in cytotoxicity against infected, stressed and tumour cells (Wrobel *et al.*, 2007; Marlin *et al.*, 2017). γδ$^+$ T cells also promote the maturation and activation of DCs and monocytes (Leslie *et al.*, 2002; Conti *et al.*, 2005; Eberl *et al.*, 2009); as well as promoting B and T cell responses and impairing the immunosuppressive activity of Tregs (Brandes, Willimann and Moser, 2005; Petermann *et al.*, 2010; Petrasca and Doherty, 2014).

Vδ2$^-$ cells include those cells carrying a Vδ1 or Vδ3 chain. Human Vδ1$^+$ cells are the most abundant γδ$^+$ T cells at epithelial sites, such as the intestine and skin. They are cytotoxic and secrete IFN-γ, essential for the elimination of viruses, especially cytomegalovirus (CMV) (Déchanet *et al.*, 1999; Sell *et al.*, 2015), fungi and tumour cells. Antigen presentation is driven by MHC class I polypeptide-related protein A (MICA) and B (MICB). Vδ1$^+$ cells can also recognize endogenous phospholipids presented by non-classical MHC molecules of the CD1 family (Adams, Gu and Luoma, 2015).

Of note, murine γδ⁺ T cells can also be activated independently of their TCR, in response to pathogen products through TLRs (Martin *et al.*, 2009) and cytokines via cytokine receptors (Sutton *et al.*, 2009). Whether a similar activation pattern also occurs in humans is not yet known.

1.1.1.3.2 Mucosal Associated Invariant T cells

Mucosal associated invariant T (MAIT) cells represent 1-10% of total blood-circulating T cells in healthy adults, and are of great importance in microbial infections (Salou, Franciszkiewicz and Lantz, 2017). MAIT cells develop in the thymus but undergo selection through the MHC-related 1 (MR1) molecule expressed on CD4⁺CD8⁺ double positive (DP) thymocytes (Seach et al., 2013). After selection, MAIT cells exit the thymus and migrate mainly to mucosal tissues, but also to the liver and lungs. MAIT cells express the invariant TCR alpha chain Vα7.2 predominantly paired with the J segment J33 (Vα7.2-Jα33), but also with the J12 (Vα7.2-Jα12) and J20 (Vα7.2-Jα20) segments. These VJ elements combine with a restricted set of TCR-β chains to build a functional TCR. MAIT cells are mainly negative for CD4 and CD8 or express the CD8 homodimer CD8αα on their surface (Reantragoon *et al.*, 2013). They have an effector-memory phenotype and express the lectin family NK receptor CD161, the IL-18 receptor (IL-18Rα), and tissue-homing chemokine receptors, such as CCR6 and CCR9 (Chandra and Kronenberg, 2015; Koay, Godfrey and Pellicci, 2018). Like γδ⁺ T cells, MAIT cells can be activated both in a TCR-dependent or independent manner (Slichter et al., 2016). TCR-activation is restricted by MR1 molecules presenting bacterial transitory neo-antigens derived of the metabolism of vitamins B2 and B9. Upon TCR-engagement, MAIT cells secrete IFN-γ, TNF-α and IL-17 (van Wilgenburg *et al.*, 2016). MAIT cells also display cytotoxic activity and release granzyme B and perforin (Kurioka *et al.*, 2015). TCR-independent activation involves the presence of cytokines, such as IL-12, IL-15, IL-18 and IL-23; which promote the secretion of IFN-γ, granzyme B and IL-17 (Ussher *et al.*, 2014; Slichter *et al.*, 2016). Some studies have also shown a synergistic effect between inflammatory signals and TCR engagement (Slichter *et al.*, 2016).

A further group of ILLs share properties of T and NK cells, and are named natural killer T cells (NKTs), representing a very rare population in human blood (less than 0.1%) (Kenna *et al.*, 2003). Invariant NKT cells (iNKTs), also termed type 1 NKT cells, display an invariant TCR alpha chain (Vα24-J18) that preferentially combines with the Vβ11 element. iNKTs participate in the clearance of bacteria, parasite, fungi and also viruses (Juno, Keynan and Fowke, 2012; Kinjo, Kitano and Kronenberg, 2013). They display an activated phenotype and typical markers of the NK lineage, such as CD161, CD56 and CD16. They recognize pathogen-associated or endogenous lipids presented by the non-classical MHC molecule CD1d on APCs. iNKTs sense danger-associated molecular patterns (DAMPs) and rapidly produce proinflammatory cytokines that promote activation of NK cells, T cells, B cells, DCs and macrophages. These cells can be sub-classified according to the cytokines they release. The most

common subsets are iNKT1, iNKT2 and iNKT17, which mirror the Th1, Th2 and Th17 secretory profiles (Chandra and Kronenberg, 2015).

Similar to other innate-like cells, iNKT cells can also be indirectly activated through cytokine signalling or NK receptors (Reilly, Wands and Brossay, 2010; Brennan, Brigl and Brenner, 2013).

1.2 PURINERGIC SIGNALLING

Purine nucleotides and nucleosides are important messengers in extracellular cell communication. Purinergic signalling plays a significant role in numerous organ systems, including the immune system (Burnstock and Burnstock, 2006); and therefore, is considered a potential therapeutic target for the treatment of immune-related disorders (Burnstock, 2017), such as multiple sclerosis or asthma.

Under physiological conditions, purine nucleotides are mostly intracellular, and contribute to cell metabolism as energy reservoirs and/or enzyme cofactors. ATP is present at high concentrations (1-10 mM) in the intracellular compartment (Beis and Newsholme, 1975; Traut, 1994; Burnstock, 2017), whereas the extracellular concentration of ATP is considerably lower (nanomolar range) (Ryan *et al.*, 1996; Gorman, Feigl and Buffington, 2006). ATP can be physiologically released in an active or passive fashion to the extracellular milieu, where it promotes autocrine and paracrine effects. The active release of purine nucleotides occurs predominantly by exocytosis or through membrane-bound proteins (Lazarowski, 2012). In addition, a variety of stimuli, including hypoxia, apoptosis, cell stress and proinflammatory molecules may trigger the active release of ATP through pannexin channels and connexin hemichannels (Dosch *et al.*, 2018).

Upon cell damage, injured cells release passively large amounts of ATP to the extracellular compartment, leading to a rapid increase of extracellular ATP (eATP). High levels of eATP are recognized as a danger signal by the immune system, triggering an inflammatory response (Idzko *et al.*, 2007; Boeynaems, Communi and Robaye, 2012a; Rodrigues, Tomé and Cunha, 2015; Amores-Iniesta *et al.*, 2017; Cauwels *et al.*, 2017). eATP is exposed to several ectonucleotidases that mediate its degradation to adenosine diphosphate (ADP) and adenosine monophosphate (AMP). These enzymes include ectonucleoside triphosphate diphosphohydrolases (ENTPDases), such as CD39; alkaline phosphatases; and ectonucleotide pyrophosphatases/phosphodiesterases (ENPPs) (Zimmermann, 2000). Additionally, the ectoenzyme CD38 mediates the catabolism of nicotinamide adenine dinucleotide (NAD$^+$) to ADP-ribose, which is converted to AMP by ENPP1 (Horenstein *et al.*, 2013; Quarona *et al.*, 2013). Extracellular AMP can be further degraded by the ectoenzyme CD73 (ecto-5′-nucleotidase), which mediates the hydrolysis of AMP into adenosine (Ado) (Antonioli *et al.*, 2013), a molecule with immunosuppressive properties (Haskó *et al.*, 2008; Haskó and Cronstein,

2013). Adenosinergic signalling is tightly regulated by adenosine deaminase (ADA), an enzyme that is found both in the cytosol and extracellularly; either as a membrane-bound complex together with CD26 or soluble in the plasma and serum. ADA is responsible for the irreversible degradation of Ado into inosine. Ado can also be transported to the cytosol by nucleoside transporters, and further converted to AMP by intracellular adenosine kinases (Cekic and Linden, 2016).

During acute inflammation, high levels of ATP accumulate at the site of inflammation, promoting infiltration of inflammatory cells (Kronlage *et al.*, 2010) and release of proinflammatory molecules (Ferrari, La Sala, *et al.*, 2000; Monção-Ribeiro *et al.*, 2014). Tissue injury, inflammation and possibly an insufficient degradation rate contribute to the maintenance of high concentrations of eATP at the inflammatory site. On the contrary, during resolution of inflammation, the ratio between eATP and eAdo shifts in favour to Ado. Ultimately, high levels of Ado and low concentration of ATP contribute to the resolution of inflammation (Eltzschig, Sitkovsky and Robson, 2012; Cekic and Linden, 2016; Faas, Sáez and de Vos, 2017). Therefore, the extracellular purinergic microenvironment determines the balance between a proinflammatory and anti-inflammatory status (Faas, Sáez and de Vos, 2017).
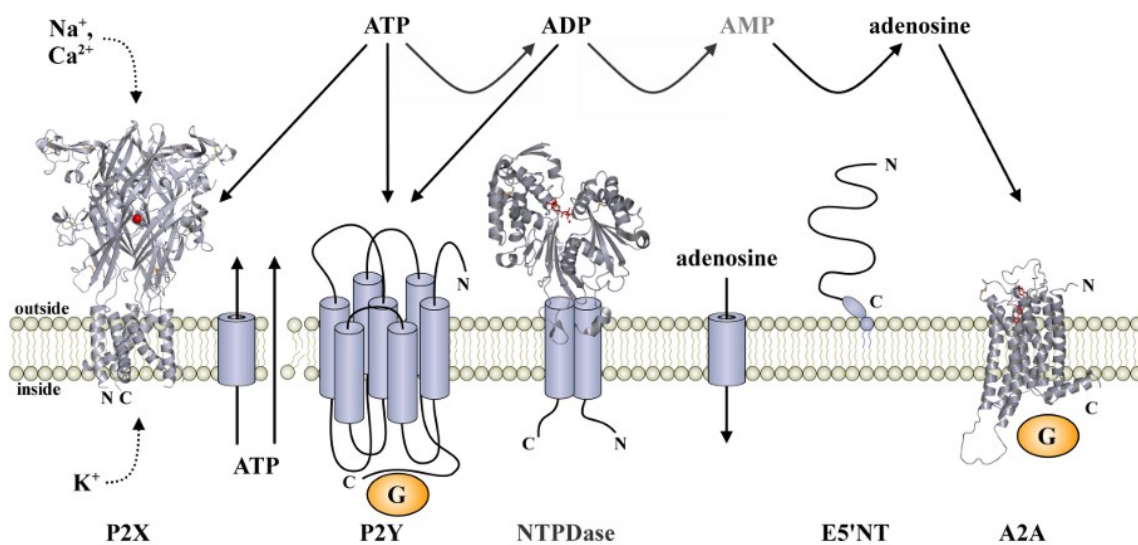
© Norbert Sträter

Figure 2. ATP and its downstream metabolites induce different responses through signalling via different purinergic receptors. Damaged or injured cells release large amounts of ATP to the extracellular compartment. Purinergic receptors are subdivided in three different subtypes: P1, P2X and P2Y receptors. ATP is the only purine nucleotide inducing the activation of P2X receptors, whereas both ATP and ADP, among other purine nucleotides, trigger the activation of P2Y receptors. Released ATP is recognized as a danger signal by the immune system, promoting inflammatory responses through signalling via P2 receptors. Different ectonucleotidases are responsible for the complete degradation of ATP to ADP and AMP, and ultimately to adenosine, which binds to P1 receptors and induces various immune-regulatory effects.

Purinergic signalling is mediated by purinergic receptors (**Figure 2**). To date, three different families of purinergic receptors have been identified: the P1 or adenosine receptors; and the P2X and P2Y receptors, which bind to ATP and/or other nucleotides (Cekic and Linden, 2016).

1.2.1 <u>P1 receptors</u>

P1 receptors (P1Rs) are membrane-bound proteins composed of seven transmembrane domains coupled to G-proteins on the intracellular side. Coupling to a specific G-protein subtype determines the signalling cascade and the outcome of the response (Sheth *et al.*, 2014). There are four known subtypes of P1 receptors (A1, A2A, A2B and A3); all of them binding to Ado. A1R and A2AR are high affinity receptors, whereas activation of the A2BR and A3R receptors requires higher concentrations of Ado (Fredholm *et al.*, 2001).

Ado signalling in immune cells is mainly mediated by A2A and A2B receptors, and both receptors have been reported to be upregulated following inflammation. The majority of immune cells express A2AR on their surface, whereas the expression of A2BR is mainly restricted to DCs and macrophages (Cekic and Linden, 2016). Engagement of Ado triggers distinct immunosuppressive effects, including the secretion of anti-inflammatory IL-10 by macrophages and the inhibition of secretion of TNF-α and IL-12 by DCs and macrophages. Ado signalling also leads to weaker neutrophil responses and impaired T cell proliferation and cytokine production (Haskó *et al.*, 2008; Haskó and Cronstein, 2013).

1.2.2 <u>P2 receptors</u>

P2 receptors (P2Rs) are excitatory receptors present on a variety of immune cells, and in general, promote inflammatory responses. To date, eighteen functional nucleotide-binding P2 receptors have been described in humans; classified into two different families: the ionotropic P2X receptors (P2XRs) and the metabotropic P2Y receptors (P2YRs).

1.2.2.1 P2Y receptors

P2Y receptors are homo-or-heterotrimeric receptors that belong to the superfamily of G-protein coupled receptors. They are grouped into two subfamilies based on sequence homology and signal transduction: the first subfamily (P2Y1, P2Y2, P2Y4, P2Y6 and P2Y11) is coupled to Gq-proteins; while the second subfamily (P2Y12, P2Y13, and P2Y14) is coupled to G_i-proteins (von Kügelgen and Hoffmann, 2016). The most common ligand of the P2YR family is ATP, although some receptors are more promiscuous and also bind to other nucleotides, such as ADP, uridine triphosphate (UTP) and uridine diphosphate (UDP) (Jacobson *et al.*, 2009). Indeed, ATP concentration determines binding to

certain subtypes of P2YRs and the outcome of the response. In addition, the same nucleotide can function as an agonist or as an antagonist for different receptors (Idzko, Ferrari and Eltzschig, 2014).

P2YRs are expressed virtually in all human tissues, and they are involved in physiological events, such as lipid metabolism, platelet aggregation, bone remodelling and distinct responses in the nervous system (Boeynaems, Communi and Robaye, 2012b). P2YRs are present in different immune cell types, including neutrophils, macrophages, endothelial cells, microglia and DCs. Activation of P2YRs is involved in chemotaxis and immune cell differentiation and maturation, and therefore, is associated to several inflammatory conditions, such as psoriasis and Crohn´s disease (Jacob *et al.*, 2013; Le Duc *et al.*, 2017).

1.2.2.2 P2X receptors

P2X receptors are ATP-gated membrane-bound ion channels that do not resemble any other ion channels or proteins at the molecular level. Seven distinct members (P2X1-P2X7) encompass the P2XR family. Functional receptors require the arrangement of three subunits, which range from 270 aa (P2X4) to 595 aa (P2X7) (Nicke *et al.*, 1998). Interestingly, while P2X7 only forms homodimers, some other P2X receptors can form heterotrimeric ion channels (P2X1/2; P2X1/4; P2X1/5; P2X2/3; P2X2/6 and P2X4/6) (Cekic and Linden, 2016). Each subunit is characterized by an intracellular amino-terminus tail, a long intracellular carboxyl-terminus tail, two hydrophobic transmembrane domains (TM1 and TM2) and a big extracellular loop that contains the binding site for ATP (Alves *et al.*, 2014). Activation of P2XR requires the binding of one ATP molecule to the binding pocket of each pair of monomers. Ligand binding induces a conformational change and the opening of the ion channel, allowing flux of cations (K^+, Na^+ and Ca^{2+}) and depolarization of the plasma membrane (Egan and Khakh, 2004; Samways, Li and Egan, 2014).

P2X receptors are widely expressed throughout the human systems and tissues, underlining the important role of these ionotropic receptors in a variety of tissues and physiological processes, including neurotransmission, smooth muscle contraction and immune cell activation (North, 2002; Kaczmarek-Hájek *et al.*, 2012).

1.3 THE P2X7 RECEPTOR

The P2X7 receptor (P2X7), previously referred as P2Z (Gordon, 1986), is the most relevant and most investigated P2X subtype in the field of immunology due to its role in promoting inflammatory responses (Di Virgilio *et al.*, 2017; Giuliani *et al.*, 2017). Each subunit of the homotrimer has a molecular weight of 72 kDa and a length of 595 aa (Bartlett, Stokes and Sluyter, 2014). A unique

characteristic of the P2X7 subunit is its very long carboxyl-terminal domain, which is indispensable for pore formation (Adriouch *et al.*, 2002; Smart *et al.*, 2003; Becker *et al.*, 2008; Alves *et al.*, 2014).

ATP is the only physiological nucleotide that serves as a ligand for P2X7 in humans, although some other non-nucleotide substances, such as bactericidal peptides released during inflammation, can also activate P2X7 (Di Virgilio *et al.*, 2018). Unlike other members of the P2XR family, P2X7 has a low affinity to ATP, and therefore, high concentrations of ATP (EC ≥ 100 µM) are required in order to induce its activation (Surprenant *et al.*, 1996; Donnelly-Roberts *et al.*, 2009). The lower affinity of P2X7 to ATP is probably a consequence of the size, accessibility and the amino acid composition of the ATP-binding pocket (Di Virgilio *et al.*, 2017). Furthermore, the high activation threshold of P2X7 is thought to serve as a control mechanism to prevent its activation under physiological conditions (Jiang, 2009).

In addition to ATP, extracellular NAD$^+$ (eNAD) triggers the activation of P2X7 in mice. Activation by eNAD is mediated by the mono-ADP-ribosyltransferase ARTC2.2, which catalyses the transfer of an ADP-ribose moiety from a NAD molecule to an arginine residue at position 125 (Arg125), located in the immediate vicinity of the ATP-binding pocket (Adriouch *et al.*, 2008). In humans, *ART2* is a pseudogene (Haag *et al.*, 1994); therefore unresponsiveness of P2X7 to NAD$^+$ in humans is most likely to be caused by the lack of ART2 and ADP-ribosyltransferase activity (Rissiek *et al.*, 2017).

1.3.1 Genetic variations of the human *P2RX7* gene

The *P2RX7* gene is located at the chromosomal position 12q24.31 and consists of 13 exons spanning 53 kb (G. N. Buell *et al.*, 1998). *P2RX7* is highly polymorphic, with thousands of single-nucleotide polymorphisms (SNPs) and several naturally occurring splice variants reported to date (Bartlett, Stokes and Sluyter, 2014; Di Virgilio et al., 2017). Genetic variations can lead to a loss or gain of function in P2X7. For instance, the SNPs H155Y, H270R and A348T result in different sensitivity to ATP, being the allelic variants 155Y, 270R and 348T, the ones conferring higher sensitivity (Cabrini et al., 2005; Stokes et al., 2010). Several SNPs on the P2RX7 gene have been linked to susceptibility to infections, such as tuberculosis (Fernando et al., 2007); and to different diseases, such as cardiovascular diseases (Gidlöf et al., 2012), rheumatoid arthritis (Portales-Cervantes et al., 2012) and osteoporosis (Bartlett, Stokes and Sluyter, 2014; Kasuya et al., 2017).

In humans, nine alternative splice variants (P2XB-P2XJ) of *P2RX7* occur naturally; all of them differing in their functional properties from the original and full-length P2X7A variant (Sluyter, 2017). For instance, P2XB is a truncated isoform with a shorter C-terminus, and therefore lacks the ability to form the large pore (Sluyter and Stokes, 2011; Bartlett, Stokes and Sluyter, 2014; Di Virgilio *et al.*,

2017). P2X7C, P2X7E and P2X7G are also C-terminally truncated isoforms. Alternative splicing also generates variants that lack or contain additional exons, or that results in a null allele.

1.3.2   Expression of P2X7 in the immune system

P2X7 is expressed in the surface of most cells of the hematopoietic lineage (Idzko, Ferrari and Eltzschig, 2014), but also in many other tissues and cell types (Burnstock and Knight, 2004; Bartlett, Stokes and Sluyter, 2014), including epithelial cells (Welter-Stahl et al., 2009) and cells in the nervous system (Sperlagh et al., 2006). Within the immune system, P2X7 expression is particularly high in both human and murine monocytes, macrophages (Gu et al., 2000; Burnstock and Knight, 2004), microglia (Inoue, 2008; He et al., 2017) and DCs (Surprenant et al., 1996; Mutini et al., 1999). P2X7 is also expressed on neutrophils, eosinophils, mast cells, T cells, B cells, NK cells and NKT cells (Wang et al., 2004; Beldi et al., 2008; Idzko, Ferrari and Eltzschig, 2014). In mice, Tregs and iNKTs are the lymphocytes expressing the highest levels of P2X7 (Heiss et al., 2008; Hubert et al., 2010; Rissiek et al., 2014). Up to now, very little is known about the expression pattern and function of P2X7 in human T cells.

In addition, P2X7 is also found in the lipid rafts from certain murine cell types, such as lymphoma or lung epithelial cells. Leucocytes and platelets also express large amounts of P2X7 intracellularly, and P2X7 has also been identified in the phagosomes of macrophages in mice (Gu et al., 2000; Kuehnel et al., 2009; Sluyter, 2017).

1.3.3   P2X7-mediated downstream effects in immune cells

Engagement of ATP induces a reversible conformational rearrangement that allows the influx of Ca^{2+} and Na^+ and efflux of K^+ (Surprenant *et al.*, 1996; Bartlett, Stokes and Sluyter, 2014). Activation of P2X7 leads to distinct downstream responses depending on the cell type (**Figure 3**).

1.3.3.1   Assembly of the inflammasome and release of proinflammatory cytokines

P2X7 activation triggers the processing and release of the proinflammatory cytokines IL-1β and IL-18 by monocytes, macrophages, DCs and microglial cells via inflammasome activation (Perregaux *et al.*, 2000; Ferrari *et al.*, 2006; Pelegrin and Surprenant, 2006; Englezou *et al.*, 2015; He *et al.*, 2017). Inflammasomes are a group of multiprotein intracellular complexes implicated in cell damage and immune responses against pathogens. Among all inflammasomes, the NLRP3 inflammasome, also known as NALP3, has been associated with the pathogenesis of multiple inflammatory diseases (Guo, Callaway and Ting, 2015). The production of IL-1β and IL-18 requires two different signals. First, sensing of microbial molecules, such as lipopolysaccharide (LPS) by the toll-like receptor 4 (TLR4),

triggers synthesis of inactive pro-IL1β and pro-IL18 and its accumulation in the cytoplasm of the cells. Thus, a second stimulus is required for the processing and release of mature IL-1β and IL-18 (Dowling and O'Neill, 2012). The activation of P2X7 is one of the mechanisms capable of inducing the relocalisation and assembly of the NLRP3 inflammasome. Although the exact mechanism behind this is yet to be discovered, the efflux of K^+ ions seems to be responsible for its recruitment (Pétrilli et al., 2007). The NLRP3 inflammasome complex consists of the NOD-like receptor NALP3 protein, the apoptosis-associated speck-like protein containing a card (ASC) adaptor protein and the inactive enzyme procaspase-1. Dimerization of NLRP3 receptors enables recruitment of the ASC protein through the pyrin domain (PYD). ASC, which also contains a caspase activation and recruitment domain (CARD), binds to the CARD domain of procaspase-1; triggering a conformational change and the subsequent proteolytic cleavage of procaspase-1 and its conversion to active caspase-1. Free caspase-1 mediates the cleavage of immature pro-IL1β and pro-IL18 into biologically active IL-1β and IL-18 (He, Hara and Núñez, 2016) (**Figure 3A**). The exact mechanisms how IL-1β is released to the extracellular compartment is still debated (Giuliani *et al.*, 2017).

1.3.3.2 Shedding of surface proteins

P2X7 activation also leads to the activation of metalloproteases of the ADAM (A disintegrin and metalloprotease) family, which are responsible for the rapid shedding of the ectodomain of several proteins from the cell membrane (**Figure 3B**). P2X7-mediated shedding has been demonstrated for proteins such as CD62L in many immune cell types (Gu, Bendall and Wiley, 1998; Scheuplein *et al.*, 2009), CD27 in murine T cells (Moon *et al.*, 2006), IL6R in monocytes (Garbers *et al.*, 2011), TNF-α in microglia (Suzuki *et al.*, 2004) and CD23 in B cells (Pupovac *et al.*, 2015).

1.3.3.3 Pore formation and induction of cell death

ATP-P2X7 interaction induces the rapid and reversible externalization of phosphatidylserine (PS) on the outer leaflet of the plasma membrane of T cells (Elliott *et al.*, 2005; Scheuplein *et al.*, 2009); which is associated with influx of Na^+ and Ca^{2+} (B. Rissiek *et al.*, 2015). PS exposure has also been reported in other cell types, such as erythrocytes and monocytes (Sluyter, Shemon and Wiley, 2007; Ward *et al.*, 2010). Persistent stimulation by ATP induces the opening of a secondary non-selective pore permeable to organic cationic molecules up to 900 Da (Steinberg *et al.*, 1987) (**Figure 3B**). The mechanism behind pore formation is still unclear: it may be directly mediated by P2X7 itself or by P2X7 in association with other proteins such pannexin 1 (Gulbransen et al., 2012). Prolonged P2X7 activation leads to membrane blebbing and ultimately to cell death of especially sensitive cell types, such as murine Tregs (Scheuplein et al., 2009).
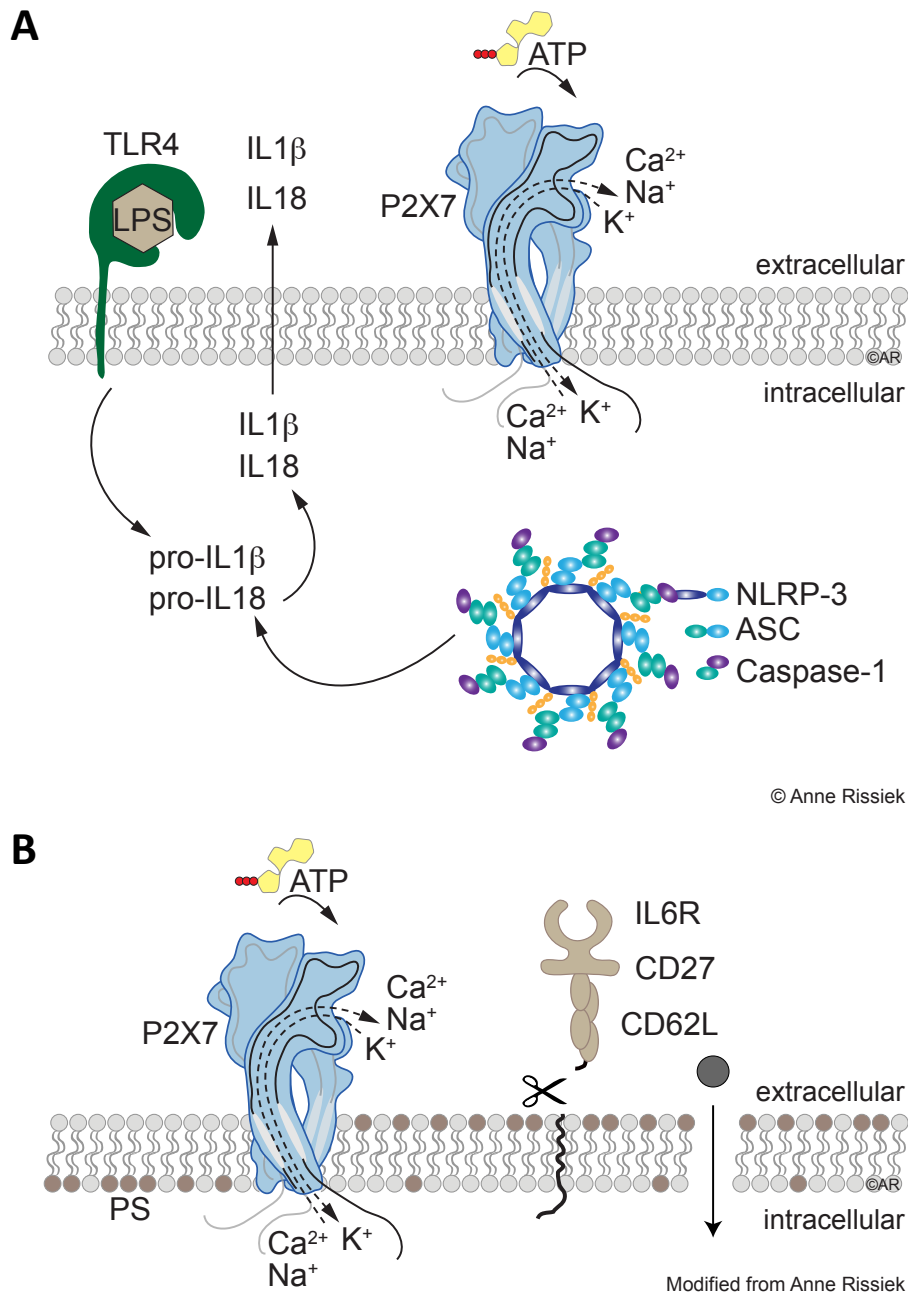
Figure 3. Extracellular ATP induces different P2X7-mediated downstream responses. Binding to extracellular ATP induces the opening of the P2X7 ion channel, allowing the passage of Ca^{2+} and Na^+ to the intracellular compartment and K^+ to the extracellular compartment. (**A**) Sensing of LPS through TLR4 leads to the synthesis of the precursor forms of IL-1β and IL-18 (pro-IL1β and pro-IL18, respectively) by monocytes and macrophages. Engagement of ATP to P2X7 on these immune cell subsets triggers activation of the NLRP3 inflammasome, which mediates the conversion of pro caspase-1 to active caspase-1. Activated caspase-1 catalyses the proteolytic cleavage of the precursor forms to active IL-1β and IL-18, which can then be secreted to the extracellular milieu. (**B**) P2X7 activation in T cells, and also in other immune cell types, induces the exposure of PS on the outer leaflet of the plasma membrane and activation of metalloproteases that catalyse the shedding of surface proteins such as CD62L and CD27. Prolonged activation of P2X7 leads to the opening of a non-selective secondary pore, allowing the passage of large molecules, membrane blebbing and, ultimately to cell death of especially sensitive cell types.

1.3.4 Role of P2X7 signalling in T cell biology

P2X7 signalling is involved in the development, differentiation and activation of T cells. Thymocytes undergoing negative selection in the thymus release substantial amounts of ATP, which upon binding to P2X7, contribute to enhanced programmed cell death (Lépine *et al.*, 2006). The strength of γδ-TCR signalling in double negative (DN) cells, which express both the pre-TCRα and γδ-TCR, is a decisive factor in αβ versus γδ-lineage fate decision during T cell maturation in mice. Strong signalling through the γδ-TCR complex supports the commitment to the γδ-lineage, whereas a weaker signalling favours development of thymocytes towards the αβ-lineage (Haks *et al.*, 2005; Hayes, Li and Love, 2005). Also, the ATP-P2X7 axis provides an additional signal favouring γδ-lineage commitment. The absence or blockade of P2X7 results in increased transition of murine γδ T cells to the double positive (DP) stage. Immature γδ T cells exhibit higher expression of P2X7 and release higher quantities of ATP to the extracellular milieu than DN3 stage thymocytes. Therefore, both P2X7 and secreted ATP contribute to a stronger signal favouring commitment to γδ lineage (Frascoli et al., 2012).

Activation of P2X7 induces cell death of murine Tregs (Rissiek *et al.*, 2014) and dampens their immunosuppressive potential (Schenk *et al.*, 2011). High concentrations of eATP are needed to induce cell death, whereas just the brief exposure to low concentrations of NAD^+ is required (Seman et al., 2003). Of note, wild type (WT) mice have more Tregs than P2X7-deficient mice (B. Rissiek *et al.*, 2015). T cells show different sensitivity to ATP according to their activation and differentiation status. Murine naïve T cells are more sensitive to NAD^+-induced cell death (NICD) than activated effector T cells (Rissiek *et al.*, 2014). Controversially, a different study shows that intestinal effector and memory $CD4^+$ T cells display higher levels of P2X7 than naïve cells, and therefore, are more susceptible to NICD (Hashimoto-Hill *et al.*, 2017). A similar scenario also seems to occur in humans: while intermediate concentrations of ATP increase proliferation of activated T cells, high concentrations of ATP induce apoptosis of these cells but promote proliferation of Tregs. These opposed effects might be explained by signalling through other P2 receptors (Trabanelli *et al.*, 2012).

The role of ATP in the proliferation of human T cells was first described by Baricordi et al, 1996. While high concentrations of ATP induce cell death of immune cells (Yoon *et al.*, 2007), low concentrations of ATP induce proliferation of conventional T cells (Adinolfi *et al.*, 2005). Upon TCR engagement, T cells release ATP to the extracellular compartment, which can stimulate P2X1, P2X4 and P2X7 in an autocrine manner, contributing to T cell proliferation (Schenk *et al.*, 2008; Woehrle *et al.*, 2010). In this scenario, activation of P2X7 induces the mobilization of calcium ions and increases cellular energy stores and production of IL-2; promoting the activation and proliferation of T cells (Adinolfi *et al.*, 2005; Yip *et al.*, 2009). Moreover, upregulation of P2X7 upon T-cell stimulation in Jurkat cells (Yip et al 2009) and overexpression of P2X7 receptors in the human cell line HEK293 (Adinolfi *et al.*, 2005)

results in increased T cell proliferation. ATP released from activated T cells also acts on neighbouring cells, inducing calcium waves that regulate motility of murine and human T cells through P2X4 and P2X7 receptors (Wang *et al.*, 2014).

ATP and P2X7 signalling are also involved in the polarization of murine T cells. P2X7 promotes T cell differentiation towards a Th17 phenotype and inhibits their conversion to Tregs. P2X7 antagonism rescues the differentiation of naïve CD4^{+} T cells to Tregs (Schenk *et al.*, 2011). Similarly, eATP from commensal bacteria induces the secretion of IL-6, IL-23 and TGF-β by a subset of murine DCs cells in the intestine, promoting the differentiation of Th17 cells. Th17 cell differentiation was inhibited in the presence of unspecific P2 receptor antagonists (Atarashi *et al.*, 2008), most likely via inhibition of P2X7; although this was not tested in this study. In the tumour environment, P2X7-dependent release of IL-1β is required for the optimal differentiation of IFNγ-producing CD8^{+} T cells (Aymeric *et al.*, 2010). P2X7 also contributes to the differentiation of Th1 cells in a mouse model for malaria. In this work, the expansion of Th1 cells correlated to increased cell death of Tfh cells (Salles *et al.*, 2017). A similar effect was seen in another study, in which P2X7 activation limited the number of Tfh cells in the small intestine of mice (Proietti *et al.*, 2014).

1.3.5   P2X7 in host-defence and disease

Purinergic signalling is involved in the chemotaxis of inflammatory cells, antimicrobial activity and release of proinflammatory cytokines (Di Virgilio *et al.*, 2017). P2X7 is essential for the host defence against bacterial, viral, fungal and parasite infections. However, different studies using P2X7-deficient mice and pharmacological inhibitors of P2X7 show that P2X7 activation can in fact improve or worsen the course of infection depending on the pathogen, severity and circumstances of infection (Savio *et al.*, 2018). **Table 1** summarizes the consequences of P2X7 activation in several pathogen infections.

Table 1. Effects of P2X7 modulation in infectious diseases.

Disease	Species	Role of P2X7	Method and immune consequences	Reference
Sepsis	Mice	Negative	P2X7 KO mice (CLP model): - ↑ survival - ↓ immune response: ↓ production of IL-1β, IL-6, IL-12, IL-17, and IL-4 and ↓ lung infiltration.	(Santana *et al.*, 2015)
Septic encephalopathy	Mice	Negative	P2X7 KO mice (CLP model) and P2X7 antagonist A438079: - ↑ survival - ↓ immune response (↓ production of IL-1β) - ↓ leucocyte adhesion (↓CXCL1 and CX3CL1)	(H. Wang *et al.*, 2015)

Sepsis	Mice	Positive	P2X7 KO mice (CLP model) and P2X7 antagonist oATP: - ↓ survival - ↑ immune response (↑ production of IL-1β, IL-6, TNF-α) - ↑bacterial burden P2X7 agonists MgATP and bzATP: A438079 (CLP model): - ↑ bacterial clearance by macrophages	(Csóka *et al.*, 2015)
Sepsis	Human	Negative	Gain-of-function mutations: - Association with severe sepsis and sepsis shock	(Geistlinger *et al.*, 2012)
Mycobacterium tuberculosis (H37Rv)	Mice	Positive	P2X7 KO mice: - ↑Tregs - ↑bacterial burden in lung tissue	(Santos *et al.*, 2013)
Mycobacterium tuberculosis (Bejiing 1471)	Mice	Negative	P2X7 KO mice: - Delayed mortality - ↓ leucocyte infiltration - ↓ necrotic death of macrophages - ↓ bacterial burden and bacillus dissemination	(Amaral *et al.*, 2014)
Mycobacterium Tuberculosis	Human	Positive	Loss-of-function SNP at position 1513: - Increased susceptibility to extra-pulmonary tuberculosis - ↓ bacterial clearance by macrophages	(Fernando *et al.*, 2007)
Chlamydia trachomatis	Human and mice	Positive	ATP treated macrophages infected with Chlamydia: - PLD activation - Phagolysosome formation - Acidification of the phagolysosome and ↑clearance of bacteria	(Coutinho-Silva *et al.*, 2003)
Dengue virus	Human	Positive	Virus-infected monocytes: - ↑ production of NO - ↓ viral load - ↓ production of TNF, CXCL8, CCL2 and CXCL10.	(Corrêa *et al.*, 2016)
HIV-1 virus	Human	Negative	- Release of HIV-1 virus from VCC of virus-infected primary MDMs.	(Graziano *et al.*, 2015)
HIV-1 virus	Human	Negative	P2X7 antagonists oATP and BBG: - ↓ HIV replication in primary human macrophages	(Hazleton, Berman and Eugenin, 2012)
Influenza virus	Mice	Negative	P2X7 KO mice: - ↑ survival - ↓ neutrophil infiltration - ↓ production of IFNγ, TNFα, IL-6 CXCL8, CCL2 and CXCL10.	(Leyva-Grado *et al.*, 2017)

CLP (cecal ligation puncture); PLD (phospholipase D); oATP (oxidized ATP); VCC (virus-containing compartments).

Adapted from Savio *et al.*, 2018

P2X7 is associated with the pathogenesis of many diseases from different systems in the body; typically due to enhanced inflammatory responses caused by release of IL-1β and other proinflammatory cytokines (Savio *et al.*, 2018). **Table 2** describes the contribution of P2X7 to multiple diseases with inflammatory component.

Table 2. Protective effects of P2X7 genetic ablation or pharmacological inhibition in inflammatory diseases.

Disease	Mechanism	Consequences	Reference
Chronic inflammatory & neuropathic pain	P2rx7 KO	- ↓ release of IL-1β - Absence of inflammatory and neuropathic hypersensitivity	(Chessell *et al.*, 2005)
Acute lung injury	PI: A438079	- ↓ NLRP3 inflammasome activation - ↓ release of IL-1β, IL-17A and IFN-γ	(Wang *et al.*, 2015)
Lung inflammation and fibrosis	P2rx7 KO	- ↓ lung inflammation - ↓ fibrosis markers	(Riteau *et al.*, 2010)
Allergic airway inflammation	P2rx7 KO	- ↓ asthmatic airway inflammation - ↓ airway eosinophilia - ↓ goblet cell hyperplasia - ↓ bronchial hyperresponsiveness to methacholine	(Müller *et al.*, 2011)
	PI: KN62		
Experimental glomerulonephritis	P2rx7 KO	- Better renal function - ↓ proteinuria - ↓ glomerular injury	(Taylor *et al.*, 2009)
	PI: A-438079	- Prevention of antibody-mediated glomerulonephritis	
	PI: 13A7	- ↓ albuminuria - ↓ inflammation markers - ↓ kidney damage	(Danquah *et al.*, 2016)
Experimental autoimmune encephalomyelitis	P2rx7 KO	- ↓ incidence of the disease - ↓ astroglial activation and axonal damage	(Sharp *et al.*, 2008)
Type 1 Diabetes	P2rx7 KO	- Prevention of the disease - ↓ immune cell infiltration - No alteration of pancreatic islet number and area	(Vieira *et al.*, 2016)
	PI: BBG		
Allergic contact dermatitis	PI: 13A7	- ↓ gain in ear weight - ↓ levels of IL-6 and IL-1β	(Danquah *et al.*, 2016)
Anti-collagen-induced arthritis	P2rx7 KO	- ↓ susceptibility to disease - ↓ swelling and redness of affected joints - ↓ destruction of cartilage	(Labasi *et al.*, 2002)
Experimental colitis	PI: BBG	- ↓ severity of colitis - ↓ myeloperoxidase activity - ↓ collagen deposition - ↓ levels of IL-1β	(Marques *et al.*, 2014)

		- Attenuated murine colitis. - ↓ NF-κB activation - ↓ expression of active caspase-1 in lamina propria immune cells - ↓levels of IL-1β and TNF in colon tissues	
	PI: A438079	- Attenuated murine colitis. - ↓ NF-κB activation - ↓ expression of active caspase-1 in lamina propria immune cells - ↓levels of IL-1β and TNF in colon tissues	(Wan *et al.*, 2016)
	P2rx7 KO	- ↓ weight loss - ↓ tissue damage - ↑migration and accumulation of Tregs in the colon	(Figliuolo *et al.*, 2017)
Liver fibrosis	PI: A438079	- ↓ cell injury - ↓ inflammatory infiltration and cell injury - ↓ collagen accumulation in the liver - ↓ levels of TNF-α, IL-1β and CCL2 in the serum - ↓ NFκB activation	(Huang *et al.*, 2014)
	PI: BBG oATP	- ↓liver fibrosis - ↓ IL-6, TNF-α, IL-1β and other inflammatory mediators in the liver - ↑portal-systemic collateral vascular responsiveness	(Tung *et al.*, 2015)

P2rx7-defficient mice (P2rx7 KO); PI (pharmacological inhibition); BBG (brilliant blue-G); CCL2 (chemokine (C-C motif) ligand 2); oATP (oxidized ATP).

Also, P2X7 is highly expressed by many tumours and promotes tumour cell growth (Adinolfi *et al.*, 2012). Tumorigenesis occurs under physiological concentrations of ATP (Di Virgilio, 2012). Controversially, high concentrations of ATP lead to tumour cell death in many types of cancer (Savio *et al.*, 2018) and potentiates the efficacy of cytotoxic drugs (Pacheco *et al.*, 2016).

1.3.6   Therapies and tools

P2X7 antagonists have shown promising results in preclinical trials for the treatment of inflammatory diseases, such as glomerulonephritis, multiple sclerosis, inflammatory pain and rheumatoid arthritis (Arulkumaran et al., 2011; Bartlett et al., 2014; Bhattacharya and Biber, 2016; Carroll et al., 2009; Guile et al., 2009). However, some compounds, AZD9056 (NCT00520572) and CE-224,535 (NCT00628095) provided no extra benefit on clinical trials (Keystone *et al.*, 2012; Stock *et al.*, 2012); while other showed limitations in terms of selectivity, dosage and adverse effects (Friedle, Curet and Watters, 2010; Bartlett, Stokes and Sluyter, 2014).

An alternative therapeutic approach is the use of nanobodies (Nbs). Nbs are the smallest antigen variable binding domain (V_HH) of heavy chain only antibodies (hcAbs) present in camelids (Arbabi-Ghahroudi, 2017). Nbs exhibit numerous advantages over conventional Abs. Their smaller size, biochemical characteristics and the length and flexibility of their CDR3 region, enables them to reach and bind epitopes otherwise inaccessible to conventional Abs (Muyldermans, 2013). Furthermore,

Nbs are weakly immunogenic, and present high stability, solubility and tissue penetration (Wesolowski *et al.*, 2009; Unciti-Broceta *et al.*, 2013). They are also easy to reformat by genetic manipulation. The genetic linkage of multiple Nbs with same specificity (multivalent Nb) increases the avidity of the construct. Linkage to other Nbs with different specificity and/or linkage to certain protein domains provide additional functions or can direct the Nbs towards a specific target tissue (Wesolowski *et al.*, 2009; Farrington *et al.*, 2014). For instance, fusion to an albumin-specific nanobody or Fc-domain results in an increased half-life of the Nb (Tijink et al., 2008).

2. <u>AIMS OF THE STUDY</u>

The laboratory of Professor Koch-Nolte has generated P2X7-specific nanobodies for the positive and negative modulation of P2X7 function in mice. They have recently shown that *in vivo* administration of P2X7-specific nanobodies ameliorates allergic contact dermatitis and experimental glomerulonephritis in mice (Danquah et al., 2016), underlining the potential of P2X7-specific nanobodies as a therapeutic drug for the treatment of inflammatory disorders. Professor Koch-Nolte´s laboratory has also generated a highly specific nanobody targeting P2X7 in humans; designated Dano1 (Danquah *et al.*, 2016).

In line with these findings, the main goal of this doctoral thesis is **to assess the potential of the anti-human P2X7 nanobody Dano1 as a tool to modulate the function of the P2X7 receptor in human immune cells**. The specific aims are:

1. To assess the expression of the P2X7 receptor on distinct human immune cell subpopulations.

2. To determine whether the expression of P2X7 is modulated upon activation of human T cells.

3. To investigate the relevance of P2X7 activation or blockade in human T cells.

3. <u>MATERIAL AND METHODS</u>

3.1 MATERIALS

3.1.1 <u>Blood and tissue samples</u>

Sample	Source	Ethics protocol
Peripheral blood from healthy adults	Volunteers	PV5139
Peripheral blood from children	Center for Obstetrics and Pediatrics	PV5482
Buffy coats from healthy adults	Blood Bank	-
Gut tissue from obese patients	Center for Internal Medicine	PV4889

3.1.2 <u>General equipment</u>

Equipment	Company, Location
Analytical balance LA 124i	VWR International, Radnor (PA), USA
Centrifuge 5424R	Eppendorf, Hamburg, Germany
Centrifuge 5810R	Eppendorf, Hamburg, Germany
Centrifuge Allegra X-30R	Beckman Coulter, Brea (CA), USA
Centrifuge Biofuge fresco	Heraeus, Hanau, Germany
Freezer -20°C	Liebherr, Bulle, Switzerland
Freezer -80°C	Thermo Fisher Scientific, Waltham (MA), USA
Inverted Microscope	Olympus, Shinjuku, Tokyo, Japan
Micro centrifuge Galaxy MiniStar	VWR, Radnor (PA), USA
Multi-channel pipettes (100 µl/300 µl)	Eppendorf, Hamburg, Germany
Neubauer cell chamber	Merienfeld, Lauda-Königshofen , Germany
pH-Meter WTW pH523	Xylem, Rye Brook (NY), USA
PIPETBOY acu 2	Integra Biosciences, Biebertal, Germany
Pipettes 2.5/10/20/200/1000 µl	Eppendorf, Hamburg, Germany
Pipettes 20/200 µl	Gilson, Villiers le Bel, France
Precision balance Precisa 400M	Oehmen Labortechnik, Essen, Germany
Refrigerator/freezer	Liebherr, Bulle, Switzerland
Scout Pro Digital scale	Ohaus, Parsippany (NJ), USA
Thermomixer 5436	Eppendorf, Hamburg, Germany
Thermoshaker with heated lid	CLF, Emersacker, Germany

Vacuum pump Vacusafe	Integra Biosciences, Biebertal, Germany
Vortex mixer	Heidolph, Schwabach, Germany
Vortex mixer	Scientific industries, Bohemia (NY), USA
Water bath	GFL, Burgwedel, Germany

3.1.3 Materials for cell culture

Chemical reagents and their manufacturers

Adenosine triphosphate (ATP)	Sigma-Aldrich, St. Louis (MO), USA
Apyrase	Sigma-Aldrich, St. Louis (MO), USA
AZ10606120 (P2X7 antagonist)	Tocris, Ellisville (MO), USA
Benzoylbenzoyl ATP (bzATP)	Tocris, Ellisville (MO), USA
Biocoll	Merck, Darmstadt, Germany
Bovine serum albumin (BSA)	Thermo Fisher Scientific, Waltham (MA), USA
Brefeldin A solution, 1000X	eBioscience, San Diego (CA), USA
Dimethyl sulfoxide (DMSO)	AppliChem, Darmstadt, Germany
Ethanol (70 %) for disinfection	Th. Geyer, Renningen, Germany
Ethylenediaminetetraacetic acid (EDTA), 0.5 M	AppliChem, Darmstadt, Germany
Fetal bovine serum (FBS)	Biochrom, Berlin, Germany
Fetal calf serum (FCS)	Merck, Darmstadt, Germany
Human serum (Type AB)	Merck, Darmstadt, Germany
JNJ47965567 (P2X7 antagonist)	R&D Systems, Minneapolis (MN), USA
L-glutamine, 200 mM	Thermo Fisher Scientific, Waltham (MA), USA
Lipopolysaccharide (LPS)	Sigma-Aldrich, St. Louis (MO), USA
Nigericin	Sigma-Aldrich, St. Louis (MO), USA
Penicillin (10000 U/ml)/ Streptomycin (10000 µg/ml)	Thermo Fisher Scientific, Waltham (MA), USA
Phosphate-buffered saline (PBS) (1x, 10x)	Thermo Fisher Scientific, Waltham (MA), USA
Poly-L-lysine solution 0.01%	Sigma-Aldrich, St. Louis (MO), USA
RPMI 1640 with or w/o phenol red	Thermo Fisher Scientific, Waltham (MA), USA
Sodium dichloroisocyanurate (ChlorClean)	Carl Roth, Karlsruhe, Germany
Trypan blue, 0.4 %	Sigma-Aldrich, St. Louis (MO), USA
Tuerk solution	Sigma-Aldrich, St. Louis (MO), USA
X-VIVO 15 medium	Lonza, Basel, Switzerland

Cell culture media and their composition

Full RPMI Medium	10 % FCS (heat inactivated) 1 % penicillin/streptomycin 2 mM L-glutamine in RPMI
T cell medium	10 % human serum (heat inactivated) 1 % penicillin/streptomycin 2 mM L-glutamine in RPMI
Freezing medium I	90 % RPMI, 10 % FCS
Freezing medium II	40 % RPMI, 40 % FCS, 20 % DMSO

Buffers and solutions and their composition

10X MACS buffer	20 mM EDTA, 5 % BSA (w/v) in 10X PBS
Permeabilisation/blocking buffer	1% BSA + 0.2% Saponin in 1X PBS
Trypan blue solution	0.4 % trypan blue solution, 1:10 in PBS

Reagents for the stimulation of immune cells

HDMAPP ammonium salt	Echelon Biosciences, Salt Lake City (UT), USA
Human recombinant IL-2 (Tecine)	Roche, Basel, Switzerland
Ionomycin calcium salt	Sigma-Aldrich, St. Louis (MO), USA
Phorbol myristate acetate (PMA)	Sigma-Aldrich, St. Louis (MO), USA
Phytohemagglutinin PHA	Sigma-Aldrich, St. Louis (MO), USA
Purified anti-human CD28 antibody (CD28.2)	BioLegend, San Diego (CA), USA
Purified anti-human CD3 antibody (OKT3)	BioLegend, San Diego (CA), USA
Retinoic acid	Sigma-Aldrich, St. Louis (MO), USA

Kits for the separation of immune cells and their manufacturers

Monocytes isolation Kit II	Milteny Biotec, Bergisch Gladbach, Germany

3.1.4 Materials for molecular biology

Isolation kits

Nucleospin Blood Kit (DNA, RNA and protein purification)	Macherey-Nagel, Düren, Germany

NucleoSpin Gel and PCR Clean-up	Macherey-Nagel, Düren, Germany
QIAshredder	Qiagen, Hilden, Germany
RNeasy Plus Mini Kit	Qiagen, Hilden, Germany

Chemical reagents and their manufacturers

DNase I	Qiagen, Hilden, Germany
Ethanol ≥99,8%	Roth, Karlsruhe, Germany
Proteinase K	Macherey-Nagel, Düren, Germany
β-mercaptoethanol, 50 mM	Invitrogen, Carlsbad (CA), USA

Chemical reagents, materials and equipment for conventional PCR

6X DNA loading dye	Thermo Fisher Scientific, Waltham (MA), USA
Biovision 3026MX UV-Illuminator	Biovision Technologies, Exton (PE), USA
Deoxyribonucleotide triphosphates (dNTPS)	Merck, Burlington (MA), USA
DNA gel electrophoresis 40-0708	Peqlab Biotechnologie, Erlangen, Germany
GeneRuler 1 Kb DNA ladder	Thermo Fisher Scientific, Waltham (MA), USA
KOD Buffer (10X)	Merck, Burlington (MA), USA
KOD Polymerase	Merck, Burlington (MA), USA
Laminar Air Flow Class III	Gelaire, Seven Hills (NSW), Australia
LE Agarose	Biozym Scientific, Hessisch Oldendorf, Germany
Magnesium sulphate (MgSO4)	Merck, Burlington (MA), USA
Nulcease-free water	Thermo Fisher Scientific, Waltham (MA), USA
Quick load 100 bp DNA ladder	Biolabs, Ipswich (MA), USA
Roti-Safe Gel Stain	Roth, Karlsruhe, Germany
Scout Pro Digital scale	Ohaus, Parsippany (NJ), USA
T3 PCR Thermocycler	Biometra, Göttingen, Germany
TAE gel running buffer 50X	ApplicChem GmbH, Darmstadt, Germany
TI 1 Transilluminator (UV)	Biometra, Göttingen, Germany

List of primers

P2RX7 genotyping

P2RX7 (Exon 5) Forward Primer	5' TAGGATGGGCTTGATGGAAG 3'
P2RX7 (Exon 5) Reverse Primer	5' TAGGACCCAGGACTTTGCAG 3'
P2RX7 (Exon 8) Forward Primer	5' TGGCTATGCAGGGAGATGT 3'
P2RX7 (Exon 8) Reverse Primer	5' GCCTTGGAAACCAAAATTAGTC 3'
P2RX7 (Exon 11) Forward Primer	5' CCAGCTGGTTGTGTACATCG 3'
P2RX7 (Exon 11) Reverse Primer	5' TGATTTGGGCCTAATTTTCG 3'

ENTPD1 genotyping

ENTPD1 Forward Primer	5' GTAGAGGGAGGAAAT AG 3'
ENTPD1 Reverse Primer	5' TGGCTACTCATGCTAT 3'

Equipment for DNA and RNA quantification

Nanodrop 2000c	Thermo Fisher Scientific, Waltham (MA), USA

Materials for cDNA transcription

0.1 M Dithiothreitol (DTT)	Invitrogen, Carlsbad (CA), USA
DEPC-H2O	Invitrogen, Carlsbad (CA), USA
dNTPS (dATP, dCTP, dGTP, dTT; 100 mM)	Invitrogen, Carlsbad (CA), USA
First Strand Buffer 5X	Invitrogen, Carlsbad (CA), USA
M-MLV Reverse Transcriptase	Invitrogen, Carlsbad (CA), USA
Random primers	Invitrogen, Carlsbad (CA), USA

Materials for real-time PCR (Taqman assays)

GAPDH taqman probe; Hs02578991_g1	Thermo Fisher Scientific, Waltham (MA), USA
IL1B taqman probe; Hs00174097_m1	Thermo Fisher Scientific, Waltham (MA), USA
IL6 taqman probe; Hs00985639_m1	Thermo Fisher Scientific, Waltham (MA), USA
Maxima Probe/ROX qPCR Master Mix	Thermo Fisher Scientific, Waltham (MA), USA
TNF taqman probe; Hs01113624_g1	Thermo Fisher Scientific, Waltham (MA), USA

Materials for real-time PCR (SYBR Green assays)

Maxima SYBR Green/ROX qPCR Master Mix	Thermo Fisher Scientific, Waltham (MA), USA

Equipment for real time-PCR

StepOne Plus Real Time PCR system	Applied Biosystems, Foster City (CA), USA

List of primers

Reference Genes

RPL13A Forward Primer	5' ATCTTGTGAGTGGGGCATCT 3'
RPL13A Reverse Primer	5' GCTTGCTGTTGTACACAGGG 3'
18S Forward Primer	5' CGGCTACCACATCCAAGGAA 3'
18S Reverse Primer	5' GCTGGAATTACCGCGGCT 3'

Genes of interest

P2RX7 Forward Primer	5' TCTTCGTGATGACAAACTTTCTCAA 3'
P2RX7 Reverse Primer	5' GTCCTGCGGGTGGGATACT 3'

3.1.5 Materials for isolation of immune cells from human gut tissue

Chemical reagents and their manufacturers

Collagenase IV from Clostridium histolyticum	Sigma-Aldrich, St. Louis (MO), USA
Dithiothreitol (DTT)	AppliChem, Darmstadt, Germany
DNase I	AppliChem, Darmstadt, Germany
Hanks´ balanced salt solution 10X (HBSS)	Thermo Fisher Scientific, Waltham (MA), USA
HEPES	Roth, Karlsruhe, Germany
Percoll	GE Healthcare, Little Chalfont, UK

Buffers and solutions and their composition

DTT solution (for 500ml)	50 ml 10X HBSS 50 ml HEPES-bicarbonate buffer 50 ml FBS 350 ml dH2O 15.4 mg DTT/100 ml (Fc: 1 mM)

HEPES-bicarbonate buffer 10X	23.8 g HEPES (Fc: 100 mM) 21 g NaHCO3 (Fc: 250 mM) in 1 litre of ddH2O (pH adjusted to 7.2 with HCl)
Collagenase solution (for 500 ml)	500 ml RPMI 55 ml FBS 5.5 ml 100X HGPG 1 ml 0.5 M of CaCl2 1 ml 0.5 M MgCl2 100 U/ml collagenase
HGPG 100X	59.6 g HEPES 14.6g L-glutamine 1x106 U penicillin 1 g streptomycin In 500 ml RPMI (pH adjusted pH to 7.2 with HCl)

3.1.6 Materials for flow cytometry

Fluorochrome-conjugated reagents ant their manufacturers

Live/dead dyes

L/D succinimidyl ester Pacific Orange	Invitrogen, Carlsbad, CA, USA
L/D succinimidyl ester AF750	Thermo Fisher Scientific, Waltham (MA), USA

Proliferation dyes

Proliferation dye eFluor670	Thermo Fisher Scientific, Waltham (MA), USA

Fluorochrome-conjugated antibodies and their manufacturers

Specificity	Fluorochrome	Clone	Company
Lineage markers			
CD2	FITC	RPA-2.10	Becton Dickinson, Franklin Lakes (NJ), USA
CD3	APC-Cy7	UCHT1	BioLegend, San Diego (CA), USA
CD3	PerCP-Cy5.5	OKT3	Thermo Fisher Scientific, Waltham (MA), USA
CD3	V510	OKT3	BioLegend, San Diego (CA), USA
CD3	APC-Cy7	OKT3	BioLegend, San Diego (CA), USA
CD3	BV650	UCHT1	BioLegend, San Diego (CA), USA
CD4	APC	SK3	BioLegend, San Diego (CA), USA
CD4	AF488	RPA-T4	BioLegend, San Diego (CA), USA
CD4	V500	RPA-T4	Becton Dickinson, Franklin Lakes (NJ), USA
CD4	APC-Cy7	RPA-T4	BioLegend, San Diego (CA), USA

CD8α	V510	RPA-T8	BioLegend, San Diego (CA), USA
CD8	BV421	RPA-T8	BioLegend, San Diego (CA), USA
CD8α	Pacific Blue	RPA-T8	BioLegend, San Diego (CA), USA
CD8β	PE	2ST8.5H7	Becton Dickinson, Franklin Lakes (NJ), USA
CD8	PE-Cy7	SK1	BioLegend, San Diego (CA), USA
CD8α	FITC	RPA-T8	BioLegend, San Diego (CA), USA
CD14	V450	MφP9	Becton Dickinson, Franklin Lakes (NJ), USA
CD14	FITC	M5E2	BioLegend, San Diego (CA), USA
CD16	APC-Cy7	3G8	BioLegend, San Diego (CA), USA
CD19	PE-Cy7	HIB19	BioLegend, San Diego (CA), USA
CD20	V450	L27	Becton Dickinson, Franklin Lakes (NJ), USA
CD20	FITC	2H7	BioLegend, San Diego (CA), USA
CD24	PerCP-Cy5.5	ML5	BioLegend, San Diego (CA), USA
CD33	BV421	WM53	BioLegend, San Diego (CA), USA
CD45	V510	HI30	BioLegend, San Diego (CA), USA
CD56	PE-Cy7	B159	Becton Dickinson, Franklin Lakes (NJ), USA
CD56	BV421	HCD56	BioLegend, San Diego (CA), USA
CD56	APC	HCD56	BioLegend, San Diego (CA), USA
CD127	PerCP-Cy5.5	A019D5	BioLegend, San Diego (CA), USA
CD161	BV421	HP-3G10	BioLegend, San Diego (CA), USA
CD161	PE	HP-3G10	BioLegend, San Diego (CA), USA
CD163	PerCP-Cy5.5	GHI/61	BioLegend, San Diego (CA), USA

Activation markers

CD25	PE	M-A251	Becton Dickinson, Franklin Lakes (NJ), USA
CD25	BV421	BC96	BioLegend, San Diego (CA), USA
CD80	PE	L307.4	Becton Dickinson, Franklin Lakes (NJ), USA
HLA-DR	FITC	G46-6	Becton Dickinson, Franklin Lakes (NJ), USA

Maturation markers

CD27	APC-Cy7	O323	BioLegend, San Diego (CA), USA
CD28	PE-Cy7	CD28.2	BioLegend, San Diego (CA), USA
CD45RA	PE-Cy7	HI100	BioLegend, San Diego (CA), USA
CD45RA	BV421	HI100	BioLegend, San Diego (CA), USA
CD62L	FITC	DREG-56	BioLegend, San Diego (CA), USA
CD62L	PE	DREG-56	Becton Dickinson, Franklin Lakes (NJ), USA
CD69	APC-Cy7	FN50	BioLegend, San Diego (CA), USA

CD197 (CCR7)	AF647	G043H7	BioLegend, San Diego (CA), USA

Ectoenzymes

CD38	PerCP-Cy5.5	HIT2	BioLegend, San Diego (CA), USA
CD38	AF488	HIT2	BioLegend, San Diego (CA), USA
CD39	PE-Cy7	A1	BioLegend, San Diego (CA), USA
CD73	PE	AD2	BioLegend, San Diego (CA), USA

Chemokine receptors

CD183 (CXCR3)	AF488	1C6/CXCR3	Becton Dickinson, Franklin Lakes (NJ), USA
CD194 (CCR4)	PE-Cy7	L291H4	BioLegend, San Diego (CA), USA
CD196 (CCR6)	PerCP-Cy5.5	G034E3	BioLegend, San Diego (CA), USA
CX3CR1	PE-Cy7	2A9-1	BioLegend, San Diego (CA), USA

T cell receptor chain markers

Tγδ	FITC	11F2	Becton Dickinson, Franklin Lakes (NJ), USA
Tγδ	PE	11F2	Becton Dickinson, Franklin Lakes (NJ), USA
Tγδ	PE-Cy7	11F2	Becton Dickinson, Franklin Lakes (NJ), USA
Vδ1	FITC	TS-1	Thermo Fisher Scientific, Waltham (MA), USA
Vδ2	APC	123R3	Milteny Biotec, Bergisch Gladbach, Germany
Vδ2	PE	B6	Becton Dickinson, Franklin Lakes (NJ), USA
Vδ2	FITC	B6	BioLegend, San Diego (CA), USA
Vα7.2	APC	3C10	BioLegend, San Diego (CA), USA
Vα7.2	PE	3C10	BioLegend, San Diego (CA), USA
Vγ9	FITC	IMMU 360	Beckman Coulter, Brea (CA), USA
Vα24	FITC	6B11	BioLegend, San Diego (CA), USA

Other antibodies

rh IgG1Fc	-	110-HG	R & D Systems, Minneapolis (MN), USA
ASC	-	N-15	Santa Cruz Biotechnology, Dallas (TX), USA
Rabbit Fc (rbFc)	PE	-	Dianova, Hamburg, Germany
IgD	PE	IA6-2	BioLegend, San Diego (CA), USA

Fluorochrome-conjugated nanobodies and their providers

Specificity	Fluorochrome	Clone	Provider
hP2X7 (Dano1)	AF647/ -	3c23	Professor Dr. Friedrich Koch- Nolte, UKE
mARTC2.2	AF647/ -	s+14	Professor Dr. Friedrich Koch- Nolte, UKE
Toxin A, *C.difficile*	-	L+8	Professor Dr. Friedrich Koch- Nolte, UKE

Chemical reagents and their manufacturers

Bovine serum albumin (BSA)	Thermo Fisher Scientific, Waltham (MA), USA
Clean solution	Becton Dickinson, Franklin Lakes (NJ), USA
Flow sheath fluid	Becton Dickinson, Franklin Lakes (NJ), USA
Rinse solution	Becton Dickinson, Franklin Lakes (NJ), USA
Sodium azide (NaN_3)	Sigma-Aldrich, St. Louis (MO), USA
Fixation buffer	eBioscience, San Diego (CA), USA
Permeabilisation Buffer 10X	eBioscience, San Diego (CA), USA
Paraformaldehyde (PFA)	Morphisto GmbH, Frankfurt, Germany
DAPI	Merck, Darmstadt, Germany

Flow cytometry buffers and their composition

FACS buffer	0.1 % BSA, 0.02 % NaN3 in 1X PBS

Flow cytometry equipment and materials and their manufacturers

FACS Aria Fusion (FACS Core Facility, UKE)	Becton Dickinson, Franklin Lakes (NJ), USA
FACS Aria IIIu (FACS Core Facility, UKE)	Becton Dickinson, Franklin Lakes (NJ), USA
FACSCanto II	Becton Dickinson, Franklin Lakes (NJ), USA
FACSCelesta	Becton Dickinson, Franklin Lakes (NJ), USA

3.1.7   Materials for enzyme-linked immunosorbent assay (ELISA)

Buffers, solutions and their composition

ELISA wash buffer	0.05 % Tween-20 in 1X PBS
Stop solution	2N H2SO4

Commercially available kits

Human IL-1 beta ELISA Ready-SET-Go	eBioscience, San Diego (CA), USA

Equipment

Plate reader Victor3 1240	PerkinElmer, Waltham (MA), USA

3.1.8 General consumables

Material	Company
Cellstar polypropylene tubes (15 ml, 50 ml)	Greiner bio-one, Kremsmünster, Austria
5 mL polystyrene round bottom tubes	Sarstedt, Nümbrecht, Germany
Cell scraper	TPP, Trasadingen, Switzerland
Cell strainer	Sigma-Aldrich, St. Louis (MO), USA
epT.I.P.S (1000 µl)	Eppendorf, Hamburg, Germany
Examination gloves	UKE, Hamburg, Germany
Millipore Express PLUS 0.22 µm	Merck, Darmstadt, Germany
Petri dish	Nunc, Roskilde, Denmark
Pipette tips (10 µl, 200 µl, 1000 µl)	Sarstedt, Nümbrecht, Germany
Reagent reservoir	Starlab, Hamburg, Germany
SafeSeal tubes (1.5 ml, 2 ml)	Sarstedt, Nümbrecht, Germany
Scalpel	Cardinal Health, Dublin (OH), USA
Serological pipettes	Sarstedt, Nümbrecht, Germany
S-Monovette Z-Gel/K3E	Sarstedt, Nümbrecht, Germany

3.1.9 Software

Material	Company
4 peaks	Nucleobytes B.V., Aalsmeer, The Netherlands
Adobe Illustrator CS2	Adobe Systems, San Jose (CA), USA
FACSDiva	Becton Dickinson, Franklin Lakes (NJ), USA
Finch TV	Gospiza, Inc., Seattle (WA), USA
FlowJo 10.4	FlowJo LLC, Ashland (OR), USA
GraphPad Prism 6.07	GraphPad Software, La Jolla (CA), USA
Mendeley (Desktop 1.18 and web)	Elsevier, New York City (NY), USA
Microsoft Office Professional 2010	Microsoft, Redmond (WA), USA
Nanodrop 2000/ 2000c software	Thermo Fisher Scientific, Waltham (MA), USA
StepOne Software 2.3	Applied Biosystems, Foster City (CA), USA

3.2 METHODS

All buffers and solutions were prepared using purified water (ddH$_2$O) or phosphate-buffered saline without calcium (Ca^{2+}) and magnesium (Mg^{2+}) (PBS$^{-/-}$), if not stated otherwise.

3.2.1 Donors

3.2.1.1 Human blood

Human peripheral blood from adult healthy individuals at the UKE was freshly drawn in EDTA or heparin collection tubes. Buffy coats from healthy individuals were kindly provided by the Blood Bank at the UKE. All donors were of legal age. Informed consent was obtained from all volunteers. Of note, blood samples were obtained and handled according to corresponding ethics protocol (Ethikkommission der Ärztekammer Hamburg, Regulationsmechanismen von Immunzellen; PV5139).

Human peripheral blood from a child with cryopyrin associated periodic syndrome (CAPS) was kindly provided by Dr. med. Kai Lemberg from the Center for Obstetrics and Pediatrics at the UKE, and handled according to corresponding ethics protocol (Frühkindliche, medizinische Eingriffe, Auswirkungen auf die Entwicklung des Immunsystems; PV5482).

3.2.1.2 Human gastrointestinal tissue

Human gastrointestinal tissue was obtained as discarded material from the ileum part of the small intestine from patients undergoing laparoscopic gastric bypass surgery due to morbid obesity at the UKE. Gut samples were kindly provided by Prof. Nicola Gagliani from the Center for Internal Medicine in the UKE. Of note, human tissue was obtained and handled according to corresponding ethics protocol (PV4889).

3.2.1.3 T cell lines

T cell lines were derived from human peripheral blood mononuclear cells (PBMCs) from adult healthy donors.

3.2.2 <u>Isolation of human cells</u>

3.2.2.1 Isolation of peripheral blood mononuclear cells

PBMCs from peripheral blood or buffy coats were isolated by density gradient centrifugation using Biocol density gradient medium. Biocol is a hydrophilic polymer that allows the separation of cells according to size, density and shape. Blood was diluted with two parts of PBS $^{-/-}$ at room temperature (RT). Afterwards, 30 ml of diluted blood were carefully layered over 20 ml of Biocol in a 50 ml Falcon tube, and centrifuged for 25 min at 800 xg with slow acceleration and break at RT. After centrifugation, mononuclear cells constitute a monolayer at the interphase between plasma and the separation medium, whereas erythrocytes deposit as a substantial pellet at the bottom of the tube. The monolayer was then recovered by aspiration and washed twice with cold PBS; first for 10 min at 650 xg and afterwards for 5 min at 450 xg at 4°C. The total cell number was manually assessed using a Neubauer counting chamber. Dead cells were excluded by dye exclusion using Trypan blue. Subsequently, the formula *N° of cells x Dilution factor x 10000 = n° of cells/ml* was used to calculate the total amount of cells. Isolated PBMCs were immediately used for further experiments.

3.2.2.2 Isolation of infiltrating immune cells from human gut tissue

Pieces of small intestine tissue were obtained as discard material from patients undergoing bariatric surgery. The intestinal tissue was placed into a Petri dish containing Roswell Park Memorial Institute medium (RPMI). Circular folds of gut mucosa were separated from the muscular layer and fat tissue, cut into small pieces of approximately 0.5 cm and incubated in 1mM dithiothreitol (DTT) solution for 20 min at 37°C, while shaking. Afterwards, the remaining tissue and medium were filtered through a metal cell strainer and washed twice with PBS supplemented with 1% fetal bovine serum (FBS) (450xg, 5 min 4°C). The supernatant, which contains the intraepithelial lymphocytes (IELs), was collected and kept at 4°C. To further isolate the lamina propria lymphocytes (LPLs), the remaining pieces of small intestine were collected, minced with a scalpel and treated with collagenase IV solution (1mg/ml) containing freshly added DNase I (10 U/ml) for 45 min, in a 5% CO_2 incubator at 37°C, while shaking. The digested intestinal tissue was further homogenized through a metal strainer, washed once with PBS supplemented with 1% FBS, and the flow-through was collected. The supernatants containing IELs or LPLs were pooled together and pelleted by centrifugation for 10 min, at 515 xg, at 4°C. From the pooled cells, leukocytes were additionally enriched by Percoll gradient centrifugation. First, Percoll osmolarity was adjusted by adding 1 part 10X PBS to 9 parts of Percoll. Percoll solution was further diluted with 6 parts of RPMI supplemented with 1% FBS to create a 40% Percoll solution, and used to resuspend the cell pellet. Next, 4 ml of the cell suspension were

carefully layered over 4 ml of isotonic Percoll solution (67%) and centrifuged at 450 xg for 20 min with low acceleration and break. Infiltrating lymphocytes were collected from the interphase by aspiration, washed once with 1X PBS supplemented with 1% FBS, at 450 xg for 5 min, and resuspended in RPMI medium supplemented with 10% FBS.

3.2.3   Magnetic-activated cell sorting

Magnetic-activated cell sorting (MACS) is a method that allows the separation of distinct cell populations based on magnetic nanoparticles that are coated with antibodies against specific surface molecules. Magnetically-labelled cells are then retained to separation columns. Using this technique, cells can be positively or negatively selected. Positive selection is achieved by labelling of the cells of interest, whereas negative selection is achieved by targeting all the other populations but the one of interest (Miltenyi *et al.*, 1990).

3.2.3.1 Enrichment of human monocytes

Human monocytes were enriched from PBMCs by negative selection using the human monocyte Isolation Kit II (Milteny Biotec) according to the manufacturer´s protocol. Briefly, a total of $4 \cdot 10^7$ PBMCs were passed through a 30 µM cell filter to avoid the clogging of the column, and centrifuged for 10 min at 290 xg. Next, cells were incubated in a solution containing MACS buffer, and antibodies against Fc-receptors (FcR) and biotin-conjugated antibodies against the following antigens: CD3, CD7, CD16, CD19, CD56, CD123 and CD235a, for 10 min at 4°C. Afterwards, anti-biotin magnetic MicroBeads, which bind to the biotinylated antibodies, were added to the cells and followed by 15 min incubation at 4°C. Cells were washed twice at 290 xg for 10 min and resuspended in MACs buffer. The cell suspension was run through a MACS LS column and washed thrice with 3 ml of MACS buffer. The effluent containing the monocyte enriched fraction was then collected in a Falcon tube. Cells retained in the columns were eluted outside of the magnetic field and used as control to assess the purity of the process. Both fractions were stained using antibodies against lineage markers (**Table 3**) for 15 min at RT, and the purity was finally assessed by flow cytometry.

Table 3. List of antibodies used for the assessment of purity after MACS isolation.

Fluorochrome	V450	V510	AF488	PE	PerCP-Cy5.5	PE-Cy7	APC	APC-Cy7
Antigen	CD14	CD45	CD4	TCRγδ	CD3	CD19	CD56	CD16

3.2.4   Flow cytometry

Flow cytometry is one of the most widely used methods in cell-based research. It allows the simultaneous analysis of both physical and chemical properties on single cells. The fluidics system

forces cells to move single file in droplets through a beam of light. The system is equipped with mirrors, filters and optical detectors that collect the light scattered by the cells, and photomultipliers (PMTs) that convert the optical signal into electrical pulses. Electrical pulses are then further processed and converted into digital data. Each cell emits the light from the laser in two different ways: the Forward Scatter (FSC), providing information about the size or area; and the Side Scatter (SSC), which relates to the internal complexity of the cell (Adan et al., 2017; Cossarizza et al., 2017). Using this technique, distinct immune cell populations can be identified by using antibodies against different cell markers. To this end, antibodies are conjugated to fluorochromes, chemical compounds that absorb light at certain wavelengths and re-emit it at a distinct wavelength. The emitted light is detected by different fluorescence detectors. Of note, some fluorochromes are excited or emit light at a similar wavelength, which may cause interference among them. This phenomenon is known as spillover, and the method applied to correct the overlapping emission spectra is known as compensation. Flow cytometry also allows the sorting of live cells based on fluorescence labelling [section 3.2.4.4].

Unless otherwise stated, washing steps were performed with 1X PBS $^{-/-}$ at 450 xg and at RT.

3.2.4.1   Staining of surface molecules

A total of $0.5 \cdot 10^6$ to $1 \cdot 10^6$ cells were used for staining of molecules expressed on the cell plasma membrane. Cells were transferred to FACS tubes washed once with PBS or RPMI and resuspended in PBS or RPMI. To block unspecific binding of the antibodies, cells were incubated with human IgG (hIgG) for 5 min at RT. Cells were further incubated with antibodies against markers of interest diluted in FACS Buffer for 30 min. After washing, cells were resuspended in $150 - 200 \, \mu l$ FACS buffer and analysed by flow cytometry.

In case of staining whole blood, 50 µl of blood were stained as described above instead. After the incubation with the staining antibodies and washing with PBS, erythrocyte lysis was performed by addition of 1 ml 1X lysing solution for 10 min at RT in the dark.

Staining of human P2X7 was carried out using the following strategy. Due to a low expression of the receptor, a staining control for P2X7 was performed. To this end, two tubes were required for each staining. In the first tube, cells were stained with an antibody cocktail containing the P2X7-specific nanobody Dano1, whereas the cells from the second tube were stained with the same antibody cocktail containing a nanobody against mouse ARTC2.2 instead. As mentioned in the introduction, ARTC2.2 is not expressed in humans. Thus, the second tube serves as isotype control (IC), which is needed to ensure the specificity of the P2X7 signal.

3.2.4.2 Exclusion of dead cells and cell counting

Dead cells were excluded using the amine-reacting life/dead (L/D) fluorescent dyes Pacific Orange (PacO, 1µg/ml) or Alexa Fluor 750 (AF750, 1µg/ml). In cells with intact cell membranes, these dyes cannot penetrate the plasma membrane and bind only to amines present on the cell membrane. However, disruption of the plasma membrane occurring during cell death facilitates binding to the amines present inside the cell, therefore resulting in a more intense signal.

L/D was added 10 min after the addition of the surface staining antibodies, and the cell suspension was kept at 4°C for the following 20 min. Cells were then washed once with FACS buffer or RPMI to remove the excess of reactive dye.

3.2.4.3 Staining of intracellular molecules

For the intracellular staining (ICC) of cytokines and/or transcription factors (TFs), cells were resuspended in serum free X-VIVO-15 medium and stimulated with 50 ng/ml of phorbol-myristate-acetate (PMA) and 1 µg/ml of ionomycin (Iono) for 5 hours in the incubator at 37°C and 5% CO_2. To prevent the release of cytokines into the medium, 10 µg/ml of brefeldin A (BfA) was added 30 min after stimulation with PMA/Iono. BfA is a substance that inhibits the transport of proteins from the endoplasmic reticulum to the Golgi apparatus, resulting in an accumulation of cytokines inside the cell.

After stimulation cells were washed and stained for cell surface molecules and live/dead dye as described in sections 3.2.4.1 and 3.2.4.2. After washing twice, first with cold PBS and then with PBS with 0.2% bovine serum albumin (BSA), pelleted cells were resuspended in 1 ml of 1X fixation/permeabilisation buffer and further incubated for 1 h at 4°C in the dark. After washing twice with 1X permeabilisation buffer, antibodies against the cytokines and/or TFs of interest were added, and the cell suspension was incubated for 30 min at 4°C in the dark. Finally, cells were washed once with FACS Buffer, resuspended in 200 µl FACS buffer and analysed by flow cytometry [section 3.2.4.5].

3.2.4.4 Sorting of immune cell types

Flow cytometry also enables the separation of different cell populations according to their fluorescent properties. As mentioned before, the liquid stream consists of a cascade of droplets that are screened one after the other. When a cell matches the desired criteria for sorting, in our case based on the expression of certain surface markers; an electrical pulse is applied to the droplet.

Consequently, the cell will be deflected from the stream and collected separately from the other cells (Ibrahim and van den Engh, 2007).

Prior to sorting, cells were stained for surface markers [section 3.2.4.1] and then filtered through a 30 µM cell strainer. Sorted cells were collected in FBS-coated sterile FACS tubes. Details on the immune cell populations of interest and the markers used for the sorting are listed in **Table 4**.

Table 4. List of the immune cell populations of interest and the markers used for their characterisation.

Immune cell types	Markers	Immune cell types	Markers
TCD3$^+$ cells	CD3$^+$	Tγδ$^+$Vδ2$^-$	CD3$^+$TCRγδ$^+$Vδ2$^-$
TCD4$^+$ cells	CD3$^+$CD4$^+$	Tγδ$^+$Vδ1$^+$	CD3$^+$TCRγδ$^+$Vδ1$^+$
TCD8$^+$ cells	CD3$^+$CD8$^+$	MAIT cells	CD3$^+$CD8$^+$CD161$^+$Vα7.2$^+$
Tγδ$^+$	CD3$^+$TCRγδ$^+$	NK cells	CD3$^-$CD56$^+$
Tγδ$^+$Vδ2$^+$	CD3$^+$TCRγδ$^+$Vδ2$^+$	Monocytes	Gated according to FSC-A and SSC-A

3.2.4.5 Data acquisition

Flow cytometry was performed on a BD FACS Canto II or FACS Celesta flow cytometer. Cell sorting was performed on a BD FACS Aria IIIu flow cytometer. When needed for further cell culture, cells were sorted on a BD FACS Aria Fusion under sterile conditions. All flow cytometers use the FACS Diva software. FACS data were later analysed with FlowJo software.

3.2.5 Generation of human T cell lines

Human T cell lines are useful tools to study the phenotype and function of T cells *in vitro*. For this study, TCD4$^+$, Tγδ$^+$ (Vδ1$^+$ and Vδ2$^+$) and MAIT cell lines were generated. PBMCs were isolated from blood of healthy donors [section 3.2.2.1] and FACS-sorted [section 3.2.4.4] using the markers listed in **Table 4**.

Sorted cells were washed, resuspended in T cell medium and seeded into individual wells onto a round-bottom 96-well plate at a density of $2 \cdot 10^4$ - $1 \cdot 10^5$ cells/well. To simulate Ag presentation, sorted cells were cultured with $2 \cdot 10^5$ heterologous human PBMCs irradiated with 39 grays for 13 min (3 grays/min) in order to avoid their proliferation during *in vitro* culture. Each cell population was cultured under specific conditions (**Table 5**) and incubated in a 5% CO$_2$ incubator at 37°C. TCD4 cells were stimulated with phytohaemagglutinin (PHA, 2.5 µg/ml,) and self-produced IL-2 supernatant (Dilution: 1:2000). Tγδ$^+$ Vδ1$^+$ cells were stimulated with PHA (2.5 µg/ml) and IL-2 supernatant (1:400). Tγδ$^+$ Vδ2$^+$ cells were cultured with (E)-4-hydroxy-dimethylallyl pyrophosphate (HDMAPP, 10 nM) and IL-2 supernatant (1:400). MAIT cells (CD8$^+$, CD161$^+$, Vα7.2$^+$) were stimulated with soluble anti-CD3 (0.4 µg/ml,), recombinant IL-2 (rec IL-2, 100 U/ml) and recombinant IL-7 (rec IL-7, 10 ng/ml). Cell

growth and cell culture contamination were checked daily with an inverted microscope. Every 3 to 4 days, approximately half of the medium was removed and exchanged for fresh medium containing fresh IL-2. Cell passage was performed when required in order to maintain the exponential growth of the cell lines. To this end, half of the cell suspension was transferred into a new well and fresh medium with fresh IL-2 was added. After 12 to 14 days in culture, cells were restimulated. Cells were harvested, washed once with 1X PBS and manually counted. $1 \cdot 10^4$ cells from each cell line were then seeded into a new 96-well plate with $2 \cdot 10^5$ feeder cells and stimulated as specified above. The remaining cells were frozen and put back into culture when needed. Cells were restimulated for a maximum of 5 rounds, and restimulation rounds were annotated to keep track of the culture.

Table 5. Specific conditions for the treatment of the distinct cell lines.

	TCD4$^+$	Vδ1$^+$	Vδ2$^+$	MAIT
Reagents	PHA IL-2 supernatant	PHA IL-2 supernatant	HDMAPP IL-2 supernatant	soluble anti-CD3 recombinant IL-2 (rIL-2)

3.2.6 *In vitro* assays

3.2.6.1 Activation of human T cells

Activation of CD4$^+$ and CD8$^+$ T cells was determined by the expression of the activation markers CD25 and CD69 on the cell surface. PBMCs from healthy donors were resuspended in T cell medium and stimulated with soluble anti-CD3 (0.5 µg/ml). To assess the influence of P2X7 blockade on T cell activation, cells were then seeded onto a round-bottom 96-well plate at $0.5-1 \cdot 10^5$ cells per well in the absence or presence of Dano1 (100 nM) or a control-Nb against mouse ARTC2.2 (100 nM) in a final volume of 200 µl. Nbs were used in different formats, such as monomers (mon), dimers (dim), fused to the rabbit Fc-portion of IgG (rbFc) or linked to the albumin-binding nanobody Alb8 (dimAlb). Nbs were added a second time after 2 days of culture. After 4 days in culture in a 5% CO_2 incubator at 37°C, cells were stained with antibodies against the markers listed in **Table 6**. Subsequently, the *in vitro* activation of living T cells was monitored by flow cytometry.

Table 6. List of antibodies used for the assessment of T cell activation *in vitro*.

Fluorochrome	V450	V500	FITC	PerCP-Cy5.5	PE	PE-Cy7	APC-Cy7
Marker	CD25	live/dead	CD4	CD3	TCRγδ	CD8	CD69

FACS-sorted CD4, CD8 and γδ T cells from healthy donors were resuspended in full RPMI medium and seeded onto a round-bottom 96-well plate pre-coated with anti-CD3 at a cell density of $1 \cdot 10^5$ cells per well. Coating was performed with 200 µl of PBS containing 1 µg/ml soluble anti-CD3, at 37°C for 3 hours. Before seeding of the cells, the 96-well plate was washed twice with PBS under sterile conditions. Cells were further stimulated with 5 µg/ml of soluble anti-CD28, and incubated in a 5%

CO_2 incubator for 9 days at 37°C. Cells were collected every odd day for RNA isolation [see section 3.2.8.2]. As a control, FACS-sorted cells at day 0 and PBMCs were also collected.

3.2.6.2 Proliferation of human T cells

Proliferation of $CD4^+$ and $CD8^+$ T cells was determined by eFluor dye dilution by flow cytometry. PBMCs from healthy donors were resuspended in eFluor670 (2 µM) and incubated in a 5% CO_2 incubator at 37°C for 10 min. eFluor labelling was stopped by addition of full RPMI and an incubation on ice for 5 min. Afterwards, cells were washed twice and resuspended in full RPMI in the absence or presence of soluble anti-CD3 (0.4 µg/ml). Cells were seeded onto a round-bottom 96-well plate at $0.8\text{-}1 \cdot 10^5$ cells per well in a final volume of 200 µl, in the absence or presence of Dano1 or a control Nb against mouse ARTC2.2 (100 nM). After 4 to 5 days in culture, cells were stained with antibodies against CD4 and CD8 and proliferation of living T cells was assessed by flow cytometry (see **Table 6** for Fluorochrome-conjugated antibodies).

3.2.6.3 Stimulation of human T cells with retinoic acid

PBMCs were resuspended in full RPMI medium and seeded onto a round-bottom 96-well plate at a density of $2 \cdot 10^5$ cells per well in a final volume of 200 µl. Cells were stimulated with soluble anti-CD3 (0.5 µg/ml), and cultured in the absence or presence of 1, 10 or 100 nM of retinoic acid (RA) in a 5% CO_2 incubator at 37°C for 5 days.

Cells were harvested daily, and transferred to an eppendorf tube. After centrifugation (450 xg, 5min), supernatants were collected and frozen at -20°C. Cells were then resuspended in PBS, transferred into FACS tubes and stained for the following markers (**Table 7**). The expression of P2X7 was monitored over time by flow cytometry [section 3.2.4.1].

Table 7. List of antibodies used for the assessment of RA effect in T cell activation *in vitro*.

Fluorochrome	BV421	V500	FITC	PerCP-Cy5.5	PE	PE-Cy7	APC	APC-Cy7
Marker	CD25	Live/dead	CD2	CD38	CD8β	CD8α	P2X7	CD4

3.2.6.4 Uptake of 4',6-diamidino-2-phenylindole (DAPI)

4',6-diamidino-2-phenylindole (DAPI) is a fluorescent dye that binds to double stranded DNA. The uptake of DAPI was used as readout to assess P2X7-dependent pore formation on different immune cell types. PBMCs or gut-infiltrating leukocytes were isolated [sections 3.2.2.1 and 3.2.2.2] and resuspended in RPMI medium. A total of $1 \cdot 10^6$ PBMCs were incubated in the absence or presence of Dano1 (100 nM) or Control Nb (100 nM) at 4°C for 30 min. As a control condition, cells were incubated with 10 U/ml of apyrase in a 5% CO_2 incubator at 37°C for 20 min. Afterwards, cells were

loaded with DAPI and incubated for further 30 min in the absence or presence of 0.5, 1.5 or 4.5 mM ATP in a water bath pre-heated at 37°C. Immediately after, cells were placed at 4°C in order to stop the reaction, washed with cold RPMI medium, and stained for 30 min at 4°C with one of the antibody cocktails listed in **Table 8**. After washing twice with cold RPMI medium, cells were resuspended in 100 µl FACS buffer, kept on ice and measured by flow cytometry.

Table 8. List of antibodies used for the identification of immune cells and assessment of uptake of DAPI.

Fluorochrome	BV421	V500	FITC	PerCP-Cy5.5	PE	PE-Cy7	APC	APC-Cy7
(1) Marker	DAPI	CD8	Vδ1; Vγ9; Vα24	CD3	CD161	TCRγδ	Vα7.2 Vδ2	CD4
(2) Marker	DAPI	CD3	CD8; CD20	CD127	CD25	CD39	CD56	CD4

3.2.6.5 Shedding of CD62L extracellular domain

The shedding of the extracellular domain of CD62L was also used as readout to assess the function of the P2X7 receptor *in vitro*. Cells were treated as described in section 3.2.6.4. The antibodies used for flow cytometric analysis are listed in **Table 9**.

Table 9. List of antibodies used for the identification of immune cells and assessment of CD62L shedding.

Fluorochrome	BV421	V500	FITC	PerCP-Cy5.5	PE	PE-Cy7	APC	APC-Cy7
(1) Marker	CD56	CD8	Vδ1; Vγ9; Vα24	CD3	CD62L	TCRγδ; CD19	Vδ1	CD4
(2) Marker	CD161	CD3	CD62L	CD127	CD25	CD8	Vα7.2	CD4

3.2.6.6 Suboptimal stimulation of T cells

The role of P2X7 as co-stimulatory molecule under suboptimal stimulation of the TCR was determined by proliferation of CD4$^+$ and CD8$^+$ T cells and expression of the activation markers CD25 and CD69 over time. First, PBMCS were labelled with eFluor dye as detailed in section 3.2.6.2. Next, a total of $1 \cdot 10^5$ PBMCs were resuspended in full RPMI medium and seeded onto a 96-well round-bottom plate at a final volume of 200 µl/well. Cells were stimulated with different concentrations of soluble anti-CD3 (0.1; 0.5; 1; 10 and 100 ng/ml) under the absence or presence of ATP (1.5; 4.5 mM), Dano 1 (100 nM) or apyrase (10 U/ml), and incubated for 4 days in a 5% CO_2 incubator at 37°C. T cell proliferation and activation were assessed after 36 h and 96 h by flow cytometry using the antibodies listed in **Table 10**.

Table 10. List of antibodies used for the assessment of T cell activation and proliferation *in vitro*.

Fluorochrome	BV421	BV500	FITC	PerCP-Cy5.5	PE	PE-Cy7	APC	APC-Cy7
Marker	CD25	L/D	CD3	CD4	Tγδ	CD8	eFluor	CD69

3.2.6.7 Induction of inflammasome assembly (ASC specks)

The activation of the inflammasome was assessed by formation of ASC specks. This method relies on the recruitment of ASC into large protein complexes in the cytosol (Sester et al., 2015). To this end, a total of $1 \cdot 10^6$ PBMCs from healthy donors were stimulated with 100 ng/ml LPS in the absence or presence of 200 nM of Dano1 or a control nanobody against Toxin A from *Clostridium difficile* (clone L+8) for 2 h at 37°C. Immediately after, cells were further stimulated either with 2.5 or 5 mM ATP, or with 10 μM or 20 μM nigericin for 30 min at 37°C. Afterwards, cells were fixed with 2% paraformaldehyde (PFA) for 10 min on ice (4°C), washed with FACS buffer at 450 xg for 5 min, and subsequently permebealised with 0.2% saponin. Cells were stained with rabbit anti-ASC primary antibody for 90 min at 4°C, washed with cold FACS buffer for 5 min at 450 xg and stained with PE-conjugated anti-rabbit secondary antibody and a BV421-conjugated antibody against CD33 for further 45 min at 4°C. After staining, cells were washed once with FACS buffer and measured by flow cytometry. ASC specks were defined by a lower pulse width to pulse area after gating on $CD33^+$ cells.

3.2.6.8 Stimulation of NF-κB-induced gene transcription

A total of $2.5 \cdot 10^4$ purified monocytes [section 3.2.3.1] were seeded onto a 24 flat-bottom well plate coated with 300 μl of 0.01% poly-L-lysine solution for 25 min at RT. Cells were stimulated with LPS (1 μg/ml) in RPMI medium in the absence or presence of different constructs of Dano1 (100 nM) or a control Nb (100 nM) at 37°C, 5% CO_2. After incubation for a period of 3 h, cells were lysed with lysing solution RLT buffer and detached from the well plate using a scrapper. Cells were then collected, and resuspended in RLT + 1% β-mercaptoethanol, and stored at -80°C until day of use. mRNA was isolated from frozen samples and transcribed into complementary deoxyribonucleic acid (cDNA) according to the manufacturer's instructions; as detailed in sections 3.2.8.2 and 3.2.8.4, respectively. cDNA was further used for real-time polymerase chain reaction (Real-time PCR) [section 3.2.8.5.1] and gene expression of the *IL6*, *IL1B* and *TNF* genes were determined.

3.2.6.9 Stimulation of human monocytes

Aliquots of heparinized blood from healthy donors were stimulated with LPS (1 μg/ml) in the presence or absence of serial dilutions of Dano1, a control Nb or the small molecule inhibitors JNJ 47965567 and AZ10606120, in a 5% CO_2 incubator for 1.5 h at 37°C. Blood samples were further incubated for 30 minutes with the indicated concentrations of ATP in a water bath pre-heated at 37°C. Occasionally, the P2X7 receptor agonist benzoyl-ATP (bzATP), which exhibits greater potency than ATP, was used instead. To bring the reaction to an end, blood aliquots were placed on ice immediately after incubation. Plasma was aspirated after centrifugation of the blood at 736 xg for 5

min at 4°C. Finally, plasma was diluted 1:4 in RPMI medium and stored overnight at 4°C. The levels of IL-1β were determined the next day by enzyme-linked immunosorbent assay (ELISA) [section 3.2.7].

3.2.7 Enzyme-linked immunosorbent assay (ELISA)

Levels of IL-1β in plasma were determined by sandwich ELISA according to the manufacturer´s instructions (Ready-SET-Go, eBioscience). Treatment of the samples and obtention of the plasma is described in section 3.2.6.9. Briefly, a Maxisorp ELISA plate was coated overnight with capture antibody against IL-1β at 4°C. The procedure consisted of a capture antibody, the sample and a detection antibody conjugated with biotin. Afterwards avidin conjugated with horseradish peroxidase (HRP) was added. The addition of tetramethylbenzidine (TMB) as a substrate started the oxidative reaction, which was left to proceed about 10 min, or until the liquid turned into dark blue. The reaction was stopped using 2N H_2SO_4. Washing was performed 3-5 times with 300 µl of wash buffer between all steps. Standards were diluted in RPMI, and RPMI was also used as blank. Absorbance was read at 450 nm in a plate reader VICTOR3 spectrophotometer. The standard curve covered the range of 3.9 pg/ml to 2000 pg/ml. Data were analysed using Microsoft Excel 2010.

3.2.8 Gene expression assessment

3.2.8.1 Isolation of DNA from human blood

Genomic DNA was extracted from whole blood using the Nucleospin Blood (DNA, RNA and protein purification) Kit following the steps detailed in the manufacturer's instructions (Macherey-Nagel). Briefly, 200 µl of blood, 25 µl of proteinase K and 200 µl of a specific buffer (Buffer 3) were incubated at 70°C for 15 min. After incubation and addition ethanol (100%), the mix was pipetted into a NucleoSpin blood column and centrifuged at 11363 xg for 1 min. After two washing steps, the residual ethanol was removed by an additional centrifugation at 11363 xg for 1 min. Finally, DNA was eluted in 100 µl elution buffer pre-heated at 70°C, after a 1 min centrifugation 11363 xg. DNA concentration was determined [section 3.2.8.3] and samples were stored at -20°C until use.

3.2.8.2 Isolation of RNA from human cells

PBMCs and sorted immune cells were centrifuged at 1800 rpm for 10 min at 4°C and resuspended in RLT lysing solution + 1% β-mercaptoethanol. The cell suspension was then snap-frozen in liquid nitrogen and immediately stored at -80°C until day of use. RNA extraction was performed using the RNeasy Plus Mini Kit, following the steps detailed in the protocol provided by the manufacturer (Qiagen). Frozen samples containing cell lysate were removed from the -80°C and left at RT until

completely thawed. The lysate was then transferred into a QIAshredder spin column, centrifuged at full speed (15870 xg) for 2 min and the flow-through was collected. Afterwards, 1 volume of ethanol (70%) was added to the lysate until complete homogenization was achieved. Next, the mix was transferred to an RNeasy spin column, centrifuged at 13520 xg for 15 sec and the flow-through was discarded. Following, buffer RW1 was added into the column, and the mix was centrifuged as stated before. In order to remove any trace of DNA, the mix was incubated with DNase I (375 U/ml) for 15 min at RT. Subsequently, buffer RW1 was added onto the spin column, followed by a centrifugation at 13520 xg for 15 sec, and the flow-through was discarded. After two washing steps with buffer RPE, the column was centrifuged at full speed for 1 min. Finally, RNA was eluted in 30 µl of RNase-free water after centrifugation at 9391 xg for 1 min. RNA concentration was determined [section 3.2.8.3] and immediately used for cDNA synthesis or frozen in liquid nitrogen and stored at -80°C.

3.2.8.3 Quantification of purified DNA and RNA

The concentration of DNA and RNA from human blood, PBMCs and purified/sorted immune cells was determined by spectrophotometry at 260 nm. To this end, the following conversion factors were used: A260 = 1 = 50 µg/ml or A260 = 1 = 40 µg/ml for DNA and RNA samples, respectively. The purity was determined with the ratio of the absorbance at A_{260} divided by the absorbance at A_{280}; considering as pure a range between 1.8-2.0 and 2.0-2.2 for DNA and RNA, respectively.

3.2.8.4 Synthesis of cDNA

Isolated mRNA from PBMCs, sorted immune cells or purified monocytes was used as template for the synthesis of cDNA in a reverse transcription polymerase chain reaction. To that end, two different reactions were performed; the first one by incubating the RNA with random primers and dNTPs for 5 min at 65°C, and afterwards by incubating the mix with First Strand Buffer, DTT, diethyl pyrocarbonate (DEPC) treated water and M-MLV reverse transcriptase, for 50 min at 37°C and 15 min at 70°C. The final concentration and volume for each reagent are detailed in **Table 11**.

Table 11. List of reagents for the synthesis of cDNA.

Reaction 1		Reaction 2	
Reagents	**Volume**	**Reagents**	**Volume**
RNA	10 µl	Reaction 1 Mix	12 µl
Random hexamers (3 µg/µl)	1 µl	First Strand Buffer (1x)	4 µl
dNTPs (30 mM)	1 µl	DTT (0.1 M)	2 µl
	Σ = 12 µl	H₂O	1 µl
		MLV-RT (200 U/µl)	1 µl
			Σ = 20

3.2.8.5 Real time polymerase chain reaction

Real-Time polymerase chain reaction (Real-Time PCR) was performed using TaqMan or SYBR Green assays.

3.2.8.5.1 TaqMan assays

TaqMan assays were run to measure gene expression of the interleukin 6 (*IL6*, Hs00985639_m1), interleukin-1β (*IL1B*, Hs00174097_m1), Tumor Necrosis Factor (*TNF*, Hs01113624_g1) and Glyceraldehyde 3-phosphate dehydrogenase (*GAPDH*, Hs02758991_g1) genes on purified monocytes. Each TaqMan assay includes a mix with a set of primers and a reporter probe labelled with fluorescence. Real-time PCR reactions were carried out on a 96 Fast PCR-well plate using Maxima Probe/ROX qPCR master mix, a gene-specific TaqMan probe and cDNA in a final volume of 20 μl. The plate was then measured on a StepOne Plus Real-Time PCR System in accordance with the manufacturer's instructions (Applied Biosystems); by denaturation at 95°C for 10 min, followed by 40 cycles at 95°C for 15 sec and 60°C for 40 sec. Melting curve analyses were performed to verify the amplification specificity. Information on the concentration and volume for each reagent is detailed in **Table 12**. The relative gene expression was calculated using the ΔΔCt method. For the analysis, data were normalised to the expression of the reference gene *GAPDH*. Non LPS-stimulated samples in the absence of nanobodies were used as calibrator.

Table 12. List of reagents for qPCR reaction using a TaqMan assay.

Reagents	Volume
Maxima Probe/Rox qPCR master mix	10 μl
Gene-specific taqMan probe (3 μg/μl)	1 μl
Nuclease-free water	4 μl
cDNA	5 μl
	Σ = 20 μl

3.2.8.5.2 SYBR Green assays

SYBR Green assays were run to measure gene expression of 18S ribosomal RNA (*18S*), ribosomal protein L13a (*RPLA13*) and the seven members of the P2X receptor family *(P2RX1-P2RX7)* on PBMCs and sorted immune cells. SYBR Green is an intercalating dye that binds preferentially to double-stranded DNA. Real-time PCR reactions were carried out on a 96 Fast PCR-well plate using Maxima SYBR Green/ROX qPCR master mix, a pair of specific primers and cDNA in a final volume of 20 μl. The optimal pre-dilution of the cDNA was previously checked according to the reference genes *RPLA13* and *18S* for the distinct sorted immune cell types. Reaction products were measured following the protocol mentioned in <u>section 3.2.8.5.1</u>. Information on the concentration and volume for each

reagent is detailed in **Table 13**. Data were normalised to the expression of the reference genes *RPLA13* and *18S* and total PBMCs were used as calibrator.

Table 13. List of reagents for qPCR reaction using a SYBR Green assay.

Reagents	Volume
Maxima SYBR Green/ROX qPCR master mix	10 µl
Forward primer	1 µl
Reverse primer	1 µl
Nulcease-free water	3 µl
cDNA	5 µl
	Σ = 20 µl

3.2.9 <u>Genotyping</u>

Three prominent SNPs that confer different sensitivity to ATP have been identified in the human *P2RX7* gene. These SNPs, which are encoded in exons 5, 8 and 11, result in the variation of one amino acid at the following positions: 155 (H→Y), 270 (H→R) and 348 (A→T) (Stokes et al., 2010). Similarly, a SNP located in the first intron of the *ENTPD1* gene correlates with the expression of CD39 on Tregs and conventional CD4$^+$ T cells (A. Rissiek *et al.*, 2015). DNA was isolated from peripheral blood from healthy volunteers [<u>section 3.2.8.1</u>] and genotyped using PCR.

3.2.9.1 Polymerase Chain Reaction

PCR is a technique used to amplify a particular region of DNA. This method relies on the usage of an enzyme termed DNA polymerase, which is able to synthesize multiple copies of DNA by addition of deoxyribonucleotide triphosphates (dNTPs) to a DNA region that has been previously flanked by a specific pair of primers (Mullis *et al.*, 1986). PCR reactions typically consist of 25-30 cycles of an initial denaturation step of the double stranded DNA (dsDNA) at 90-95°C, followed by the annealing of the primers at 50-65°C and the elongation of the complementary strand of DNA at a 69-72°C for 45 sec. The PCR reaction was carried in a suitable buffer with required salts and magnesium sulfate ($MgSO_4$). Details on the PCR reactions and the program for the optimal amplification of the *ENTPD1* gene and exons 5, 8 and 11 of the *P2RX7* gene are to be found in **Table 14** and **Table 15**, respectively. The PCR reaction was transferred into a 0.2 ml PCR tube, and DNA template was added and mixed carefully. Afterwards, PCR tubes were placed in a PCR Thermocycler.

Table 14. List of reagents for the amplification of SNPs present in the *P2RX7* and *ENTPD1* genes.

	P2RX7	*ENTPD1*
Reagents	**Volume [µl]**	**Volume [µl]**
H_2O	31	13.2
KOD Buffer (10X)	5	4
dNTPS (2 mM)	5	4
$MgSO_4$ (25 mM)	2	2.4
Forward Primer (10 µM)	2	1.2
Reverse Primer (10 µM)	2	1.2
KOD Polymerase (1 U/ µl)	1	0.8
DNA Template	2	13.2
Final volume	**50**	**40**

Table 15. Protocol for the amplification of the SNP targeting region.

Step	Temperature [°C]	Time (min)
1	94°C	5 min
2	94°C	30 sec
3	60°C	30 sec
4	72°C	1 min
5	Step 2 to 4 x 10 times with a decrease of 1°C at step 3 at each cycle	
6	94°C	30 sec
7	50°C	30 sec
8	72°C	1 min
9	Step 6 to 8 x 25 times	
10	70°C	10 min

3.2.9.2   Agarose gel electrophoresis of PCR product

Products from PCR were fractioned due to their size in an agarose gel electrophoresis. Gels with 1-1.5% agarose were made with 1X TAE buffer containing 0.5 µg/ml of Rotisafe. Samples were prepared with 6X loading buffer, loaded into individual pockets of the gel and ran at an intensity of 90 V. As a reference for molecular-weight size marker, 8 µl of DNA ladder 100 bp or 1 kb were used. DNA bands were visualized using a UV-Transilluminator and photographed for documentation. DNA bands were then excised from the gel for further processing [section 3.2.9.3].

3.2.9.3 Extraction of DNA fragments from an agarose gel

The elution of DNA fragments from agarose gels was carried out with the NucleoSpin Gel and PCR Clean-up according to manufacturer's instructions (Macherey-Nagel). DNA fragments were excised from agarose gel under UV light using a clean scalpel, and incubated with NT1 buffer at 58°C for 15 min, until dissolved. Afterwards, the mix was transferred onto a Nucleospin column, and washed twice with Buffer NT3 at 15870 xg for 1 min in a microcentrifuge. To ensure that no residual carryovers of buffers are present, the column was centrifuged at 15870 xg for 1 min. Purified DNA was finally eluted in 15 µl of de-ionized water by a 1 min centrifugation at 15870 xg. Before sequencing, DNA concentration was determined as described in <u>section 3.2.8.3</u>.

3.2.9.4 Sequencing of DNA

Sequencing was performed by the company Eurofins Genomics using the Sanger Sequencing method (Sanger, Nicklen and Coulson, 1977). The sequencing reaction consists of 150 ng of purified DNA diluted in de-ionized water and 2 µl of the specific primer (10 µM) in a final reaction volume of 17 µl. The mix was transferred to labelled-specific safe-lock tubes (Mix2Seq Kit) provided by the manufacturer. Results were analyzed using the software 4 Peaks.

3.2.10 <u>Statistical analysis</u>

Data representation and statistical analysis were performed using the GraphPad Prism 6.0 software. The two-tailed Student's T test was used for comparisons between two groups; both for paired and unpaired data. For comparisons among multiple groups, the analysis of variance (One-way ANOVA) with Bonferroni post-test was used for unpaired data, and repeated measures (RM) one way ANOVA was used for paired data. A p-value ≤ 0.05 was considered significant.

4. <u>RESULTS</u>

The results of this thesis will be presented in two sections. In the first part, I will address the expression and function of the P2X7 receptor on human monocytes. Here, I will also show evidence of the potential of the P2X7-specific nanobody Dano1 as a therapeutic drug candidate in humans. In the second part, I will show the expression and function of P2X7 on human lymphocytes, focusing on the T cell compartment.

4.1 EXPRESSION AND FUNCTION OF P2X7 ON HUMAN MONOCYTES AND MACROPHAGES

4.1.1 <u>Monocytes show high expression of P2X7 on the cell surface</u>

P2X7 is expressed by most immune cells, particularly in monocytes (Wang et al., 2004). In humans, circulating monocytes are classified according to the expression of CD14 and CD16 in classical (CD14$^+$CD16$^-$), intermediate (CD14$^+$CD16$^+$) and non-classical monocytes (CD14^{dim}CD16$^+$) (Ziegler-Heitbrock, 2000). We used flow cytometry to investigate whether there are any differences in the expression of P2X7 on the different monocyte subpopulations. The gating strategy for the analysis is shown in **Figure 4A**. Leucocytes were identified among live single cells by the expression of CD45, and monocytes were gated according to the expression of CD14 and CD16. The expression of P2X7 was assessed using the P2X7-specific nanobody Dano1, as it will be done in all experiments in this thesis. In order to ensure that the signal obtained is specific, we compared the Median Fluorescence Intensity (MFI) of Dano1 staining with the MFI of an irrelevant nanobody control, namely a nanobody recognizing murine ARTC2.2, a molecule which is not existing in humans. The comparison between the control and specific staining is shown for all experiments, and the statistical analysis comparing different cell types is performed on the resulting signal after subtraction of the control.

In line with published data, we observed high expression of P2X7 on the surface of all peripheral monocyte subtypes (**Figure 4**). Of note, all monocyte subpopulations show a similar level of P2X7 expression (**Figure 4B, C**). However, when the specific (subtracted) signal of the three subpopulations is compared, it becomes evident that CD14^{dim}CD16$^+$ (non-classical) monocytes express less P2X7 than the other subpopulations, and this difference is significant when compared to CD14$^+$ CD16$^+$ monocytes **Figure 4E**).
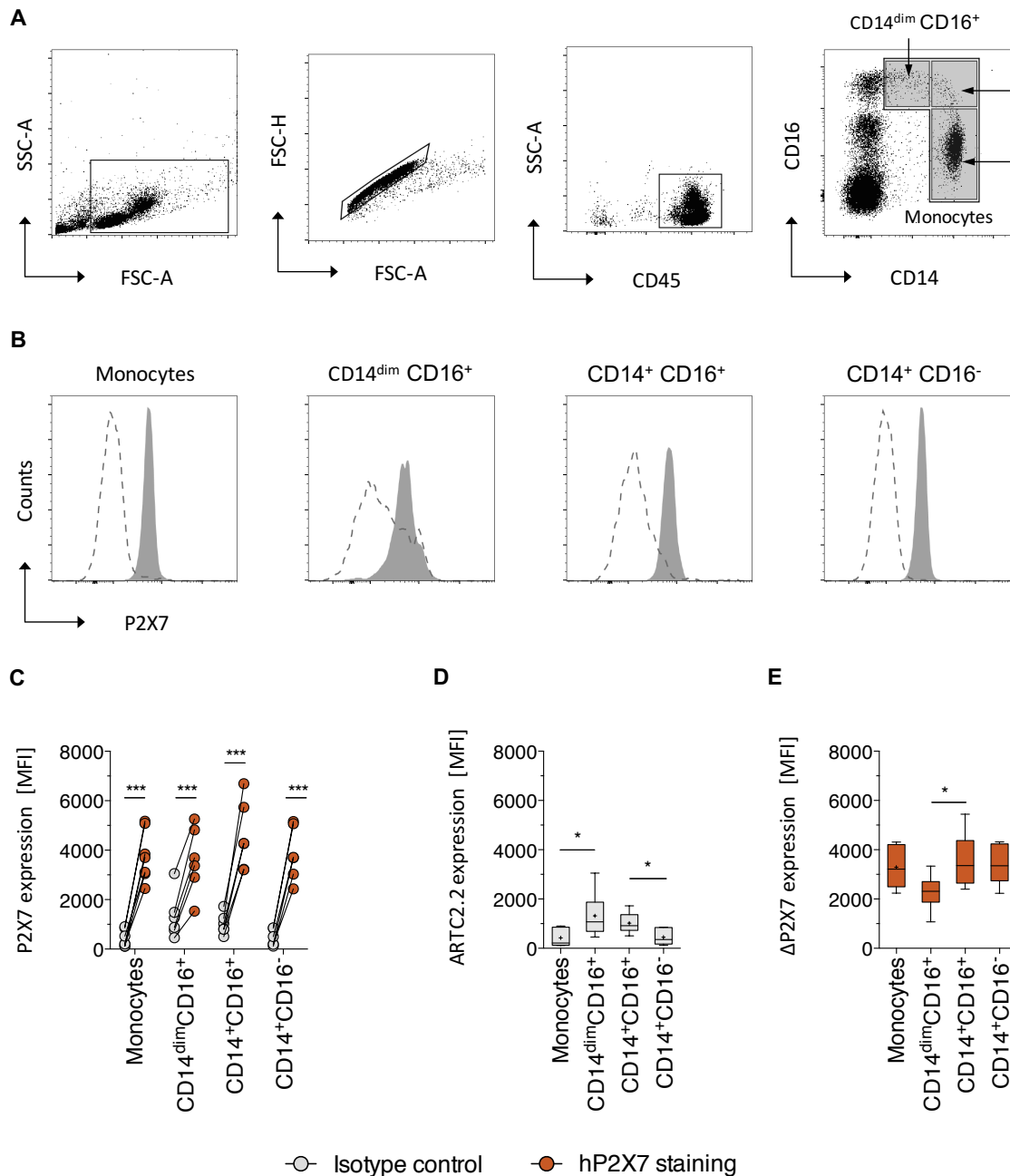
Figure 4. All monocytes subtypes express high levels of P2X7 on the cell surface. (**A**) Dot plots show the gating strategy for the identification of different monocytes subtypes in PBMC samples. (**B**) Expression of surface P2X7 (Median Fluorescence Intensity (MFI) in whole monocytes and in CD14^{dim}CD16^{+}, CD14^{+}CD16^{+}, and CD14^{+}CD16^{-} monocyte subtypes. (**C**) Comparison of P2X7 expression and background for the different monocyte subtypes. P values were determined by paired Student's t test *** = <0.001. (**D-E**) Box and whiskers plots for MFI ± SD of the IC (**D**) and P2X7 expression after subtraction of the MFI of the IC (MFI P2X7 staining − MFI IC) (**E**). P values were determined by paired RM one-way ANOVA, followed by Bonferroni post-test: * = <0.05. Data correspond to one representative donor (**B**) or six healthy individuals (**C-E**).

## 4.1.2 P2X7 blockade by Dano1 impairs ATP-dependent oligomerisation of the inflammasome

LPS stimulation of monocytes induces the synthesis of the IL-1β and IL-18 precursors, resulting in the accumulation of pro-IL-1β in the cytoplasm. A second stimulus is required for the processing of mature IL-1β. ATP-gating of P2X7 can provide such a second signal, triggering the recruitment and polymerisation of ASC proteins into large complexes termed ASC specks. The binding of ASC to procaspase-1 induces the proteolytic cleavage and conversion of procaspase-1 into active caspase-1, which mediates the maturation of immature pro-IL-1β and pro-IL-18 into active IL-1β and IL-18, respectively (Ferrari et al., 2006; Cheng et al., 2009). To assess the potential of P2X7 nanobodies for human therapy, we first investigated the ability of the P2X7-specific nanobody Dano1 for blocking the formation of ASC specks. For this, we used a recently described flow cytometry-based protocol (Sester *et al.*, 2015), which relies on the detection of changes in the pulse of emitted fluorescence upon inflammasome activation. The authors showed that the relocalisation of ASC into dense specks induces an increased height of the fluorescent pulse associated with a decrease in the fluorescent pulse width, which is easy to detect by flow cytometry and, in contrast to microscope-based strategies, allows for exact quantification of ASC formation.
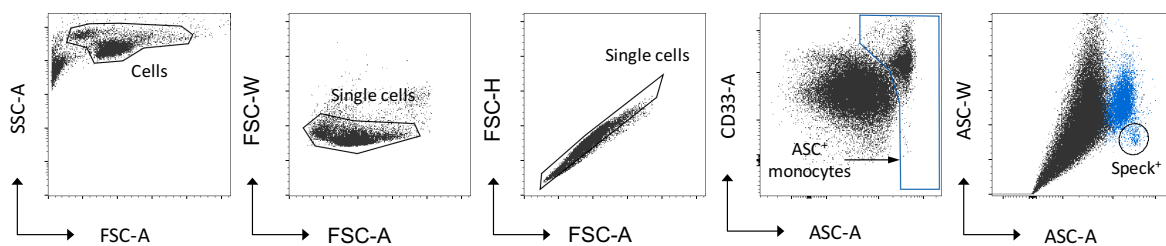
Figure 5. Gating strategy for the detection of ASC specks in human blood monocytes for monitoring of inflammasome oligomerisation. PBMCs were fixed and stained with an antibody against the adaptor protein ASC, following treatment with LPS (100 ng/ml) and ATP (2.5 or 5 mM). Cells were gated based on their size and granularity in the plot FSC-A/SSC-A in order to exclude debris from the analysis. Doublets were excluded in the FSC-A/FSC-W (W=width) and FSC-H/FSC-A plots. Monocytes were identified using the myeloid marker CD33, and the formation of ASC specks (black circle) was calculated as the percentage of ASC-positive monocytes (blue gate).

LPS-stimulated PBMCs were stained with the myeloid marker CD33 and with an antibody directed against the intracellular ASC adaptor protein. Flow cytometry analysis was performed in accordance with the gating strategy described in the original paper (Sester et al., 2015). Briefly, after exclusion of cell debris and doublets, cells were gated according to the expression of CD33 and ASC (CD33$^+$ASC$^+$ cells). ASC specks were defined by ASC-W versus ASC-A, considering as speck$^+$ cells the population displaying a reduction in the fluorescent pulse width (**Figure 5**).

As expected, priming with LPS alone did not result in ASC-speck formation in healthy donors, and neither did stimulation with ATP alone (**Figure 6A**). In contrast, stimulation of LPS-primed human PBMCs with low (2.5 mM) or high (4.5 mM) concentrations of ATP induced the recruitment and assembly of the inflammasome into specks (**Figure 6**). Furthermore, addition of Dano1, but not a control nanobody, prior to stimulation with ATP, resulted in a significant blockade of ASC-speck formation (**Figure 6B**).
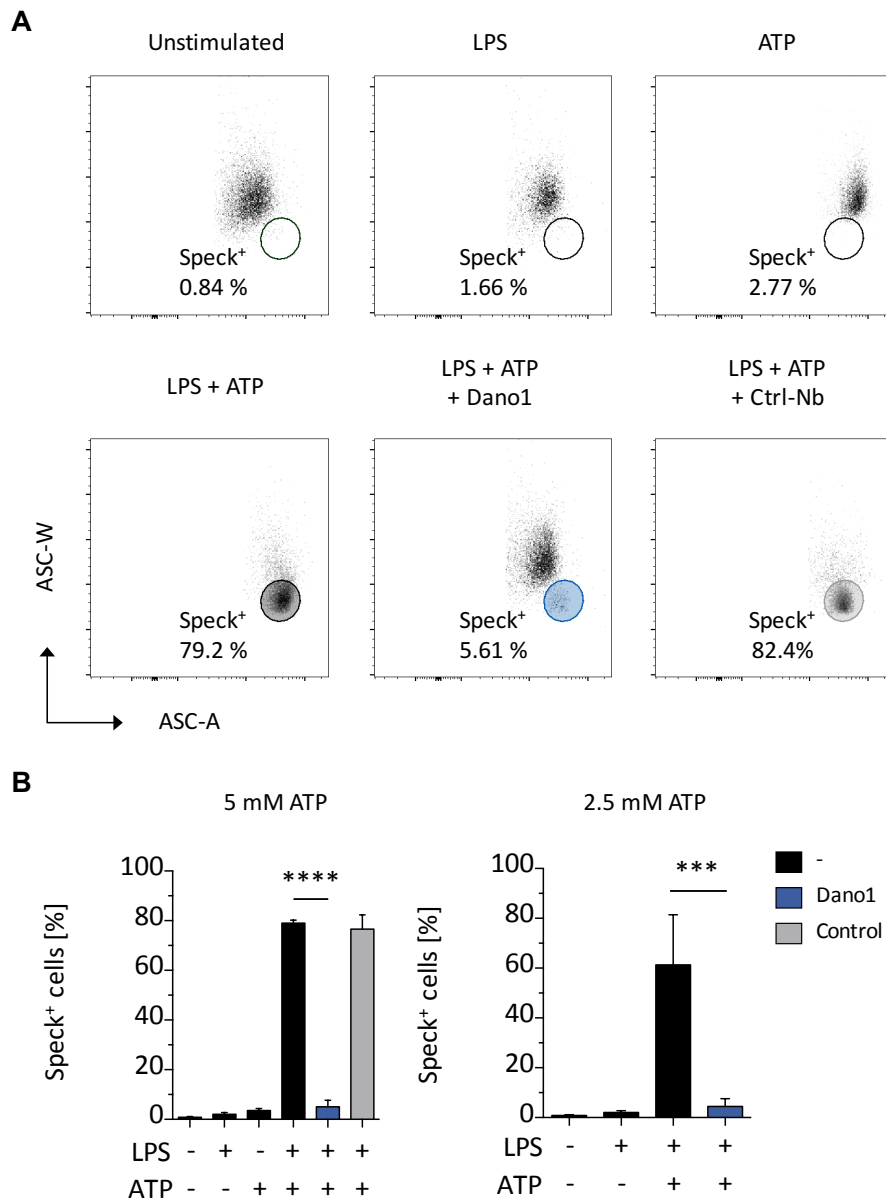
Figure 6. Dano1 blocks ATP-dependent activation of the inflammasome. Human PBMCs were treated for 2 hours with LPS (100ng/ml) and with ATP (2.5 mM and 5 mM) for 0.5 hours in the absence or presence of the P2X7-specific Nb Dano1-mFc (fused to Fc domain of mouse IgG1) or a control Nb-mFc against Toxin A from *C. difficile* (200 nM). (**A**) Representative FACS plots showing the formation of ASC-specks: upper row from left to right (unstimulated, + LPS, + ATP); lower row from left to right (LPS + ATP (5mM), LPS + ATP (5mM) + Dano1-mFc, LPS + ATP (5mM) + control Nb-mFc). (**B**) Percentage of ASC-speck+ monocytes (Mean ± SD, n = 3 donors) upon stimulation with 5 mM (left) or 2.5 mM ATP (right). Data is representative of one experiment of a set of two (n=6). P values were determined by one-way ANOVA, followed by Bonferroni post-test: ***= <0.001.

Inflammasomes are also activated by a large variety of microbial molecules, danger signals and crystalline substances, in a P2X7-independent fashion (Cullen et al., 2015). To further confirm the specificity of Dano1 to block ATP-dependent inflammasome activation, we stimulated PBMCs with different concentrations of nigericin instead of ATP. Similar to ATP, nigericin induced recruitment and oligomerisation of ASC in LPS-primed PBMCs but not in unprimed PBMCs (**Figure 7**). Nigericin induces the opening of Pannexin-1 channels, leading to a decrease in intracellular levels of K^+ and the subsequent activation of the inflammasome (Pelegrin and Surprenant, 2007). Interestingly, stimulation with nigericin did not result in such a clear population of speck$^+$ cells, as it was the case upon stimulation with ATP (**Figure 6A, 7A**). As expected, Dano1 was only effective after treatment with ATP **Figure 6B**), but had little if any effect on P2X7-independent inflammasome activation induced by nigericin (**Figure 7**). Additionally, preincubation with a control nanobody also did not alter inflammasome activation. These results indicate that Dano-1 blocks inflammasome activation in response to ATP in human monocytes.
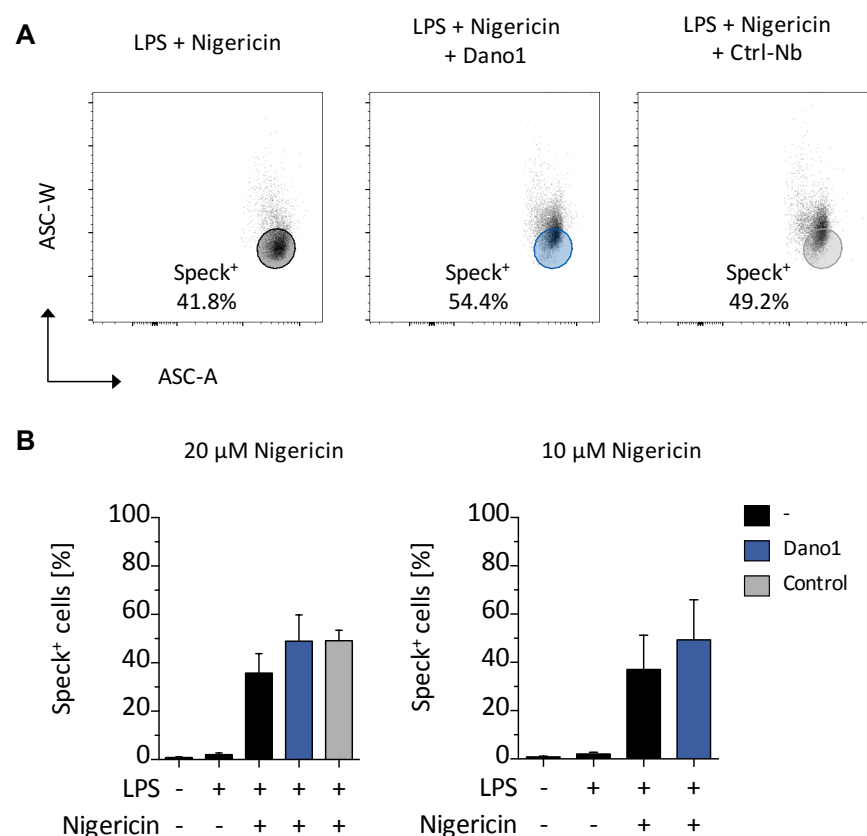

Figure 7. Dano1 does not have an effect on P2X7-independent inflammasome activation. Human PBMCs were treated for 2 hours with LPS (100ng/ml) and with nigericin (10μM and 20 μM) for 0.5 hours in the absence or presence of the P2X7-specific Nb Dano1-mFc or a control Nb-mFc (200 nM). (**A**) Representative FACS plots showing the formation of ASC-specks under specific conditions. From left to right: LPS + Nigericin (20 μM); LPS + Nigericin (20 μM) + Dano1-mFc; LPS + Nigericin (20 μM) + control Nb-mFc. (**B**) Percentage of ASC-speck$^+$ cells (Mean ± SD, n = 3 donors) upon stimulation with 20 μM (left) or 10 μM nigericin (right). Data are representative of one experiment of a set of two (n=6). P values were determined by one-way ANOVA, followed by Bonferroni post-test.

4.1.3 Dano1 abolishes ATP-induced release of IL-1β by monocytes

IL-1β is an important mediator of the inflammatory response, and is involved in a variety of cellular activities, including cell proliferation, differentiation, and apoptosis. In contrast to other proinflammatory cytokines, IL-1β is synthesized as a precursor and cleaved by caspase-1 to produce the mature form, which is subsequently released (Dinarello, 2009). The role of P2X7 for inducing the cleavage of the precursor pro-IL1β has been extensively investigated (Giuliani et al., 2017). To evaluate the potential of Dano1 in blocking IL-1β production, we used a surrogate inflammation *in vitro* model, which is the stimulation of freshly obtained human blood with LPS and ATP, and subsequent measurement of IL-1β production in the serum after incubation.

First, we aimed to determine an optimal concentration of ATP to induce an adequate release of IL-1β to be measured by ELISA. As shown in **Figure 8A**, both concentrations of ATP (2.5 and 5 mM) induced the release of high amounts of IL-1β. Of note, the lack of one of the two signals, either priming with LPS or treatment with ATP, resulted in no release of IL-1β. Furthermore, preincubation with Dano 1 significantly prevented the release of IL-1β (**Figure 8A**).

Second, to further confirm the capacity of Dano1 to antagonise P2X7 *in vitro*, we treated human blood with the P2X7 receptor agonist benzoyl-ATP (bzATP), which exhibits greater potency than ATP. Unlike stimulation with ATP, where a concentration higher than 0.5 mM is needed to induce release of IL-1β (**Figure 8C**), the same concentration of bzATP induced a sizeable release of the cytokine (**Figure 8B**). As we expected, Dano1, but not a control Nb, efficiently blocked the release of IL-1β after stimulation with both ATP and bzATP (**Figure 8A, B**).
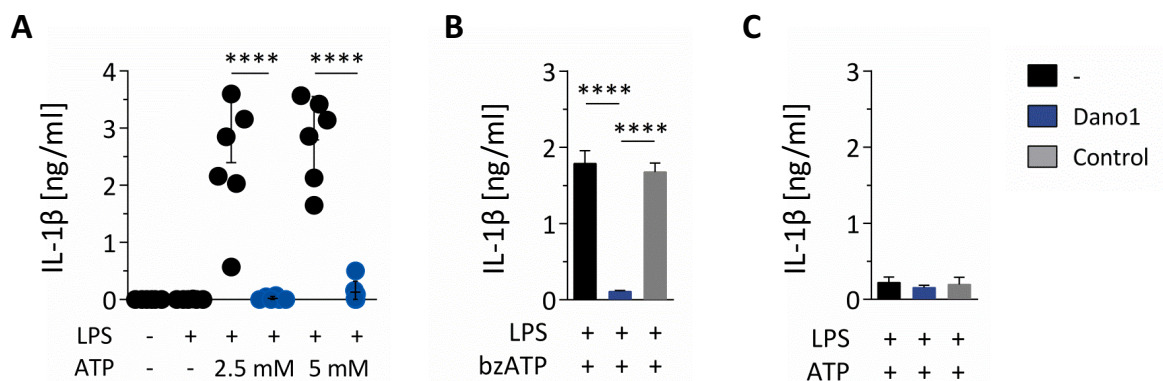
Figure 8. Dano1 blocks the ATP-dependent release of IL-1β by LPS-primed human monocytes. Fresh human blood was treated with LPS (1μg/ml) for 1.5 hours at 37°C, 5% CO2, and further incubated with ATP or bzATP for 0.5 hour at 37°C. Levels of IL-1β [ng/ml] in plasma were monitored by ELISA. (**A**) LPS-treated human blood was incubated with either 2.5 mM or 5 mM of ATP under the absence or presence of 100nM Dano1-rbFc (n=6). (**B-C**) LPS-treated human blood was incubated with 0.5 mM bzATP (**B**) or ATP (**C**) under the absence or presence of 100 nM of Dano1-mFc or a control Nb-mFc (α-Toxin A *C.difficile*) (n=3). P values were determined by one-way ANOVA, followed by Bonferroni post-test: **** = <0.0001.

Finally, to assess the specificity of the signal blocked, we used blood of a patient with cryopyrin-associated periodic syndrome (CAPS). CAPS are rare autoinflammatory diseases characterized by a gain-of-function mutation in the NLRP3 inflammasome that leads to its constitutive activation, bypassing the signal provided by external stimuli such as ATP (Cordero, Alcocer-Gómez and Ryffel, 2018). The patient with CAPS presented a very high production of IL-1β after stimulation with only LPS, while stimulation with LPS alone resulted in no production of IL-1β in the healthy control. Interestingly, Dano1 did not abolish the massive production of IL-1β in the patient with CAPS (**Figure 9**), demonstrating the specificity of Dano1 for blocking ATP-P2X7-dependent activation of the inflammasome but not constitutive activation of the inflammasome.
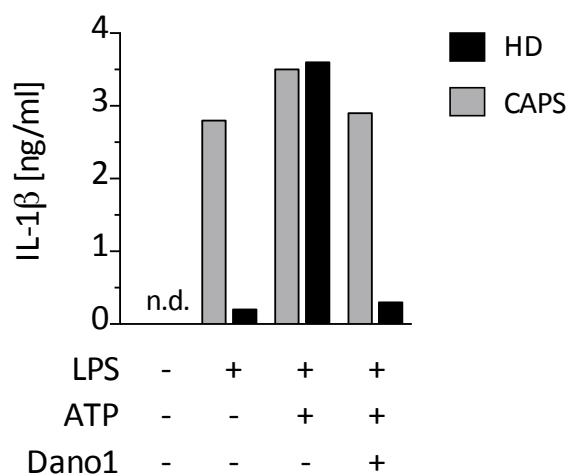
Figure 9. Dano1 specifically blocks ATP-induced release of IL-1β by LPS-primed human monocytes. Fresh human blood from a healthy donor (black) or a patient with CAPS (grey) was treated with LPS (1µg/ml) for 1.5 hours at 37°C, 5% CO2, and further incubated with ATP (2.5 mM) for 0.5 hour at 37°C under the absence or presence of Dano1-mon. Data are of a single experiment. Legend: HD = healthy donor; CAPS: patient with cryopyrin-associated periodic syndrome.

4.1.4   Dano1 exhibits higher potency for blocking P2X7 compared to currently used antagonists

To evaluate the potential of Dano1 as a therapeutic drug, we compared the blocking capacity of the nanobody with two small molecule antagonists that are currently in preclinical development, JNJ47965567 (Jansen) and AZ10606120 (AstraZeneca). All healthy donors responded to the treatment with great secretion of IL-1β, which was abolished when the blood was preincubated with Dano1 (**Figure 10**). Dano1 blocked ATP-induced release of IL-1β at subnanomolar IC50 (0.13 ± 0.05 nM), while both small-molecule antagonists were used at submicromolar IC50 (JNJ47965567 = 253.1 ± 197.2; and AZ10606120 = 352.6± 31.8). Therefore, Dano 1 demonstrated up to 2000-fold higher potency than the small-molecule antagonists currently in preclinical development.
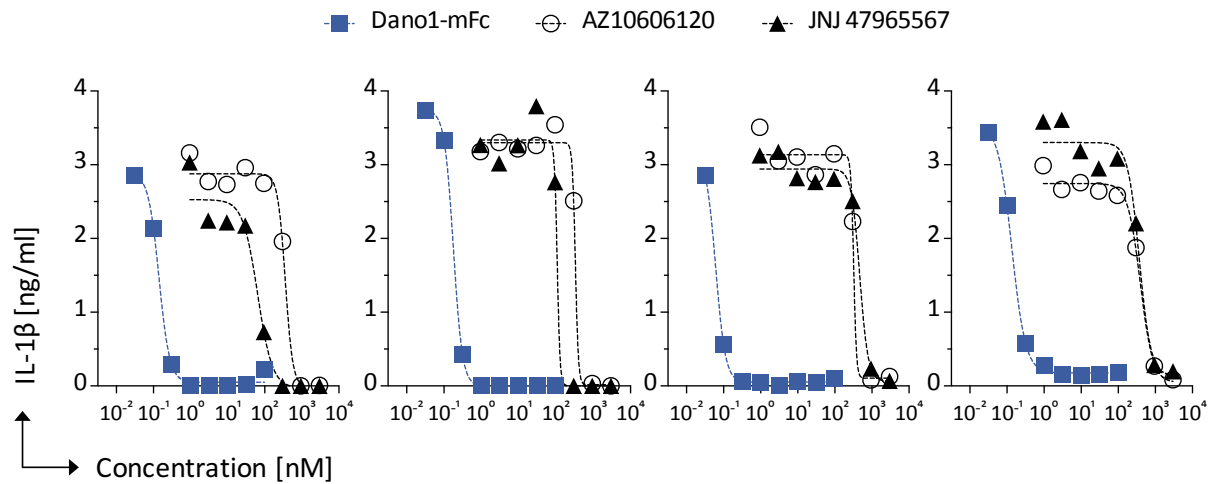
Figure 10. **Dano 1 blocks ATP-induced release of IL-1β at subnanomolar IC50 values.** Fresh human blood was treated with LPS (1µg/ml) for 1.5 hours at 37°C, 5% CO_2, and further incubated with 2.5 mM ATP in the presence of serial dilutions of Dano1-mFc or the small-molecule antagonists JNJ47965567 or AZ10606120. Data are of four healthy donors (n=4).

Altogether, our data demonstrate the specificity of Dano1 for blocking P2X7-mediated induction of IL-1β, underlining its potential as an innovative pre-clinical drug candidate (Danquah *et al.*, 2016).

4.1.5 Multimeric nanobodies exhibit enhanced potency than the monomeric constructs

Since the lab of Prof. Nolte had previously demonstrated that dimerisation of mouse specific P2X7-nanobodies improved binding affinity and enhanced their functional potency (Danquah *et al.*, 2016), we assessed whether multimerisation of Dano1 would also enhance its blocking capacity. Dimeric nanobodies were obtained by genetic linkage of two monomers with a 35 glycine-serine linker (Gly/Ser) (Danquah *et al.*, 2016). To investigate their blocking potential, LPS-primed human blood was incubated with different formats of the nanobody Dano1: in its monomeric form, as a dimer and as a dimer fused with the Fc domain of rabbit IgG. All nanobody constructs showed a good antagonist effect and blocked the release of IL-1β (**Figure 11**). Furthermore, dimerisation of Dano1 and fusion to an Fc domain resulted in lower IC50 values (Dano1-mon = 3.74 nM; Dano1-dim = 0.57 nM; Dano1-rbFc = 0.07 nM). Therefore, bivalent Nbs exhibit higher potency than monomeric constructs.
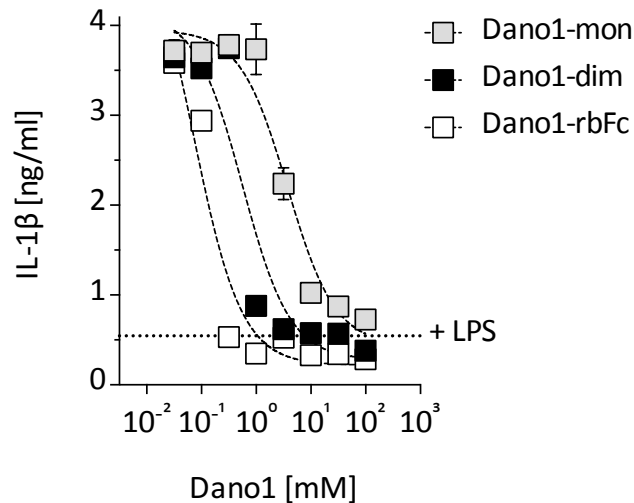
Figure 11. Dimerisation of Dano1 results in enhanced blocking of IL-1β release by LPS-primed human monocytes. LPS-treated human blood was incubated with serial dilutions of Dano1-mon (monomer), Dano1-dim (dimer) or Dano1-rbFc (fused to rabbit Fc) prior to stimulation with ATP (2.5 mM). Data are representative of a single experiment (n=1).

4.1.6   Dano1 can also alter the transcription of genes regulated by the NF-κB pathway

Beyond IL-1 production, which is driven by inflammasome activation, we wanted to address whether Dano1 would exert an effect on other major inflammatory pathways, for instance the transcription of genes controlled by NF-κB signalling. To this end, we stimulated monocytes with LPS and measured the transcription of *IL1B*, *IL6* and *TNF* by qRT-PCR. For this experiment, we used two different constructs of the nanobodies, one fused with the Fc-domain of rabbit IgG (rbFc), and the other construct fused to the albumin-binding nanobody Alb8 (dimAlb); both resulting in an increased half-life of the Nb *in vivo* (Tijink *et al.*, 2008)*.* Our results show that Dano1 does not impair P2X7-independent transcription of *IL1B* (**Figure 12A**) and *IL6* (**Figure 12B**). Similarly, treatment under the presence of a control Nb did also not have an effect on the transcription of these genes (**Figure 12A, B**). Unexpectedly, we detected a reduced expression of the *TNF* gene after treatment in the presence of both Dano1 and a control Nb (**Figure 12C**). Of note, this effect was reproduced in three independent experiments, regardless of the specificity and format of the Nbs.
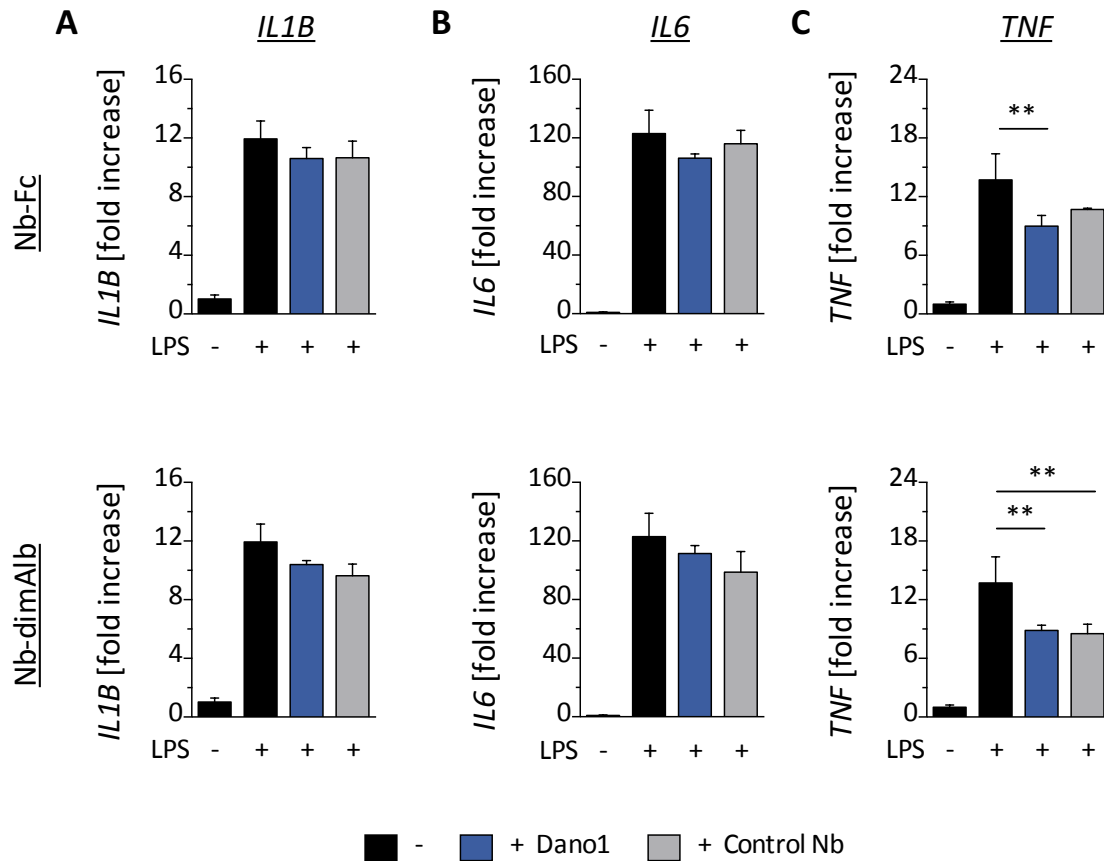
Figure 12. Dano1 decreases the expression of *TNF* but not *IL1B* and *IL6* in LPS-treated human monocytes. P2X7-independent activation of NF-κB–mediated transcription of *IL6*, *IL1B* and *TNF* in purified human blood monocytes was monitored by quantitative reverse transcription PCR (qRT-PCR) after priming with LPS for 3 hours in the absence or presence of either 200 nM Dano1-mFc or control Nb-mFc (upper row), or Dano1-dimAlb or control Nb-dimAlb (lower row). Control nanobody was specific for mouse ARTC2.2. (**A-C**) The graphs show the fold increase in the transcription of *IL1B* (**A**), *IL6* (**B**) and *TNF* (**C**) genes (Mean ± SD, n = 4). Data are relative to the expression of the reference gene *GAPDH* and were calculated using the delta-delta Ct formula (2–ΔΔCt). Data are representative of three independent experiments. P values were determined by one-way ANOVA, followed by Bonferroni post-test: ** = <0.01.

4.2 EXPRESSION AND FUNCTION OF P2X7 ON HUMAN LYMPHOCYTES

4.2.1 NK cells exhibit the highest expression of surface P2X7 among all lymphocytes

In order to determine the expression of P2X7 in lymphocytes, we designed antibody panels for the identification of the lymphocyte subsets. We first analysed the expression of P2X7 on the three major types of lymphocytes: B cells (CD19^{+}), T cells (CD3^{+}) and NK cells (CD16^{+} CD3^{-} CD19^{-}). Classical monocytes were gated based on the expression of CD14 (**Figure 13A**), and used as positive control for the expression of P2X7.
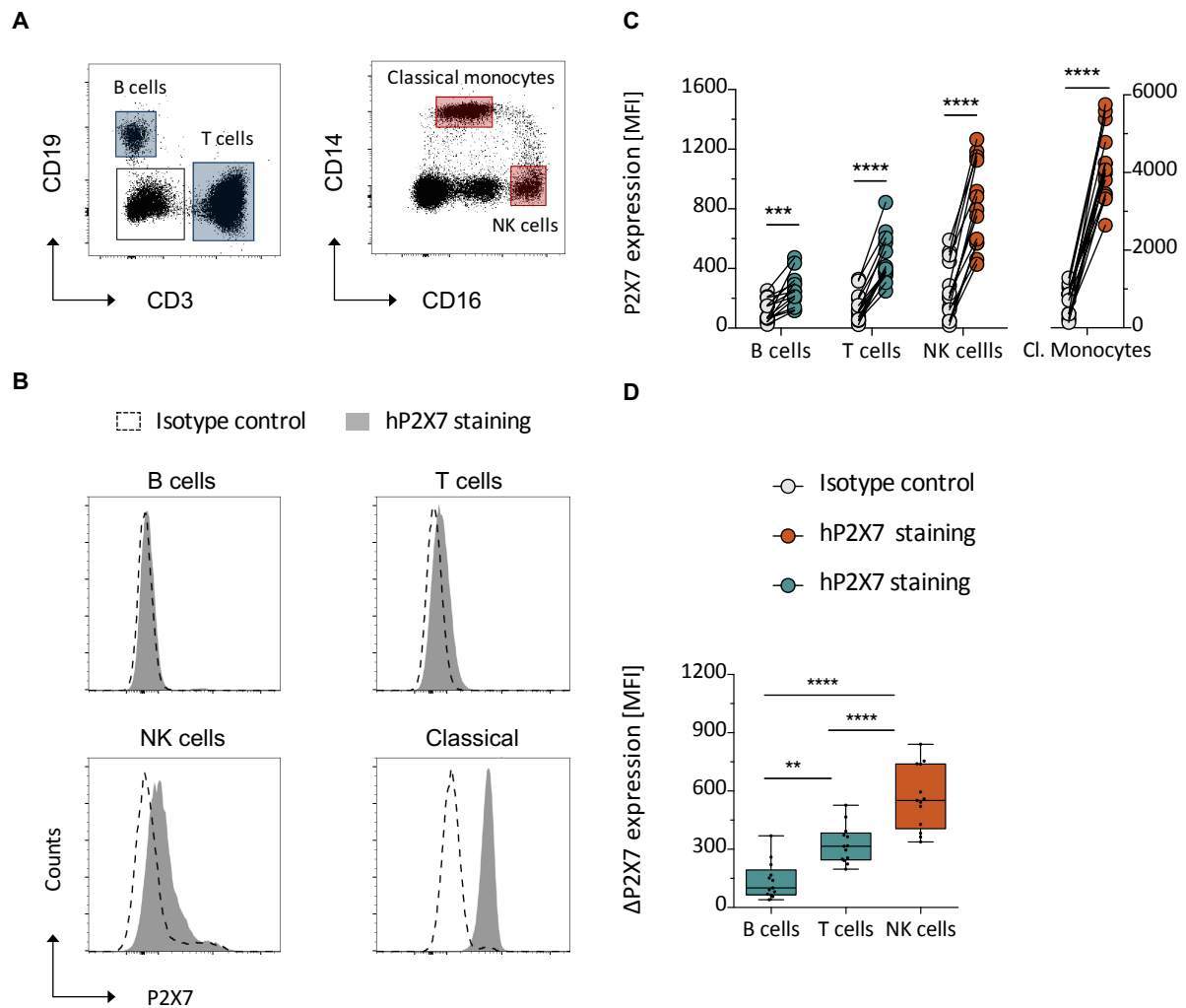
Figure 13. P2X7 is differentially expressed among distinct lymphocyte populations. (**A**) Gating strategy for the identification of the different lymphocyte subtypes and classical monocytes. (**B**) P2X7 expression (MFI) on the surface of B cells (CD19$^+$), T cells (CD3$^+$), NK cells (defined as CD3$^-$CD19$^-$CD16$^+$ in the lymphocyte gate) and classical monocytes (CD3$^-$CD19$^-$CD14$^+$). The number of cells in the histogram plot was normalised for each population. (**C**) Expression of P2X7 (MFI) and background signal detected on the IC for the different immune cell subtypes. (**D**) Expression of P2X7 (MFI ± SD) after subtracting the MFI of the IC from the MFI of the P2X7 staining (MFI P2X7 - MFI IC). Histograms in (**B**) are representative of one donor while thirteen healthy donors are shown in (**C-D**). P values were determined by paired Student's t test, or by paired RM one-way ANOVA, followed by Bonferroni post-test: * = <0.05; ** = <0.01; *** = <0.001; **** = <0.0001. Legend: red = innate immune cells // blue: adaptive immune cells.

Due to the complexity of the P2X7 staining, we first determined for each cell subset whether there are differences between the MFI of the P2X7 staining and the MFI of the isotype control (IC). We found significant differences between the MFI of both stainings in all immune cell populations (**Figure 13C**). Of note, we did not find any differences in the MFI among isotype controls. All lymphocyte subsets displayed relatively low amounts of P2X7 compared to classical monocytes (**Figure 13B, C**). Interestingly, NK cells expressed significantly higher levels of P2X7 than T and B cells, the latter showing negligible specific staining. To further confirm these results, we subtracted the IC from the P2X7 staining in order to obtain a single MFI value for the comparison of P2X7 expression.

After subtraction, we confirmed the higher expression of P2X7 on NK cells compared to T and B cells (**Figure 13D**).

Our data suggest a distinct pattern of expression within the lymphocyte compartment, where NK cells express the most P2X7 on their surface, followed by T cells and ultimately by B cells.

4.2.2 CD4$^+$ CD25$^+$ CD127$^-$ regulatory T cells express lower levels of P2X7 than conventional CD4 T cells

We next aimed to assess the pattern of expression within the T cell compartment. Tregs were gated according to expression of CD25 and CD127 (CD4$^+$ CD25^{high} CD127$^-$) within the CD4 T population. The remaining CD4 T cells were considered "conventional CD4 T cells" (**Figure 14A**).
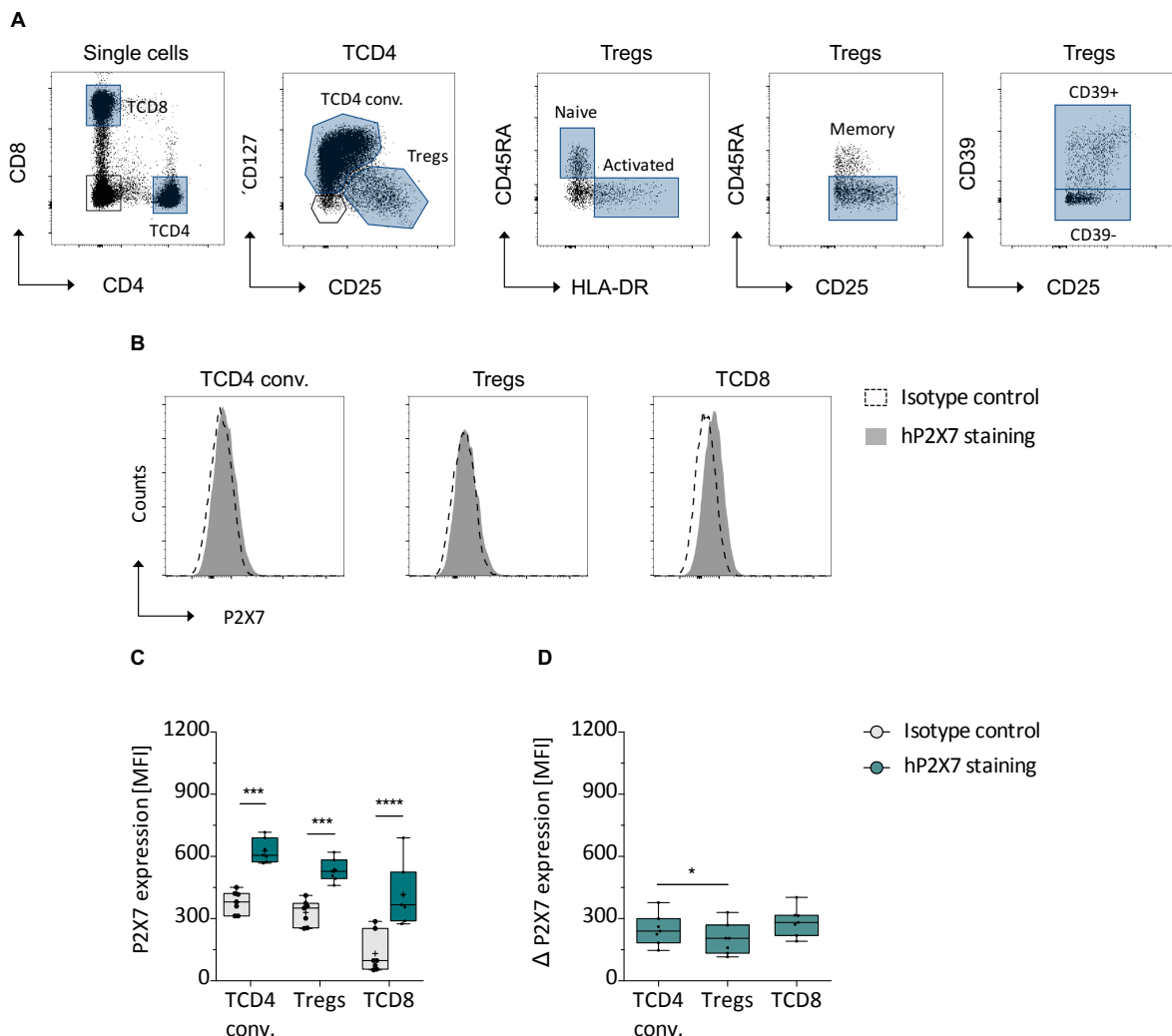
Figure 14. Human Tregs express lower levels of P2X7 than conventional CD4 T cells (**A**) Gating strategy for the identification of distinct T cell subtypes. (**B**) P2X7 expression (MFI) on the surface of CD8 T cells (CD3$^+$CD8$^+$), conventional CD4 T cells (TCD4conv., CD4$^+$ CD25$^{-/low}$ CD127$^+$) and Tregs (CD4$^+$CD25$^+$CD127$^-$). Number of cells was normalised. (**C**) Expression of P2X7 (MFI ± SD) and background signal detected on the IC of distinct T cell subsets. (**D**) Expression of P2X7 (MFI ± SD) after subtraction of the MFI of the IC from the MFI of the P2X7 staining (MFI P2X7 - MFI IC) on the surface of distinct T cell subsets. Data are representative of one (**B**) or seven

(**C-D**) healthy donors. P values were determined by paired Student's t test, or by paired RM one-way ANOVA, followed by Bonferroni post-test: * = <0.05; ** = <0.01; *** = <0.001; **** = <0.0001. Legend: blue = adaptive immune cells (**C-D**).

All three T cell subsets (conventional CD4, Tregs and CD8) showed low levels of P2X7 on their surface (**Figure 14B, C**), but still significantly different from the negative control (**Figure 14C**). At first, it seems that CD8 cells had lower levels of P2X7, however, when the negative staining was subtracted, CD8 T cells showed similar expression of P2X7 than CD4 T cells, while Tregs had the lowest expression (**Figure 14D**). Therefore, the apparent differences seen in **Figure 14C** were rather caused by the lower fluorescent signal of the stainings in CD8 T cells using this constellation of surface markers.

4.2.3 P2X7 is preferentially expressed in effector and memory CD4 T cells

We next investigated at which stage of maturation/differentiation do T cells express higher levels of P2X7. To this end, we used CD27 and CD45RA to define naive (CD27$^+$ CD45RA$^+$), central memory (CM, CD27$^+$ CD45RA$^-$), effector memory CD45RA positive (TEMRA, CD27$^-$CD45RA$^+$) and effector memory (EM, CD27$^-$ CD45RA$^-$) phenotypes in CD4 and CD8 T cells. In addition, we identified effector T cells based on the lack of expression of CD27 and CD28 (CD27$^-$CD28$^-$ cells). The gating strategy for the identification of the distinct effector subsets is represented on **Figure 15A**. TEMRA CD4 T cells were not analysed due to insufficient cell number.

All cell subsets were significantly positive (although with low expression) for P2X7 (**Figure 15B, C**). Interestingly, CM CD4 T cells showed higher expression of surface P2X7 than the whole population of CD4 T cells (**Figure 15C**). These results were confirmed by comparison of P2X7 staining after subtraction of IC (**Figure 15D**). We also observed that CM and EM cells expressed higher levels of P2X7 than naïve CD4 T cells (**Figure 15D**).
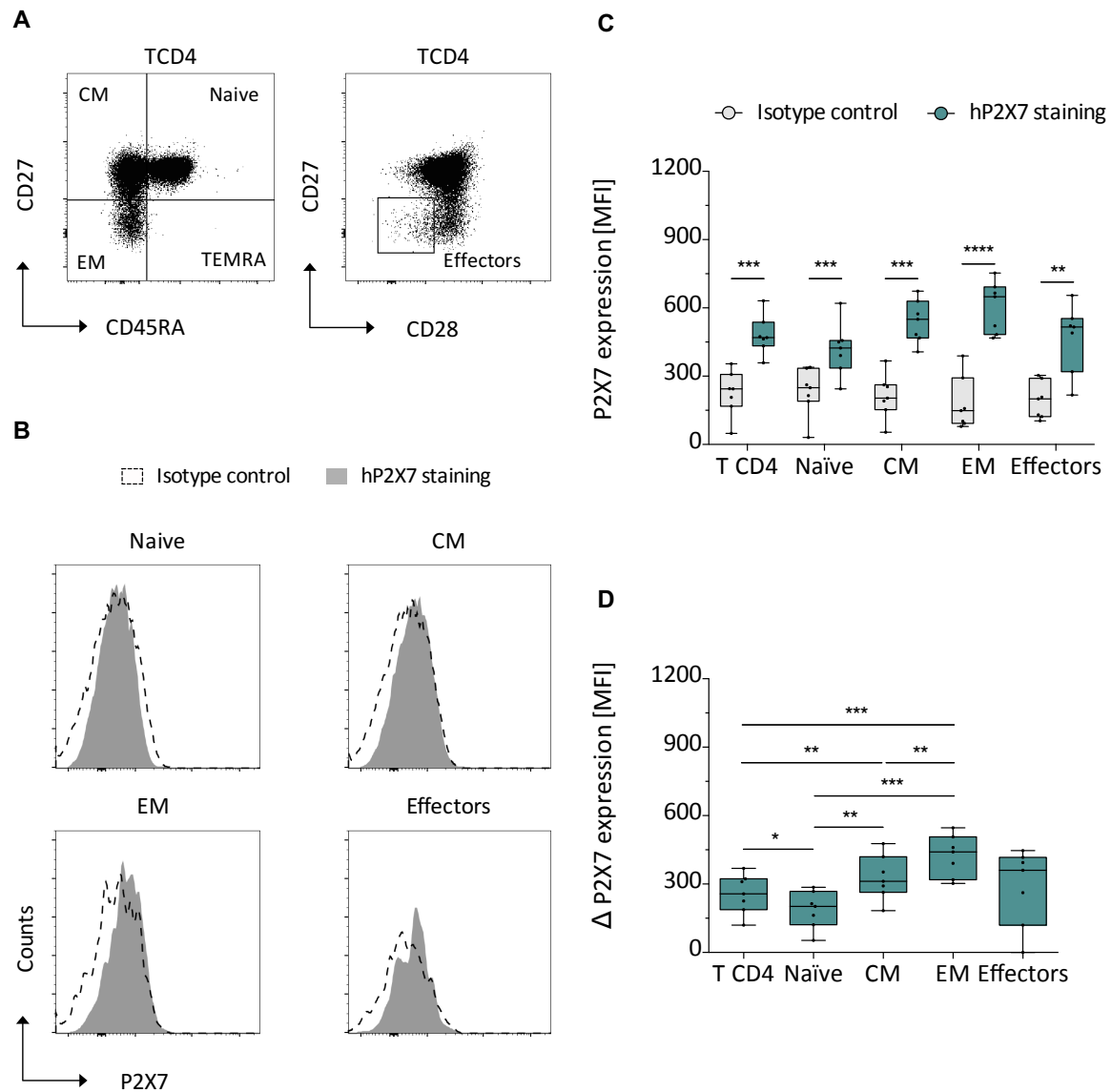
Figure 15. CD4 T cells with effector phenotype express higher levels of P2X7 than naïve cells. (**A**) Gating strategy for the identification of different T cell effector subtypes. (**B**) P2X7 expression (MFI) on the surface of naïve (CD27$^+$CD45RA$^+$), central memory (CM, CD27$^+$CD45RA$^-$), effector memory (EM, CD27-CD45RA$^-$) and effectors (CD27$^-$CD28$^-$) CD4 T cells. (**C**) Expression (MFI ± SD) of P2X7 and background signal detected on the IC on the surface of different CD4 effector subsets. (**D**) Expression of P2X7 (MFI ± SD) after subtraction of the MFI of the IC from the MFI of the P2X7 staining (MFI P2X7 - MFI IC) on the surface of different effector CD4 T cell effector subsets. Data are representative of one (**B**) or seven (**C-D**) healthy donors. P values were determined by paired Student's t test, or by RM one-way ANOVA, followed by Bonferroni post-test: * = <0.05; ** = <0.01; *** = <0.001; **** = <0.0001. Legend: blue = adaptive immune cells (**C-D**).

Similarly, we also determined the pattern of P2X7 expression within distinct Tregs subpopulations according to maturation status (**Figure 14A**); and observed that activated (HLA-DR$^+$), memory (CD45RA) and CD39$^+$ Tregs expressed higher levels of P2X7 than naïve Tregs (CD45RA$^+$) (data not shown).

Since P2X7 is involved in the polarization of T cells towards the Th1 and Th17 phenotypes (Schenk *et al.*, 2011; Salles *et al.*, 2017), we assessed the expression of P2X7 on distinct Th subtypes defined

according to expression of different chemokine receptors (Becattini *et al.*, 2015). Th17 cells were identified as CCR6$^+$ CCR4$^+$ CXCR3$^-$, Th1/Th17 cells as CCR6$^+$ CCR4$^-$CXCR3$^+$, Th2 as CCR6$^-$ CCR4$^+$ CXCR3$^-$ and Th1 as CCR6$^-$ CCR4$^-$ CXCR3$^+$ (**Figure 16A**). All T helper cell subtypes (**Figure 16C**) tend to express higher levels of P2X7 than whole CD4 cells, which contain the naïve subset, and P2X7 expression was significantly higher on Th1 and Th17 cells (**Figure 16D**).
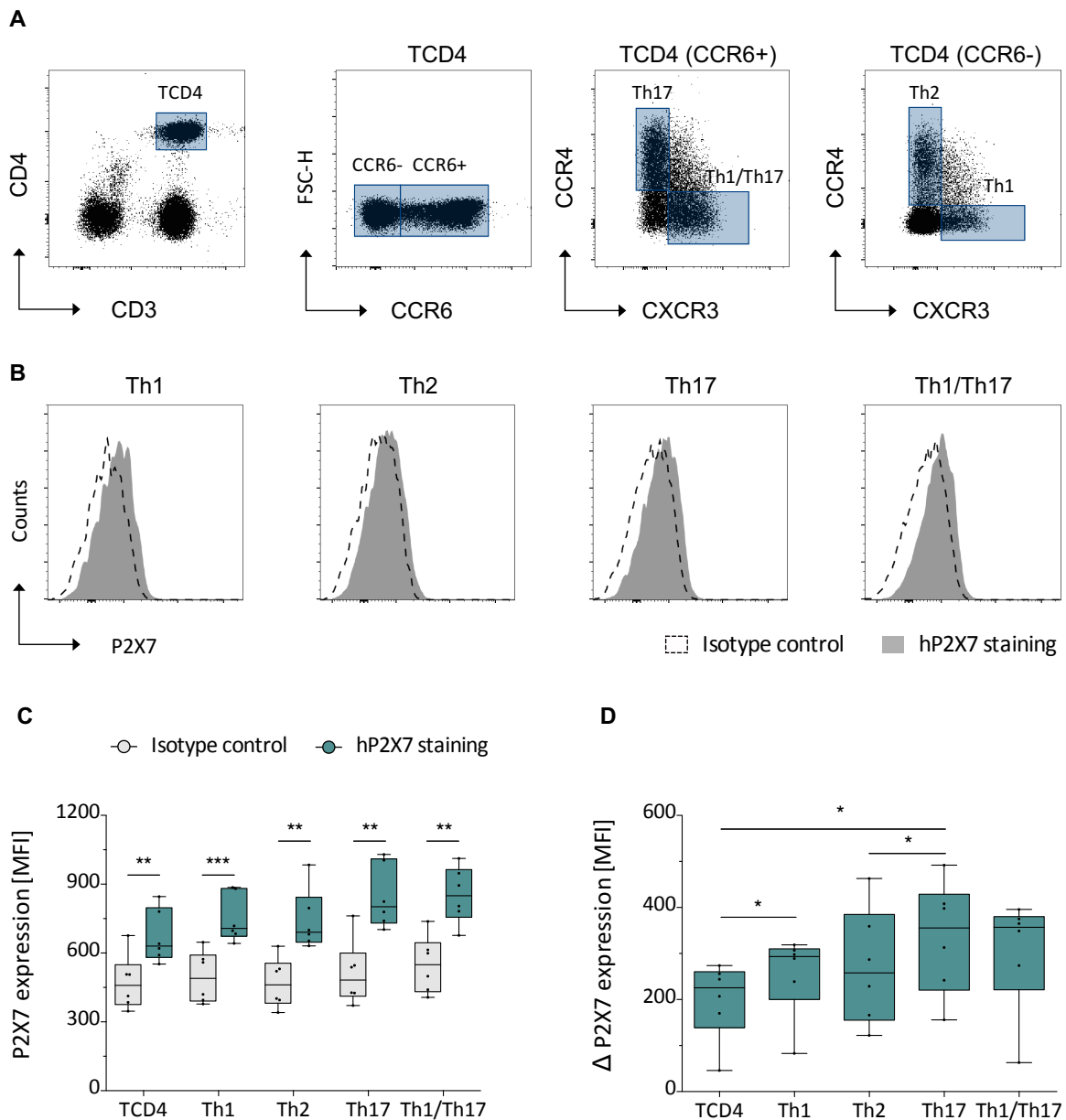
Figure 16. Proinflammatory Th1 and Th17 cells express higher levels of P2X7. (**A**) Gating strategy for the identification of distinct T helper cells. (**B**) P2X7 expression (MFI) on the surface of Th17 cells (CCR6$^-$ CCR4$^+$CXCR3$^-$), Th1/Th17 (CCR6$^-$CCR4$^-$CXCR3$^+$), Th2 (CCR6$^+$CCR4$^+$CXCR3$^-$) and Th1 cells (CCR6$^+$CCR4$^-$CXCR3$^+$). (**C**) Expression of P2X7 (MFI ± SD) and background signal detected on the IC on the surface of distinct T helper cells. (**D**) Expression of P2X7 (MFI ± SD) after subtraction of the MFI of the IC to the MFI of the P2X7 staining (MFI P2X7 - MFI IC) on the surface of distinct T helper cells. Data are representative of one (**B**) or six (**C-D**) healthy donors. P values were determined by paired Student's t test, or by RM one-way ANOVA, followed by Bonferroni post-test: * = <0.05; ** = <0.01; *** = <0.001. Legend: blue = adaptive immune cells.

In contrast to CD4 T cells, we did not find any differences on the expression of P2X7 on the different CD8 effector subsets, neither before nor after subtraction of the IC (**Figure 17**).
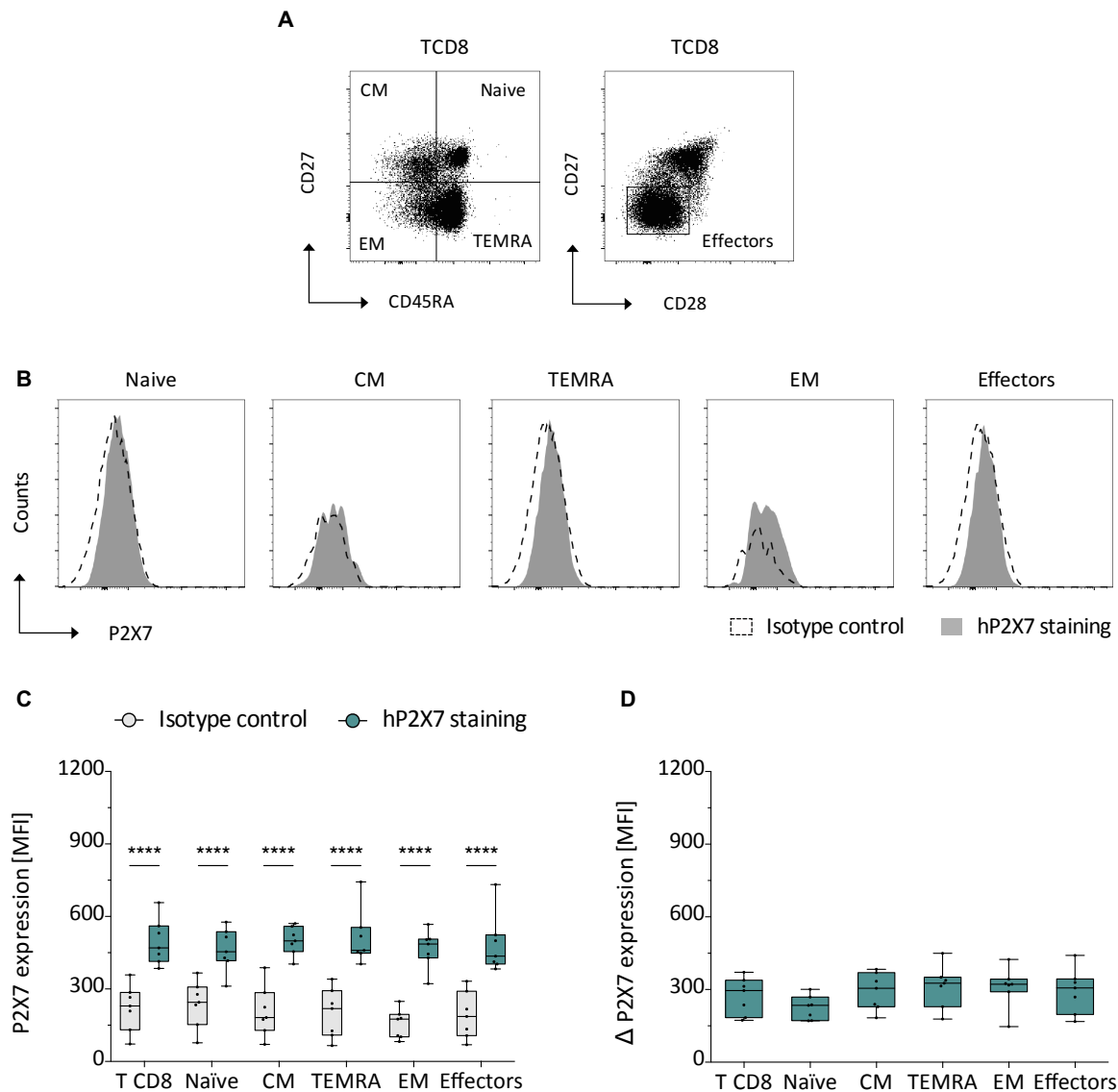
Figure 17. All CD8 T cell subsets express similar levels of P2X7 on the cell surface. (**A**) Gating strategy for the identification of different T cell effector subtypes. (**B**) P2X7 expression (MFI) on the surface of naive (CD27$^+$CD45RA$^+$), central memory (CM, CD27$^+$CD45RA$^-$), effector memory CD45RA positive (TEMRA, CD27$^-$ CD45RA$^+$), effector memory (EM, CD27-CD45RA$^-$) and effectors (CD27$^-$CD28$^-$) CD8 T cells. (**C**) Expression (MFI ± SD) of P2X7 and background signal detected on the IC on the surface of different CD8 effector subsets. (**D**) Expression of P2X7 (MFI ± SD) after subtraction of the MFI of the IC from the MFI of the P2X7 staining (MFI P2X7 - MFI IC) on the surface of different effector CD8 T cell effector subsets. Data are representative of one (**B**) or seven (**C-D**) healthy donors. P values were determined by paired Student's t test, or by RM one-way ANOVA, followed by Bonferroni post-test: **** = <0.0001. Legend: blue = adaptive immune cells.

In summary, CD4 T cells with an activated, effector or memory phenotype express higher levels of P2X7 within CD4 T cells. This pattern was also observed in Tregs, even though they show very low amounts of P2X7. In contrast, the effector phenotype does not correlate with the expression of P2X7 on CD8 T cells, which expressed similar amounts of P2X7 independently of their effector phenotype.

4.2.4 Innate-like lymphocytes exhibit higher levels of P2X7 than conventional T cells

Since NK cells express the highest levels of P2X7 within the lymphocyte compartment, we asked whether other innate lymphocytes or innate-like lymphocytes would also express higher levels of P2X7. In humans, 1-6% of circulating T cells belong to the γδ lineage, being T cells harbouring the Vδ2 chain the most abundant (50-90%) γδ T cell subtype. The gating strategy for the identification of γδ T cells is shown in **Figure 18A**.

T cells from the γδ lineage expressed higher levels of P2X7 on their surface when compared to conventional CD4 and CD8 T cells (**Figure 18**). Within γδ T cells, Vδ2$^+$ cells were the ones expressing the highest levels among all T cell subsets (**Figure 18B**). After subtraction of the unspecific signal, we confirmed the higher expression of P2X7 in both γδ T cells (all) and Vδ2$^+$ cells compared to conventional T cells and Vδ2$^-$ cells (**Figure 18D**).

Another T cell population with a semi-invariant TCR and innate properties are MAIT cells, identified as CD3$^+$ Vα7.2$^+$ CD161$^+$ in **Figure 19A**. Interestingly, MAIT cells exhibited similar expression of P2X7 than γδ T cells (**Figure 19 B-D**), and therefore higher than conventional T cells.

We next assessed P2X7 on the whole population of innate lymphoid cells (ILCs), defined as CD3$^-$ CD127$^+$CD161$^+$, and the two major NK cell subsets: NK dim (CD3$^-$ CD56^{dim}) and NK bright cells (CD3$^-$ CD56^{high}). The gating strategy for the identification of all immune cell populations is represented in **Figure 19A**. We observed higher expression of P2X7 on ILCs and both NK subsets than αβ T cells (**Figure 19E, F**).
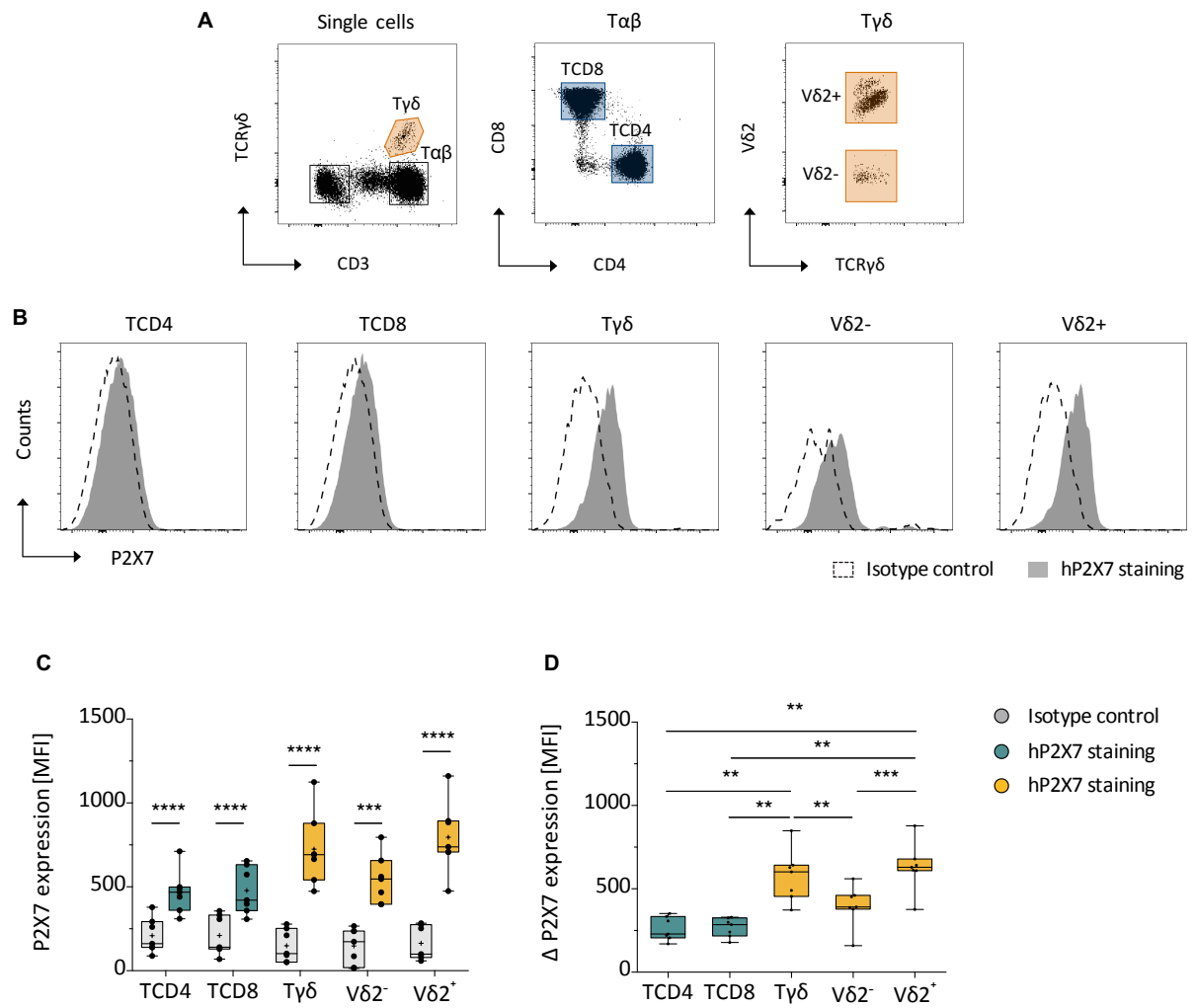
Figure 18. γδ T cells express higher levels of P2X7 than conventional T cells. (**A**) Gating strategy for the identification of different immune cell populations. (**B**) P2X7 expression (MFI) on the surface of CD4 (CD3$^+$CD4$^+$), CD8 (CD3$^+$CD8$^+$), γδ (CD3$^+$TCRγδ$^+$), Vδ2$^+$ (CD3$^+$TCRγVδ2$^+$), Vδ2$^-$ (CD3$^+$TCRγVδ2$^-$) T cells. Number of cells was normalised. (**C**) Expression of P2X7 (MFI ± SD) and background signal detected on the IC on the surface of distinct T cell subsets. (**D**) Expression of P2X7 (MFI ± SD) after subtraction of the MFI of the IC from the MFI of the P2X7 staining (MFI P2X7 - MFI IC) on the surface of T cell subsets. Data are representative of one (**B**) or seven (**C-D**) healthy donors. P values were determined by paired Student's t test, or by RM one-way ANOVA, followed by Bonferroni post-test: ** = <0.01; *** = <0.001; **** = <0.0001. Legend: orange = innate-like lymphocytes // blue = adaptive immune cells.
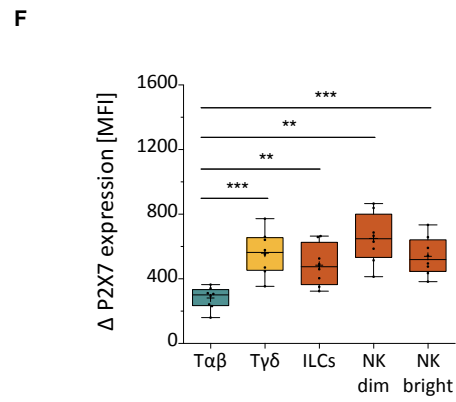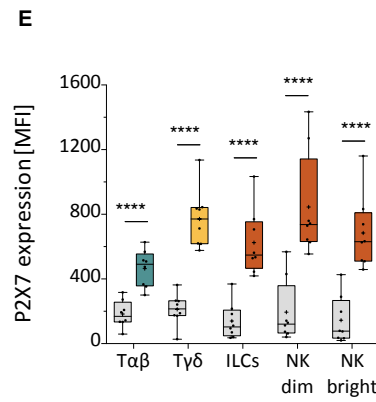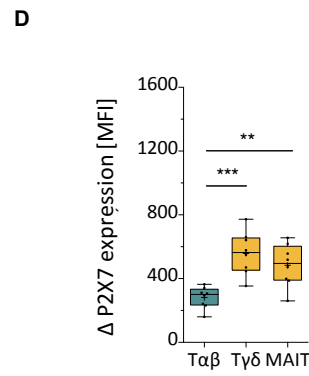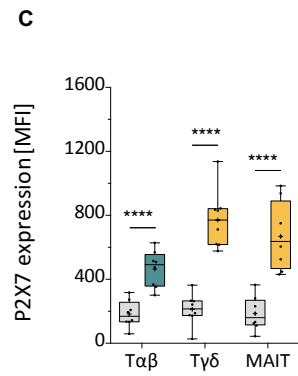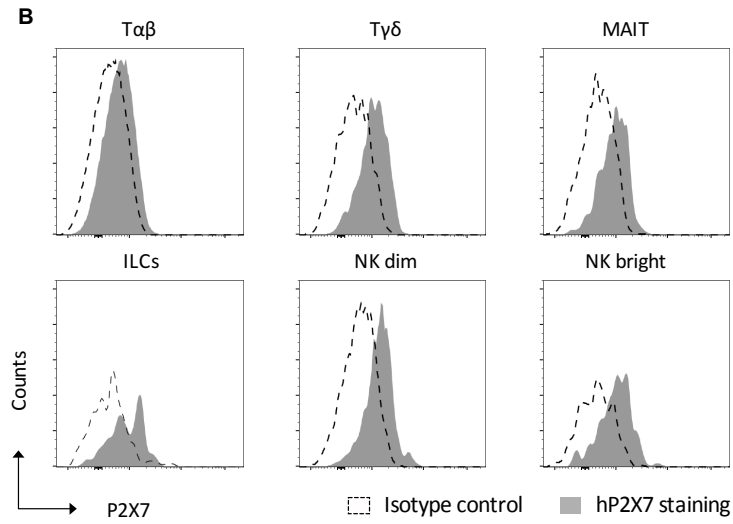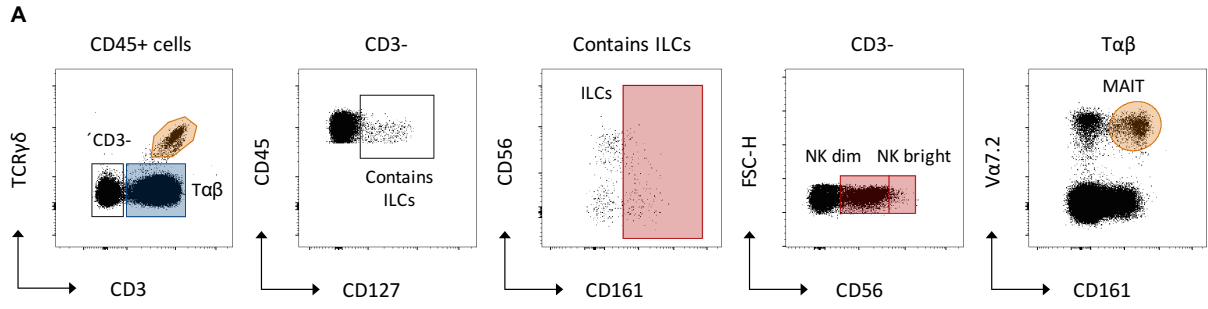
Figure 19. Innate-like lymphocytes and innate like cells express higher levels of P2X7 than conventional T cells. (**A**) Gating strategy for the identification of different immune cell populations. (**B**) P2X7 expression (MFI) on the surface of αβ (CD3$^+$TCRγδ$^-$), γδ (CD3$^+$TCRγδ$^+$), MAIT (CD3$^+$CD161$^+$Vα7.2$^+$), ILCs (CD3$^-$ CD127$^+$ CD161$^+$), NK dim (CD3$^-$CD56^{dim}) and NK bright cells (CD3$^-$CD56^{high}). Number of cells was normalised. (**C** and **E**) Expression of P2X7 (MFI ± SD) and background signal detected on the IC on the surface of distinct immune cells. (**D** and **F**) Expression of P2X7 (MFI ± SD) after subtraction of the MFI of the IC from the MFI of the P2X7 staining (MFI P2X7 - MFI IC) on the surface of distinct immune cells. Data are representative of one (**B**) or seven (**C-F**) healthy donors. P values were determined by paired Student's t test, or by RM one-way ANOVA, followed by Bonferroni post-test: ** = <0.01; *** = <0.001; **** = <0.0001. Legend: red= innate immune cells // orange = innate-like lymphocytes // blue = adaptive immune cells.

Our data demonstrates that innate cells (NK cells, ILCs) and innate-like lymphocytes (MAIT cells, γδ T cells) express higher levels of P2X7 on the cell surface than conventional T cells. Therefore, P2X7 expression reveals a distinct pattern that correlates to the "innateness" of the lymphocytes.

4.2.5 γδ T cells also exhibit higher amounts of P2X7 at the mRNA level

To further confirm this pattern, we determined the *ex vivo* expression of P2X7 at the mRNA level in sorted T cell subsets by qRT-PCR. The gating strategy for the identification and sorting of the different T cell subpopulations is shown in **Figure 20A**. The sample "CD3 T cells" included all T cell subpopulations; and therefore was used as experimental calibrator. P2X7 mRNA expression was more than threefold higher in γδ T cells than in conventional T cells (**Figure 20B**), thus confirming that innate-like γδ T cells exhibit higher levels of P2X7 both at the surface and mRNA level. As represented in the graph, the expression of *P2RX7* varies among the different donors, which may be a consequence of genetic variations (SNPs) in the *P2RX7* gene.
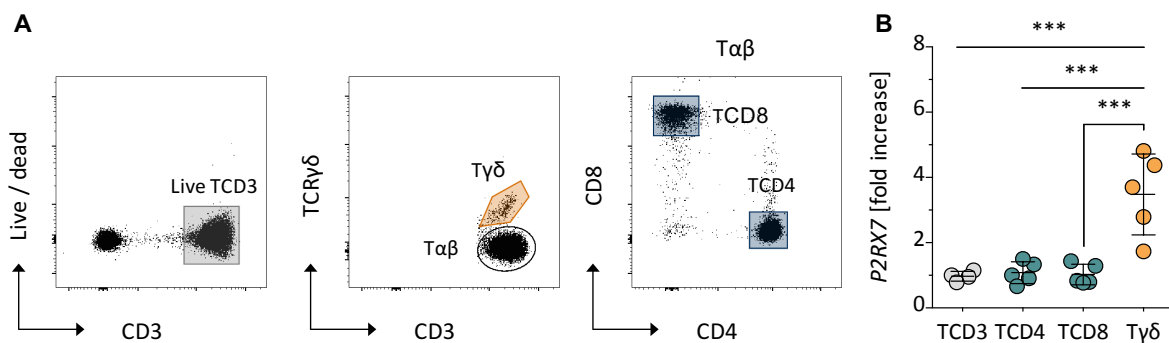
Figure 20. γδ T cells exhibit higher expression of the *P2RX7* gene than conventional T cells. The expression of *P2RX7* in sorted CD3$^+$ T cells, CD3$^+$CD4$^+$ T cells, CD3$^+$CD8$^+$ T cells and CD3$^+$TCRγδ$^+$ T cells was monitored by qRT-PCR. (**A**) Gating strategy for the identification and sorting of T cell subsets. (**B**) Fold increase in the transcription of *P2RX7*. Data are relative to the expression of the reference gene *RPL13A*; using CD3$^+$ T cells (TCD3) as calibrator. Relative gene expression (Mean ± SD) was calculated using the delta-delta Ct formula ($2^{-\Delta\Delta Ct}$). Data are representative of five healthy donors (n=5). P values were determined by one-way ANOVA, followed by Bonferroni post-test: *** = <0.001.

4.2.6 Innate-like T cell-derived cell lines exhibit higher levels of P2X7 than CD4 and CD8 conventional cell lines

Since innate-like lymphocytes are rare events in peripheral blood in many donors, we generated T cell lines derived from sorted γδ T cells, MAIT and also from CD4 T cells from human peripheral blood in order to obtain sufficient cells for mechanistic studies.

The purity of the cell lines was always higher than 70% for the MAIT-derived cell line and higher than 90% for the other T cell-derived cell lines (**Figure 21A**). Similar to what we saw in peripheral blood, γδ and MAIT-derived T cell lines tend to express higher levels of P2X7 than the CD4-derived T cell line (**Figure 21B**). Furthermore, within the γδ-derived T cell line, cells expressing the Vδ2 chain exhibited higher levels of P2X7 than TγVδ2⁻ cells (**Figure 21B**).

In line with our previous findings, these data confirm the distinct pattern of P2X7 expression within the T cell compartment. However, the γδ T cell lines created lost the expression of P2X7 after several rounds of stimulation, and therefore, could not be further used for testing P2X7 function.
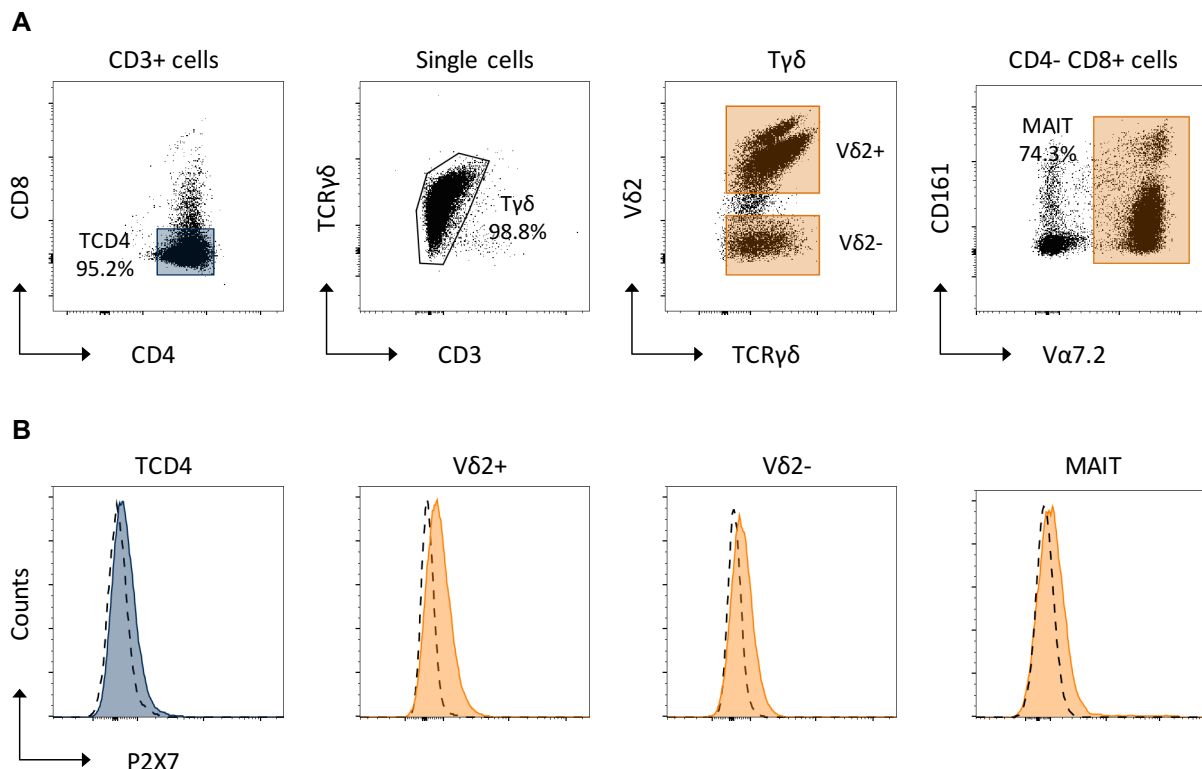
Figure 21. Cell lines derived from innate-like lymphocytes express higher levels of P2X7 than cell lines derived from CD4 T cells. CD4 T cells, γδ T cells and MAIT cells from human peripheral blood were sorted by flow cytometry and cultured under specific conditions. (**A**) Purity (percentage) of each cell line upon specific gating. (**B**) Overlaid histograms of the expression of P2X7 for the different T cell-derived cell lines. Data correspond to day 3 (MAIT-derived T cell line) or day 11 (CD4- and γδ-derived T cell lines) after stimulation. Data (Median Fluorescence Intensity (MFI)) are of one representative donor. Legend: dotted line= isotype control; filled histogram= P2X7 expression; blue= adaptive CD4 T cells and orange= innate-like lymphocytes.

4.2.7 RNA transcription of *P2RX7* increases upon T cell activation

The higher expression of P2X7 on activated/effector T cells prompted us to investigate whether P2X7 is upregulated upon activation. Since both signals from the IC and P2X7 staining increase upon activation, we assessed changes in the transcription of *P2RX7* upon stimulation of sorted CD4, CD8 and γδ T cells with soluble αCD3 for 9 days. All T cell subsets from all donors upregulated *P2RX7* over the course of time compared to day zero (**Figure 22**). In line with cell surface expression, the basal expression of *P2RX7* was higher on γδ T cells than in CD4 and CD8 T cells, and this differential expression was maintained over time (**Figure 22**). Upregulation of P2X7 was characterized by a peak one day after activation, followed by a decrease on the mRNA levels on day three. This pattern was very prominent on γδ T cells, which after a downregulation of P2X7 expression on day 2, showed a steady increase in gene expression. CD4 T cells showed a similar profile of upregulation, but reached the maximum of expression already on day one. Nevertheless, the upregulation upon day three was less marked than in γδ T cells (**Figure 22**). In contrast, CD8 T cells exhibited a progressive upregulation of P2X7 in two of the donors (**Figure 22A, B**), reaching the highest levels of P2X7 on day 9 for all donors (**Figure 22**). All donors were genotyped for three SNPs (H155Y, H270R and A348T) in the *P2RX7* gene, which result in different sensitivity to ATP; being the allelic variants 155Y, 270R and 348T, the ones conferring higher sensitivity (Cabrini et al., 2005; Stokes et al., 2010). The genotypes of the different donors are as follows: D1 (HY/RH/AT), D2 (YY/RR/TT) and D3 (HH/RR/TT). Although the pattern of expression between the different cell types was similar among all donors, genetic variations could explain the differences in *P2RX7* expression.

Altogether, our data indicate that T cells upregulate *P2RX7* expression upon activation, and that this effect is more pronounced in γδ T cells.
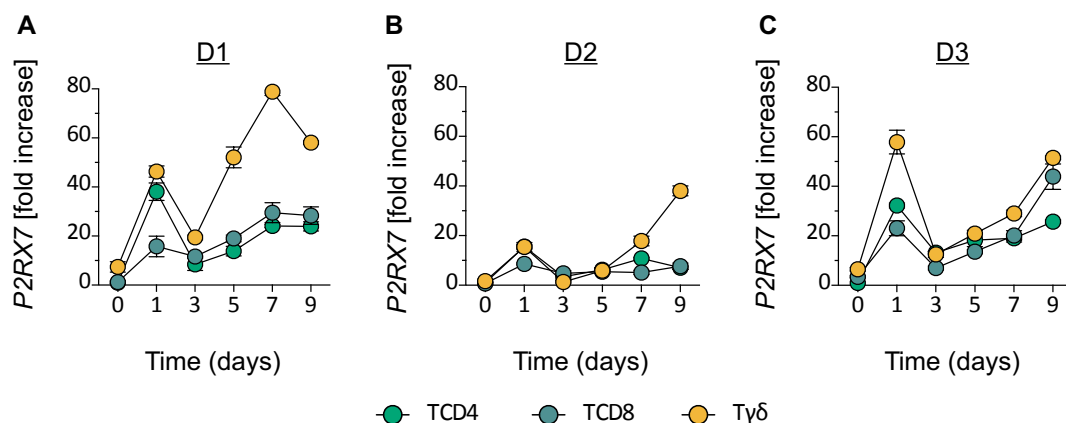
Figure 22. *P2RX7* gene expression in T cells is upregulated upon T cell stimulation *in vitro*. Sorted CD3+CD4+ T cells, CD3+CD8+ T cells and CD3+TCRγδ+ T cells were stimulated with soluble αCD3 antibodies for 9 days. The expression of *P2RX7* was determined by qRT-PCR. Data are relative to the expression of the reference gene *RPL13A*, and basal expression of *P2RX7* of CD4 T cells was used as the calibrator sample. (**A-C**) Relative gene expression of *P2RX7* in CD4 T cells (green), CD8 T cells (blue) and γδ T cells (orange) for each donor (D1-D3; n=3).

4.2.8 The expression of P2X7 in human intestinal T cells is similar to peripheral T cells

In the mouse intestine, both conventional CD8αβ$^+$ and unconventional intraepithelial CD8αα$^+$ T cells express more P2X7 than their peripheral counterparts (Heiss *et al.*, 2008). In patients with Crohn´s disease P2X7 is expressed in higher levels in the mucosa layer of the colon (Neves *et al.*, 2014). Therefore, we investigated P2X7 expression on human T cells from the small intestine from two donors undergoing bariatric surgery. The gating strategy used for the identification of different T cell subsets is shown in **Figure 23A**. In contrast to mice, human intestinal cells did not exhibit high levels of P2X7 on the surface, but rather similar to the levels observed on T cells in the periphery (**Figure 23B**). Again, γδ T cells from the intestine also seem to express higher levels of P2X7 than CD4 and CD8 T cells (**Figure 23B**).

Both eATP and purinergic signalling are implicated in exacerbated intestinal inflammatory responses (Diezmos, Bertrand and Liu, 2016; Wan *et al.*, 2016; Figliuolo *et al.*, 2017). Indeed, Wang and colleagues reported higher levels of eATP in colon tissues of mice suffering from colitis (Wan *et al.*, 2016); underlining the need for controlling the levels of ATP to prevent excessive inflammation in the intestine (Friedman *et al.*, 2009; Kusu *et al.*, 2013). Thus, we investigated the expression of the ATP-metabolising ectoenzymes CD39 and CD73 on human gut T cells. In peripheral blood, the expression of CD39 is highly variable (2-70%) on Tregs, whereas CD4 and CD8 T cells express lower levels of this ectoenzyme (A. Rissiek *et al.*, 2015). Our data show that 80% of intestinal CD8 T cells from one donor expressed CD39 (**Figure 24B**), although this was not the case for the other donor (> 5% of CD39$^+$ CD8 T cells). In contrast, expression of CD39 was almost negligible in conventional CD4 T cells (**Figure 24B**). Tregs represent a low percentage of intraepithelial lymphocytes (IELTs), but are more abundant among lamina propria lymphocytes (LPLs) (Lutter *et al.*, 2018). We observed low frequency (>2.5%) of Tregs in human gut tissue, which included both IELTs and LPLs, and CD39 was only partially detected in one of the donors (**Figure 24B**).

We found that most CD8 T cells from the intestine and also in periphery express very high levels of CD73, while expression of CD73 seems to be higher in intestinal CD4 T cells compared to the periphery (**Figure 24**). Even though CD39 and CD73 are rarely co expressed in human peripheral T cells (**Figure 24A**) (Mandapathil *et al.*, 2010), we observed coexpression of the two ectoenzymes in nearly 75% of intestinal CD8 T cells of one of the donors (**Figure 24B**).
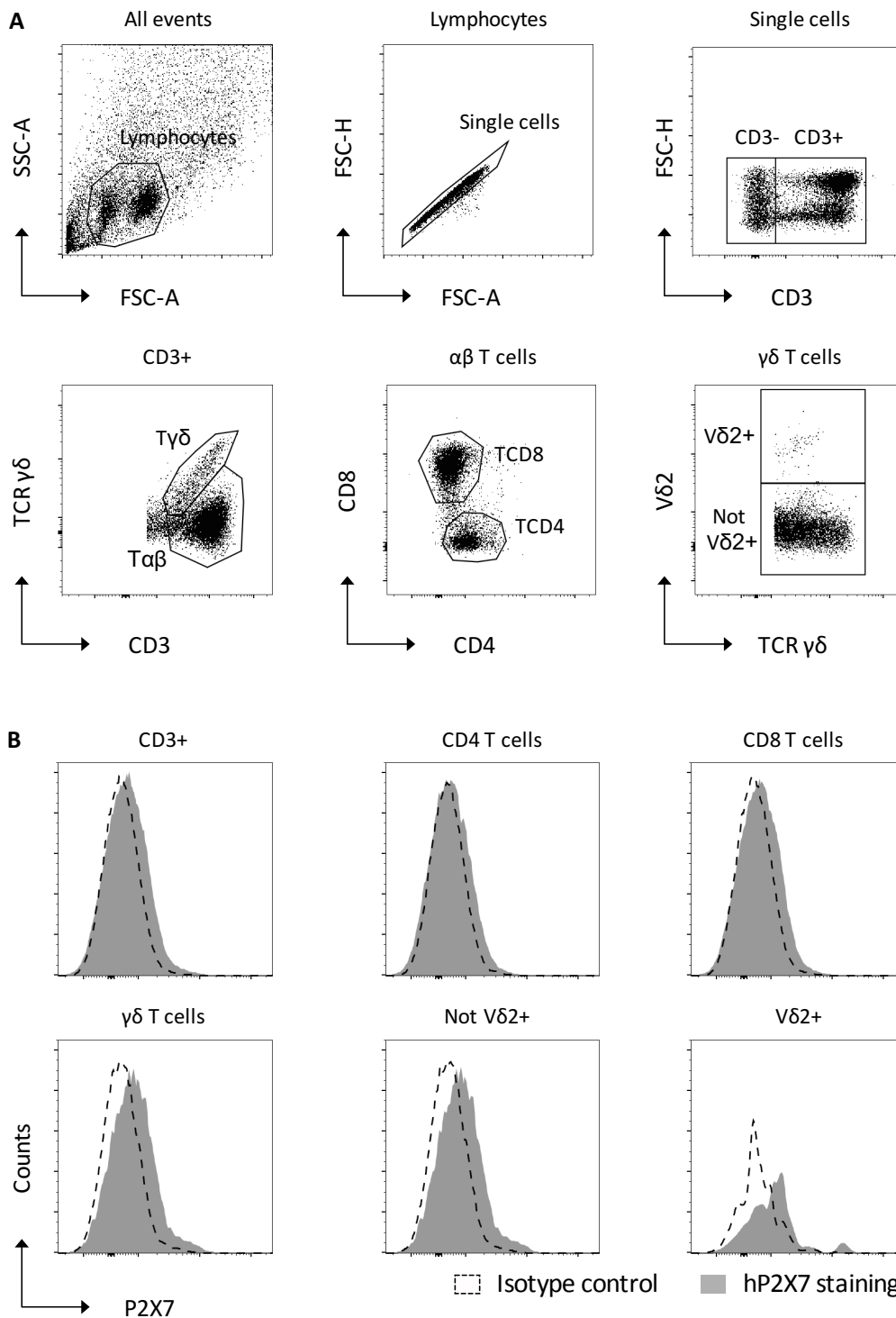
Figure 23. Human intestinal T cells express similar amounts of P2X7 than T cells from the periphery. *Ex vivo* expression of P2X7 on the surface of human intestinal T cells. (**A**) Gating strategy for the identification of different T cell subsets. (**B**) P2X7 expression (MFI) on the surface of αβ (CD3$^+$TCRγδ$^-$), CD4 (CD4$^+$), CD8 (CD8$^+$), γδ (CD3$^+$TCRγδ$^+$), Vδ2 (Vδ2$^+$) and not Vδ2 T cells (Vδ2$^-$). Number of cells was normalised. Data are of a single donor (n=2).
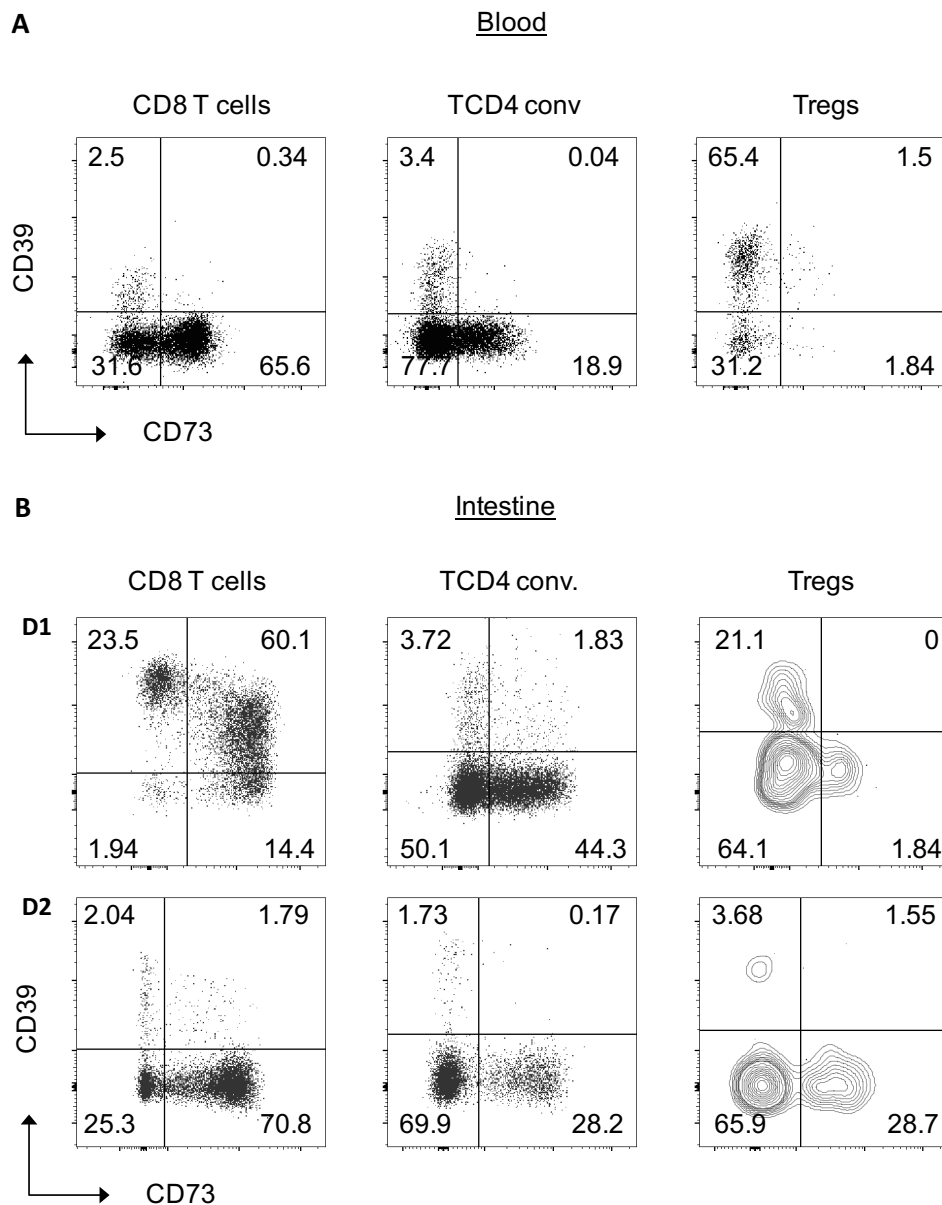
Figure 24. The ectoenzyme CD73 is highly expressed in human intestinal CD8 T cells. Percentage of CD39 and CD73 positive peripheral (**A**) and intestinal (**B**) CD4 T cells (CD3$^+$CD4$^+$), CD8 T cells (CD3$^+$CD8$^+$) and Tregs (CD4$^+$CD25$^+$CD127$^-$). Data are of one (**A**) or two (**B**) individual donors.

In summary, we report similar expression of P2X7 between intestinal and peripheral T cells in humans. We also report high and similar expression of the ectoenzyme CD73 between human intestinal and peripheral CD8 T cells, whereas the expression of CD73 seems to be higher in intestinal CD4 T cells.

4.2.9 Retinoic acid does not induce P2X7 upregulation on human T cells

The human intestine is colonized by a complex population of microorganisms and, intestinal T cells are in constant activation to maintain homeostasis. In the intestine of mice, CD8 and effector and

memory CD4 T cells express high levels of P2X7 on the surface, which increases their sensitivity to extracellular nucleotides and P2X7-mediated cell death (Heiss *et al.*, 2008; Hashimoto-Hill *et al.*, 2017). Retinoic acid (RA), which is produced by epithelial and stromal cells, and DCs, (Iwata, 2009; Hall *et al.*, 2011) is abundant in the small intestine (Hall *et al.*, 2011) and an important determinant of gut immunity (Czarnewski *et al.*, 2017). In mice, RA mediates upregulation of P2X7 on T cells (Heiss *et al.*, 2008; Hashimoto-Hill *et al.*, 2017). To investigate whether this also occurs in humans, we polyclonaly stimulated PBMCs and determined the effect of increasing concentrations of RA on P2X7 expression in gut T cells, namely CD4, CD8αα and CD8αβ (**Figure 25A**).
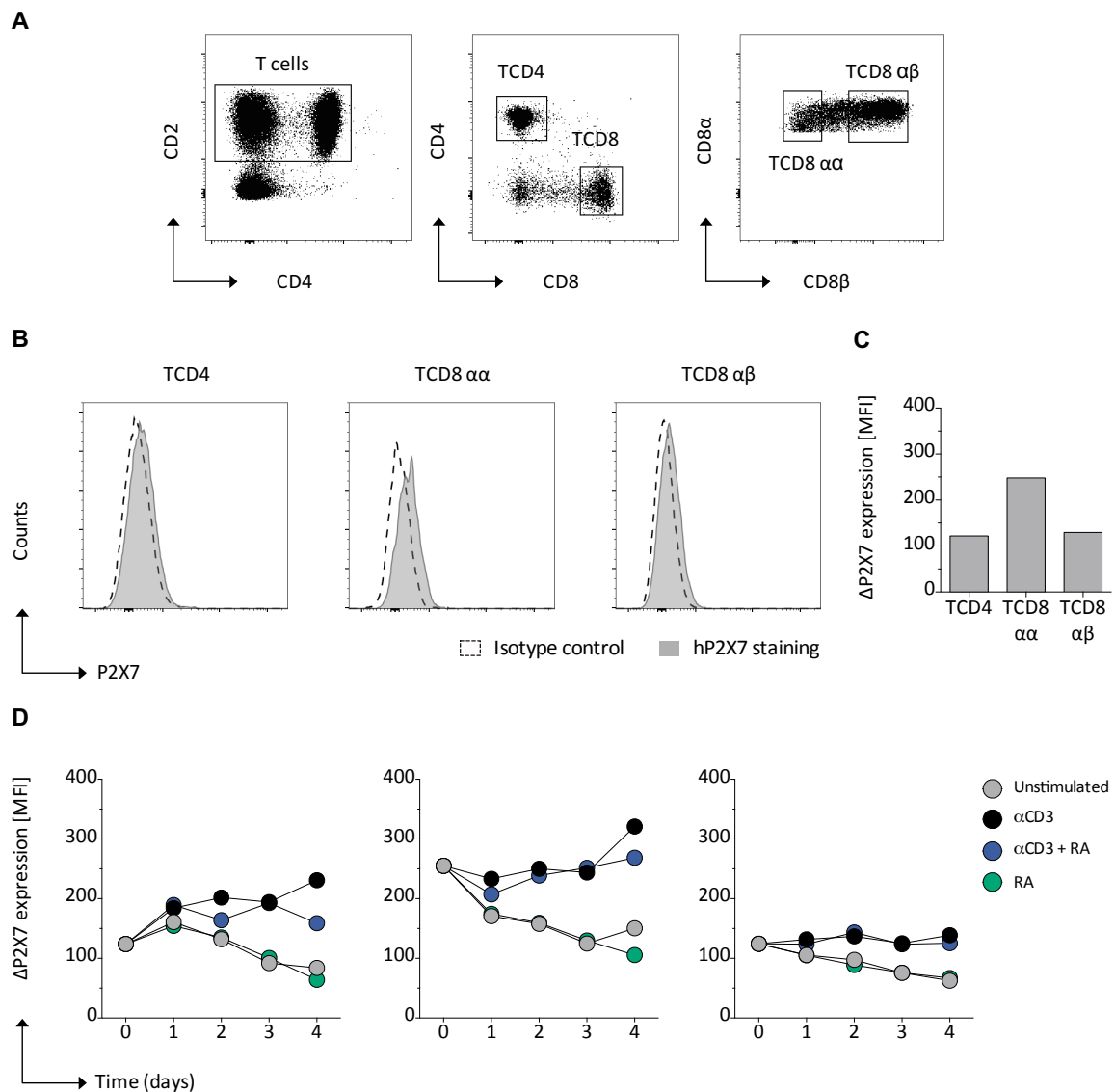
Figure 25. Stimulation of human T cells with retinoic acid (RA) does not alter the expression of P2X7. PBMCs were left untreated or stimulated with soluble αCD3 antibodies for 4 days in the presence or absence of RA (100 nM). The expression of P2X7 was determined by flow cytometry over time. (**A**) Gating strategy for the identification of distinct T cell subsets. (**B-C**) *Ex vivo* expression of P2X7 (day 0) on CD4^{+}, CD8αα^{+} and CD8αβ^{+} T cells. Data correspond to MFI of the IC (black dotted line) and P2X7 staining (grey filled histogram) (**B**) or after subtraction of the IC (ΔP2X7) (**C**). (**D**) Expression of P2X7 (MFI) after subtraction of the IC (MFI P2X7 - MFI IC) cells over the course of time. Data are representative of two independent experiments (n=2).

As shown by the upregulation of CD38 and CD25 (data not shown), T cells were similarly activated under all conditions. All three T cell subsets exhibited low basal expression of P2X7 (**Figure 25B**), being CD8αα T cells the ones expressing more (**Figure 25C**). Polyclonal T cell stimulation resulted in a moderate increase in P2X7 gene expression on CD4 and CD8αα T cells, but not in CD8αβ$^+$ T cells (**Figure 25D**). In contrast to mice, addition of RA did not result in upregulation of P2X7 on the surface of T cells, even at high concentrations (**Figure 25D**). Unstimulated cells lost expression of P2X7 over time, and RA did not revert this tendency (**Figure 25D**).

In contrast to what has been reported in mice, human intestinal T cells express low levels of P2X7, similar to those observed in T cells from the periphery. Additionally, RA does not modulate the expression of P2X7 on human T cells.

4.2.10 γδ T cells exhibit higher sensitivity to ATP-induced shedding of CD62L

The distinct pattern of expression found in innate-like lymphocytes prompted us to investigate whether a higher expression of P2X7 would imply more sensitivity to ATP. P2X7 activation results in activation of ADAM metalloproteinases and subsequent shedding of protease-susceptible membrane glycoproteins, such as CD62L (Scheuplein *et al.*, 2009) and CD27 (Moon *et al.*, 2006).
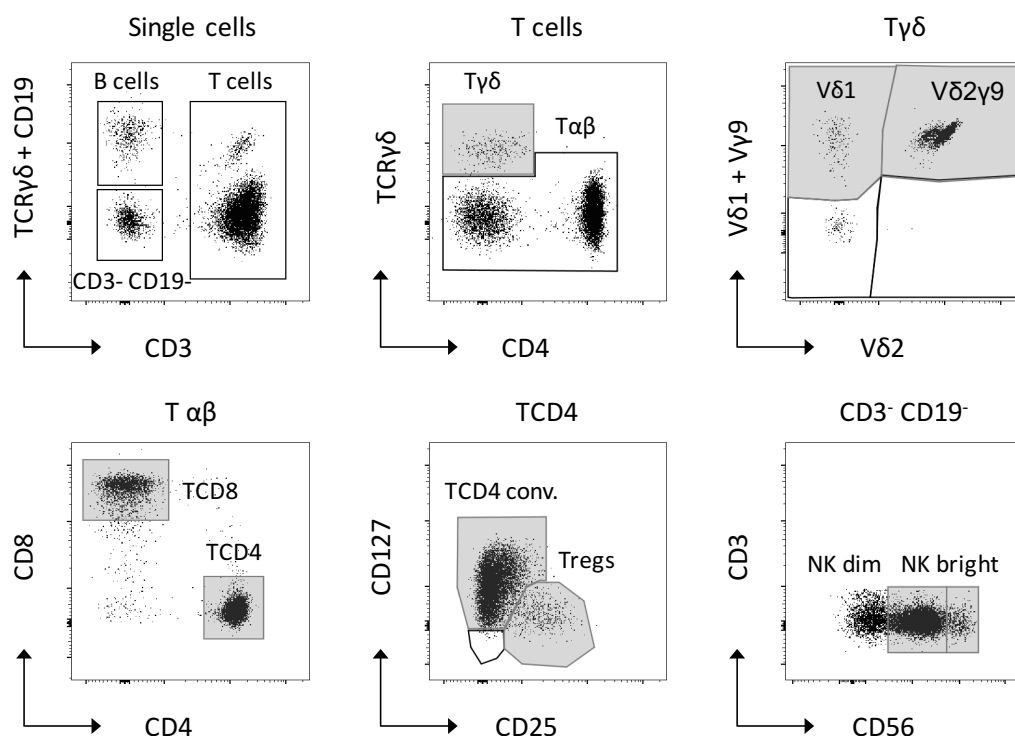
Figure 26. Gating strategy for the identification of distinct immune cell subsets. γδ T cells were identified as CD3$^+$TCRγδ$^+$ cells; and within this subset Vδ2$^+$Vγ9$^+$ and Vδ1$^+$ cells were also identified. αβ T cells were identified according to expression of CD3, CD4 (CD4 T cells) and CD8 (CD8 T cells). CD4 T cells were subdivided in conventional CD4 T cells (CD25$^-$CD127$^+$) and Tregs (CD25$^+$CD127$^-$). NK dim (CD56^{dim}) and NK bright cells (CD56^{high}) were gated within CD3$^-$CD19$^-$ cells.

Thus, we assessed the shedding of CD62L upon incubation of PBMCs with ATP. The gating strategy for the identification of the different immune cell types is shown in **Figure 26**. Although the surface expression of P2X7 was relatively low in Tregs, the dramatic effects of P2X7 activation on murine Treg cells (Hubert *et al.*, 2010) prompted us to assess sensitivity to ATP in their human counterparts. Our readout is the percentage of cells expressing surface CD62L. Due to the high variability in the expression of CD62L among donors, data were standardised and the baseline frequency of CD62L$^+$ cells (without addition of exogenous ATP) was set at 100% for each donor. Thus, the frequency of CD62L$^+$ cells after addition of different concentrations of ATP is relative to the frequency without addition of ATP.
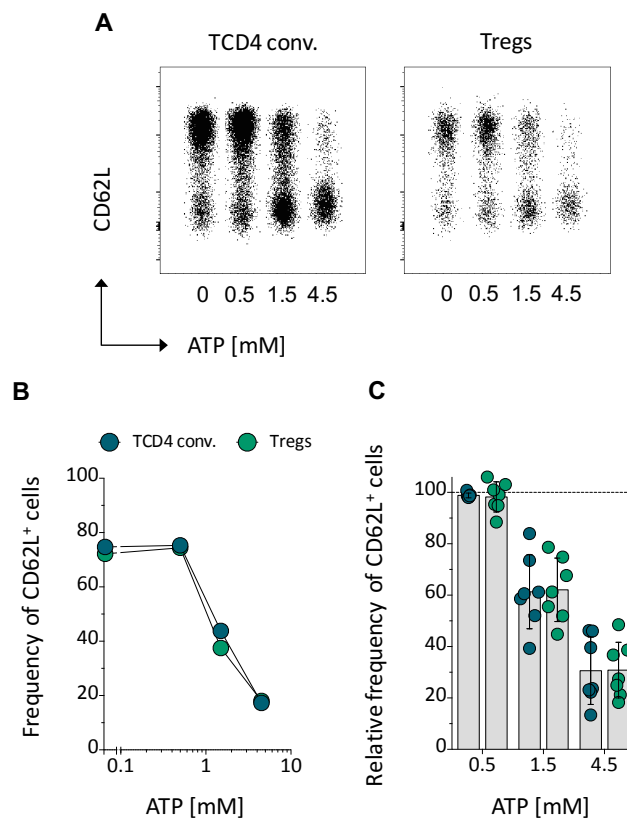
Figure 27. Conventional CD4 T cells and Tregs exhibit similar sensitivity to ATP-induced shedding of CD62L. Human PBMCs were stimulated with different concentrations of ATP for 30 min and the shedding of CD62L on conventional CD4 T cells (TCD4 conv., blue) and Tregs (green) was determined by flow cytometry. (**A**) Concatenated FACS plots of CD62L$^+$ conventional CD4 T cells (left) and CD62L$^+$ Tregs (right). (**B**) Frequency of CD62L$^+$ conventional CD4$^+$ T cells and Tregs upon stimulation with ATP. (**C**) Frequency of CD62L$^+$ conventional CD4 T cells and CD62L$^+$ Tregs upon stimulation with ATP relative to the basal frequency of CD62L$^+$ cells (no exogenous ATP). Basal frequency of CD62L$^+$ cells is represented by a dotted black line at 100%. Data are representative of one (**A** and **B**) or seven (**C**) healthy donors. P values were determined by paired Student's t test for the comparison of two groups, and paired RM one-way ANOVA followed by Bonferroni post-test for the comparison of three or more groups.

Shedding of CD62L was observed upon addition of 1.5 mM of ATP (≈ 40% loss) and stimulation with 4.5 mM of ATP, led to a 70% decrease of CD62L$^+$ cells in both T cell subsets (**Figure 27A-C**). However, we did not find any significant differences in ATP-induced shedding of CD62L between Tregs and conventional CD4 T cells in response to ATP (**Figure 27C**).

Next, we compared the sensitivity to ATP of innate-like γδ T cells with conventional CD4 and CD8 T cells. All three populations showed shedding of CD62L upon addition of 1.5 mM ATP, although to a different extent. In some donors, γδ T cells started to react already upon stimulation with 0.5 mM ATP. Interestingly, we observed that upon addition of 1.5 mM of ATP, shedding of CD62L is nearly complete in γδ T cells (**Figure 28**), while only half of CD4 and CD8 T cells lost CD62L from the cell membrane. Not even the highest concentration of ATP (4.5mM) resulted in complete loss of CD62L$^+$ conventional T cells (**Figure 28**). Of note, CD8 T cells proved to be more sensitive to ATP stimulation, in line with its slightly higher expression levels of P2X7 or it may be because MAIT cells were not excluded from the CD8 gate.
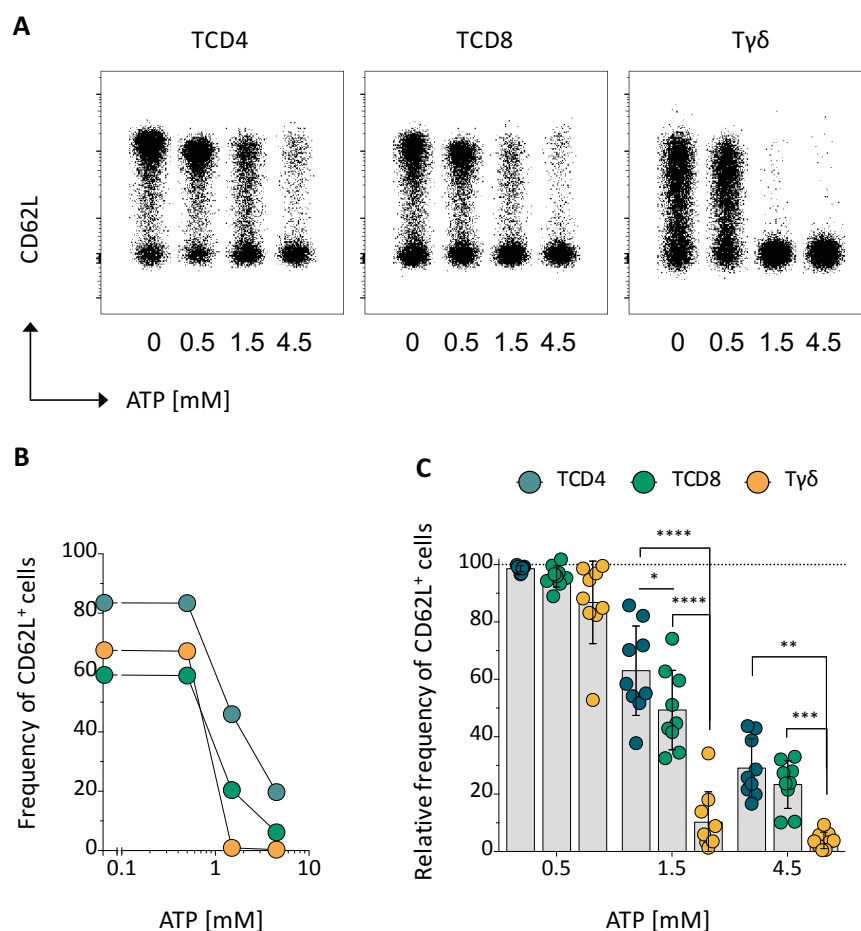
Figure 28. γδ T cells exhibit higher sensitivity to ATP-induced shedding of CD62L. Human PBMCs were stimulated with different concentrations of ATP for 30 min and the shedding of CD62L on CD4 (blue), CD8 (green) and γδ T cells (orange) was determined by flow cytometry. (**A**) Concatenated FACS plots of CD62L$^+$ CD4 (left) and CD62L$^+$ CD8 (middle) and CD62L$^+$γδ T cells (right) stimulated under different conditions (**B**) Frequency of CD62L$^+$ CD4 and CD62L$^+$ CD8 and CD62L$^+$ γδ T cells upon stimulation with ATP. (**C**) Frequency of CD62L$^+$CD4,

CD62L$^+$CD8 and CD62L$^+$ γδ T cells upon stimulation with ATP relative to the basal frequency of CD62L$^+$ cells (no exogenous ATP). Basal frequency of CD62L$^+$ cells is represented by a dotted black line at 100%. Data are representative of one (**A** and **B**) or nine (**C**) healthy donors. P values were determined by paired Student's t test for the comparison of two groups, and paired RM one-way ANOVA followed by Bonferroni post-test for the comparison of three or more groups: * = <0.05; *** = <0.001; **** = <0.0001.

Within γδ T cells, even though Vδ2$^+$ T cells express more P2X7 on their surface than Vδ2$^-$ T cells, Vδ1 cells proved more sensitive to ATP than Vδ2γ9 T cells (**Figure 29**); since at the lowest concentration of ATP (0.5mM) 30% of Vδ1 cells had already lost CD62L from their surface, while only 10% did so in the Vδ2γ9 population. At higher concentrations of ATP, both γδ T cell subsets had completely shed CD62L from the cell surface (**Figure 29**).
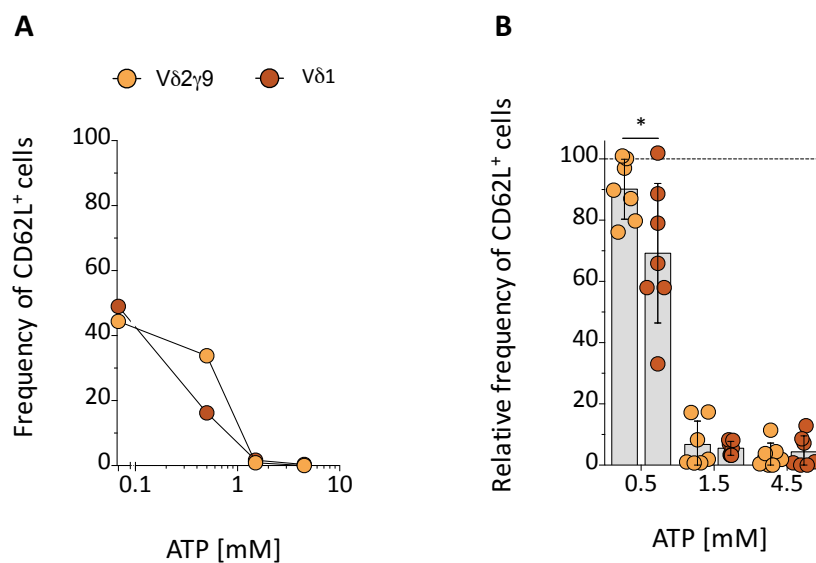
Figure 29. Vδ1 T cells are more sensitivity to ATP-induced shedding of CD62L than Vδ2γ9 T cells at low concentration of ATP. Human PBMCs were stimulated with different concentrations of ATP for 30 min and the shedding of CD62L on Vδ1 (red) and Vδ2Vγ9 (orange) T cells was determined by flow cytometry. (**A**) Frequency of CD62L$^+$ Vδ1 and CD62L$^+$ Vδ2γ9 T cells upon stimulation with ATP. (**B**) Frequency of CD62L$^+$ Vδ1 and CD62L$^+$ Vδ2γ9 T cells upon stimulation with ATP relative to the basal frequency of CD62L$^+$ cells (no exogenous ATP). Basal frequency of CD62L$^+$ cells is represented by a dotted black line at 100%. Data are representative of one (**A**) or seven (**C**) healthy donors. P values were determined by paired Student's t test for the comparison of two groups, and paired RM one-way ANOVA followed by Bonferroni post-test for the comparison of three or more groups.

NK cells are the paradigm of innate lymphocytes. The expression of CD56 differentiates two NK subsets, the more immature CD56^{high}, and the highly cytolytic CD56^{dim}. We have previously shown that NK cells express the highest levels of P2X7 at the cell surface among all lymphocytes. Accordingly, shedding of CD62L was significantly higher on both NK subsets compared to CD4 T cells in response to ATP (1.5 and 4.5 mM) (**Figure 30B**). We also observed lower frequency of CD62L$^+$ cells on the NK dim subset than in NK bright cells upon stimulation with 1.5 mM ATP (**Figure 30B**), in line with its effector phenotype.

In summary, NK cells are highly sensitive to high concentrations of ATP. Furthermore, the pattern of CD62L shedding in NK cells is similar to the pattern found in γδ T (**Figure 30D**).
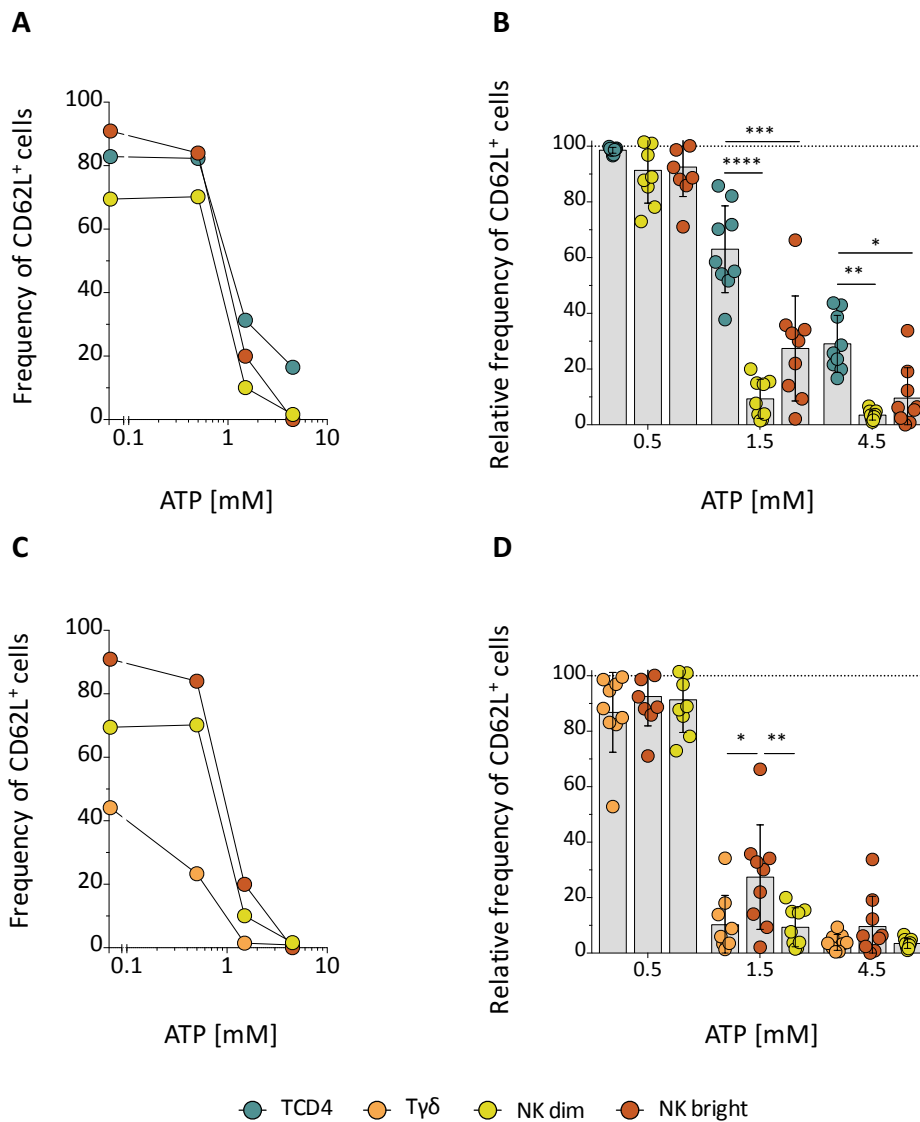
Figure 30. NK cells also exhibit higher sensitivity to ATP than conventional CD4 T cells. Human PBMCs were stimulated with different concentrations of ATP for 30 min and the shedding of CD62L on conventional CD4 T cells (blue), γδ T cells (orange), NK dim (yellow) and NK bright (red) was determined by flow cytometry. (**A** and **C**) Frequency of CD62L$^+$ NK dim, NK bright, CD4 T cells (**A**) and γδ T cells (**C**) upon stimulation with ATP. (**B** and **D**) Frequency of CD62L$^+$ NK dim, NK bright, CD4 T cells (**B**) and γδ T cells (**D**) upon stimulation with ATP relative to the basal frequency of CD62L$^+$ cells (no exogenous ATP). Basal frequency of CD62L$^+$ cells is represented by a dotted black line at 100%. Data are representative of one (**A** and **C**) or eight-nine (**B** and **D**) healthy donors. P values were determined by paired Student's t test for the comparison of two groups, and paired RM one-way ANOVA followed by Bonferroni post-test for the comparison of three or more groups: * = <0.05; ** = <0.01; *** = <0.001; **** = <0.0001.

Overall, the magnitude of response to ATP among lymphocytes is as follows: NK dim and γδ T cells > NK bright > CD8 T cells > CD4 T cells, resembling the magnitude of surface expression of P2X7 on these immune cells.

4.2.11 ATP-induced shedding of CD62L is mediated by P2X7

In order to confirm the role of P2X7 in CD62L shedding, we preincubated PBMCs with Dano1 or a control Nb prior to stimulation with ATP. As control, PBMCs were also preincubated with apyrase, an enzyme that catalyses the hydrolysis of ATP to AMP and inorganic phosphate, thus eliminating the ligand of P2X7 and preventing its activation. Preincubation with Dano 1 or apyrase abolished ATP-induced shedding of CD62L. In contrast, preincubation with a control nanobody did not have any effect on ATP-induced shedding of CD62L (**Figure 31**), confirming the role of P2X7 in this response.
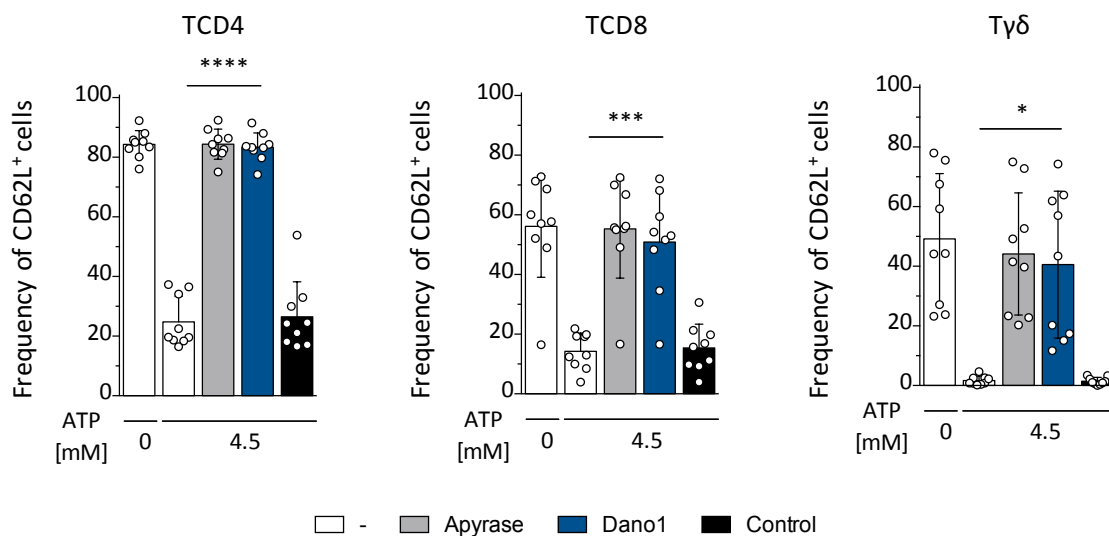
Figure 31. Dano1 inhibits P2X7-mediated shedding of CD62L in response to ATP. Human PBMCs were preincubated with 100 nM of Dano1 (blue) or a control Nb (black), 10 U/ml apyrase (grey) or RPMI as control (white) for 20 min at RT or 37°C (apyrase) prior to stimulation with ATP (4.5 mM) for further 30 min. Frequency of CD62L$^+$ cells (Mean ± SD, n=9) was assessed by flow cytometry. P values were determined by paired RM one-way ANOVA followed by Bonferroni post-test for the comparison of three or more groups: * = <0.05; *** = <0.001; **** = <0.0001.

4.2.12 Innate-like lymphocytes exhibit higher sensitivity to ATP-induced pore formation

Activation of P2X7 triggers the opening of a secondary non-selective pore permeable to cationic molecules with a molecular mass up to 900 Da (Steinberg *et al.*, 1987). Therefore, we measured the uptake of DAPI as a surrogate approach for P2X7 activation. To study this aspect, we stimulated PBMCs with ATP and measured the uptake of DAPI by flow cytometry. The gating strategy for the identification of immune cells is shown in **Figure 32**. In this case, we also identified Tregs according to the expression of CD39, and MAIT cells as CD8$^+$CD161$^+$Vα7.2$^+$ cells. Since MAIT cells are relatively rare in human blood (1-10%) (Salou, Franciszkiewicz and Lantz, 2017), and that they mostly harbour a memory phenotype (characterized by the absence of CD62L) (Chandra and Kronenberg, 2015), determination of ATP-induced shedding of CD62L was not reliable in this subset.
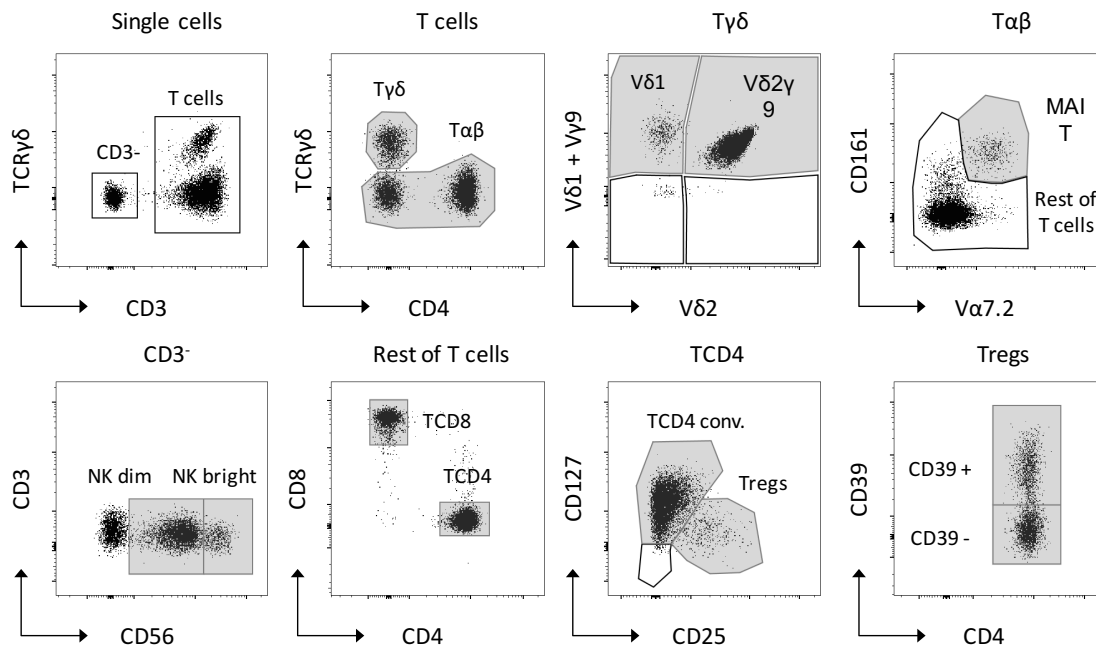
Figure 32. Gating strategy for the identification of distinct immune cell subsets. γδ T cells were identified as CD3$^+$TCRγδ$^+$ cells; and within this subset Vδ2$^+$Vγ9$^+$ and Vδ1$^+$ cells were also identified. αβ T cells were gated according to expression of CD3, and CD8 T cells according to expression of CD8. Conventional CD4 T cells were identified as CD25$^-$CD127$^+$ and Tregs (CD25$^+$CD127$^-$) were subdivided according to expression of CD39. MAIT cells were identified as CD8$^+$CD161$^+$Vα7.2$^+$ cells. NK dim (CD56^{dim}) and NK bright cells (CD56^{high}) were gated within CD3$^-$CD19$^-$ cells.

The uptake of DAPI was induced upon stimulation with 1.5 mM of ATP in both human Tregs and conventional CD4 T cells (**Figure 33**). Similar to what we observed for the shedding of CD62L, both T cell subsets followed a similar pattern (**Figure 33B**), confirming that human Tregs do not exhibit higher sensitivity to ATP (**Figure 33C**).
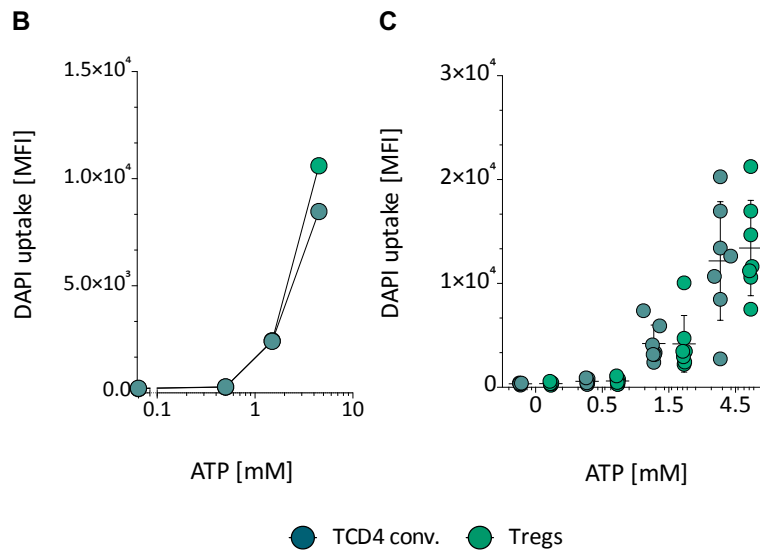
Figure 33. Conventional CD4 T cells and Tregs exhibit similar sensitivity to ATP-induced pore formation. Human PBMCs were stimulated with different concentrations of ATP for 30 min and the uptake of DAPI was monitored by flow cytometry. (**A**) Uptake of DAPI (Median fluorescence intensity, MFI) by conventional CD4 T cells (TCD4 conv., left) and Tregs (right). (**B-C**) Comparison of uptake of DAPI, MFI (**B**) and MFI ± SD (**C**), by TCD4 conv. (blue) and Tregs (green). Data are representative of one (**A-B**) or seven (**C**) healthy donors. P values were determined by paired Student's t test for the comparison of two groups and paired RM one-way ANOVA followed by Bonferroni post-test for the comparison of three or more groups.

We next investigated ATP-induced pore formation of γδ T cells in comparison with conventional T cells (**Figure 34A, B**). Stimulation with 1.5 mM ATP and 4.5 mM ATP substantially increased the uptake of DAPI in all T cell subsets, although to a different extent (**Figure 34**). In line with previous findings, γδ T cells proved to be more sensitive to ATP than conventional T cells, regardless of the concentration of ATP (**Figure 34C**).

Within γδ T cells, the Vδ1 and Vδ2γ9 subsets exhibited similar profiles upon stimulation with different concentrations of ATP (**Figure 35A**), although in this case, Vδ2γ9 T cells were more sensitive to ATP (1.5 mM), as the uptake of DAPI was slightly higher in this subset (**Figure 35B**).
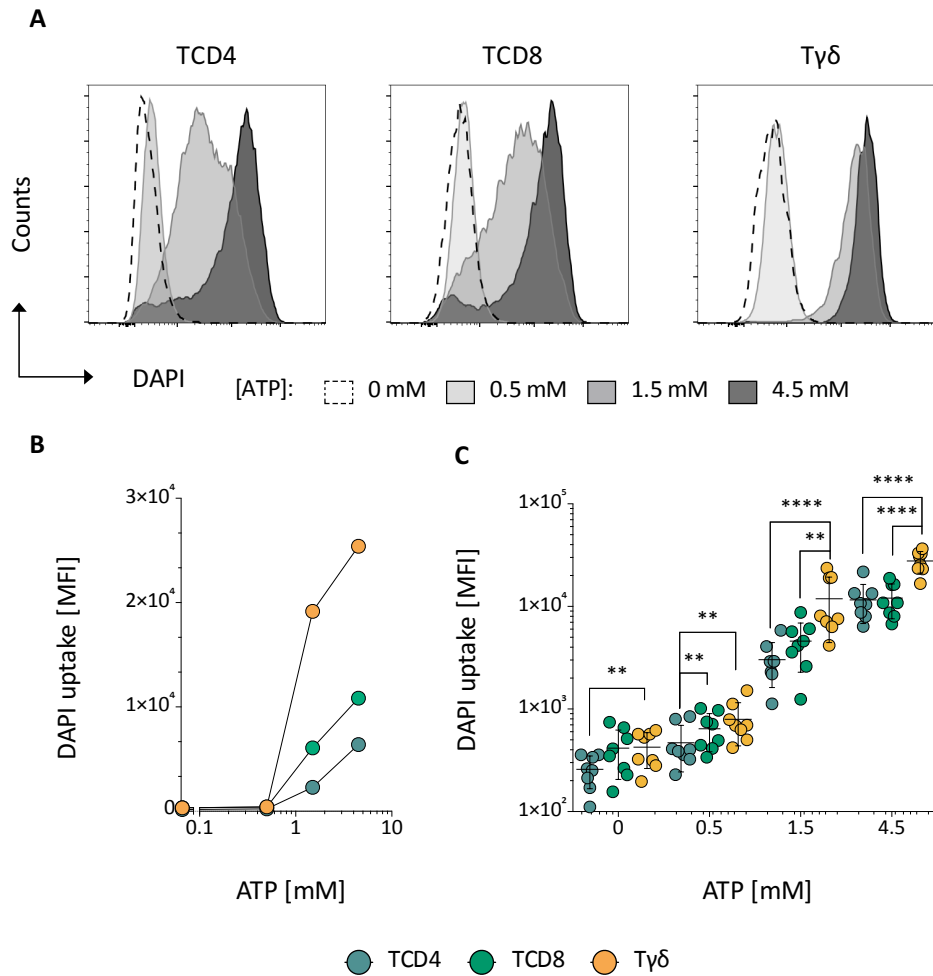
Figure 34. γδ T cells exhibit higher sensitivity to ATP-induced pore formation. Human PBMCs were stimulated with different concentrations of ATP for 30 min and the uptake of DAPI was monitored by flow cytometry. (**A**) Uptake of DAPI (MFI) by conventional CD4 T cells (left), CD8 T cells (middle) and γδ T cells (right). (**B**-**C**) Comparison of uptake of DAPI, MFI (**B**) and MFI ± SD (**C**), by CD4 T cells (TCD4, blue), CD8 T cells (TCD8, green) and γδ T cells (Tγδ, orange). Data are representative of one (**A**- **B**) or eight (**C**) healthy donors. P values were determined by paired RM one-way ANOVA followed by Bonferroni post-test for the comparison of three or more groups: * = <0.05; ** = <0.01; *** = <0.001; **** = <0.0001.
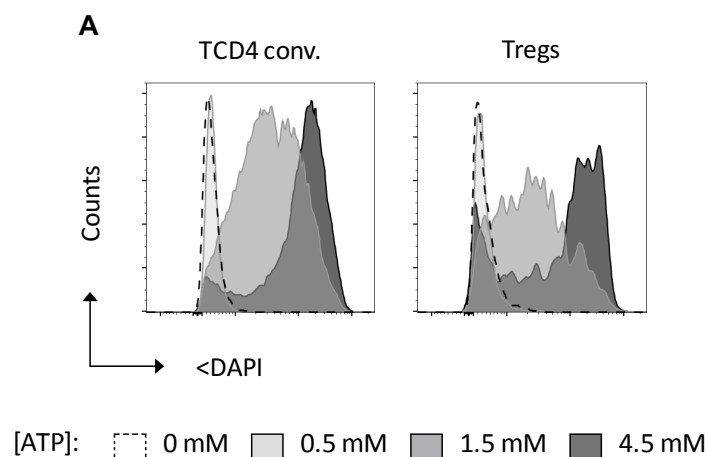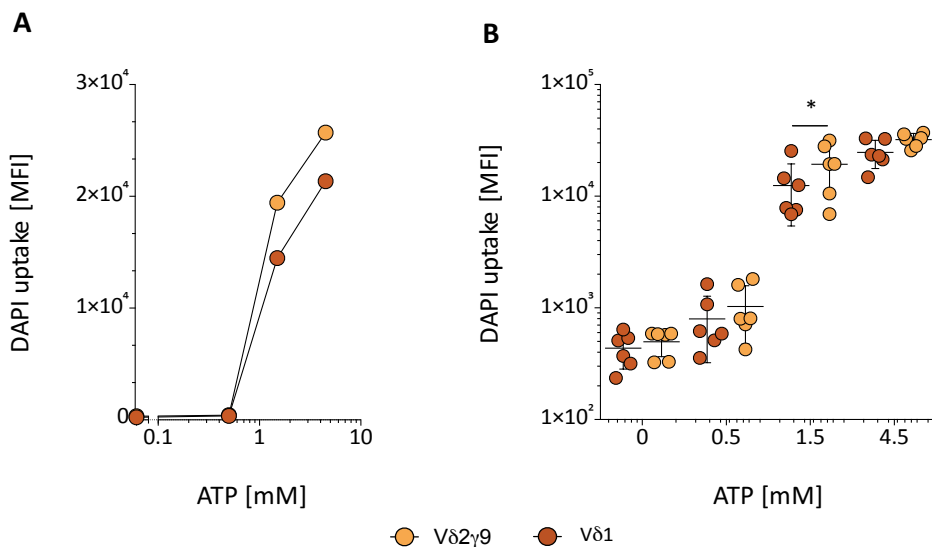
Figure 35. Vδ2γ9 T cells exhibit slightly higher sensitivity to ATP-induced pore formation. Human PBMCs were stimulated with different concentrations of ATP for 30 min and the uptake of DAPI on Vδ2γ9 (orange) and Vδ1 cells (red) was monitored by flow cytometry. Data are represented by MFI (**A**) or MFI ± SD (**B**). Data are representative of one (**A**) or six (**B**) healthy donors. P values were determined by paired Student's T Test for the comparison of two groups and paired RM one-way ANOVA followed by Bonferroni post-test for the comparison of three or more groups: * = <0.05.

DAPI uptake could also be measured in the innate-like MAIT cells (**Figure 36**). In line with other innate-like cells, MAIT cells were more sensitive to ATP-induced pore formation than conventional CD8 T cells (**Figure 36C**). Also NK cells tend to react more prominently to high concentrations of ATP than CD4 T cells (**Figure 37**), although we could only confirm this tendency on NK^{dim} cells in response to the highest concentration of ATP (data not shown).

Figure 36. Innate-like MAIT cells exhibit higher sensitivity to ATP-induced pore formation than conventional CD8 T cells. Human PBMCs were stimulated with different concentrations of ATP for 30 min and the uptake of DAPI was monitored by flow cytometry. (**A**) Uptake of DAPI (MFI) by CD8 T cells (left) and MAIT cells (right). (**B-C**) Comparison of uptake of DAPI, MFI (**B**) and MFI ± SD (**C**), by MAIT (orange) and CD8 T cells (green). Data are representative of one (**A-B**) or nine (**C**) healthy donors. P values were determined by paired Student's t test for the comparison of two groups and paired RM one-way ANOVA followed by Bonferroni post-test for the comparison of three or more groups: * = <0.05; ** = <0.01.

Figure 37. Innate and innate-like lymphocytes exhibit higher sensitivity to ATP-induced pore formation than conventional T cells. Human PBMCs were stimulated with different concentrations of ATP for 30 min and the uptake of DAPI by CD4 T cells, CD8 T cells, γδ T cells, MAIT cells, NK dim and NK bright cells was determined by flow cytometry. Data (MFI) are the mean of a total of 6-8 healthy donors.

In line with previous findings, innate and innate-like immune cells are more sensitive to ATP-mediated pore formation. In this case, the sequence of response to ATP is the following: γδ T cells > MAIT cells > NK dim > Nk bright > CD8 T cells > CD4 T cells. These data resemble the pattern of P2X7 expression seen by flow cytometry, even though NK cells express the highest levels of P2X7.

4.2.13 Dano1 efficiently blocks ATP-induced pore formation in immune cells

To confirm the role of P2X7 in pore formation upon ATP engagement, we preincubated PBMCs with Dano1, a control Nb or apyrase prior to stimulation with ATP. ATP induced the prominent uptake of DAPI by all immune cells. As expected, preincubation with Dano 1 or apyrase, but not a control Nb, decreased the uptake of DAPI to the levels measured in basal conditions (**Figure 38**).

Our data confirm that P2X7-blockade by Dano1 or removal of ATP by apyrase prevents ATP-induced pore formation in immune cells; confirming the role of P2X7 in such cellular response.
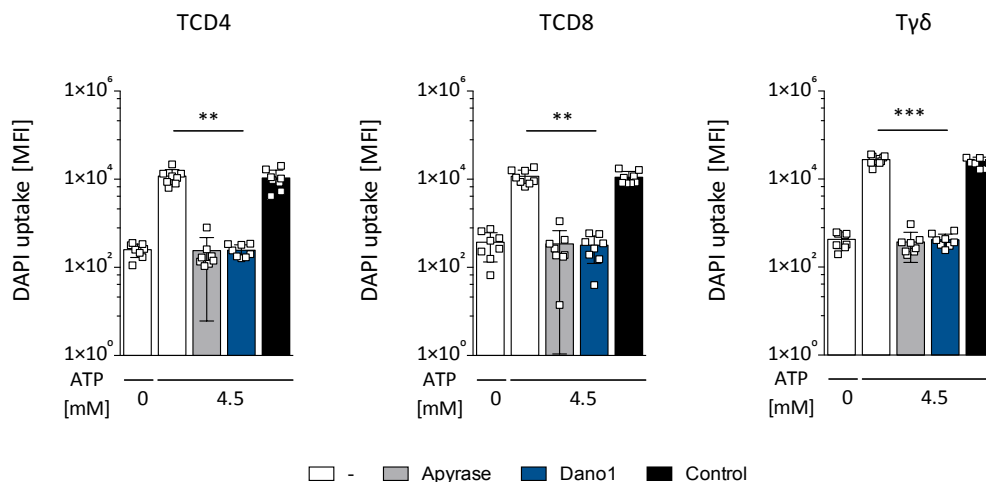
Figure 38. Dano1 inhibits P2X7-dependent pore formation induced by ATP in a variety of T cell subsets. Human PBMCs were preincubated with 100 nM of Dano1 (blue) or a control Nb (black), 10 U/ml apyrase (grey) or RPMI as control (white) for 20 min at RT or 37°C (apyrase) prior to stimulation with ATP (4.5 mM) for further 30 min. The uptake of DAPI (MFI ± SD, n=8) was determined by flow cytometry. P values were determined by paired RM one-way ANOVA followed by Bonferroni post-test for the comparison of three or more groups: * = <0.05; ** = <0.01; *** = <0.001; **** = <0.0001.

4.2.14 <u>Effector T cells are more sensitive to ATP-induced pore formation than naïve T cells</u>

Based on the higher expression of P2X7 in the surface of effector CD4 T cells, we hypothesized that effector cells might also exhibit higher sensitivity to ATP. To this end, we determined the uptake of DAPI on different T cell subsets, identified according to maturation markers (**Figure 15A, 17A**), in response to ATP. Of note, we only analysed those populations with a frequency higher than 5%. Effector memory CD4 T cells exhibited higher uptake of DAPI than naïve and central memory CD4 T cells (**Figure 39A**). Comparably, CD8 T cells with an effector profile (EM, TEMRA and effectors) were also more sensitive to ATP than naïve CD8 T cells (**Figure 39B**). Although this tendency was observed in different donors, we did not find significant differences among them. Additionally, we reconfirmed that ATP-induced pore formation occurs through P2X7 signalling, as preincubation with Dano1 prevented the uptake of DAPI in all populations (data not shown).
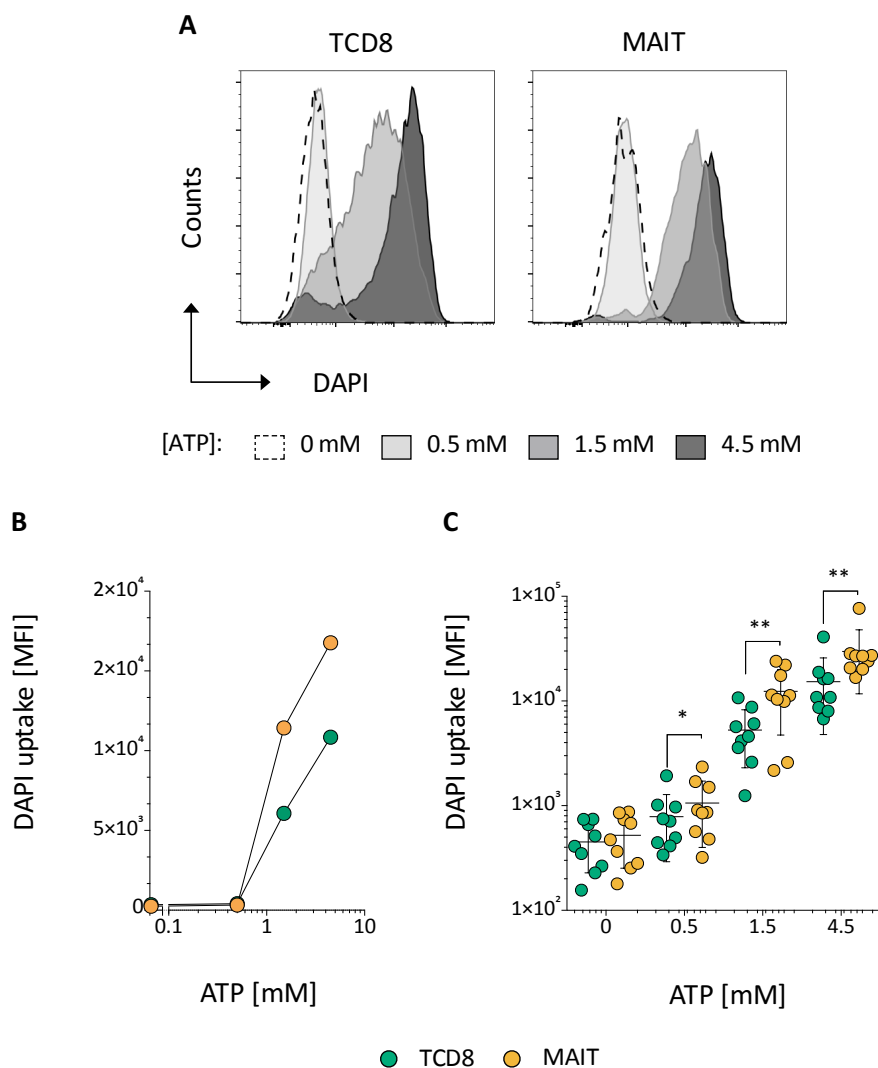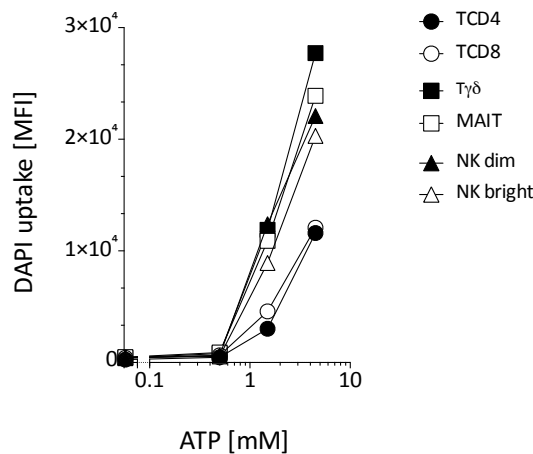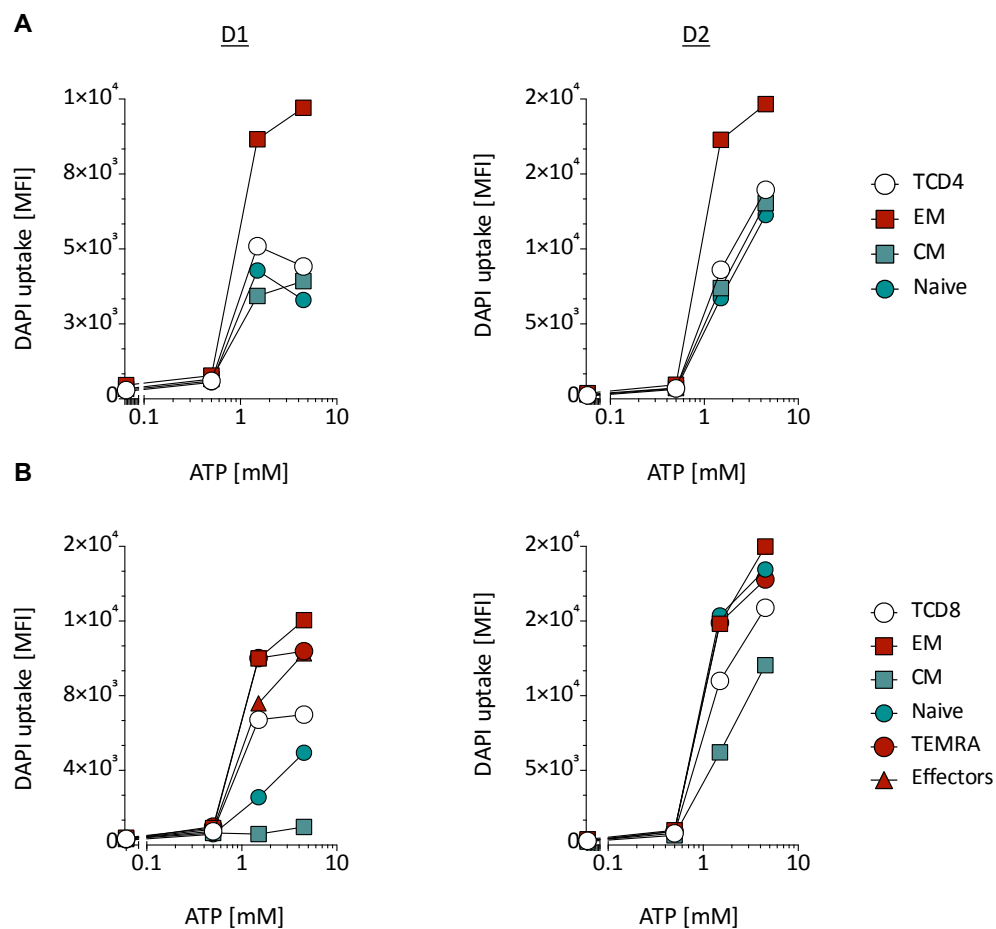
Figure 39. Effector T cells exhibit higher sensitivity to ATP-induced pore formation than naïve cells. Human PBMCs were stimulated with different concentrations of ATP for 30 min and the uptake of DAPI on naïve, central memory (CM), effector memory (EM), effectors and TEMRA CD4 (**A**) and CD8 (**B**) T cells was monitored by flow cytometry. White circles represent the whole population of CD4 and CD8 T cells. Data (MFI; n = 2 donors; D1, D2) are representative of six healthy donors.

The expression of the ATP-metabolising enzyme CD39 in Tregs is genetically determined, therefore some donors have a high proportion of CD39+ Tregs (>40%) while in some others less than 20% of Tregs express CD39 (A. Rissiek *et al.*, 2015). Moreover, CD39 is an activation marker for T cells (Maliszewski *et al.*, 1994). Therefore, we compared the sensitivity of Tregs expressing CD39 with those not expressing the ectoenzyme in response to ATP (**Figure 40**), and observed, that activated Tregs (CD39+ Tregs) react strongly to ATP than non-activated Tregs (CD39- Tregs) (**Figure 40**).
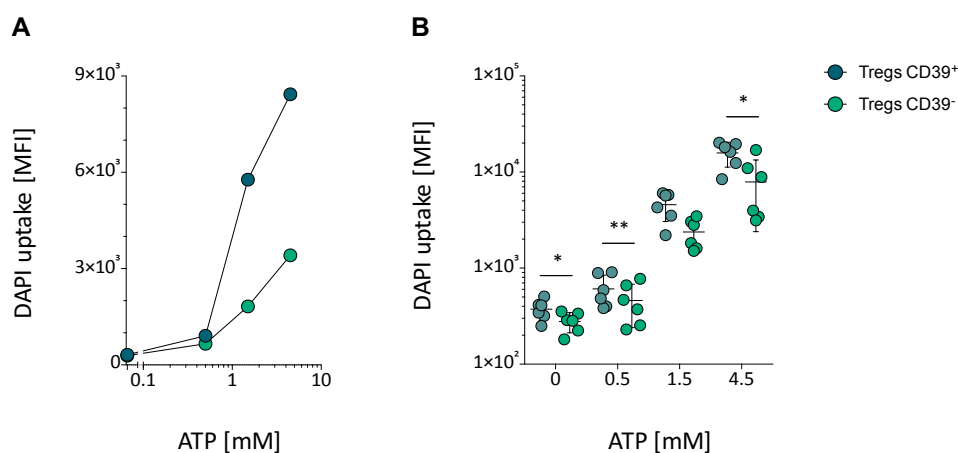
Figure 40. CD39+ Tregs exhibit higher sensitivity to ATP-induced pore formation than CD39- Tregs cells. Human PBMCs were stimulated with different concentrations of ATP for 30 min and the uptake of DAPI on CD39+ (blue) and CD39- Tregs (green) was monitored by flow cytometry. Data are represented by Median fluorescence intensity (MFI) (**A**) or MFI ± SD (**B**). Data are representative of one (**A**) or six (**B**) healthy donors. P values were determined by paired Student's t test for the comparison of two groups and paired RM one-way ANOVA followed by Bonferroni post-test for the comparison of three or more groups: * = <0.05; ** = <0.01.

These results indicate that activated and effector T cells exhibit higher sensitivity to ATP than their naïve and non-effector counterparts.

4.2.15 Blockade of the P2X7 receptor does not affect activation or proliferation of T cells *in vitro*

Up to now, our experiments described the immediate consequences of P2X7-activation in response to ATP. The next obvious aim was to determine the influence of prolonged activation of P2X7 on T cell responses. It is known that high concentrations of ATP induce P2X7-mediated cell death of murine T cells (Yoon *et al.*, 2007). In contrast, when low concentrations of ATP are present, P2X7 promotes the activation and proliferation of T cells through P2X7 signalling (Adinolfi *et al.*, 2005; Schenk *et al.*, 2008; Yip *et al.*, 2009). Thus, we first investigated whether blockade of P2X7 would

have an impact on T cell activation. For this, we stimulated human PBMCs with αCD3 antibodies in the presence of Dano1 or a control Nb, and then assessed the expression of the activation markers CD25 and CD69. The gating strategy for the identification of CD4 and CD8 T cells is shown in **Figure 41A**.

We detected high levels of CD25 and lower levels of CD69 on the surface of CD4 and CD8 T cells four days after stimulation (**Figure 41B, D**). CD25 expression increased progressively over the course of time, reaching the highest levels 96 hours after stimulation (**Figure 41C**, **E**). In contrast, CD69 was upregulated one day after stimulation, and started to decrease after 72 hours (**Figure 41C**, **E**). Blockade of P2X7 by Dano1 did not impair or increase activation of T cells (**Figure 41C, E**).
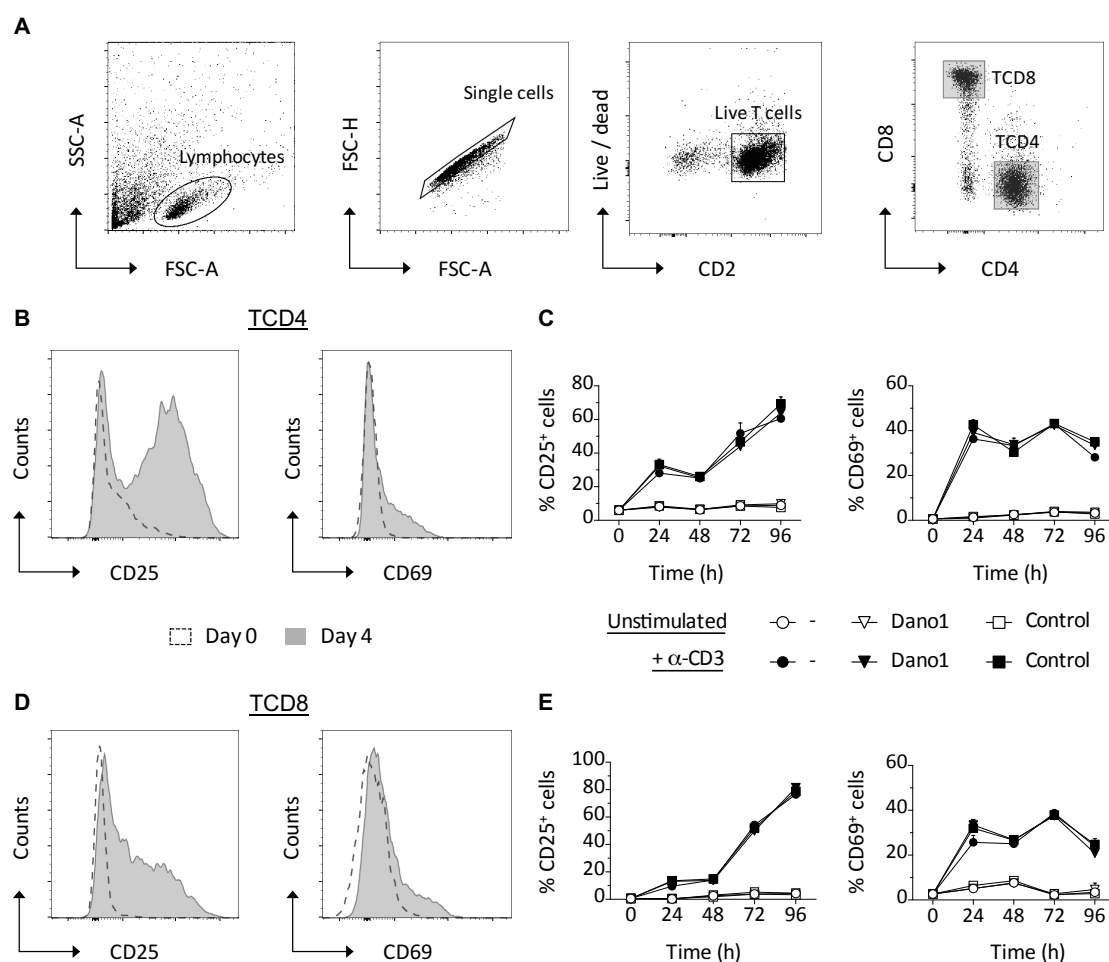
Figure 41. Dano1 does not affect activation of human T cells *in vitro*. Human PBMCs were stimulated with αCD3 antibodies (0.5 µg/ml) in the absence or presence of 100 nM of Dano1 or a control Nb (anti-mARTC2.2). T cell activation was determined by the expression of CD25 and CD69 on the cell surface. Nanobodies were used as dimers, and added on day zero and day two. (**A**) Gating strategy for the identification of CD4 (CD2$^+$CD4$^+$) and CD8 T cells (CD2$^+$CD8$^+$). (**B** and **D**) Expression of CD25 (left) and CD69 (right) in CD4 (**B**) and CD8 (**D**) T cells. Data (MFI) correspond to day 0 (black dotted line) and day four (gray filled histogram). (**C** and **E**) Percentage (Mean ± SD, n=3) of CD25$^+$ (left) CD69$^+$ (right) CD4 (**C**) or CD8 T cells (**E**). Data are representative of one donor from two independent experiments.

As a second approach, we investigated T cell proliferation on PBMCs by eFluor dye dilution by flow cytometry (**Figure 42**). The gating strategy for the identification of proliferating CD4 and CD8 T cells is

shown in **Figure 42A**. Stimulation with αCD3 antibodies induced the proliferation of CD4 and CD8 T cells (**Figure 42**) after three days in culture. Consequently, T cell proliferation was also not affected by the presence of Dano1 or a control Nb (**Figure 42B, C**).
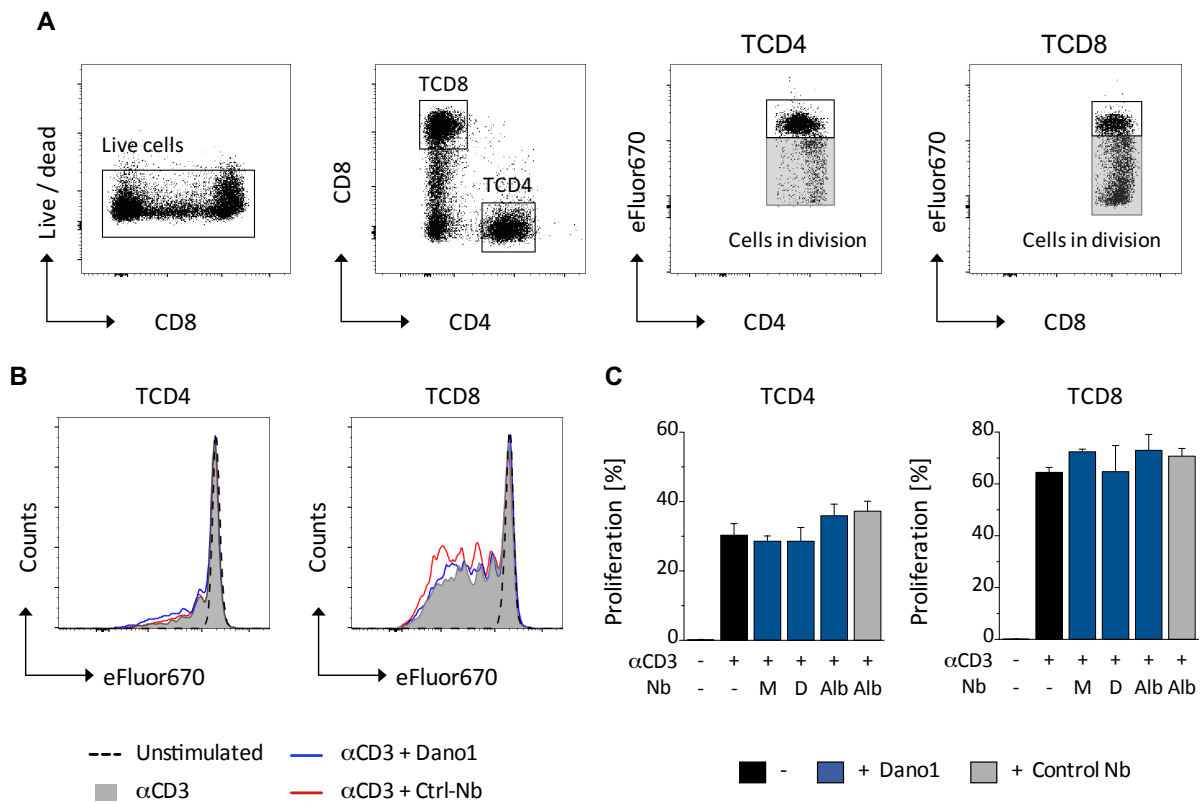
Figure 42. Dano1 does not affect proliferation of human T cells *in vitro*. Human PBMCs were stimulated with αCD3 antibodies (0.5 µg/ml) and ATP (1.5 mM or 4.5 mM) in the absence or presence of 100 nM of Dano1 or a control Nb (anti-mARTC2.2). T cell proliferation was monitored by flow cytometric analysis of eFluor dye dilution. Nanobodies were used as monomers (M), dimers (D) or fused to the albumin-binding nanobody Alb8 (Alb); and added on day zero and day two. (**A**) Gating strategy for the identification of CD4 and CD8 T cells. (**B**) Overlaid histograms (MFI) represent the amount of CD4 (left) and CD8 (right) T cells in proliferation. (**C**) Percentage of proliferating cells (Mean± SD, n =3). P values were determined by one-way ANOVA followed by Bonferroni post-test. Data are of one representative donor of a total of four donors.

Next, we tested whether ATP-mediated activation of P2X7 would influence T cell function. To this end, we stimulated human PBMCs with αCD3 antibodies or with HDMAPP (for γδ T cells), and assessed the upregulation of activation markers and T cell proliferation in the presence of exogenously added ATP. While addition of 1.5 mM of ATP did not alter upregulation of CD25 on conventional T cells, it seemed to reduce activation of γδ T cells (**Figure 43A**). At higher concentrations of ATP, all three T cell subsets showed little activation, likely due to induction of cell death. This effect could be partially blocked with Dano1, but only on conventional T cells, and not on γδ T cells (**Figure 43A**), underlining the higher sensitivity of these cells to ATP. A similar picture was obtained for the upregulation of CD69 (**Figure 43B**).
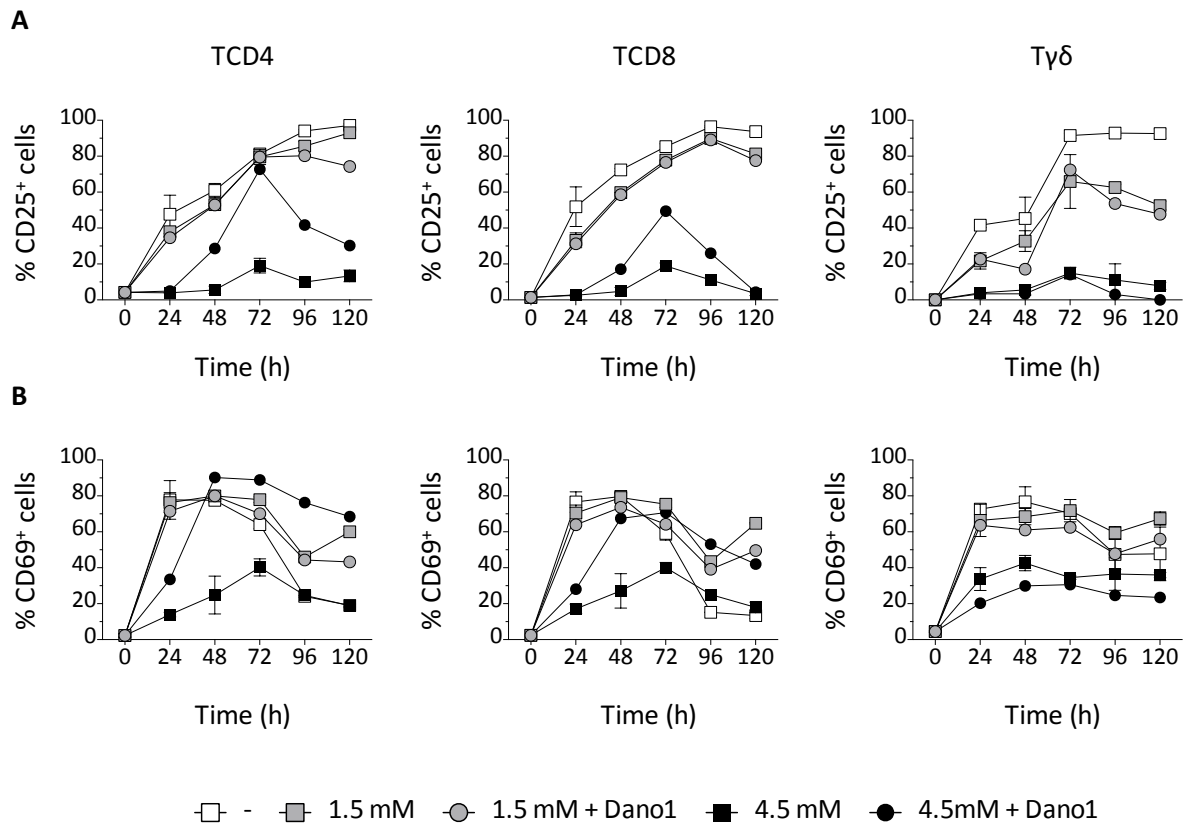
Figure 43. ATP stimulation impairs T cell activation *in vitro*. Human PBMCs were stimulated with αCD3 antibodies (0.5 µg/ml) and ATP (1.5 mM or 4.5 mM) in the absence or presence of 100 nM of Dano1. The activation of CD4 (left), CD8 (middle) and γδ T cells (right) was determined by the expression of the activation markers CD25 (**A**) and CD69 (**B**) on the cell surface. Nanobodies were used as monomers, and added on day zero and day two. Data (Mean ± SD, n=2) are representative of a single donor.

Similarly, ATP also impaired T cell proliferation in a dose-dependent manner, leading to a complete lack of proliferation upon addition of the highest concentration of ATP (4.5 mM) (**Figure 44**). Even though only live cells were included in the analysis, it is likely that the high concentration of ATP triggers the initiation of apoptosis, so that even the cells that survive are not able to proliferate normally. Additionally, blockade of P2X7 did not inhibit the effects caused by ATP, regardless of its concentration (**Figure 44**).

These data suggest that blockade of P2X7 does not have an impact on T cell activation or proliferation *in vitro*. However, we cannot exclude the contribution of other P2 receptors in this scenario.
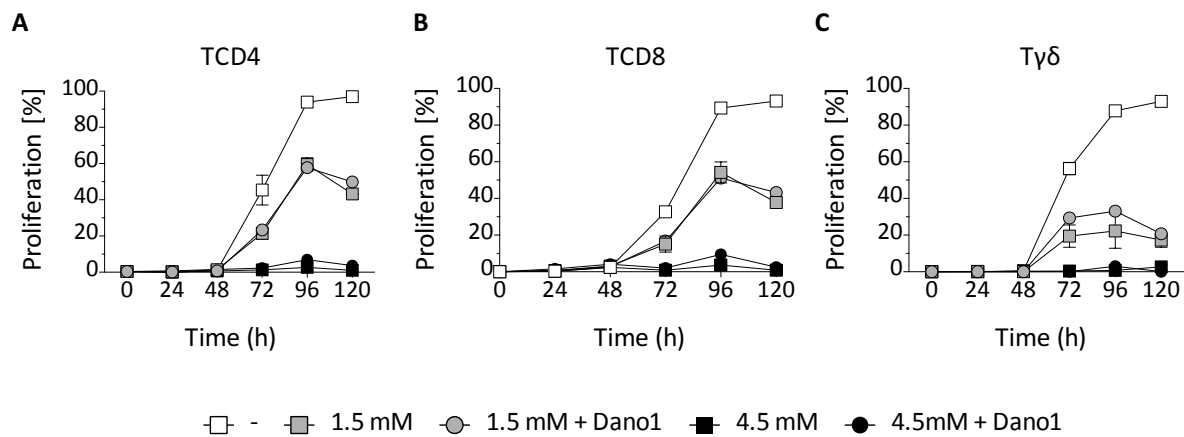
Figure 44. ATP stimulation impairs T cell proliferation *in vitro*. Human PBMCs were stimulated with αCD3 antibodies (0.5 µg/ml) and ATP (1.5 mM or 4.5 mM) in the absence or presence of 100 nM of Dano1. The proliferation of CD4 (**A**), CD8 (**B**) and γδ T cells (**C**) was monitored by flow cytometric analysis of eFluor dye dilution. Nanobodies were used as monomers, and added on day zero and day two. Percentage of proliferating cells (Mean ± SD, n=2) are from a single donor.

4.2.16 P2X7 does not provide costimulation under suboptimal stimulation of the TCR *in vitro*

Finally, we hypothesized that P2X7 might act as a costimulatory signal under suboptimal TCR-stimulation, especially on innate-like lymphocytes, since they respond independently of TCR stimulation. To this end, we determined T cell activation and proliferation on human PBMCs in response to increasing concentrations of αCD3 and ATP (**Figure 45**), mimicking a condition of suboptimal stimulation. At 1nM of αCD3, the stimulation of conventional CD4 T cells was optimal, while γδ T cells could only be fully stimulated upon 10nM of αCD3. Addition of exogenous ATP (1.5 mM) had little if any effect on T cell activation, since surface levels of CD69 and CD25 remained similar (**Figure 45A, B**); but resulted in diminished T cell proliferation (**Figure 45C**).

Presence of the ATP-degrading enzyme apyrase also resulted in impaired T cell proliferation (**Figure 45C**), whereas blockade of P2X7 using Dano1 did not alter ATP-induced effects (**Figure 45**); suggesting that other P2 receptors may come into play.

Although we only analysed one donor, our results suggest that prolonged interaction of T cells with ATP affects T cell proliferation and activation in a dose-dependent manner, regardless of the strength of TCR stimulation. Furthermore, blockade of P2X7 does not seem to be sufficient to prevent the effects induced by prolonged stimulation with ATP in long-term assays.
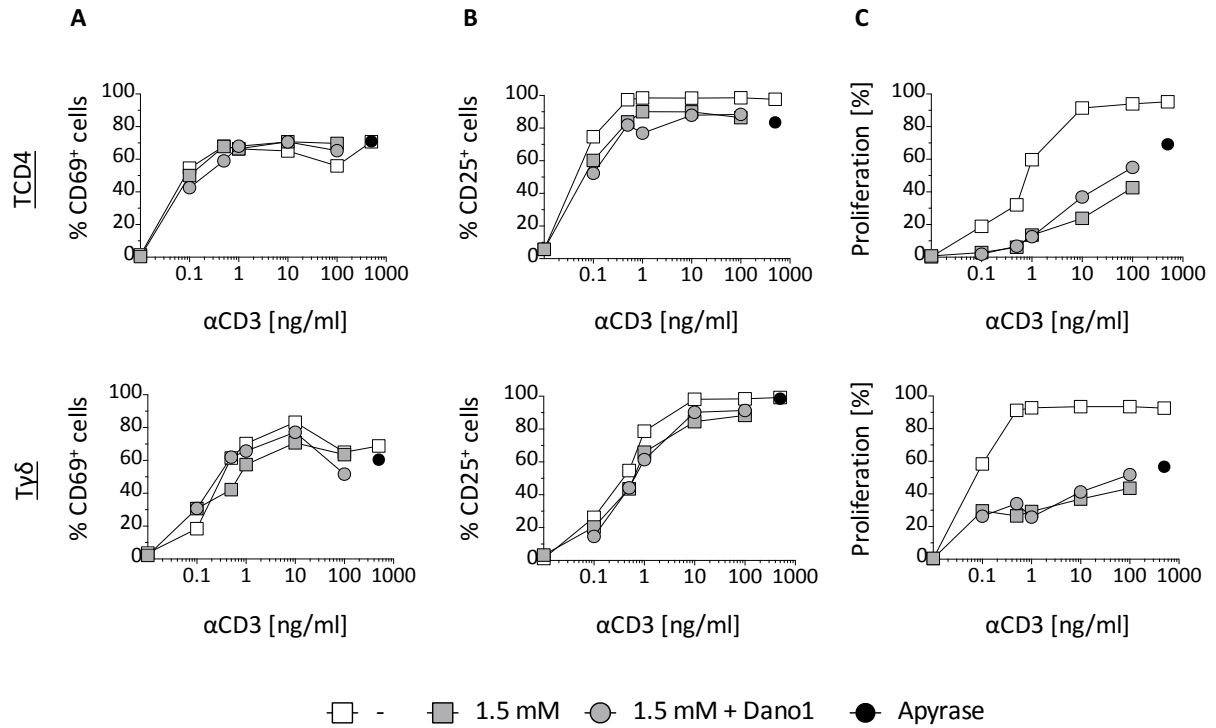
Figure 45. ATP does not act as a costimulatory signal under suboptimal stimulation of the TCR. eFluor labelled PBMCs were stimulated with different concentrations of αCD3 antibodies and ATP in the absence or presence of Dano1 (monomer). The percentage of CD69^{+} (**A**), CD25^{+} (**B**) or proliferating (**C**) CD4 (upper row) and γδ T cells (bottom row) was determined by flow cytometry. Data are from a single donor.

5. <u>DISCUSSION</u>

ATP is predominantly located intracellularly in physiological conditions. Damaged cells release large quantities of ATP to the extracellular compartment, which can bind to purinergic P2 receptors on the surface of immune cells, triggering, in most of the cases, inflammatory responses (Faas, Sáez and de Vos, 2017). P2 signalling induces a variety of responses, such as activation and proliferation of T cells, degranulation of neutrophils, and production of reactive oxygen species (ROS) and inflammatory cytokines by monocytes and macrophages (Idzko *et al.*, 2007; Boeynaems, Communi and Robaye, 2012a; Pettengill *et al.*, 2013; Rodrigues, Tomé and Cunha, 2015; Cekic and Linden, 2016; Danquah *et al.*, 2016; Amores-Iniesta *et al.*, 2017; Cauwels *et al.*, 2017). Among all P2 receptors, P2X7 is the most studied in the field of immunology due to its striking contribution to inflammation. The binding of ATP to P2X7 triggers the activation of the inflammasome and maturation of the proinflammatory cytokine IL-1β (Lister *et al.*, 2007), which is essential for the host-response and resistance to pathogens, but it also exacerbates damage during chronic disease and acute tissue injury. Indeed, P2X7 is associated with the pathogenesis of a variety of inflammatory disorders, thus attracting the attention of many researchers as a potential target for therapy (Mehta *et al.*, 2014; Burnstock, 2017; Burnstock and Knight, 2018).

In this study, we identified innate-like lymphocytes (ILLs) as the cell type expressing the highest levels of P2X7 and reacting more promptly to ATP among all T cell subsets. Furthermore, we show the potential of the P2X7-specific nanobody Dano1 as a promising drug candidate for the treatment of human disease.

5.1 P2X7 EXPRESSION AND FUNCTION IN HUMAN IMMUNE CELLS

We first set out to assess the expression of P2X7 on immune cell types using a nanobody (Dano1) that recognizes human P2X7 with high specificity (Danquah *et al.*, 2016). The low expression of P2X7 in several immune cell subtypes still required the use of a stringent negative control in order to ensure the specificity of the P2X7 signal.

P2X7 is virtually expressed by all immune cell populations and most tissues in the body (Burnstock and Knight, 2004; Sperlagh *et al.*, 2006; Welter-Stahl *et al.*, 2009; Bartlett, Stokes and Sluyter, 2014; Idzko, Ferrari and Eltzschig, 2014). Within granulocytes, human eosinophils (Ferrari, Idzko, *et al.*, 2000) and mast cells (Wareham et al., 2009) express P2X7. The expression of a functional receptor in neutrophils is still controversial (Martel-Gallegos et al., 2010). Although there are no studies reporting its expression in human basophils, P2X7 is expressed by bone marrow-derived basophils in

mice (Tsai et al., 2015). Data arising from our lab shows little if any expression of P2X7 in the surface of all granulocyte subtypes (data not shown), and the discrepancy could be due to a false positive signal arising from the high autofluorescence signal common to all granulocytes. In agreement with published data, we observed the highest expression of P2X7 in human monocytes, both on the cell surface and at mRNA level. We detected lower expression of P2X7 in non-classical monocytes (CD14^{dim} CD16$^+$) compared to the classical (CD14$^+$ CD16$^-$) and intermediate (CD14$^+$ CD16$^+$) subsets. Non-classical monocytes release lower amounts of IL-1β after exposure to LPS or LPS + bzATP than classical and intermediate monocytes due to a higher degradation rate of the pro-IL-1β transcript (Hadadi et al., 2016). We postulate that the lower expression of P2X7 on this subset might contribute to less efficient processing of pro-IL-1β to active IL-1β, suggesting a correlation between expression and function of P2X7.

While murine lymphocytes have been characterized in terms of P2X7 expression, very little is known about the expression of P2X7 in human lymphocytes. According to Gu and colleagues, human NK, T and B cells show similar expression of P2X7; low on the cell membrane, but much higher intracellularly (Gu et al., 2000). In our hands, NK cells express the highest levels of P2X7, both on the surface and at the mRNA level. In contrast, P2X7 is functional on B cells even though it is barely detectable at the cell surface (Gu et al., 2000; Pupovac et al., 2015). The controversial data in this field might be explained by the usage of different reagents targeting the human P2X7R. The monoclonal antibody (mAb) ´L4´ is the most widely used antibody for the detection of human P2X7 by flow cytometry. MAb L4 partially blocks P2X7 function in human monocytes, while Dano1 completely blocks its function in vitro (G. Buell et al., 1998; Danquah et al., 2016), which might be a consequence of binding to different epitopes (Danquah, unpublished).

There is general consensus that human T cells express P2X7 (Budagian et al., 2003; Sluyter and Wiley, 2014), however, whether distinct T cell subsets exhibit different levels of P2X7 has not been reported yet. Our data show a distinct pattern of P2X7 expression among human T cells, being ILLs and cells with an effector phenotype the ones expressing the highest levels of the receptor. ILLs, including γδ T cells, mucosal associated invariant T cells (MAIT) and invariant NKT cells (iNKTs), are a class of T cells that exhibit properties from both innate and adaptive immunity (Vermijlen and Prinz, 2014). In contrast to conventional αβ T cells, ILLs display a highly restricted TCR repertoire: human MAIT cells express the Vα7.2 chain predominantly in combination with the Vβ2 and Vβ13 chains (Tilloy et al., 1999; Lepore et al., 2014), while human iNKTs combine the Vα24-Jα18 preferentially with the Vβ11 chain (Dellabona et al., 1994). Due to their low frequency in human peripheral blood, iNKT cells were not included in this work (Montoya et al., 2007). γδ T cells are unique in that they rearrange the TCR γ and TCR δ chains instead of the classical TCR α and TCR β chains, being most of γδ T cells circulating

in blood Vγ9δ2^{+} cells. ILLs are not restricted by classical MHC class I or II molecules, but by non-classical MHC molecules instead. MR1 molecules present vitamin B metabolites to MAIT cells. Antigen presentation to iNKT cells is mostly mediated by CD1d molecules; while MICA, MICB and butyrophilins present antigen to γδ T cells (Harly *et al.*, 2012; Prinz, Silva-Santos and Pennington, 2013; Reantragoon *et al.*, 2013; Adams, Gu and Luoma, 2015). Remarkably, ILLs respond rapidly upon antigen encounter and therefore become activated at the early stages of infections.

In mice, T cells expressing higher levels of P2X7 exhibit higher sensitivity to P2X7-induced cell death and P2X7-dependent shedding of CD62L from the cell surface (Aswad and Dennert, 2006). However, Safya and colleagues have recently reported that T cell sensitivity to ATP does not strictly rely on P2X7 expression but rather depends on the activation and differentiation status of conventional T cells. Both activated (CD69^{+}) naïve and memory T cells exhibit higher exposure of phosphatidylserine (PS) and pore formation in response to ATP than their non-activated (CD69^{-}) counterparts. In contrast, non-activated T cells exhibit higher sensitivity to ATP-induced shedding of CD62L than activated T cells; underlining dissimilitude between the different P2X7-mediated cellular responses in distinct T cell subsets (Safya *et al.*, 2018). We observed a correlation between P2X7 expression and sensitivity to ATP in human T cells. Thus, ILLs do not only show the highest expression of P2X7 but also exhibit the highest sensitivity to ATP within the T cell compartment. We also observed a correlation between T cell activation status and sensitivity to ATP, being effector conventional T cells more sensitive to ATP than naïve T cells. We also report upregulation of *P2RX7* expression upon activation, especially in γδ T cells. The higher expression and sensitivity of P2X7 in T cells with an effector profile might serve as a "checkpoint" to limit excessive inflammatory responses. Higher expression of P2X7 in activated T cells would also support the role of P2X7 as a regulatory mechanism to induce cell death of T cells, when a strong effector response is no longer necessary. Indeed, P2X7-induced cell death of effector intestinal CD4 T cells is determinant for the control of experimental colitis (Hashimoto-Hill *et al.*, 2017), and genetic ablation of P2X7 worsens experimental autoimmune encephalomyelitis (EAE) by impairing apoptosis of activated lymphocytes (Chen and Brosnan, 2006); highlighting the contribution of P2X7 in limiting effector T cell responses.

P2X7-mediated cell death of immune cells occurs at high (millimolar) concentrations of ATP (Yoon *et al.*, 2007), compatible with an inflammatory milieu. Extracellular NAD^{+} (eNAD[+]) can also activate P2X7 in mice; and just the brief exposure to low concentrations of NAD^{+} induces cell death of sensitive murine T cell subtypes, especially Tregs and iNKT cells (Seman *et al.*, 2003; Hubert *et al.*, 2010; Rissiek *et al.*, 2014). Instead, low concentrations of ATP promote the activation and proliferation of T cells through P2X7 signalling (Baricordi *et al.*, 1999; Adinolfi *et al.*, 2005; Schenk *et al.*, 2008; Yip *et al.*, 2009). A higher expression of P2X7 could imply stronger contribution of P2X7 during TCR activation.

ILLs can be activated in a TCR-independent manner via stimulation of innate receptors (NK receptors, TLRs) or through cytokine signalling (Martin *et al.*, 2009; Sutton *et al.*, 2009; Reilly, Wands and Brossay, 2010; Brennan, Brigl and Brenner, 2013; Ussher *et al.*, 2014; Slichter *et al.*, 2016). We speculate that P2X7 signalling could act as a cofactor under suboptimal stimulation of the TCR and modulate the function of T cells during inflammation, especially of ILLs.

Extracellular ATP (eATP) does not only induce the activation of P2X7, but also of all P2X and several P2Y receptors, namely P2Y1, P2Y24, P2Y11 and P2Y13 (Cekic and Linden, 2016). Since P2X7 shows the lowest affinity for ATP among all P2 receptors, we have used high concentrations of ATP in this study, which might have activated other P2 receptors. Additionally, eATP is exposed to the activity of ectonucleotidases, such as CD39 and CD73, which mediate its hydrolysis into adenosine (Ado); a molecule that induces immunosuppressive functions on immune cells upon binding to P1 receptors (Haskó *et al.*, 2008). Thus, different concentrations of ATP and its downstream metabolites may trigger contrasting responses through signalling via different receptors (Idzko, Ferrari and Eltzschig, 2014; Spaans et al., 2014), revealing the complex network of purinergic signalling. We report that specific blocking of P2X7 does not impair proliferation or activation of human CD4 and CD8 T cells *in vitro*. Since physiological concentrations of ATP (1-50 nM) do not induce the proliferation of activated CD4 T cells (Trabanelli et al., 2012), we attributed the lack of effect in our assays to insufficient release of ATP by T cells, and therefore the inability to activate P2X7; although we did not measure the concentration of ATP present in the media. Upon TCR engagement, both P2X1 and P2X4 receptors translocate to the immune synapse and bind pericellular eATP. Engagement of ATP induces Ca^{2+} entry, activation of nuclear factors of activated T cells (NFATs) and synthesis of IL-2; which are crucial downstream responses for the activation and proliferation of T cells. Inhibition of P2X1 and P2X4 receptors prevents the uptake of Ca^{2+} and diminishes the synthesis of IL-2. These effects are more prominent when using non-selective P2 antagonists or P2X4-specific antagonists than inhibitors of P2X1 or P2X7 (Schenk *et al.*, 2008; Woehrle *et al.*, 2010). Ledderose and colleagues recently showed that naïve T cells release ATP in response to the chemokine SDF-1α, and that ATP binding to P2X4 contributes to the migration of human and murine T cells (Ledderose et al., 2018), underlining the role of P2X4 in T cell biology. It is then plausible that P2X7 blockade did not alter the proliferation or activation of T cells in our experiments due to the compensatory effect of other P2X receptors, most likely P2X4. Stimulation of T cells with high doses of ATP prominently decreased the activation and proliferation of T cells, probably due to ATP-induced cell death of T cells. In line with our findings, stimulation of activated CD4 T cells with a high concentration of ATP (1mM), but still lower than the concentrations used in our study, impairs T cell proliferation (Trabanelli *et al.*, 2012). The same study showed that stimulation of activated CD4 T cells with 250 nM ATP induces T cell proliferation, and

that this effect was counteracted upon degradation of ATP by apyrase. We observed that blockade of P2X7 was not sufficient to inhibit the effects of high concentrations of ATP on T cell proliferation and activation, again underlining the promiscuous use of P2 receptors. Whether the inhibition of P2X7 upon stimulation with low or intermediate concentrations of ATP would prevent the activation or proliferation of T cells needs to be further investigated.

Activation of metalloproteinases and subsequent shedding of susceptible membrane glycoproteins, and to a lesser extent pore formation occur relatively shortly after P2X7 activation. In contrast to the lack of effect seen on long-term assays like T cell proliferation, we observed that blocking of P2X7 efficiently inhibited shedding of CD62L and pore formation on immune cells upon stimulation with ATP. In long-term assays, ATP is produced, metabolised and it engages, in a sustained or intermittent manner, with different P2 receptors. Blocking P2X7 with Dano1 does not exclude the contribution of ATP and its metabolites to other purinergic receptors (Cekic and Linden, 2016). For instance, activation of the P2Y11 receptor impairs P2X7-mediated pore formation induced by eATP; but does not affect the influx of Ca^{2+} (Dreisig et al., 2018). Thus, studying the proximal effects immediately after P2X7 activation, such as influx of Ca^{2+} ions, would markedly reduce prolonged interaction of ATP with other P2 receptors. Using multicolour flow cytometry, we could still distinguish the Ca^{2+} signalling on different immune cell subsets, and clarify whether higher sensitivity of P2X7 to ATP on ILLs occurs immediately or requires a longer time of interaction. Alternatively, to elucidate the role of a single receptor such as P2X7 would require the use of specific inhibitors for all other P2 receptors. The use of a P2X7-specific agonist or the generation of P2X7-specific Nbs that potentiate the function of human P2X7, as it is the case of the Nb 14D5 in mice (Danquah et al., 2016), would also provide valuable information about what actually occurs after exclusively activating P2X7. Finally, it should be taken into account that these data arise from in vitro studies, and might not completely mirror the concentrations or interactions that occur in vivo.

5.2 DISCREPANCIES BETWEEN HUMAN AND MURINE P2X7

The murine P2X7 receptor shares 80% sequence identity to the human P2X7 receptor (Bartlett, Stokes and Sluyter, 2014). However, several discrepancies exist between the two species. For instance, ATP is the only purine nucleotide able to induce P2X7 activation in humans, whereas in mice, the ecto–ADP-ribosyltransferase ARTC2.2 can also trigger its activation in response to $eNAD^+$ (Seman et al., 2003; Adriouch et al., 2008). The relevance of this pathway in humans is not yet completely understood, since a premature stop codon in the ART2 pseudogene prevents its expression in human cells (Haag et al., 1994) and, consequently, NAD^+ does not induce apoptosis of human Tregs or PBMCs (Cortés-Garcia et al., 2016). Four additional variants of ART (ART1, ART3,

ART4 and ART5) exist in humans (Glowacki *et al.*, 2009). Within the immune system, ART1 is expressed in lymphocytes, monocytes and granulocytes (Grahnert *et al.*, 2002; Koch-Nolte *et al.*, 2006; Cortés-Garcia *et al.*, 2016). ART3 is expressed in different tissues, such as muscle and brain; while ART4 is highly expressed by erythrocytes and slightly expressed by monocytes (Koch-Nolte *et al.*, 2006). ART5 is found in similar tissues as ART3 (Koch-Nolte *et al.*, 2006), but is also detected in lymphocytes (Cortés-Garcia *et al.*, 2016). From these variants, however, only ART1 and ART5 exhibit ADP-ribosyltransferase activity (Koch-Nolte *et al.*, 2006). Since ART5 lacks the C-terminal GPI anchor and only exists in soluble form (Glowacki *et al.*, 2001); it is generally believed that ART1 is the only one able to parallel the ribosyltransferase functions of murine ARTC2.2 (Koch-Nolte *et al.*, 2006; Cortés-Garcia *et al.*, 2016).

Genetic variations affect both the human and murine P2X7, leading to differences in the expression, sensitivity and function of P2X7 (Wiley *et al.*, 2003; Bartlett, Stokes and Sluyter, 2014). A distinct allelic variant (P451L) resulting in the substitution of a proline by a leucine in the C-terminal cytosolic tail of P2X7 leads to lower sensitivity to ATP. Both C57BL/6 and DBA mice, among other strains, carry the 451L mutation and exhibit lower sensitivity to ATP than many other strains of mice, such as BALB/c and non-obese diabetic (NOD) mice (Adriouch *et al.*, 2002). Additionally, different immune cell types express different P2X7 splice variants. Murine T cells preferentially express the highly sensitive P2X7 variant (P2X7k), whereas macrophages predominantly express the classical P2X7 variant (P2X7a) (Schwarz *et al.*, 2012). Of note, eNAD$^+$ only induces ARTC2.2-mediated activation of the P2X7k variant (Schwarz *et al.*, 2012). The lower sensitivity of T cells from C57BL/6 mice might also be attributed to a lower expression of P2X7 on the cell surface (Hubert et al., 2010). The identification of different splice variants revealed that two different strains of P2X7-deficient mice, namely the GSK (GlaxoSmithKline) and Pfizer lines, are not complete knockouts for P2X7 (Bartlett, Stokes and Sluyter, 2014). Since the P2X7k variant originates from a novel exon 1, T cells from GSK mice express a fully functional P2X7 receptor (Nicke *et al.*, 2009). In Pfizer mice, both P2X713b and P2X71c splice variants escaped genetic deletion, although in this particular case, P2X7 is not functional on immune cells (Simon R J Taylor *et al.*, 2009). It is not known whether an analogous splice variant to the highly sensitive P2X7K also exists in humans. Polymorphisms in the human *P2RX7* gene can also lead to a loss-or-gain of function of P2X7. To date, three different gain-of-function (GOF) SNPs (H155Y, H270R, and A348T) and several loss-of-function (LOF) SNPs (V76A, G150R, R276H, R307Q, T357S, E496A, I568N) have been identified (Cabrini *et al.*, 2005; Fuller *et al.*, 2009; Stokes *et al.*, 2010; Bartlett, Stokes and Sluyter, 2014; Caseley *et al.*, 2014; Di Virgilio *et al.*, 2017). Some other SNPs, such as the Q460R, do not lead to significant changes in the function of P2X7 per se (Roger *et al.*, 2010); but when co inherited with other GOF SNPs, generate GOF

haplotypes (Cabrini *et al.*, 2005; Barden *et al.*, 2006; Stokes *et al.*, 2010). Many of these polymorphisms are associated with susceptibility to infection, such as toxoplasmosis (Jamieson *et al.*, 2010) and tuberculosis (Fernando *et al.*, 2007); and also with the pathogenesis of numerous diseases, such as rheumatoid arthritis (Al-Shukaili *et al.*, 2011), ischemic stroke and ischemic heart disease (Gidlöf *et al.*, 2012), chronic pain (Sorge *et al.*, 2012), multiple sclerosis (Gu *et al.*, 2015) and osteoporosis (Gartland *et al.*, 2012).

The expression pattern of P2X7 on immune cells also differs between the two species. While both species exhibit the highest levels of P2X7 on monocytes and macrophages, the expression pattern is different within the T cell compartment. In mice, P2X7 is highly expressed on Tregs and in iNKTs (Hubert *et al.*, 2010; Rissiek *et al.*, 2014); whereas we observe the highest expression of P2X7 on ILLs in humans. Remarkably, we found Tregs expressing very low levels of P2X7 within human T cells. Murine Tregs are highly sensitive to P2X7-mediated cell death (Rissiek *et al.*, 2014); whereas neither ATP (1mM) nor NAD (60 µM) are able to induce cell death or shedding of CD62L on human CD39$^+$ or CD39$^-$ Tregs *in vitro* (Cortés-Garcia *et al.*, 2016). In contrast to these findings, we did observe shedding of CD62L and induction of pore formation on Tregs upon stimulation with higher doses of ATP (≥ 1.5 mM). Upon stimulation with ATP, murine Tregs are more sensitive to P2X7-mediated shedding of CD62L and pore formation than conventional T cells (Safya *et al.*, 2018). We however report practically identical sensitivity to ATP in human Tregs and conventional CD4 T cells. Also in contrast to what Cortés-Garcia and colleagues reported, we observed higher levels of P2X7 and higher sensitivity to ATP in CD39$^+$ Tregs than in their negative counterparts. CD39 is an ectoenzyme that converts eATP into ADP and AMP; which can be further degraded to Ado by CD73 (Antonioli *et al.*, 2013). Degradation of ATP prevents its binding to P2 receptors and therefore exacerbated inflammatory responses. Since CD39$^+$ Tregs exhibit stronger immunosuppressive activity (Borsellino *et al.*, 2007; Herrath *et al.*, 2014; A. Rissiek *et al.*, 2015), we expected lower levels of P2X7 on the cell surface of this subset. In addition to its role in the catabolism of ATP, CD39 is considered an activation marker for T cells (Maliszewski *et al.*, 1994). The higher expression of P2X7 on CD39$^+$ Tregs and CD39$^+$ conventional CD4 T cells correlates to our data showing higher expression on effector/activated T cells. We postulate that higher expression of P2X7 could have a dual role in human CD39$^+$ T cells: During the onset of inflammation, ATP concentration is high, suppressing Treg function. Towards resolution of inflammation, conventional T cells upregulate CD39 in order to eliminate ATP and facilitate adenosine production. Lower concentrations of ATP could then induce proliferation and activation of regulatory T cells, dampening the inflammatory response, and maintaining Treg function (Kinsey *et al.*, 2012; Ohta *et al.*, 2012). CD39$^+$ Tregs are also more sensitive to ATP-induced pore formation. Safya and colleagues suggest that ATP-induced pore formation

activity by murine Tregs could facilitate release of ATP and therefore its conversion into AMP and ultimately into Ado (Safya *et al.*, 2018). Although CD39 and CD73 are rarely co expressed in human Tregs (Mandapathil *et al.*, 2010), CD73 is also functional as a soluble molecule. Thus, we believe that a similar release of ATP by CD39^{+} Tregs and subsequent conversion to Ado might also occur in humans. Tuning the availability of ATP is a promising therapeutic option to modulate the immune response, and deserves further study to elucidate the consequences of different concentrations of eATP in the different human T cell types, according to expression of P2X7, threshold for activation and activation status of the cells.

In addition to the high levels of ATP released in response to cell damage (Wan *et al.*, 2016), gut microbiota generate and secrete large amounts of ATP to the extracellular compartment (Iwase *et al.*, 2010; Hironaka *et al.*, 2013). In mice, eATP from commensal bacteria induces the secretion of IL-6, IL-23 and TGF-β by DCs, promoting the polarization of T cells towards a Th17 phenotype (Atarashi *et al.*, 2008). An exacerbated Th17 response is strongly associated with gut inflammation. Thus, strategies that reduce eATP or blocking ATP-mediated Th17 differentiation are beneficial to control gut inflammation (Friedman *et al.*, 2009; Neves *et al.*, 2014; Wan *et al.*, 2016; Figliuolo *et al.*, 2017). P2X7 is widely expressed throughout the intestine in mice, both in the epithelium and immune cells (Diezmos, Bertrand and Liu, 2016). Murine conventional CD8αβ and unconventional CD8αα T cells of the intestinal epithelium and lamina propria express higher amounts of P2X7 than CD8 T cells from the periphery (Heiss *et al.*, 2008). In contrast, we report similarly low expression of P2X7 on the surface of intestinal T cells and peripheral immune cells in humans; although we did not directly compare the expression of P2X7 in intestinal and peripheral T cells from the same donor. Retinoic acid mediates the upregulation of P2X7 on the surface of murine T cells (Heiss *et al.*, 2008; Hashimoto-Hill *et al.*, 2017), but we did not observe any upregulation of P2X7 on human T cells. Nevertheless, individuals with Crohn´s disease show increased expression of P2X7 in the mucosa of the colon and higher levels of proinflammatory cytokines (Neves *et al.*, 2014), suggesting a potential role of P2X7 in this disease. Thus, it would be worth investigating whether intestinal T cells from patients suffering from inflammatory disorders of the gastrointestinal tract express higher levels of P2X7 than healthy individuals.

5.3 THE P2X7 NANOBODY DANO1 AS A POTENTIAL THERAPEUTIC DRUG

The role of P2X7 in the pathogenesis of inflammatory disorders is mainly driven by the maturation and subsequent release of the proinflammatory cytokine IL-1β (Ferrari et al., 2006; Baroni et al., 2007; Gicquel et al., 2015; Giuliani et al., 2017). Experimental animal models are extremely useful for testing the safety and efficacy of newly generated drugs, as well as for understanding the molecular

mechanisms of the therapy. Since P2X7 clearly contributes to exacerbated inflammatory responses, the blockade or genetic ablation of P2X7 in animal models results in amelioration of the symptomatology and/or increased survival of the mice (see **Table 2**). Still, drug effectivity in experimental models does not imply a similar outcome in human clinical trials. The P2X7 inhibitors AZD9056 (NCT00520572) and CE-224,535 (NCT00628095) did not demonstrate any additional benefit for the treatment of rheumatoid arthritis in phase II clinical trials (Keystone et al., 2012; Stock et al., 2012). The AZD9056 inhibitor also failed to translate into benefits for patients suffering from osteoarthritis (study code: D1522c00001) and chronic obstructive pulmonary disease (study code: D1521C00002) (A. Stockley et al., 2008; Arulkumaran, Unwin and Tam, 2011); but it did reduce pain intensity in patients suffering from chronic pain (EudraCT-2005-002319-26) (Eser et al., 2015). The reason for this discrepancy could be due to specific differences in the expression of P2X7 and the protein isoform (determined by different allelic and splice variants), which may lead to different sensitivity to ATP in mice and humans.

Nanobodies (Nbs) are highly promising tools not only for research, but also for therapy (Arezumand et al., 2017; Bannas, Hambach and Koch-Nolte, 2017; Koch et al., 2017). At present, eight different Nbs are being tested in clinical trials by the pharmaceutical company Ablynx (Ghent, Belgium). From these, Nbs against the IL-6R and against the von Willebrand factor showed promising and beneficial effects in phase II clinical trials against rheumatoid arthritis (NCT01284569) (Van Roy et al., 2015) and acquired thrombotic thrombocytopenic purpura (NCT01020383) (Peyvandi et al., 2016); underlining the potential of Nbs for the treatment of inflammatory diseases.

Owing to their small size and the length and flexibility of their CDR3 region, Nbs are able to bind to epitopes that are normally inaccessible to conventional antibodies (Abs) (Muyldermans, 2013). Nbs induce weak immunogenicity due to their short-half life and a high sequence homology with the human variable V_H domain (Unciti-Broceta et al., 2013), and they can be genetically optimized to further reduce its immunogenicity (Vincke et al., 2009). Furthermore, the fusion of target-specific Nbs to other Nbs with a different specificity and/or to specific protein domains enables targeting to a specific tissue or results in increased half-life of the Nb (Wesolowski et al., 2009; Farrington et al., 2014). Indeed, injection of a nanobody against P2X7 ameliorated inflammation in glomerulonephritis and allergic contact dermatitis in mice (Danquah et al., 2016).

Monocytes, macrophages, DCs and mast cells produce IL-1β, which is a pivotal mediator in inflammation (Ren and Torres, 2009). Different from other cytokines, which are produced as mature forms and released through the classical secretory pathway, IL-1β is produced as a precursor (pro-IL1β) upon TLR stimulation and becomes active after cleavage of the precursor form by caspase-1 (Garlanda, Dinarello and Mantovani, 2013). Both the processing and release of IL-1β are tightly

regulated in order to avoid exacerbated inflammation (Charles A. Dinarello, 2011). Signals that induce the processing of pro-IL1β include nigericin, ATP, flagelin, uric acid and silica crystals, and aluminium hydroxide, among others (Charles A Dinarello, 2011; Cullen *et al.*, 2015). These compounds trigger various cellular signals, although the efflux of K^+ ions seems to be the origin of inflammasome activation (Muñoz-Planillo *et al.*, 2013). Processing of IL-1β also occurs independently of caspase-1. Cellular stress, dectin-1 or activation of Fas receptors can also induce the cleavage of pro-IL1β through activation of caspase-8. Alternatively, proteases released from neutrophils and mast cells during inflammation can also mediate the processing of pro-IL1β in the extracellular compartment (Charles A Dinarello, 2011; Afonina *et al.*, 2015).

High concentrations of ATP accelerate the conversion of the precursor into active IL-1β (Charles A Dinarello, 2011). Activation of P2X7 and overproduction of IL-1β mediate exacerbated inflammatory responses and are implicated in the pathology of many inflammatory disorders and autoimmune diseases, such as rheumatoid arthritis, chronic and neuropathic pain, inflammatory bowel disease, cardiovascular diseases, acute lung injury, lung inflammation and fibrosis, experimental glomerulonephritis, experimental autoimmune encephalomyelitis, multiple sclerosis, type 1 diabetes (T1D), allergic contact dermatitis and cancer (Labasi *et al.*, 2002; Chessell *et al.*, 2005; Sharp *et al.*, 2008; S. R.J. Taylor *et al.*, 2009; Riteau *et al.*, 2010; Coccia *et al.*, 2012; H. Wang *et al.*, 2015; Vieira *et al.*, 2016; Danquah *et al.*, 2016; Di Virgilio *et al.*, 2017; Lin and Edelson, 2017; Chen *et al.*, 2018). (Charles A Dinarello, 2011). In this thesis, we tested the potential of Dano 1 for modulating human immune cells and demonstrated the specificity of Dano1 for the blocking of P2X7 function *in vitro*. Using a surrogate inflammation model with LPS, we showed that Dano1 efficiently blocks the assembly of the inflammasome in peripheral monocytes, as well as the release of proinflammatory IL-1β. Dano1 exhibited much higher potency than the small-molecule antagonists JNJ47965567 and AZ10606120, both currently in preclinical development. We confirmed the specificity of Dano1 in P2X7-induced inflammasome activation, since blockade of P2X7 had no effect in a patient with constitutive activation of the inflammasome.

IL-1β contributes to the conversion of naïve CD4 T cells towards the proinflammatory Th17 phenotype (Chung *et al.*, 2009; Lasigliè *et al.*, 2011). The engagement of ATP to P2X receptors, especially P2X7, promotes polarization of murine T cells towards the Th1 and Th17 helper phenotype (Atarashi *et al.*, 2008; Schenk *et al.*, 2011; Purvis *et al.*, 2014; Salles *et al.*, 2017), while inhibiting their conversion into $CD4^+$ $CD25^+$ Tregs and type 1 regulatory T cells (Tr1 cells) (Schenk *et al.*, 2011; Mascanfroni *et al.*, 2015). Our data show that proinflammatory Th1 and Th17 cells show higher levels of P2X7 on the surface, suggesting a role of P2X7 also in the polarization of human T cells; although such contribution has not been reported so far. P2X7 activation is also involved in cellular

metabolism (Di Virgilio *et al.*, 2017). On the one hand, basal activation of P2X7 increases the concentration of Ca^{2+} in the mitochondria and cellular energy stores in P2X7-transfected HEK cells; thus promoting cell growth (Adinolfi *et al.*, 2005). Moreover, it also enhances the efficiency of aerobic glycolysis in P2X7-expressing HEK cells (Amoroso *et al.*, 2012), supporting cell proliferation under glucose-deprived conditions. On the other hand, P2X7 contributes to oxidative phosphorylation metabolism, which is necessary for the generation and function of memory CD8 T cells (Borges da Silva *et al.*, 2018). IL-1β and IL-23 are sufficient to induce and maintain an adequate rate of aerobic glycolysis needed to support the metabolic needs for Th17 differentiation. It is plausible that P2X7 may contribute to the shifting towards the glycolytic pathway and promote polarization of T cells towards certain Th phenotypes, namely the proinflammatory Th1 and Th17; although the specific conditions that influence its contribution to a specific metabolic programming have not yet been identified.

Although we could not elucidate the specific function of P2X7 on T cells, both the contribution of IL-1β in Th17 polarization and the higher expression of P2X7 in several effector T cell subtypes indicate that P2X7 could also be a potential target for T-cell driven diseases. Th17 cells play a critical role in the pathogenesis of autoimmune diseases (Tesmer *et al.*, 2008; Jadidi-Niaragh and Mirshafiey, 2011; Han *et al.*, 2015). Dano1 could be a suitable drug for the treatment of diseases mediated by Th1 or Th17 cells, such as rheumatoid arthritis, multiple sclerosis, psoriasis or inflammatory bowel disease; not only by reducing IL-1β production but also by directly modulating the function of T cells. Since P2X7-mediated cell death of murine Tregs favours inflammation (Di Virgilio *et al.*, 2017; Figliuolo *et al.*, 2017), and the presence of ATP inhibits the conversion of murine Th17 cells into IL-10 producing cells *in vitro* (Fan *et al.*, 2016); it is feasible that blockade of P2X7 could counteract such effects on T cells and suppress inflammation *in vivo*. Nonetheless, due to differences in the expression and sensitivity of P2X7 on murine and human T cells it is first necessary to fully determine the role of P2X7 and the effect of ATP concentration on different human T cell subsets.

Since allelic variants influence P2X7 sensitivity to ATP (Fuller *et al.*, 2009), a comprehensive analysis of the genotype should be performed before Dano1 could go into the clinics. In this study, we genotyped all donors for three different SNPs associated with the sensitivity to ATP: H155Y, H270R, and A348T. The originally published reference sequence of human P2X7 (Rassendren *et al.*, 1997) contains the variant H-H-A, which completely differs from the ancestral variant (Y-R-T). All three aminoacids in the ancestral variant confer higher sensitivity to ATP. These allelic variants occur at a frequency of 24.77% for 155Y, 75.23% for R270 and 32.24% for T349 in the Iberian population in Spain; although there are prominent differences among different human populations (Gibbs *et al.*, 2015). We observed clear differences in the magnitude of the response to ATP stimulation among

donors. Nevertheless, Dano1 completely blocked P2X7 function in all donors, regardless of the genotype.

Our group recently identified a SNP in the CD39 gene (*ENTPD1*) that strongly correlates with the expression levels of CD39 in the surface of T cells (A. Rissiek *et al.*, 2015). In line with this finding, we aimed to investigate whether the expression of P2X7 and sensitivity to ATP is higher in individuals carrying the "high sensitive SNPs". While levels of CD39 expression on Tregs can be predicted by analysing a single SNP, the combination of the three GOF SNPs in the *P2RX7* gene generates 36 different viable variants. To date, there are no data reporting whether the presence of just one of the aminoacids in the heterozygous form is sufficient to induce higher sensitivity, or whether the combination of two or more aminoacids at the different positions is needed. Although this is a very interesting aspect, our sample size was too small to contribute to this topic. Still, we did observe that most of the donors differ in one or more amino acids at positions 155, 270 and 348 (see **Table 16**). We believe that once the influence of each of three GOF SNPs in the *P2RX7* gene has been elucidated, it would be worth investigating whether there is a correlation between the different genotypes of the *ENTPD1* and *P2RX7* genes in humans; for instance whether individuals carrying the SNP associated with higher expression of CD39 would also carry a P2X7 variant associated with lower expression and sensitivity of P2X7.

Table 16. Genotypes (SNPs H155Y, H270R and A348T) of the different donors.

	SNPs				SNPs		
Donors	H155Y	H270R	A348T	Donors	H155Y	H270R	A348T
1	YY	RR	AA	24	YY	RR	AT
2	HY	HR	AT	25	HY	RR	AT
3	HY	RR	AT	26	YY	RR	TT
4	HY	RR	AT	27	HY	RR	AT
5	HH	HR	AT	28	YY	HR	AA
6	HH	HR	AT	29	HY	RR	AA
7	HY	RR	TT	30	YY	RR	AT
8	HY	RR	AA	31	HY	RR	AT
9	HY	HR	AT	32	HY	HR	AT
10	YY	RR	TT	33	HY	RR	AA
11	HH	HH	AT	34	HY	RR	AT
12	HY	HH	AA	35	YY	RR	TT
13	YY	HR	AT	36	HY	HR	AT
14	HH	HR	AA	37	HH	HR	AT
15	HY	RR	TT	38	YY	HR	AT
16	YY	HR	AT	39	HY	HH	AA
17	HY	RR	TT	40	HY	HR	AT
18	YY	HR	AT	41	HH	RR	TT
19	HY	HR	AA	42	YY	RR	TT
20	YY	RR	AA	43	HH	RR	TT
21	HY	RR	AT	44	HY	RR	AT
22	HH	RR	AA	45	YY	RR	AT
23	HY	HR	AA	46	HY	HR	AA

6. <u>ABSTRACT</u>

Injured and dying cells release large amounts of adenosine triphosphate (ATP) to the extracellular milieu, which is recognized as a danger signal by the immune system. Released ATP engages purinergic receptors, such as P2X7, promoting inflammation. Extracellular ATP is exposed to degradation, therefore ATP and its downstream metabolites may trigger contrasting responses by signalling through different purinergic receptors. P2X7 is expressed in most human tissues and immune cells. ATP binding activates P2X7 and induces the influx of Ca^{2+} and Na^+ and efflux of K^+, triggering distinct cellular responses depending on the cell type. Persistent stimulation by ATP induces the opening of a non-selective pore permeable to organic cationic molecules, and ultimately leads to cell death. In monocytes, P2X7 activation results in the activation of the inflammasome and subsequent processing of the proinflammatory cytokines IL-1β and IL-18. IL-1β is pivotal for host immune response against pathogens, but is also associated with exacerbated inflammatory responses. Experiments performed in P2X7-deficient animal models and using pharmacological blockers have demonstrated that P2X7 plays a key role in autoinflammatory and autoimmune diseases, highlighting its potential as a target for therapy.

While in mice P2X7 is prominently expressed on regulatory T cells (Tregs) and invariant natural killer cells (iNKTs); we found that in human peripheral blood, innate-like lymphocytes (ILLs) express the highest levels of P2X7 among lymphocytes, and are the most sensitive to ATP. ILLs exhibit properties from both innate and adaptive immunity and, in contrast to conventional T cells, become rapidly activated upon antigen encounter. Activated and effector T cells also show higher expression of P2X7 and sensitivity to ATP than naïve T cells. These data suggest a role of P2X7 as a "checkpoint" to limit excessive effector immune responses. We also demonstrated the high specificity of Dano1 for blocking P2X7-mediated cellular responses in all immune cells. Dano1 efficiently inhibited activation of the inflammasome and release of IL-1β in a surrogate model of inflammation with LPS. Remarkably, Dano1 exhibited up to 2000-fold higher potency in preventing release of IL-1β than small-molecule antagonists currently in preclinical development.

In conclusion, we proved the potential of the P2X7-specific nanobody Dano1 for blocking P2X7 function in humans, underlining Dano1 as a promising drug candidate for the treatment of human inflammatory diseases. Since we observed higher expression of P2X7 on the surface of proinflammatory T helper (Th) subsets, we postulate that Dano1 could also be a potential therapy against Th1 and Th17 cell-driven diseases; not only by reducing IL-1β production but also by directly modulating the function of T cells.

7. <u>ZUSAMMENFASSUNG</u>

Absterbende und gestresste Zellen geben große Mengen an Adenosintriphosphat (ATP) in den extrazellulären Raum ab, welches dort vom Immunsystem als Gefahrensignal erkannt wird. Freigesetztes ATP bindet an purinerge Rezeptoren, wie zum Beispiel P2X7, und wirkt auf diesem Wege entzündungsfördernd. Extrazelluläres ATP kann in unterschiedliche Metabolite abgebaut werden, die wiederum an andere purinerge Rezeptoren binden und teilweise antagonistische Immunantworten auslösen. P2X7 wird in den meisten humanen Geweben und Immunzellen exprimiert. ATP aktiviert P2X7 und induziert damit den Influx von Ca^{2+} und Na^+, sowie den K^+ efflux. Damit werden, in Abhängigkeit vom Zelltyp verschiedene Reaktionen ausgelöst. Anhaltende Stimulation durch ATP induziert das Öffnen von nichtselektiven Zellporen, durchgängig für organische, kationische Moleküle, was letztendlich zum Zelltod führt. In Monozyten vermittelt die Aktivierung von P2X7 die Aktivierung von Inflammasomen und damit einhergehend die Prozessierung von entzündungsfördernden Zytokinen, wie IL-1β und IL-18. IL-1β ist entscheidend für die Immunantwort gegen Pathogene, aber auch assoziiert mit einer Verschärfung der Entzündungsreaktion. Experimente in P2X7-defizienten Tiermodellen und der Gebrauch von pharmakologischen Antagonisten konnte zeigen, dass P2X7 eine Schlüsselrolle bei der Vermittlung von autoentzündlichen Reaktionen und Autoimmunerkrankungen spielt. Diese Ergebnisse unterstreichen die Rolle von P2X7 als potentielles Zielmolekül für Therapien.

Während P2X7 in der Maus primär von regulatorischen T-Zellen (Tregs) und invarianten natürlichen Killerzellen (iNKTs) exprimiert wird, konnten wir zeigen, dass in humanem peripheren Blut innate-like lymphocytes (ILLs), verglichen mit anderen Lymphozyten, die höchste P2X7-Expression aufweisen und am empfindlichsten auf ATP reagieren. ILLs weisen sowohl Eigenschaften von Zellen des angeborenen als auch des erworbenen Immunsystems auf. Anders als konventionelle T-Zellen werden ILLs unverzüglich nach Antigenkontakt aktiviert. Aktivierte und Effektor T-Zellen zeigten im Vergleich zu naiven T-Zellen ebenfalls eine höhere P2X7-Expression und Empfindlichkeit gegenüber ATP auf. Diese Daten legen nahe, dass P2X7 als Kontrollpunkt zur Limitierung von ausufernden Immunantworten dient. Wir konnten ebenfalls zeigen, dass Dano1, ein therapeutischer Nanobody gegen P2X7, die P2X7-vermittelten zellulären Antworten in allen Immunzellen spezifisch blockiert. In einem LPS-Entzündungsmodell inhibierte Dano1 die Aktivierung von Inflammasomen und die Ausschüttung von IL-1β sehr effizient. Bemerkenswerterweise zeigte Dano1 dabei eine zweitausendfach höhere Wirkung bei der Inhibierung der Zytokinausschüttung als niedermolekulare Antagonisten aus der aktuellen präklinischen Entwicklung.

Zusammenfassend haben wir gezeigt, dass der P2X7-spezifische Nanobody Dano1 ein hohes Potential besitzt, die Funktion von P2X7 in humanen Zellen zu blockieren. Diese Ergebnisse unterstreichen Dano1 als einen vielversprechenden Kandidaten für die Behandlung von entzündlichen Erkrankungen im Menschen. Da wir eine höhere Expression von P2X7 auf der Oberfläche von entzündungsfördernden Untertypen der T-Helfer-Zellen zeigen konnten, postulieren wir, dass Dano1 auch potentiell für die Behandlung von TH1- und TH17-Zell-vermittelten Krankheiten therapeutisch eingesetzt werden könnte; nicht nur durch die Reduzierung der IL-1β Produktion, sondern auch direkt durch Modulation der T-Zellfunktion.

8. <u>ABBREVIATIONS</u>

%	Percent
18S	18S ribosomal RNA gene
Abs	Antibodies
ADA	Adenosine deaminase
ADAM	A disintegrin and metalloprotease
ADCC	Antibody-dependent cell-mediated cytotoxicity
Ado	Adenosine
ADP	Adenosine diphosphate
Ag	Antigen
AMP	Adenosine monophosphate
ANOVA	Analysis of variance
APCs	Antigen presenting cells
ASC	Apoptosis-associated speck-like protein containing a card
ATP	Adenosine triphosphate
BBG	Brilliant Blue-G
BCR	B cell receptor
BD	Becton Dickinson
BfA	Brefeldin A
BSA	Bovine serum albumin
bzATP	Benzoyl-ATP
Ca^{2+}	Calcium ions
CAPS	Cryopyrin associated periodic syndrome
CARD	Caspase activation and recruitment domain
CCL2	Chemokine (C-C motif) ligand 2
cDCs	Conventional DCs
cDNA	Complementary deoxyribonucleic acid
CLP	Cecal ligation puncture
CLRs	C-type lectin receptors

CMV	Cytomegalovirus
D segments	Diversity segments
DAMPS	Danger-associated molecular patterns
DAPI	4',6-diamidino-2-phenylindole
DCs	Dendritic cells
ddH_2O	Purified water
DEPC	Diethyl pyrocarbonate
Dim	Dimer
dimAlb	Linked to the albumin-binding domain nanobody Alb8
DMAPP	Dimethylallyl pyrophosphate
DMSO	Dimethyl sulfoxide
DN	Double negative
DNA	Deoxyribonucleic acid
dNTPs	Deoxyribonucleotide triphosphate
DP	Double positive
dsDNA	Double stranded DNA
DTT	Dithiothreitol
eATP	Extracellular ATP
ELISA	Enzyme-linked immunosorbent assay
eNAD	Extracellular NAD^+
ENPPs	Ectonucleotide pyrophosphatases /phosphodiesterases
ENTPDases	Ectonucleoside triphosphate diphosphohydrolases
FACS	Fluorescence-activated cell sorting
FBS	Fetal bovine serum
FcR	Fc receptors
FoxP3	Forkhead Box P3
FSC	Forward scatter
GOF SNPS	Gain-of-function SNPs
GAPDH	Glyceraldehyde 3-phosphate dehydrogenase gene
GATA3	GATA-binding protein 3

GSK	GlaxoSmithKline
H_2SO_4	Sulfuric acid
hcAbs	Heavy chain only antibodies
hIgG	Human IgG
HMBPP	(E)-4-Hydroxy-3-methyl-but-2-enyl pyrophosphate
HRP	Horseradish peroxidase
IC	Isotype control
ICC	Intracellular staining
IELs	Intraepithelial lymphocytes
IFN	Interferons
IFN-γ	Interferon gamma
IL-18Rα	IL-18 receptor α
IL-6R	Interleukin six receptor
ILCs	Innate lymphoid cells
ILLs	Innate-like lymphocytes
ILTs	Innate-like T cells
iNKT	Invariant NKT cell
Iono	Ionomycin
IPP	Isopentenyl pyrophosphate
J segments	Join segments
K^+	Potassium ions
kDa	Kilodalton
KIRs	Killer-cell immunoglobulin-like receptor
L/D	Life/dead
LOF SNPs	Loss-of-function SNPs
LPLs	Lamina propria lymphocytes
LPS	Lipopolysaccharides
LTi	Lymphoid tissue inducers
MACS	Magnetic-activated cell sorting
MAIT	Mucosal associated invariant T cell

mARTC2.2	Mouse ARTC2.2
mFc	Fused to the mouse Fc.portion of IgG
MFI	Median fluorescence intensity
Mg^{2+}	Magnesium ions
$MgSO_4$	Magnesium sulfatae
MHC	Major histocompatibility complex
MICA	MHC class I polypeptide-related protein A
MICB	MHC class I polypeptide-related protein B
mM	Milimols/liter
Mon	Monomer
MR1	MHC-related 1
mRNA	Messenger RNA
Na^+	Sodium ions
NAD	Adenine dinucleotide
Nbs	Nanobodies
NCRs	Natural cytotoxicity receptors
NFATs	Nuclear factors of activated T cells
NICD	NAD^+-induced cell death
NK cells	Natural killer cells
NKT	Natural killer T cell
NLRs	NOD-like receptors
NOD	Non-obese diabetic
oATP	Oxidized ATP
P1Rs	Purinergic P1 receptors
P2Rs	Purinergic P2 receptors
P2RX7	P2X7 gene (human)
P2rx7 KO	P2rx7-defficient mice
P2X7	P2X7 receptor
P2XRs	Purinergic P2X receptors
P2YRs	Purinergic P2Y receptors

PAMPS	Pathogen-associated molecular pattern
PBMCs	Peripheral blood mononuclear cells
PBS	Phosphate-buffered saline
pDCs	Plasmacytoid DCs
PFA	Paraformaldehyde
PHA	Phytohaemagglutinin
PI	Pharmacological inhibition
PLD	Phospholipase D
PMA	Phorbol-myristate-acetate
PMTs	Photomultipliers
PRRs	Pattern recognition receptors
PS	Phosphatidylserine
PYD	Pyrin domain
RA	Retinoic acid
rbFc	Fused to the rabbit Fc.portion of IgG
Rec IL-2	Recombinant IL-2
Rec IL-7	Recombinant IL-7
RLRs	RIG-I-like receptors
RNA	Ribonucleic acid
ROR	Retinoic acid receptor related orphan receptor
ROS	Reactive oxygen species
RPLA13	Ribosomal protein L13a gene
RPMI	Roswell park memorial institute medium
RT	Room temperature
SD	Standard deviation
SLO	Secondary lymphoid organs
SNP	Single nucleotide polymorphism
SSC	Side scatter
TCD4 conv.	Conventional CD4 T cells
TCR	T cell receptor

TFG-β	Transforming growth factor beta
Tfh	Follicular helper T cells
TFs	Transcription factors
Th	T helper cells
TLRs	Toll-like receptors
TMB	Tetramethylbenzidine
TNF	Tumor necrosis factor
TRA	T cell receptor alpha gene (human)
TRB	T cell receptor beta gene (human)
TRD	T cell receptor delta gene (human)
Tregs	Regulatory T cells
TRG	T cell receptor gamma gene (human)
TRMs	Tissue resident memory cells
T1D	Type 1 diabetes
Tαβ	αβ T cells (conventional T cells)
UDP	Uridine diphosphate
UTP	Uridine triphosphate
V segments	Variable segments
VCC	Virus containing compartments.
VHH	Variable binding domain of hcAbs
WT	Wild type
μg	Microgram
μL	Microliter
μM	Micromoles/liter

9. <u>REFERENCES</u>

A. Stockley, R. *et al.* (2008) 'Effects of AZD9056, a P2X7 antagonist, in patients with chronic obstructive pulmonary disease', pp. A41–A42.

Adams, E. J., Gu, S. and Luoma, A. M. (2015) 'Human gamma delta T cells: Evolution and ligand recognition.', *Cellular immunology*. NIH Public Access, 296(1), pp. 31–40. doi: 10.1016/j.cellimm.2015.04.008.

Adan, A. *et al.* (2017) 'Flow cytometry: basic principles and applications', *Critical Reviews in Biotechnology*, 37(2), pp. 163–176. doi: 10.3109/07388551.2015.1128876.

Adinolfi, E. *et al.* (2005) 'Basal activation of the P2X7 ATP receptor elevates mitochondrial calcium and potential, increases cellular ATP levels, and promotes serum-independent growth.', *Molecular biology of the cell*. American Society for Cell Biology, 16(7), pp. 3260–72. doi: 10.1091/mbc.e04-11-1025.

Adinolfi, E. *et al.* (2012) 'Expression of P2X7 Receptor Increases In Vivo Tumor Growth', *Cancer Research*, 72(12), pp. 2957–2969. doi: 10.1158/0008-5472.CAN-11-1947.

Adriouch, S. *et al.* (2002) 'Cutting edge: a natural P451L mutation in the cytoplasmic domain impairs the function of the mouse P2X7 receptor.', *Journal of immunology (Baltimore, Md. : 1950)*, 169(8), pp. 4108–12.

Adriouch, S. *et al.* (2008) 'ADP-ribosylation at R125 gates the P2X7 ion channel by presenting a covalent ligand to its nucleotide binding site', *The FASEB Journal*, 22(3), pp. 861–869. doi: 10.1096/fj.07-9294com.

Afonina, I. S. *et al.* (2015) 'Review Proteolytic Processing of Interleukin-1 Family Cytokines: Variations on a Common Theme', *Immunity*, 42, pp. 991–1004. doi: 10.1016/j.immuni.2015.06.003.

Al-Shukaili, A. *et al.* (2011) 'P2X7 receptor gene polymorphism analysis in rheumatoid arthritis', *International Journal of Immunogenetics*, 38(5), pp. 389–396. doi: 10.1111/j.1744-313X.2011.01019.x.

Alves, L. A. *et al.* (2014) 'Structural and molecular modeling features of P2X receptors.', *International journal of molecular sciences*. Multidisciplinary Digital Publishing Institute (MDPI), 15(3), pp. 4531–49. doi: 10.3390/ijms15034531.

Amaral, E. P. *et al.* (2014) 'Pulmonary Infection with Hypervirulent Mycobacteria Reveals a Crucial Role for the P2X7 Receptor in Aggressive Forms of Tuberculosis', *PLoS Pathogens*. Edited by C. M.

Sassetti. Public Library of Science, 10(7), p. e1004188. doi: 10.1371/journal.ppat.1004188.

Amores-Iniesta, J. *et al.* (2017) 'Extracellular ATP Activates the NLRP3 Inflammasome and Is an Early Danger Signal of Skin Allograft Rejection.', *Cell reports*. Elsevier, 21(12), pp. 3414–3426. doi: 10.1016/j.celrep.2017.11.079.

Antonioli, L. *et al.* (2013) 'CD39 and CD73 in immunity and inflammation.', *Trends in molecular medicine*. NIH Public Access, 19(6), pp. 355–67. doi: 10.1016/j.molmed.2013.03.005.

Arbabi-Ghahroudi, M. (2017) 'Camelid Single-Domain Antibodies: Historical Perspective and Future Outlook.', *Frontiers in immunology*. Frontiers Media SA, 8, p. 1589. doi: 10.3389/fimmu.2017.01589.

Arezumand, R. *et al.* (2017) 'Nanobodies As Novel Agents for Targeting Angiogenesis in Solid Cancers.', *Frontiers in immunology*. Frontiers Media SA, 8, p. 1746. doi: 10.3389/fimmu.2017.01746.

Arulkumaran, N., Unwin, R. J. and Tam, F. W. (2011) 'A potential therapeutic role for P2X7 receptor (P2X7R) antagonists in the treatment of inflammatory diseases.', *Expert opinion on investigational drugs*. Europe PMC Funders, 20(7), pp. 897–915. doi: 10.1517/13543784.2011.578068.

Aswad, F. and Dennert, G. (2006) 'P2X7 receptor expression levels determine lethal effects of a purine based danger signal in T lymphocytes', *Cellular Immunology*, 243(1), pp. 58–65. doi: 10.1016/j.cellimm.2006.12.003.

Atarashi, K. *et al.* (2008) 'ATP drives lamina propria TH17 cell differentiation', *Nature*, 455(7214), pp. 808–812. doi: 10.1038/nature07240.

Aymeric, L. *et al.* (2010) 'Tumor Cell Death and ATP Release Prime Dendritic Cells and Efficient Anticancer Immunity', *Cancer Research*, 70(3), pp. 855–858. doi: 10.1158/0008-5472.CAN-09-3566.

Bannas, P., Hambach, J. and Koch-Nolte, F. (2017) 'Nanobodies and Nanobody-Based Human Heavy Chain Antibodies As Antitumor Therapeutics.', *Frontiers in immunology*. Frontiers Media SA, 8, p. 1603. doi: 10.3389/fimmu.2017.01603.

Barden, N. *et al.* (2006) 'Analysis of single nucleotide polymorphisms in genes in the chromosome 12Q24.31 region points to P2RX7 as a susceptibility gene to bipolar affective disorder', *American Journal of Medical Genetics Part B: Neuropsychiatric Genetics*, 141B(4), pp. 374–382. doi: 10.1002/ajmg.b.30303.

Baricordi, O. R. *et al.* (1999) 'Increased proliferation rate of lymphoid cells transfected with the P2X(7) ATP receptor.', *The Journal of biological chemistry*. American Society for Biochemistry and Molecular Biology, 274(47), pp. 33206–8. doi: 10.1074/JBC.274.47.33206.

Baroni, M. *et al.* (2007) 'Stimulation of P2 (P2X $_7$) receptors in human dendritic cells induces the release of tissue factor-bearing microparticles', *The FASEB Journal*, 21(8), pp. 1926–1933. doi: 10.1096/fj.06-7238com.

Bartlett, R., Stokes, L. and Sluyter, R. (2014) 'The P2X7 Receptor Channel: Recent Developments and the Use of P2X7 Antagonists in Models of Disease', *Pharmacological Reviews*, 66(3), pp. 638–675. doi: 10.1124/pr.113.008003.

Becattini, S. *et al.* (2015) 'T cell immunity. Functional heterogeneity of human memory CD4$^+$ T cell clones primed by pathogens or vaccines.', *Science (New York, N.Y.)*. American Association for the Advancement of Science, 347(6220), pp. 400–6. doi: 10.1126/science.1260668.

Becker, D. *et al.* (2008) 'The P2X $_7$ Carboxyl Tail Is a Regulatory Module of P2X $_7$ Receptor Channel Activity', *Journal of Biological Chemistry*, 283(37), pp. 25725–25734. doi: 10.1074/jbc.M803855200.

Beis, I. and Newsholme, E. A. (1975) 'The contents of adenine nucleotides, phosphagens and some glycolytic intermediates in resting muscles from vertebrates and invertebrates.', *The Biochemical journal*, 152(1), pp. 23–32.

Beldi, G. *et al.* (2008) 'Natural killer T cell dysfunction in CD39-null mice protects against concanavalin A-induced hepatitis', *Hepatology*, 48(3), pp. 841–852. doi: 10.1002/hep.22401.

Boehm, T. (2012) 'Evolution of Vertebrate Immunity', *Current Biology*, 22(17), pp. R722–R732. doi: 10.1016/j.cub.2012.07.003.

Boeynaems, J.-M., Communi, D. and Robaye, B. (2012a) 'Overview of the pharmacology and physiological roles of P2Y receptors', *WIREs Membr Transp Signal*, 1, pp. 581–588. doi: 10.1002/wmts.44.

Boeynaems, J.-M., Communi, D. and Robaye, B. (2012b) 'Overview of the pharmacology and physiological roles of P2Y receptors', *WIREs Membr Transp Signal*, 1, pp. 581–588. doi: 10.1002/wmts.44.

Borges da Silva, H. *et al.* (2018) 'The purinergic receptor P2RX7 directs metabolic fitness of long-lived memory CD8+ T cells', *Nature*, 559(7713), pp. 264–268. doi: 10.1038/s41586-018-0282-0.

Born, W. K., Kemal Aydintug, M. and O'Brien, R. L. (2013) 'Diversity of γδ T-cell antigens.', *Cellular & molecular immunology*. Nature Publishing Group, 10(1), pp. 13–20. doi: 10.1038/cmi.2012.45.

Borsellino, G. *et al.* (2007) 'Expression of ectonucleotidase CD39 by Foxp3+ Treg cells: hydrolysis of extracellular ATP and immune suppression.', *Blood*. American Society of Hematology, 110(4), pp. 1225–32. doi: 10.1182/blood-2006-12-064527.

Brandes, M., Willimann, K. and Moser, B. (2005) 'Professional Antigen-Presentation Function by Human gd T Cells', *Science*, 309(5732), pp. 264–268. doi: 10.1126/science.1110267.

Brennan, P. J., Brigl, M. and Brenner, M. B. (2013) 'Invariant natural killer T cells: an innate activation scheme linked to diverse effector functions', *Nature Reviews Immunology*. Nature Publishing Group, 13(2), pp. 101–117. doi: 10.1038/nri3369.

Budagian, V. *et al.* (2003) 'Signaling through P2X7 receptor in human T cells involves p56lck, MAP kinases, and transcription factors AP-1 and NF-kappa B.', *The Journal of biological chemistry*. American Society for Biochemistry and Molecular Biology, 278(3), pp. 1549–60. doi: 10.1074/jbc.M206383200.

Buell, G. *et al.* (1998) 'Blockade of human P2X7 receptor function with a monoclonal antibody.', *Blood*, 92(10), pp. 3521–8.

Buell, G. N. *et al.* (1998) 'Gene structure and chromosomal localization of the human P2X7 receptor.', *Receptors & channels*, 5(6), pp. 347–54.

Burnstock, G. (2017) 'Purinergic Signalling: Therapeutic Developments', *Frontiers in Pharmacology*. Frontiers, 8, p. 661. doi: 10.3389/fphar.2017.00661.

Burnstock, G. and Burnstock, G. (2006) 'Pathophysiology and therapeutic potential of purinergic signaling.', *Pharmacological reviews*. American Society for Pharmacology and Experimental Therapeutics, 58(1), pp. 58–86. doi: 10.1124/pr.58.1.5.

Burnstock, G. and Knight, G. E. (2004) 'Cellular Distribution and Functions of P2 Receptor Subtypes in Different Systems', in *International review of cytology*, pp. 31–304. doi: 10.1016/S0074-7696(04)40002-3.

Burnstock, G. and Knight, G. E. (2018) 'The potential of P2X7 receptors as a therapeutic target, including inflammation and tumour progression', *Purinergic Signalling*, 14(1), pp. 1–18. doi: 10.1007/s11302-017-9593-0.

Cabrini, G. *et al.* (2005) 'A His-155 to Tyr polymorphism confers gain-of-function to the human P2X7 receptor of human leukemic lymphocytes.', *Journal of immunology (Baltimore, Md. : 1950)*, 175(1), pp. 82–9.

Caseley, E. *et al.* (2014) 'Non-Synonymous Single Nucleotide Polymorphisms in the P2X Receptor Genes: Association with Diseases, Impact on Receptor Functions and Potential Use as Diagnosis Biomarkers', *International Journal of Molecular Sciences*, 15(8), pp. 13344–13371. doi: 10.3390/ijms150813344.

Cauwels, A. *et al.* (2017) 'Extracellular ATP drives systemic inflammation, tissue damage and mortality', *Cell Death & Disease*. Nature Publishing Group, 5(3), pp. e1102–e1102. doi: 10.1038/cddis.2014.70.

Cekic, C. and Linden, J. (2016) 'Purinergic regulation of the immune system', *Nature Reviews Immunology*, 16(3), pp. 177–192. doi: 10.1038/nri.2016.4.

Chandra, S. and Kronenberg, M. (2015) 'Activation and Function of iNKT and MAIT Cells', in *Advances in immunology*, pp. 145–201. doi: 10.1016/bs.ai.2015.03.003.

Charles A Janeway, J. *et al.* (2001a) 'Principles of innate and adaptive immunity'. Garland Science.

Charles A Janeway, J. *et al.* (2001b) 'T-cell receptor gene rearrangement'. Garland Science.

Chen, L. and Brosnan, C. F. (2006) 'Exacerbation of experimental autoimmune encephalomyelitis in P2X7R-/- mice: evidence for loss of apoptotic activity in lymphocytes.', *Journal of immunology (Baltimore, Md. : 1950)*. American Association of Immunologists, 176(5), pp. 3115–26. doi: 10.4049/Jimmunol.176.5.3115.

Chen, Z. *et al.* (2018) 'The P2X7 purinergic receptor: An emerging therapeutic target in cardiovascular diseases', *Clinica Chimica Acta*. Elsevier, 479, pp. 196–207. doi: 10.1016/J.CCA.2018.01.032.

Cheng, J. *et al.* (2009) 'Kinetic properties of ASC protein aggregation in epithelial cells', *Journal of Cellular Physiology*, 222(3), p. n/a-n/a. doi: 10.1002/jcp.22005.

Chessell, I. P. *et al.* (2005) 'Disruption of the P2X7 purinoceptor gene abolishes chronic inflammatory and neuropathic pain', *Pain*, 114(3), pp. 386–396. doi: 10.1016/j.pain.2005.01.002.

Chung, Y. *et al.* (2009) 'Critical Regulation of Early Th17 Cell Differentiation by Interleukin-1 Signaling', *Immunity*, 30(4), pp. 576–587. doi: 10.1016/j.immuni.2009.02.007.

Coccia, M. *et al.* (2012) 'IL-1β mediates chronic intestinal inflammation by promoting the accumulation of IL-17A secreting innate lymphoid cells and CD4(+) Th17 cells.', *The Journal of experimental medicine*. Rockefeller University Press, 209(9), pp. 1595–609. doi: 10.1084/jem.20111453.

Colonna, M., Trinchieri, G. and Liu, Y.-J. (2004) 'Plasmacytoid dendritic cells in immunity', *Nature Immunology*, 5(12), pp. 1219–1226. doi: 10.1038/ni1141.

Conti, L. *et al.* (2005) 'Reciprocal activating interaction between dendritic cells and pamidronate-stimulated gammadelta T cells: role of CD86 and inflammatory cytokines.', *Journal of immunology (Baltimore, Md. : 1950)*, 174(1), pp. 252–60.

Cordero, M. D., Alcocer-Gómez, E. and Ryffel, B. (2018) 'Gain of function mutation and inflammasome driven diseases in human and mouse models', *Journal of Autoimmunity*. Academic Press, 91, pp. 13–22. doi: 10.1016/J.JAUT.2018.03.002.

Corrêa, G. *et al.* (2016) 'The purinergic receptor P2X7 role in control of Dengue virus-2 infection and cytokine/chemokine production in infected human monocytes', *Immunobiology*, 221(7), pp. 794–802. doi: 10.1016/j.imbio.2016.02.003.

Cortés-Garcia, J. D. *et al.* (2016) 'Evaluation of the expression and function of the P2X7 receptor and ART1 in human regulatory T-cell subsets', *Immunobiology*, 221(1), pp. 84–93. doi: 10.1016/j.imbio.2015.07.018.

Cossarizza, A. *et al.* (2017) 'Guidelines for the use of flow cytometry and cell sorting in immunological studies', *European Journal of Immunology*, 47(10), pp. 1584–1797. doi: 10.1002/eji.201646632.

Coutinho-Silva, R. *et al.* (2003) 'Inhibition of chlamydial infectious activity due to P2X7R-dependent phospholipase D activation.', *Immunity*, 19(3), pp. 403–12.

Csóka, B. *et al.* (2015) 'Extracellular ATP protects against sepsis through macrophage P2X7 purinergic receptors by enhancing intracellular bacterial killing', *The FASEB Journal*, 29(9), pp. 3626–3637. doi: 10.1096/fj.15-272450.

Cullen, S. P. *et al.* (2015) 'Diverse Activators of the NLRP3 Inflammasome Promote IL-1β Secretion by Triggering Necrosis', *Cell Reports*, 11(10), pp. 1535–1548. doi: 10.1016/j.celrep.2015.05.003.

Curotto de Lafaille, M. A. and Lafaille, J. J. (2009) 'Natural and Adaptive Foxp3+ Regulatory T Cells: More of the Same or a Division of Labor?', *Immunity*. Cell Press, 30(5), pp. 626–635. doi: 10.1016/J.IMMUNI.2009.05.002.

Czarnewski, P. *et al.* (2017) 'Retinoic Acid and Its Role in Modulating Intestinal Innate Immunity.', *Nutrients*. Multidisciplinary Digital Publishing Institute (MDPI), 9(1). doi: 10.3390/nu9010068.

Danquah, W. *et al.* (2016) 'Nanobodies that block gating of the P2X7 ion channel ameliorate inflammation', *Science Translational Medicine*, 8(366), p. 366ra162-366ra162. doi: 10.1126/scitranslmed.aaf8463.

Déchanet, J. *et al.* (1999) 'Implication of gammadelta T cells in the human immune response to cytomegalovirus.', *The Journal of clinical investigation*. American Society for Clinical Investigation, 103(10), pp. 1437–49. doi: 10.1172/JCI5409.

Dellabona, P. *et al.* (1994) 'An invariant V alpha 24-J alpha Q/V beta 11 T cell receptor is expressed in all individuals by clonally expanded CD4-8- T cells.', *The Journal of experimental medicine*, 180(3), pp. 1171–6.

Delves, P. J. and Roitt, I. M. (2000) 'The Immune System', *New England Journal of Medicine*. Edited by I. R. Mackay and F. S. Rosen, 343(1), pp. 37–49. doi: 10.1056/NEJM200007063430107.

Dempsey, P. W., Vaidya, S. A. and Cheng, G. (2003) 'The Art of War: Innate and adaptive immune responses', *Cellular and Molecular Life Sciences (CMLS)*. Birkhäuser-Verlag, 60(12), pp. 2604–2621. doi: 10.1007/s00018-003-3180-y.

Deng, Y. *et al.* (2017) 'Th9 cells and IL-9 in autoimmune disorders: Pathogenesis and therapeutic potentials', *Human Immunology*. Elsevier, 78(2), pp. 120–128. doi: 10.1016/J.HUMIMM.2016.12.010.

Diezmos, E. F., Bertrand, P. P. and Liu, L. (2016) 'Purinergic Signaling in Gut Inflammation: The Role of Connexins and Pannexins', *Frontiers in Neuroscience | www.frontiersin.org*, 1, p. 311. doi: 10.3389/fnins.2016.00311.

Dinarello, C. A. (2009) 'Immunological and Inflammatory Functions of the Interleukin-1 Family', *Annual Review of Immunology*, 27(1), pp. 519–550. doi: 10.1146/annurev.immunol.021908.132612.

Dinarello, C. A. (2011) 'A clinical perspective of IL-1β as the gatekeeper of inflammation', *European Journal of Immunology*, 41(5), pp. 1203–1217. doi: 10.1002/eji.201141550.

Dinarello, C. A. (2011) 'Interleukin-1 in the pathogenesis and treatment of inflammatory diseases.', *Blood*. American Society of Hematology, 117(14), pp. 3720–32. doi: 10.1182/blood-2010-07-273417.

Donnelly-Roberts, D. L. *et al.* (2009) 'Mammalian P2X7 receptor pharmacology: comparison of recombinant mouse, rat and human P2X7 receptors.', *British journal of pharmacology*. Wiley-Blackwell, 157(7), pp. 1203–14. doi: 10.1111/j.1476-5381.2009.00233.x.

Dosch, M. *et al.* (2018) 'Mechanisms of ATP Release by Inflammatory Cells', *International Journal of Molecular Sciences*, 19(4), p. 1222. doi: 10.3390/ijms19041222.

Dowling, J. K. and O'Neill, L. A. J. (2012) 'Biochemical regulation of the inflammasome', *Critical Reviews in Biochemistry and Molecular Biology*, 47(5), pp. 424–443. doi: 10.3109/10409238.2012.694844.

Dreisig, K. *et al.* (2018) 'Human P2Y11 Expression Level Affects Human P2X7 Receptor-Mediated Cell Death', *Frontiers in Immunology*, 9, p. 1159. doi: 10.3389/fimmu.2018.01159.

Le Duc, D. *et al.* (2017) 'P2Y Receptors in Immune Response and Inflammation', in *Advances in immunology*, pp. 85–121. doi: 10.1016/bs.ai.2017.05.006.

Dunkelberger, J. R. and Song, W.-C. (2010) 'Complement and its role in innate and adaptive immune responses', *Cell Research*, 20(1), pp. 34–50. doi: 10.1038/cr.2009.139.

Eberl, M. *et al.* (2009) 'A Rapid Crosstalk of Human γδ T Cells and Monocytes Drives the Acute Inflammation in Bacterial Infections', *PLoS Pathogens*. Edited by R. R. Isberg. Public Library of Science, 5(2), p. e1000308. doi: 10.1371/journal.ppat.1000308.

Egan, T. M. and Khakh, B. S. (2004) 'Contribution of Calcium Ions to P2X Channel Responses', *Journal of Neuroscience*, 24(13), pp. 3413–3420. doi: 10.1523/JNEUROSCI.5429-03.2004.

Elliott, J. I. *et al.* (2005) 'Membrane phosphatidylserine distribution as a non-apoptotic signalling mechanism in lymphocytes', *Nature Cell Biology*, 7(8), pp. 808–816. doi: 10.1038/ncb1279.

Eltzschig, H. K., Sitkovsky, M. V and Robson, S. C. (2012) 'Purinergic signaling during inflammation.', *The New England journal of medicine*. NIH Public Access, 367(24), pp. 2322–33. doi: 10.1056/NEJMra1205750.

Englezou, P. C. *et al.* (2015) 'P2X7R activation drives distinct IL-1 responses in dendritic cells compared to macrophages.', *Cytokine*. Elsevier, 74(2), pp. 293–304. doi: 10.1016/j.cyto.2015.05.013.

Eser, A. *et al.* (2015) 'Safety and Efficacy of an Oral Inhibitor of the Purinergic Receptor P2X7 in Adult Patients with Moderately to Severely Active Crohn's Disease', *Inflammatory Bowel Diseases*, 21(10), p. 1. doi: 10.1097/MIB.0000000000000514.

Eyerich, S. *et al.* (2009) 'Th22 cells represent a distinct human T cell subset involved in epidermal immunity and remodeling.', *The Journal of clinical investigation*. American Society for Clinical Investigation, 119(12), pp. 3573–85. doi: 10.1172/JCI40202.

Faas, M. M., Sáez, T. and de Vos, P. (2017) 'Extracellular ATP and adenosine: The Yin and Yang in immune responses?', *Molecular Aspects of Medicine*, 55, pp. 9–19. doi: 10.1016/j.mam.2017.01.002.

Fan, Z.-D. *et al.* (2016) 'Involvement of P2X7 receptor signaling on regulating the differentiation of Th17 cells and type II collagen-induced arthritis in mice', *Scientific Reports*. Nature Publishing Group, 6(1), p. 35804. doi: 10.1038/srep35804.

Farrington, G. K. *et al.* (2014) 'A novel platform for engineering blood-brain barrier-crossing bispecific biologics', *The FASEB Journal*, 28(11), pp. 4764–4778. doi: 10.1096/fj.14-253369.

Fernando, S. L. *et al.* (2007) 'A Polymorphism in the P2X $_7$ Gene Increases Susceptibility to Extrapulmonary Tuberculosis', *American Journal of Respiratory and Critical Care Medicine*, 175(4), pp. 360–366. doi: 10.1164/rccm.200607-970OC.

Ferrari, D., Idzko, M., *et al.* (2000) 'P2 purinergic receptors of human eosinophils: characterization and coupling to oxygen radical production', *FEBS Letters*. No longer published by Elsevier, 486(3), pp. 217–224. doi: 10.1016/S0014-5793(00)02306-1.

Ferrari, D., La Sala, A., *et al.* (2000) 'The P2 purinergic receptors of human dendritic cells: identification and coupling to cytokine release', *The FASEB Journal*, 14(15), pp. 2466–2476. doi: 10.1096/fj.00-0031com.

Ferrari, D. *et al.* (2006) 'The P2X7 receptor: a key player in IL-1 processing and release.', *Journal of immunology (Baltimore, Md. : 1950)*. American Association of Immunologists, 176(7), pp. 3877–83. doi: 10.4049/JIMMUNOL.176.7.3877.

Figliuolo, V. R. *et al.* (2017) 'P2X7 receptor promotes intestinal inflammation in chemically induced colitis and triggers death of mucosal regulatory T cells', *Biochimica et Biophysica Acta (BBA) - Molecular Basis of Disease*, 1863(6), pp. 1183–1194. doi: 10.1016/j.bbadis.2017.03.004.

Flajnik, M. F. and Kasahara, M. (2010) 'Origin and evolution of the adaptive immune system: genetic events and selective pressures', *Nature Reviews Genetics*, 11(1), pp. 47–59. doi: 10.1038/nrg2703.

Frascoli, M. *et al.* (2012) 'Purinergic P2X7 Receptor Drives T Cell Lineage Choice and Shapes Peripheral   Cells', *The Journal of Immunology*, 189(1), pp. 174–180. doi: 10.4049/jimmunol.1101582.

Fredholm, B. B. *et al.* (2001) 'International Union of Pharmacology. XXV. Nomenclature and classification of adenosine receptors.', *Pharmacological reviews*, 53(4), pp. 527–52.

Friedle, S. A., Curet, M. A. and Watters, J. J. (2010) 'Recent patents on novel P2X(7) receptor antagonists and their potential for reducing central nervous system inflammation.', *Recent patents on CNS drug discovery*, 5(1), pp. 35–45.

Friedman, D. J. *et al.* (2009) 'CD39 deletion exacerbates experimental murine colitis and human polymorphisms increase susceptibility to inflammatory bowel disease', *Proceedings of the National Academy of Sciences*, 106(39), pp. 16788–16793. doi: 10.1073/pnas.0902869106.

Fuller, S. J. *et al.* (2009) 'Genetics of the P2X7 receptor and human disease', *Purinergic signalling*, (5), pp. 257–262. doi: 10.1007/s11302-009-9136-4.

Garbers, C. *et al.* (2011) 'Species Specificity of ADAM10 and ADAM17 Proteins in Interleukin-6 (IL-6) Trans-signaling and Novel Role of ADAM10 in Inducible IL-6 Receptor Shedding', *Journal of Biological Chemistry*, 286(17), pp. 14804–14811. doi: 10.1074/jbc.M111.229393.

Garlanda, C., Dinarello, C. A. and Mantovani, A. (2013) 'The Interleukin-1 Family: Back to the Future', *Immunity*, 39(6), pp. 1003–1018. doi: 10.1016/j.immuni.2013.11.010.

Gartland, A. *et al.* (2012) 'Polymorphisms in the P2X7 receptor gene are associated with low lumbar spine bone mineral density and accelerated bone loss in post-menopausal women', *European Journal of Human Genetics*, 20(5), pp. 559–564. doi: 10.1038/ejhg.2011.245.

Geistlinger, J. *et al.* (2012) 'P2RX7 genotype association in severe sepsis identified by a novel Multi-Individual Array for rapid screening and replication of risk SNPs', *Clinica Chimica Acta*, 413(1–2), pp. 39–47. doi: 10.1016/j.cca.2011.05.023.

Gibbs, R. A. *et al.* (2015) 'A global reference for human genetic variation', *Nature*. Nature Publishing Group, 526(7571), pp. 68–74. doi: 10.1038/nature15393.

Gicquel, T. *et al.* (2015) 'IL-1β production is dependent on the activation of purinergic receptors and NLRP3 pathway in human macrophages', *The FASEB Journal*, 29(10), pp. 4162–4173. doi: 10.1096/fj.14-267393.

Gidlöf, O. *et al.* (2012) 'A Common Missense Variant in the ATP Receptor P2X7 Is Associated with Reduced Risk of Cardiovascular Events', *PLoS ONE*. Edited by W. Zhang, 7(5), p. e37491. doi: 10.1371/journal.pone.0037491.

Giuliani, A. L. *et al.* (2017) 'The P2X7 Receptor-Interleukin-1 Liaison.', *Frontiers in pharmacology*. Frontiers Media SA, 8, p. 123. doi: 10.3389/fphar.2017.00123.

Glowacki, G. *et al.* (2001) 'Structure, chromosomal localization, and expression of the gene for mouse ecto-mono(ADP-ribosyl)transferase ART5.', *Gene*, 275(2), pp. 267–77.

Glowacki, G. *et al.* (2009) 'The family of toxin-related ecto-ADP-ribosyltransferases in humans and the mouse', *Protein Science*, 11(7), pp. 1657–1670. doi: 10.1110/ps.0200602.

Gordon, J. L. (1986) 'Extracellular ATP: effects, sources and fate.', *The Biochemical journal*, 233(2), pp. 309–19.

Gorman, M. W., Feigl, E. O. and Buffington, C. W. (2006) 'Human Plasma ATP Concentration', *Clinical Chemistry*, 53(2), pp. 318–325. doi: 10.1373/clinchem.2006.076364.

Grahnert, A. *et al.* (2002) 'Mono-ADP-ribosyltransferases in human monocytes: regulation by lipopolysaccharide.', *The Biochemical journal*, 362(Pt 3), pp. 717–23.

Graziano, F. *et al.* (2015) 'Extracellular ATP induces the rapid release of HIV-1 from virus containing compartments of human macrophages', *Proceedings of the National Academy of Sciences*, 112(25), pp. E3265–E3273. doi: 10.1073/pnas.1500656112.

Gu, B., Bendall, L. J. and Wiley, J. S. (1998) 'Adenosine triphosphate-induced shedding of CD23 and L-selectin (CD62L) from lymphocytes is mediated by the same receptor but different metalloproteases.', *Blood*, 92(3), pp. 946–51.

Gu, B. J. *et al.* (2000) 'Expression of P2X $_7$ purinoceptors on human lymphocytes and monocytes: evidence for nonfunctional P2X $_7$ receptors', *American Journal of Physiology-Cell Physiology*, 279(4), pp. C1189–C1197. doi: 10.1152/ajpcell.2000.279.4.C1189.

Gu, B. J. *et al.* (2015) 'A rare P2X7 variant Arg307Gln with absent pore formation function protects against neuroinflammation in multiple sclerosis', *Human Molecular Genetics*, 24(19), pp. 5644–5654. doi: 10.1093/hmg/ddv278.

Gulbransen, B. D. *et al.* (2012) 'Activation of neuronal P2X7 receptor–pannexin-1 mediates death of enteric neurons during colitis', *Nature Medicine*, 18(4), pp. 600–604. doi: 10.1038/nm.2679.

Guo, H., Callaway, J. B. and Ting, J. P.-Y. (2015) 'Inflammasomes: mechanism of action, role in disease and therapeutics', *Nature Medicine*, 21(7), pp. 677–687. doi: 10.1038/nm.3893.

Haag, F. *et al.* (1994) 'Premature Stop Codons Inactivate the RT6 Genes of the Human and Chimpanzee Species', *Journal of Molecular Biology*, 243(3), pp. 537–546. doi: 10.1006/jmbi.1994.1680.

Hadadi, E. *et al.* (2016) 'Differential IL-1β secretion by monocyte subsets is regulated by Hsp27 through modulating mRNA stability', *Scientific Reports*. Nature Publishing Group, 6(1), p. 39035. doi: 10.1038/srep39035.

Haks, M. C. *et al.* (2005) 'Attenuation of γδTCR Signaling Efficiently Diverts Thymocytes to the αβ Lineage', *Immunity*, 22(5), pp. 595–606. doi: 10.1016/j.immuni.2005.04.003.

Hall, J. A. *et al.* (2011) 'The role of retinoic acid in tolerance and immunity.', *Immunity*. NIH Public Access, 35(1), pp. 13–22. doi: 10.1016/j.immuni.2011.07.002.

Han, L. *et al.* (2015) 'Th17 cells in autoimmune diseases', *Frontiers of Medicine*, 9(1), pp. 10–19. doi: 10.1007/s11684-015-0388-9.

Harly, C. *et al.* (2012) 'Key implication of CD277/butyrophilin-3 (BTN3A) in cellular stress sensing by a major human   T-cell subset', *Blood*, 120(11), pp. 2269–2279. doi: 10.1182/blood-2012-05-430470.

Hashimoto-Hill, S. *et al.* (2017) 'Contraction of intestinal effector T cells by retinoic acid-induced purinergic receptor P2X7', *Mucosal Immunology*. Nature Publishing Group, 10(4), pp. 912–923. doi: 10.1038/mi.2016.109.

Haskó, G. *et al.* (2008) 'Adenosine receptors: therapeutic aspects for inflammatory and immune diseases', *Nature Reviews Drug Discovery*, 7(9), pp. 759–770. doi: 10.1038/nrd2638.

Haskó, G. and Cronstein, B. (2013) 'Regulation of Inflammation by Adenosine', *Frontiers in Immunology*. Frontiers, 4, p. 85. doi: 10.3389/fimmu.2013.00085.

Hayes, S. M., Li, L. and Love, P. E. (2005) 'TCR Signal Strength Influences αβ/γδ Lineage Fate', *Immunity*, 22(5), pp. 583–593. doi: 10.1016/j.immuni.2005.03.014.

Hazleton, J. E., Berman, J. W. and Eugenin, E. A. (2012) 'Purinergic receptors are required for HIV-1 infection of primary human macrophages.', *Journal of immunology (Baltimore, Md. : 1950)*. American Association of Immunologists, 188(9), pp. 4488–95. doi: 10.4049/jimmunol.1102482.

He, Y. *et al.* (2017) 'The role of microglial P2X7: modulation of cell death and cytokine release.', *Journal of neuroinflammation*. BioMed Central, 14(1), p. 135. doi: 10.1186/s12974-017-0904-8.

He, Y., Hara, H. and Núñez, G. (2016) 'Mechanism and Regulation of NLRP3 Inflammasome Activation', *Trends in Biochemical Sciences*, 41, pp. 1012–1021. doi: 10.1016/j.tibs.2016.09.002.

Heiss, K. *et al.* (2008) 'High sensitivity of intestinal CD8+ T cells to nucleotides indicates P2X7 as a regulator for intestinal T cell responses.', *Journal of immunology (Baltimore, Md. : 1950)*, 181(6), pp. 3861–9.

Herrath, J. *et al.* (2014) 'Surface expression of CD39 identifies an enriched Treg-cell subset in the rheumatic joint, which does not suppress IL-17A secretion', *European Journal of Immunology*. Wiley-Blackwell, 44(10), pp. 2979–2989. doi: 10.1002/eji.201344140.

Hironaka, I. *et al.* (2013) 'Glucose Triggers ATP Secretion from Bacteria in a Growth-Phase-Dependent Manner', *Applied and Environmental Microbiology*, 79(7), pp. 2328–2335. doi: 10.1128/AEM.03871-12.

Horenstein, A. L. *et al.* (2013) 'A CD38/CD203a/CD73 ectoenzymatic pathway independent of CD39 drives a novel adenosinergic loop in human T lymphocytes.', *Oncoimmunology*. Taylor & Francis, 2(9), p. e26246. doi: 10.4161/onci.26246.

Hori, S., Nomura, T. and Sakaguchi, S. (2003) 'Control of Regulatory T Cell Development by the Transcription Factor Foxp3', *Science*, 299(5609), pp. 1057–1061. doi: 10.1126/science.1079490.

Huang, C. *et al.* (2014) 'P2X7 blockade attenuates mouse liver fibrosis', *Molecular Medicine Reports*, 9(1), pp. 57–62. doi: 10.3892/mmr.2013.1807.

Hubert, S. *et al.* (2010) 'Extracellular NAD $^+$ shapes the Foxp3 $^+$ regulatory T cell compartment through the ART2–P2X7 pathway', *The Journal of Experimental Medicine*, 207(12), pp. 2561–2568. doi: 10.1084/jem.20091154.

Ibrahim, S. F. and van den Engh, G. (2007) 'Flow Cytometry and Cell Sorting', in. Springer, Berlin, Heidelberg, pp. 19–39. doi: 10.1007/10_2007_073.

Idzko, M. *et al.* (2007) 'Extracellular ATP triggers and maintains asthmatic airway inflammation by activating dendritic cells', *Nature Medicine*, 13(8), pp. 913–919. doi: 10.1038/nm1617.

Idzko, M., Ferrari, D. and Eltzschig, H. K. (2014) 'Nucleotide signalling during inflammation', *Nature*, 509(7500), pp. 310–317. doi: 10.1038/nature13085.

Inoue, K. (2008) 'Purinergic systems in microglia', *Cellular and Molecular Life Sciences*, 65(19), pp. 3074–3080. doi: 10.1007/s00018-008-8210-3.

Iwase, T. *et al.* (2010) 'Isolation and identification of ATP-secreting bacteria from mice and humans.', *Journal of clinical microbiology*. American Society for Microbiology (ASM), 48(5), pp. 1949–51. doi: 10.1128/JCM.01941-09.

Iwata, M. (2009) 'Retinoic acid production by intestinal dendritic cells and its role in T-cell trafficking', *Seminars in Immunology*, 21(1), pp. 8–13. doi: 10.1016/j.smim.2008.09.002.

Jacob, F. *et al.* (2013) 'Purinergic signaling in inflammatory cells: P2 receptor expression, functional effects, and modulation of inflammatory responses.', *Purinergic signalling*. Springer, 9(3), pp. 285–306. doi: 10.1007/s11302-013-9357-4.

Jacobson, K. A. *et al.* (2009) 'Development of selective agonists and antagonists of P2Y receptors.', *Purinergic signalling*. Springer, 5(1), pp. 75–89. doi: 10.1007/s11302-008-9106-2.

Jadidi-Niaragh, F. and Mirshafiey, A. (2011) 'Th17 Cell, the New Player of Neuroinflammatory Process in Multiple Sclerosis', *Scandinavian Journal of Immunology*, 74(1), pp. 1–13. doi: 10.1111/j.1365-3083.2011.02536.x.

Jamieson, S. E. *et al.* (2010) 'Evidence for associations between the purinergic receptor P2X(7) (P2RX7) and toxoplasmosis.', *Genes and immunity*. NIH Public Access, 11(5), pp. 374–83. doi: 10.1038/gene.2010.31.

Janeway, C. A. (1989) 'Approaching the asymptote? Evolution and revolution in immunology.', *Cold Spring Harbor symposia on quantitative biology*. Cold Spring Harbor Laboratory Press, 54 Pt 1, pp. 1–13. doi: 10.1101/SQB.1989.054.01.003.

Juno, J. A., Keynan, Y. and Fowke, K. R. (2012) 'Invariant NKT Cells: Regulation and Function during Viral Infection', *PLoS Pathogens*. Edited by T. C. Hobman. Public Library of Science, 8(8), p. e1002838. doi: 10.1371/journal.ppat.1002838.

Kaczmarek-Hájek, K. *et al.* (2012) 'Molecular and functional properties of P2X receptors--recent progress and persisting challenges.', *Purinergic signalling*. Springer, 8(3), pp. 375–417. doi: 10.1007/s11302-012-9314-7.

Kasuya, G. *et al.* (2017) 'Structural insights into the competitive inhibition of the ATP-gated P2X receptor channel', *Nature Communications*. Nature Publishing Group, 8(1), p. 876. doi: 10.1038/s41467-017-00887-9.

Kenna, T. *et al.* (2003) 'NKT cells from normal and tumor-bearing human livers are phenotypically and functionally distinct from murine NKT cells.', *Journal of immunology (Baltimore, Md. : 1950)*, 171(4), pp. 1775–9.

Keystone, E. C. *et al.* (2012) 'Clinical evaluation of the efficacy of the P2X $_7$ purinergic receptor antagonist AZD9056 on the signs and symptoms of rheumatoid arthritis in patients with active disease despite treatment with methotrexate or sulphasalazine', *Annals of the Rheumatic Diseases*, 71(10), pp. 1630–1635. doi: 10.1136/annrheumdis-2011-143578.

Kinjo, Y., Kitano, N. and Kronenberg, M. (2013) 'The role of invariant natural killer T cells in microbial immunity.', *Journal of infection and chemotherapy : official journal of the Japan Society of Chemotherapy*. NIH Public Access, 19(4), pp. 560–70. doi: 10.1007/s10156-013-0638-1.

Kinsey, G. R. *et al.* (2012) 'Autocrine adenosine signaling promotes regulatory T cell-mediated renal protection.', *Journal of the American Society of Nephrology : JASN*. American Society of Nephrology, 23(9), pp. 1528–37. doi: 10.1681/ASN.2012010070.

Koay, H.-F., Godfrey, D. I. and Pellicci, D. G. (2018) 'Development of mucosal-associated invariant T cells', *Immunology and Cell Biology*. doi: 10.1111/imcb.12039.

Koch-Nolte, F. *et al.* (2006) 'ADP-ribosylation of membrane proteins: Unveiling the secrets of a crucial regulatory mechanism in mammalian cells', *Annals of Medicine*, 38(3), pp. 188–199. doi: 10.1080/07853890600655499.

Koch, K. *et al.* (2017) 'Selection of nanobodies with broad neutralizing potential against primary HIV-1 strains using soluble subtype C gp140 envelope trimers', *Scientific Reports*. Nature Publishing Group, 7(1), p. 8390. doi: 10.1038/s41598-017-08273-7.

Kronlage, M. *et al.* (2010) 'Autocrine Purinergic Receptor Signaling Is Essential for Macrophage Chemotaxis', *Science Signaling*, 3(132), pp. ra55-ra55. doi: 10.1126/scisignal.2000588.

Kuehnel, M. P. *et al.* (2009) 'Lipids regulate P2X7-receptor-dependent actin assembly by phagosomes via ADP translocation and ATP synthesis in the phagosome lumen', *Journal of Cell Science*, 122(4), pp. 499–504. doi: 10.1242/jcs.034199.

von Kügelgen, I. and Hoffmann, K. (2016) 'Pharmacology and structure of P2Y receptors', *Neuropharmacology*, 104, pp. 50–61. doi: 10.1016/j.neuropharm.2015.10.030.

Kurioka, A. *et al.* (2015) 'MAIT cells are licensed through granzyme exchange to kill bacterially sensitized targets', *Mucosal Immunology*. Nature Publishing Group, 8(2), pp. 429–440. doi: 10.1038/mi.2014.81.

Kusu, T. *et al.* (2013) 'Ecto-nucleoside triphosphate diphosphohydrolase 7 controls Th17 cell responses through regulation of luminal ATP in the small intestine.', *Journal of immunology (Baltimore, Md. : 1950)*. The American Association of Immunologists, Inc., 190(2), pp. 774–83. doi: 10.4049/jimmunol.1103067.

Labasi, J. M. *et al.* (2002) 'Absence of the P2X7 receptor alters leukocyte function and attenuates an inflammatory response.', *Journal of immunology (Baltimore, Md. : 1950)*, 168(12), pp. 6436–45.

Lasigliè, D. *et al.* (2011) 'Role of IL-1 Beta in the Development of Human TH17 Cells: Lesson from NLPR3 Mutated Patients', *PLoS ONE*. Edited by J. El Khoury. Public Library of Science, 6(5), p. e20014. doi: 10.1371/journal.pone.0020014.

Lazarowski, E. R. (2012) 'Vesicular and conductive mechanisms of nucleotide release', *Purinergic Signalling*, 8(3), pp. 359–373. doi: 10.1007/s11302-012-9304-9.

Ledderose, C. *et al.* (2018) 'Purinergic P2X4 receptors and mitochondrial ATP production regulate T cell migration', *Journal of Clinical Investigation*, 128(8), pp. 3583–3594. doi: 10.1172/JCI120972.

Lépine, S. *et al.* (2006) 'ATP-induced apoptosis of thymocytes is mediated by activation of P2X7 receptor and involves de novo ceramide synthesis and mitochondria', *Biochimica et Biophysica Acta (BBA) - Molecular and Cell Biology of Lipids*, 1761(1), pp. 73–82. doi: 10.1016/j.bbalip.2005.10.001.

Lepore, M. *et al.* (2014) 'Parallel T-cell cloning and deep sequencing of human MAIT cells reveal stable oligoclonal TCRβ repertoire', *Nature Communications*, 5(1), p. 3866. doi: 10.1038/ncomms4866.

Leslie, D. S. *et al.* (2002) 'CD1-mediated gamma/delta T cell maturation of dendritic cells.', *The Journal of experimental medicine*, 196(12), pp. 1575–84.

Leyva-Grado, V. H. *et al.* (2017) 'Contribution of the Purinergic Receptor P2X7 to Development of Lung Immunopathology during Influenza Virus Infection.', *mBio*. American Society for Microbiology, 8(2), pp. e00229-17. doi: 10.1128/mBio.00229-17.

Licona-Limón, P. *et al.* (2013) 'Th9 Cells Drive Host Immunity against Gastrointestinal Worm Infection.', *Immunity*. Howard Hughes Medical Institute, 39(4), pp. 744–57. doi: 10.1016/j.immuni.2013.07.020.

Lin, C.-C. and Edelson, B. T. (2017) 'New Insights into the Role of IL-1β in Experimental Autoimmune Encephalomyelitis and Multiple Sclerosis.', *Journal of immunology (Baltimore, Md. : 1950)*. NIH Public Access, 198(12), pp. 4553–4560. doi: 10.4049/jimmunol.1700263.

Lister, M. F. *et al.* (2007) 'The role of the purinergic P2X7 receptor in inflammation.', *Journal of inflammation (London, England)*. BioMed Central, 4, p. 5. doi: 10.1186/1476-9255-4-5.

Lutter, L. *et al.* (2018) 'The elusive case of human intraepithelial T cells in gut homeostasis and inflammation', *Nature Reviews Gastroenterology & Hepatology*. Nature Publishing Group, p. 1. doi: 10.1038/s41575-018-0039-0.

Ma, C. S. *et al.* (2012) 'The origins, function, and regulation of T follicular helper cells', *The Journal of Experimental Medicine*, 209(7), pp. 1241–1253. doi: 10.1084/jem.20120994.

Malhotra, S. *et al.* (2009) 'B Cell Antigen Receptor Endocytosis and Antigen Presentation to T Cells Require Vav and Dynamin', *Journal of Biological Chemistry*, 284(36), pp. 24088–24097. doi: 10.1074/jbc.M109.014209.

Maliszewski, C. R. *et al.* (1994) 'The CD39 lymphoid cell activation antigen. Molecular cloning and structural characterization.', *Journal of immunology (Baltimore, Md. : 1950)*, 153(8), pp. 3574–83.

Mandapathil, M. *et al.* (2010) 'Generation and accumulation of immunosuppressive adenosine by human CD4+CD25highFOXP3+ regulatory T cells.', *The Journal of biological chemistry*. American Society for Biochemistry and Molecular Biology, 285(10), pp. 7176–86. doi: 10.1074/jbc.M109.047423.

Marlin, R. *et al.* (2017) 'Sensing of cell stress by human γδ TCR-dependent recognition of annexin A2.', *Proceedings of the National Academy of Sciences of the United States of America*. National Academy of Sciences, 114(12), pp. 3163–3168. doi: 10.1073/pnas.1621052114.

Marques, C. C. *et al.* (2014) 'Prophylactic systemic P2X7 receptor blockade prevents experimental colitis', *Biochimica et Biophysica Acta (BBA) - Molecular Basis of Disease*, 1842(1), pp. 65–78. doi: 10.1016/j.bbadis.2013.10.012.

Martel-Gallegos, G. *et al.* (2010) 'Human neutrophils do not express purinergic P2X7 receptors', *Purinergic Signalling*, 6(3), pp. 297–306. doi: 10.1007/s11302-010-9178-7.

Martin, B. *et al.* (2009) 'Interleukin-17-Producing γδ T Cells Selectively Expand in Response to Pathogen Products and Environmental Signals', *Immunity*, 31(2), pp. 321–330. doi: 10.1016/j.immuni.2009.06.020.

Mascanfroni, I. D. *et al.* (2015) 'Metabolic control of type 1 regulatory T cell differentiation by AHR and HIF1-α.', *Nature medicine*. NIH Public Access, 21(6), pp. 638–46. doi: 10.1038/nm.3868.

Mayadas, T. N., Cullere, X. and Lowell, C. A. (2014) 'The multifaceted functions of neutrophils.', *Annual review of pathology*. NIH Public Access, 9, pp. 181–218. doi: 10.1146/annurev-pathol-020712-164023.

Mehta, N. *et al.* (2014) 'Purinergic receptor P2X7: A novel target for anti-inflammatory therapy', *Bioorganic & Medicinal Chemistry*, 22(1), pp. 54–88. doi: 10.1016/j.bmc.2013.10.054.

Meier, D. *et al.* (2007) 'Ectopic Lymphoid-Organ Development Occurs through Interleukin 7-Mediated Enhanced Survival of Lymphoid-Tissue-Inducer Cells', *Immunity*, 26(5), pp. 643–654. doi: 10.1016/j.immuni.2007.04.009.

Miltenyi, S. *et al.* (1990) 'High Gradient Magnetic Cell Separation With MACS1', *Cytometry*, 11, pp. 231–238.

Monção-Ribeiro, L. C. *et al.* (2014) 'P2X7 Receptor Modulates Inflammatory and Functional Pulmonary Changes Induced by Silica', *PLoS ONE*. Edited by J. Kanellopoulos. Public Library of Science, 9(10), p. e110185. doi: 10.1371/journal.pone.0110185.

Montoya, C. J. *et al.* (2007) 'Characterization of human invariant natural killer T subsets in health and disease using a novel invariant natural killer T cell-clonotypic monoclonal antibody, 6B11.', *Immunology*. Wiley-Blackwell, 122(1), pp. 1–14. doi: 10.1111/j.1365-2567.2007.02647.x.

Moon, H. *et al.* (2006) 'P2X receptor-dependent ATP-induced shedding of CD27 in mouse lymphocytes', *Immunology Letters*, 102(1), pp. 98–105. doi: 10.1016/j.imlet.2005.08.004.

Müller, T. *et al.* (2011) 'A Potential Role for P2X7R in Allergic Airway Inflammation in Mice and Humans', *American Journal of Respiratory Cell and Molecular Biology*, 44(4), pp. 456–464. doi: 10.1165/rcmb.2010-0129OC.

Mullis, K. *et al.* (1986) 'Specific enzymatic amplification of DNA in vitro: the polymerase chain reaction.', *Cold Spring Harbor symposia on quantitative biology*, 51 Pt 1, pp. 263–73.

Muñoz-Planillo, R. *et al.* (2013) 'K+ Efflux Is the Common Trigger of NLRP3 Inflammasome Activation by Bacterial Toxins and Particulate Matter', *Immunity*, 38(6), pp. 1142–1153. doi: 10.1016/j.immuni.2013.05.016.

Mutini, C. *et al.* (1999) 'Mouse dendritic cells express the P2X7 purinergic receptor: characterization and possible participation in antigen presentation.', *Journal of immunology (Baltimore, Md. : 1950)*, 163(4), pp. 1958–65.

Neves, A. R. *et al.* (2014) 'Overexpression of ATP-activated P2X7 Receptors in the Intestinal Mucosa Is Implicated in the Pathogenesis of Crohn's Disease', *Inflammatory Bowel Diseases*, 20(3), pp. 444–457. doi: 10.1097/01.MIB.0000441201.10454.06.

Nicke, A. *et al.* (1998) 'P2X1 and P2X3 receptors form stable trimers: a novel structural motif of ligand-gated ion channels', *The EMBO Journal*, 17(11), pp. 3016–3028. doi: 10.1093/emboj/17.11.3016.

Nicke, A. *et al.* (2009) 'A Functional P2X7 Splice Variant with an Alternative Transmembrane Domain 1 Escapes Gene Inactivation in P2X7 Knock-out Mice', *Journal of Biological Chemistry*, 284(38), pp. 25813–25822. doi: 10.1074/jbc.M109.033134.

Nikolich-Zugich, J., Slifka, M. K. and Messaoudi, I. (2004) 'The many important facets of T-cell repertoire diversity', *Nature Reviews Immunology*. Nature Publishing Group, 4(2), pp. 123–132. doi: 10.1038/nri1292.

North, R. A. (2002) 'Molecular Physiology of P2X Receptors', *Physiological Reviews*, 82(4), pp. 1013–1067. doi: 10.1152/physrev.00015.2002.

Ohta, A. *et al.* (2012) 'The development and immunosuppressive functions of CD4(+) CD25(+) FoxP3(+) regulatory T cells are under influence of the adenosine-A2A adenosine receptor pathway.', *Frontiers in immunology*. Frontiers Media SA, 3, p. 190. doi: 10.3389/fimmu.2012.00190.

Pacheco, P. A. F. *et al.* (2016) 'P2X7 receptor as a novel drug delivery system to increase the entrance of hydrophilic drugs into cells during photodynamic therapy', *Journal of Bioenergetics and Biomembranes*, 48(4), pp. 397–411. doi: 10.1007/s10863-016-9668-6.

Pelegrin, P. and Surprenant, A. (2006) 'Pannexin-1 mediates large pore formation and interleukin-1β release by the ATP-gated P2X7 receptor', *The EMBO Journal*, 25(21), pp. 5071–5082. doi: 10.1038/sj.emboj.7601378.

Pelegrin, P. and Surprenant, A. (2007) 'Pannexin-1 couples to maitotoxin- and nigericin-induced interleukin-1beta release through a dye uptake-independent pathway.', *The Journal of biological chemistry*. American Society for Biochemistry and Molecular Biology, 282(4), pp. 2386–94. doi:

10.1074/jbc.M610351200.

Perregaux, D. G. *et al.* (2000) 'ATP acts as an agonist to promote stimulus-induced secretion of IL-1 beta and IL-18 in human blood.', *Journal of immunology (Baltimore, Md. : 1950)*, 165(8), pp. 4615–23.

Petermann, F. *et al.* (2010) 'γδ T cells enhance autoimmunity by restraining regulatory T cell responses via an interleukin-23-dependent mechanism.', *Immunity.* NIH Public Access, 33(3), pp. 351–63. doi: 10.1016/j.immuni.2010.08.013.

Petrasca, A. and Doherty, D. G. (2014) 'Human VÎ´2+ Î³Î´ T Cells Differentially Induce Maturation, Cytokine Production, and Alloreactive T Cell Stimulation by Dendritic Cells and B Cells', *Frontiers in Immunology*. Frontiers, 5, p. 650. doi: 10.3389/fimmu.2014.00650.

Pétrilli, V. *et al.* (2007) 'Activation of the NALP3 inflammasome is triggered by low intracellular potassium concentration', *Cell Death & Differentiation*, 14(9), pp. 1583–1589. doi: 10.1038/sj.cdd.4402195.

Pettengill, M. *et al.* (2013) 'Soluble Ecto-5'-nucleotidase (5'-NT), Alkaline Phosphatase, and Adenosine Deaminase (ADA1) Activities in Neonatal Blood Favor Elevated Extracellular Adenosine', *The Journal of Biological Chemistry*, 288(38), pp. 27315–27326. doi: 10.1074/jbc.M113.484212.

Peyvandi, F. *et al.* (2016) 'Caplacizumab for Acquired Thrombotic Thrombocytopenic Purpura', *New England Journal of Medicine*, 374(6), pp. 511–522. doi: 10.1056/NEJMoa1505533.

Portales-Cervantes, L. *et al.* (2012) 'The His155Tyr (489C>T) single nucleotide polymorphism of P2RX7 gene confers an enhanced function of P2X7 receptor in immune cells from patients with rheumatoid arthritis', *Cellular Immunology*, 276(1–2), pp. 168–175. doi: 10.1016/j.cellimm.2012.05.005.

Prinz, I., Silva-Santos, B. and Pennington, D. J. (2013) 'Functional development of γδ T cells', *European Journal of Immunology*, 43(8), pp. 1988–1994. doi: 10.1002/eji.201343759.

Proietti, M. *et al.* (2014) 'ATP-Gated Ionotropic P2X7 Receptor Controls Follicular T Helper Cell Numbers in Peyer's Patches to Promote Host-Microbiota Mutualism', *Immunity*, 41(5), pp. 789–801. doi: 10.1016/j.immuni.2014.10.010.

Pupovac, A. *et al.* (2015) 'Activation of the P2X7 receptor induces the rapid shedding of CD23 from human and murine B cells', *Immunology and Cell Biology*. Nature Publishing Group, 93(1), pp. 77–85. doi: 10.1038/icb.2014.69.

Purvis, H. A. *et al.* (2014) 'A Negative Feedback Loop Mediated by STAT3 Limits Human Th17 Responses', *The Journal of Immunology*, 193(3), pp. 1142–1150. doi: 10.4049/jimmunol.1302467.

Quarona, V. *et al.* (2013) 'CD38 and CD157: A long journey from activation markers to multifunctional molecules', *Cytometry Part B: Clinical Cytometry*. Wiley-Blackwell, 84B(4), pp. 207–217. doi: 10.1002/cyto.b.21092.

Rassendren, F. *et al.* (1997) 'The permeabilizing ATP receptor, P2X7. Cloning and expression of a human cDNA.', *The Journal of biological chemistry*, 272(9), pp. 5482–6.

Reantragoon, R. *et al.* (2013) 'Antigen-loaded MR1 tetramers define T cell receptor heterogeneity in mucosal-associated invariant T cells', *The Journal of Experimental Medicine*, 210(11), pp. 2305–2320. doi: 10.1084/jem.20130958.

Reilly, E. C., Wands, J. R. and Brossay, L. (2010) 'Cytokine dependent and independent iNKT cell activation.', *Cytokine*. NIH Public Access, 51(3), pp. 227–31. doi: 10.1016/j.cyto.2010.04.016.

Ren, K. and Torres, R. (2009) 'Role of interleukin-1beta during pain and inflammation.', *Brain research reviews*. NIH Public Access, 60(1), pp. 57–64. doi: 10.1016/j.brainresrev.2008.12.020.

Rissiek, A. *et al.* (2015) 'The expression of CD39 on regulatory T cells is genetically driven and further upregulated at sites of inflammation', *Journal of Autoimmunity*, 58, pp. 12–20. doi: 10.1016/j.jaut.2014.12.007.

Rissiek, B. *et al.* (2014) 'ADP-Ribosylation of P2X7: A Matter of Life and Death for Regulatory T Cells and Natural Killer T Cells', in *Current topics in microbiology and immunology*, pp. 107–126. doi: 10.1007/82_2014_420.

Rissiek, B. *et al.* (2015) 'P2X7 on mouse T cells: One channel, many functions', *Frontiers in Immunology*. doi: 10.3389/fimmu.2015.00204.

Rissiek, B. *et al.* (2017) 'Ecto-ADP-ribosyltransferase ARTC2.1 functionally modulates FcγR1 and FcγR2B on murine microglia.', *Scientific reports*. Nature Publishing Group, 7(1), p. 16477. doi: 10.1038/s41598-017-16613-w.

Riteau, N. *et al.* (2010) 'Extracellular ATP Is a Danger Signal Activating P2X$_7$ Receptor in Lung Inflammation and Fibrosis', *American Journal of Respiratory and Critical Care Medicine*, 182(6), pp. 774–783. doi: 10.1164/rccm.201003-0359OC.

Rodrigues, R. J., Tomé, A. R. and Cunha, R. A. (2015) 'ATP as a multi-target danger signal in the brain', *Frontiers in Neuroscience*. Frontiers, 9, p. 148. doi: 10.3389/fnins.2015.00148.

Roger, S. *et al.* (2010) 'Single nucleotide polymorphisms that were identified in affective mood disorders affect ATP-activated P2X7 receptor functions', *Journal of Psychiatric Research*, 44(6), pp. 347–355. doi: 10.1016/j.jpsychires.2009.10.005.

Van Roy, M. *et al.* (2015) 'The preclinical pharmacology of the high affinity anti-IL-6R Nanobody® ALX-0061 supports its clinical development in rheumatoid arthritis.', *Arthritis research & therapy*. BioMed Central, 17(1), p. 135. doi: 10.1186/s13075-015-0651-0.

Ryan, L. M. *et al.* (1996) 'Adenosine triphosphate levels in human plasma.', *The Journal of rheumatology*, 23(2), pp. 214–9.

Safya, H. *et al.* (2018) 'Variations in Cellular Responses of Mouse T Cells to Adenosine-5'-Triphosphate Stimulation Do Not Depend on P2X7 Receptor Expression Levels but on Their Activation and Differentiation Stage', *Frontiers in Immunology*. Frontiers, 9, p. 360. doi: 10.3389/fimmu.2018.00360.

Sakaguchi, S. (2004) 'Naturally arising CD4+ regulatory T cells for immunologic self-tolerance and negative control of immune responses', *Annual Review of Immunology*, 22(1), pp. 531–562. doi: 10.1146/annurev.immunol.21.120601.141122.

Salles, É. M. de *et al.* (2017) 'P2X7 receptor drives Th1 cell differentiation and controls the follicular helper T cell population to protect against Plasmodium chabaudi malaria', *PLOS Pathogens*. Edited by J. Langhorne. Public Library of Science, 13(8), p. e1006595. doi: 10.1371/journal.ppat.1006595.

Salou, M., Franciszkiewicz, K. and Lantz, O. (2017) 'MAIT cells in infectious diseases', *Current Opinion in Immunology*. Elsevier Current Trends, 48, pp. 7–14. doi: 10.1016/J.COI.2017.07.009.

Samways, D. S. K., Li, Z. and Egan, T. M. (2014) 'Principles and properties of ion flow in P2X receptors.', *Frontiers in cellular neuroscience*. Frontiers Media SA, 8, p. 6. doi: 10.3389/fncel.2014.00006.

Sanger, F., Nicklen, S. and Coulson, A. R. (1977) 'DNA sequencing with chain-terminating inhibitors.', *Proceedings of the National Academy of Sciences of the United States of America*, 74(12), pp. 5463–7.

Santana, P. T. *et al.* (2015) 'The P2X7 Receptor Contributes to the Development of the Exacerbated Inflammatory Response Associated with Sepsis', *Journal of Innate Immunity*, 7(4), pp. 417–427. doi: 10.1159/000371388.

Santos, A. A. *et al.* (2013) 'Implication of purinergic P2X7 receptor in M. tuberculosis infection and host interaction mechanisms: A mouse model study', *Immunobiology*, 218(8), pp. 1104–1112. doi: 10.1016/j.imbio.2013.03.003.

Savio, L. E. B. *et al.* (2018) 'The P2X7 Receptor in Inflammatory Diseases: Angel or Demon?', *Frontiers in Pharmacology*. Frontiers, 9, p. 52. doi: 10.3389/fphar.2018.00052.

Schenk, U. *et al.* (2008) 'Purinergic Control of T Cell Activation by ATP Released Through Pannexin-1 Hemichannels', *Science Signaling*, 1(39), pp. ra6-ra6. doi: 10.1126/scisignal.1160583.

Schenk, U. *et al.* (2011) 'ATP Inhibits the Generation and Function of Regulatory T Cells Through the Activation of Purinergic P2X Receptors', *Science Signaling*, 4(162), pp. ra12-ra12. doi: 10.1126/scisignal.2001270.

Schenkel, J. M. and Masopust, D. (2014) 'Tissue-resident memory T cells.', *Immunity*. Elsevier, 41(6), pp. 886–97. doi: 10.1016/j.immuni.2014.12.007.

Scheuplein, F. *et al.* (2009) 'NAD+ and ATP Released from Injured Cells Induce P2X7-Dependent Shedding of CD62L and Externalization of Phosphatidylserine by Murine T Cells', *The Journal of Immunology*, 182(5), pp. 2898–2908. doi: 10.4049/jimmunol.0801711.

Schmitt, E. G. and Williams, C. B. (2013) 'Generation and function of induced regulatory T cells.', *Frontiers in immunology*. Frontiers Media SA, 4, p. 152. doi: 10.3389/fimmu.2013.00152.

Schwarz, N. *et al.* (2012) 'Alternative Splicing of the N-Terminal Cytosolic and Transmembrane Domains of P2X7 Controls Gating of the Ion Channel by ADP-Ribosylation', *PLoS ONE*. Edited by Z. Zhang, 7(7), p. e41269. doi: 10.1371/journal.pone.0041269.

Seach, N. *et al.* (2013) 'Double Positive Thymocytes Select Mucosal-Associated Invariant T Cells', *The Journal of Immunology*, 191(12), pp. 6002–6009. doi: 10.4049/jimmunol.1301212.

Sell, S. *et al.* (2015) 'Control of Murine Cytomegalovirus Infection by γδ T Cells', *PLOS Pathogens*. Edited by S. C. Jameson. Public Library of Science, 11(2), p. e1004481. doi: 10.1371/journal.ppat.1004481.

Seman, M. *et al.* (2003) 'NAD-Induced T Cell Death: ADP-Ribosylation of Cell Surface Proteins by ART2 Activates the Cytolytic P2X7 Purinoceptor', *Immunity*. Cell Press, 19(4), pp. 571–582. doi: 10.1016/S1074-7613(03)00266-8.

Sester, D. P. *et al.* (2015) 'A Novel Flow Cytometric Method To Assess Inflammasome Formation', *The Journal of Immunology*, 194(1), pp. 455–462. doi: 10.4049/jimmunol.1401110.

Sharp, A. J. *et al.* (2008) 'P2x7 deficiency suppresses development of experimental autoimmune encephalomyelitis', *Journal of Neuroinflammation*, 5(1), p. 33. doi: 10.1186/1742-2094-5-33.

Sheth, S. *et al.* (2014) 'Adenosine Receptors: Expression, Function and Regulation', *International Journal of Molecular Sciences*, 15(2), pp. 2024–2052. doi: 10.3390/ijms15022024.

Slichter, C. K. *et al.* (2016) 'Distinct activation thresholds of human conventional and innate-like memory T cells.', *JCI insight*. American Society for Clinical Investigation, 1(8). doi: 10.1172/jci.insight.86292.

Sluyter, R. (2017) 'The P2X7 Receptor', in *Advances in experimental medicine and biology*, pp. 17–53. doi: 10.1007/5584_2017_59.

Sluyter, R., Shemon, A. N. and Wiley, J. S. (2007) 'P2X7 receptor activation causes phosphatidylserine exposure in human erythrocytes', *Biochemical and Biophysical Research Communications*. Academic Press, 355(1), pp. 169–173. doi: 10.1016/J.BBRC.2007.01.124.

Sluyter, R. and Stokes, L. (2011) 'Significance of P2X7 Receptor Variants to Human Health and Disease', *Recent Patents on DNA & Gene Sequences*, 5(1), pp. 41–54. doi: 10.2174/187221511794839219.

Sluyter, R. and Wiley, J. S. (2014) 'P2X7 receptor activation induces CD62L shedding from human CD4+ and CD8+ T cells', *Inflammation and Cell Signaling*, 1(1). doi: 10.14800/ics.92.

Smart, M. L. *et al.* (2003) 'P2X7 receptor cell surface expression and cytolytic pore formation are regulated by a distal C-terminal region.', *The Journal of biological chemistry*. American Society for Biochemistry and Molecular Biology, 278(10), pp. 8853–60. doi: 10.1074/jbc.M211094200.

Smith, V. J. (2016) 'Immunology of Invertebrates: Cellular', in *eLS*. Chichester, UK: John Wiley & Sons, Ltd, pp. 1–13. doi: 10.1002/9780470015902.a0002344.pub3.

Sorge, R. E. *et al.* (2012) 'Genetically determined P2X7 receptor pore formation regulates variability in chronic pain sensitivity', *Nature Medicine*, 18(4), pp. 595–599. doi: 10.1038/nm.2710.

Spaans, F. *et al.* (2014) 'Danger signals from ATP and adenosine in pregnancy and preeclampsia.', *Hypertension (Dallas, Tex. : 1979)*. American Heart Association, Inc., 63(6), pp. 1154–60. doi: 10.1161/Hypertensionha.114.03240.

Sperlagh, B. *et al.* (2006) 'P2X7 receptors in the nervous system', *Progress in Neurobiology*, 78(6), pp. 327–346. doi: 10.1016/j.pneurobio.2006.03.007.

Spits, H. *et al.* (2013) 'Innate lymphoid cells — a proposal for uniform nomenclature', *Nature Reviews Immunology*, 13(2), pp. 145–149. doi: 10.1038/nri3365.

Spits, H. and Cupedo, T. (2012) 'Innate Lymphoid Cells: Emerging Insights in Development, Lineage Relationships, and Function', *Annual Review of Immunology*, 30(1), pp. 647–675. doi: 10.1146/annurev-immunol-020711-075053.

Steinberg, T. H. *et al.* (1987) 'ATP4- permeabilizes the plasma membrane of mouse macrophages to fluorescent dyes.', *The Journal of biological chemistry*, 262(18), pp. 8884–8.

Stock, T. C. *et al.* (2012) 'Efficacy and Safety of CE-224,535, an Antagonist of P2X7 Receptor, in Treatment of Patients with Rheumatoid Arthritis Inadequately Controlled by Methotrexate', *The Journal of Rheumatology*, 39(4), pp. 720–727. doi: 10.3899/jrheum.110874.

Stokes, L. *et al.* (2010) 'Two haplotypes of the P2X $_7$ receptor containing the Ala-348 to Thr polymorphism exhibit a gain-of-function effect and enhanced interleukin-1β secretion', *The FASEB Journal*. Federation of American Societies for Experimental Biology, 24(8), pp. 2916–2927. doi: 10.1096/fj.09-150862.

Stone, K. D., Prussin, C. and Metcalfe, D. D. (2010) 'IgE, mast cells, basophils, and eosinophils.', *The Journal of allergy and clinical immunology*. NIH Public Access, 125(2 Suppl 2), pp. S73-80. doi: 10.1016/j.jaci.2009.11.017.

Surprenant, A. *et al.* (1996) 'The cytolytic P2Z receptor for extracellular ATP identified as a P2X receptor (P2X7).', *Science (New York, N.Y.)*, 272(5262), pp. 735–8.

Sutton, C. E. *et al.* (2009) 'Interleukin-1 and IL-23 Induce Innate IL-17 Production from γδ T Cells, Amplifying Th17 Responses and Autoimmunity', *Immunity*, 31(2), pp. 331–341. doi: 10.1016/j.immuni.2009.08.001.

Suzuki, T. *et al.* (2004) 'Production and Release of Neuroprotective Tumor Necrosis Factor by P2X7 Receptor-Activated Microglia', *Journal of Neuroscience*, 24(1), pp. 1–7. doi: 10.1523/JNEUROSCI.3792-03.2004.

Tabarkiewicz, J. *et al.* (2015) 'The Role of IL-17 and Th17 Lymphocytes in Autoimmune Diseases.', *Archivum immunologiae et therapiae experimentalis*. Springer, 63(6), pp. 435–49. doi: 10.1007/s00005-015-0344-z.

Tanaka, Y. *et al.* (1995) 'Natural and synthetic non-peptide antigens recognized by human γδ T cells', *Nature*, 375(6527), pp. 155–158. doi: 10.1038/375155a0.

Taylor, S. R. J. *et al.* (2009) 'Lymphocytes from P2X7-deficient mice exhibit enhanced P2X7 responses.', *Journal of leukocyte biology*. The Society for Leukocyte Biology, 85(6), pp. 978–86. doi: 10.1189/jlb.0408251.

Taylor, S. R. J. *et al.* (2009) 'P2X7 Deficiency Attenuates Renal Injury in Experimental Glomerulonephritis', *Journal of the American Society of Nephrology*, 20(6), pp. 1275–1281. doi: 10.1681/ASN.2008060559.

Tesmer, L. A. *et al.* (2008) 'Th17 cells in human disease.', *Immunological reviews*. NIH Public Access, 223, pp. 87–113. doi: 10.1111/j.1600-065X.2008.00628.x.

Tijink, B. M. *et al.* (2008) 'Improved tumor targeting of anti-epidermal growth factor receptor Nanobodies through albumin binding: taking advantage of modular Nanobody technology', *Molecular Cancer Therapeutics*, 7(8), pp. 2288–2297. doi: 10.1158/1535-7163.MCT-07-2384.

Tilloy, F. *et al.* (1999) 'An invariant T cell receptor alpha chain defines a novel TAP-independent major histocompatibility complex class Ib-restricted alpha/beta T cell subpopulation in mammals.', *The Journal of experimental medicine*, 189(12), pp. 1907–21.

Trabanelli, S. *et al.* (2012) 'Extracellular ATP Exerts Opposite Effects on Activated and Regulatory CD4+ T Cells via Purinergic P2 Receptor Activation', *The Journal of Immunology*, 189(3), pp. 1303–1310. doi: 10.4049/jimmunol.1103800.

Traut, T. W. (1994) 'Physiological concentrations of purines and pyrimidines.', *Molecular and cellular biochemistry*, 140(1), pp. 1–22.

Tsai, S. H. *et al.* (2015) 'The ectoenzyme E-NPP3 negatively regulates ATP-dependent chronic allergic responses by basophils and mast cells.', *Immunity*. Elsevier, 42(2), pp. 279–293. doi: 10.1016/j.immuni.2015.01.015.

Tung, H.-C. *et al.* (2015) 'The Beneficial Effects of P2X7 Antagonism in Rats with Bile Duct Ligation-induced Cirrhosis', *PLOS ONE*. Edited by M. A. Avila, 10(5), p. e0124654. doi: 10.1371/journal.pone.0124654.

Unciti-Broceta, J. D. *et al.* (2013) 'Novel therapy based on camelid nanobodies', *Therapeutic Delivery*, 4(10), pp. 1321–1336. doi: 10.4155/tde.13.87.

Ussher, J. E. *et al.* (2014) 'CD161 [++] CD8 [+] T cells, including the MAIT cell subset, are specifically activated by IL-12+IL-18 in a TCR-independent manner', *European Journal of Immunology*, 44(1), pp. 195–203. doi: 10.1002/eji.201343509.

Vermijlen, D. and Prinz, I. (2014) 'Ontogeny of Innate T Lymphocytes â€" Some Innate Lymphocytes are More Innate than Others', *Frontiers in Immunology*, 5, p. 486. doi: 10.3389/fimmu.2014.00486.

Vieira, F. S. *et al.* (2016) 'P2X7 receptor knockout prevents streptozotocin-induced type 1 diabetes in mice', *Molecular and Cellular Endocrinology*, 419, pp. 148–157. doi: 10.1016/j.mce.2015.10.008.

Vincke, C. *et al.* (2009) 'General Strategy to Humanize a Camelid Single-domain Antibody and Identification of a Universal Humanized Nanobody Scaffold', *Journal of Biological Chemistry*, 284(5), pp. 3273–3284. doi: 10.1074/jbc.M806889200.

Di Virgilio, F. (2012) 'Purines, Purinergic Receptors, and Cancer', *Cancer Research*, 72(21), pp. 5441–5447. doi: 10.1158/0008-5472.CAN-12-1600.

Di Virgilio, F. *et al.* (2017) 'The P2X7 Receptor in Infection and Inflammation', *Immunity*, 47(1), pp. 15–31. doi: 10.1016/j.immuni.2017.06.020.

Di Virgilio, F. *et al.* (2018) 'Non-nucleotide Agonists Triggering P2X7 Receptor Activation and Pore Formation', *Frontiers in Pharmacology*. Frontiers, 9, p. 39. doi: 10.3389/fphar.2018.00039.

Vos, Q. *et al.* (2000) 'B-cell activation by T-cell-independent type 2 antigens as an integral part of the humoral immune response to pathogenic microorganisms.', *Immunological reviews*, 176, pp. 154–70.

Wan, P. *et al.* (2016) 'Extracellular ATP mediates inflammatory responses in colitis via P2 × 7 receptor signaling', *Scientific Reports*. Nature Publishing Group, 6(1), p. 19108. doi: 10.1038/srep19108.

Wang, C. M. *et al.* (2014) 'Adenosine triphosphate acts as a paracrine signaling molecule to reduce the motility of T cells.', *The EMBO journal*. European Molecular Biology Organization, 33(12), pp. 1354–64. doi: 10.15252/embj.201386666.

Wang, H. *et al.* (2015) 'P2RX7 sensitizes Mac-1/ICAM-1-dependent leukocyte-endothelial adhesion and promotes neurovascular injury during septic encephalopathy', *Cell Research*, 25(6), pp. 674–690. doi: 10.1038/cr.2015.61.

Wang, L. *et al.* (2004) 'P2 receptor mRNA expression profiles in human lymphocytes, monocytes and CD34+ stem and progenitor cells.', *BMC Immunology*, 5(1), p. 16. doi: 10.1186/1471-2172-5-16.

Wang, S. *et al.* (2015) 'Blockage of P2X7 attenuates acute lung injury in mice by inhibiting NLRP3 inflammasome', *International Immunopharmacology*, 27(1), pp. 38–45. doi: 10.1016/j.intimp.2015.04.035.

Ward, J. R. *et al.* (2010) 'Temporal interleukin-1beta secretion from primary human peripheral blood monocytes by P2X7-independent and P2X7-dependent mechanisms.', *The Journal of biological chemistry*. American Society for Biochemistry and Molecular Biology, 285(30), pp. 23147–58. doi: 10.1074/jbc.M109.072793.

Wareham, K. *et al.* (2009) 'Functional evidence for the expression of P2X1, P2X4 and P2X7 receptors in human lung mast cells', *British Journal of Pharmacology*, 157(7), pp. 1215–1224. doi: 10.1111/j.1476-5381.2009.00287.x.

Welter-Stahl, L. *et al.* (2009) 'Expression of purinergic receptors and modulation of P2X7 function by the inflammatory cytokine IFNγ in human epithelial cells', *Biochimica et Biophysica Acta (BBA) - Biomembranes*. Elsevier, 1788(5), pp. 1176–1187. doi: 10.1016/J.BBAMEM.2009.03.006.

Wesolowski, J. *et al.* (2009) 'Single domain antibodies: promising experimental and therapeutic tools in infection and immunity', *Medical Microbiology and Immunology*, 198(3), pp. 157–174. doi: 10.1007/s00430-009-0116-7.

Wiley, J. S. *et al.* (2003) 'An Ile-568 to Asn Polymorphism Prevents Normal Trafficking and Function of the Human P2X $_7$ Receptor', *Journal of Biological Chemistry*, 278(19), pp. 17108–17113. doi: 10.1074/jbc.M212759200.

van Wilgenburg, B. *et al.* (2016) 'MAIT cells are activated during human viral infections', *Nature Communications*. Nature Publishing Group, 7, p. 11653. doi: 10.1038/ncomms11653.

Woehrle, T. *et al.* (2010) 'Pannexin-1 hemichannel-mediated ATP release together with P2X1 and P2X4 receptors regulate T-cell activation at the immune synapse', *Blood*, 116(18), pp. 3475–3484. doi: 10.1182/blood-2010-04-277707.

Wrobel, P. *et al.* (2007) 'Lysis of a Broad Range of Epithelial Tumour Cells by Human ?? T Cells: Involvement of NKG2D ligands and T-cell Receptor- versus NKG2D-dependent Recognition', *Scandinavian Journal of Immunology*, 66(2–3), pp. 320–328. doi: 10.1111/j.1365-3083.2007.01963.x.

Yip, L. *et al.* (2009) 'Autocrine regulation of T-cell activation by ATP release and P2X 7 receptors', *The FASEB Journal*, 23(6), pp. 1685–1693. doi: 10.1096/fj.08-126458.

Yoon, M.-J. *et al.* (2007) 'Extracellular ATP Is Involved in the Induction of Apoptosis in Murine Hematopoietic Cells', *Biological & Pharmaceutical Bulletin*, 30(4), pp. 671–676. doi: 10.1248/bpb.30.671.

Zhang, Y. and Huang, B. (2017) 'The Development and Diversity of ILCs, NK Cells and Their Relevance in Health and Diseases', in, pp. 225–244. doi: 10.1007/978-981-10-5987-2_11.

Zhu, J., Yamane, H. and Paul, W. E. (2010) 'Differentiation of Effector CD4 T Cell Populations', *Annual Review of Immunology*, 28(1), pp. 445–489. doi: 10.1146/annurev-immunol-030409-101212.

Ziegler-Heitbrock, H. W. L. (2000) 'Definition of human blood monocytes', *Journal of Leukocyte Biology*. Wiley-Blackwell, 67(5), pp. 603–606. doi: 10.1002/jlb.67.5.603.

Zimmermann, H. (2000) 'Extracellular metabolism of ATP and other nucleotides', *Naunyn-Schmiedeberg's Archives of Pharmacology*. Springer-Verlag, 362(4–5), pp. 299–309. doi: 10.1007/s002100000309.
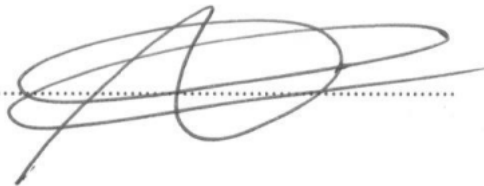
10. <u>ACKNOWLEDGEMENTS</u>

11. <u>EIDESSTATTLICHE VERSICHERUNG</u>

Ich versichere ausdrücklich, dass ich die Arbeit selbständig und ohne fremde Hilfe verfasst, andere als die von mir angegebenen Quellen und Hilfsmittel nicht benutzt und die aus den benutzten Werken wörtlich oder inhaltlich entnommenen Stellen einzeln nach Ausgabe (Auflage und Jahr des Erscheinens), Band und Seite des benutzten Werkes kenntlich gemacht habe.

Ferner versichere ich, dass ich die Dissertation bisher nicht einem Fachvertreter an einer anderen Hochschule zur Überprüfung vorgelegt oder mich anderweitig um Zulassung zur Promotion beworben habe.

Ich erkläre mich einverstanden, dass meine Dissertation vom Dekanat der Medizinischen Fakultät mit einer gängigen Software zur Erkennung von Plagiaten überprüft werden kann.

Unterschrift: ....